Establishing tissue-specific chromatin organization during development of the epidermis

Nuclear architecture of different layers of murine epidermis and the role of p63 and Satb1 in establishing tissue-specific organization of the epidermal differentiation complex locus

Michał Ryszard Gdula

Submitted for the degree of Doctor of Philosophy

Centre for Skin Sciences

Division of Medical Sciences

School of Life Sciences

University of Bradford

2011

Dedicated to my Parents and sister Agnieszka thanks to whose sacrifice and support I could pursue my fascinations and interests.

Acknowledgement

I would like to pay special thanks and appreciation to my supervisor Professor Vladimir Botchkarev for his tremendous support, encouragement and co-operation in all my work.

I would like to also thank Dr Michael Fessing for guiding me into the “FISH” world and for our three-year-long fruitful cooperation.

I am extremely indebted to Dr Andrei Mardaryev and Dr Natasha Botchkareva for their advice and assistance.

I wish to acknowledge and to thank my friends Mr. Krzysztof Poterłowicz, Dr Julian Laubenthal and Dr Mohammed Ikram Ahmed both for their support during my work and for sharing our day-to–day PhD student life.

Last but not least I would like to thank Kinga for brightening my life and not letting me to sink entirely into the chromatin world.

Contents:

Abstract

During development, multipotent stem cells establish tissue-specific programmes of gene expression that underlie a process of differentiation into specialized cell types.

It was shown in the study that changes in the nuclear architecture during terminal keratinocyte differentiation show correlation with the dynamics of the transcriptional and metabolic activity. In particular, terminal differentiation is accompanied by the decrease of nuclear volume, elongation of its shape, reduction of the number and fusion of nucleoli, increase in the number of centromeric clusters and a dramatic decrease of the transcriptional activity.

Global changes in the nuclear architecture of epidermal keratinocytes are associated with marked remodelling of the higher-order chromatin structure of the epidermal differentiating complex (EDC). EDC is positioned peripherally in the epidermal nuclei at E11.5 when its genes show low expression levels and relocates towards the nuclear interior at E16.5 when EDC genes are markedly upregulated.

P63 transcription factor serving as a master regulator of epidermal development is involved in the control of EDC relocation in epidermal progenitor cells. The epidermis of E16.5 p63KO exhibits significantly more peripheral positioning of the EDC loci, compared to wild-type.

The genome organizer Satb1 serving as a direct p63 target controls higher order chromatin folding of the central part of *EDC* and Satb1 knockout mice show alterations of epidermal development and expression of the EDC encoded genes.

Thus, this study shows that the programme of epidermal development and terminal differentiation is regulated by p63 and other factors and include marked remodelling of three-dimensional nuclear organization and positioning of tissue specific gene loci. In addition to the direct involvement of p63 in controlling the expression of tissue-specific genes, p63 via regulation of the chromatin remodelling factors such as Satb1 promotes establishing specific conformation of the EDC locus required for efficient expression of terminal differentiation-associated genes.

Abbreviations

3C - chromatin conformation capture assay

ANOVA - analysis of variance test

AT -adenine thymine

BAC - bacterial artificial chromosome

CB - Cajal bodies

CE - cornified envelope

CT - chromosome territory

CT-IT - chromosome territory-interchromatin compartment model

DOP -PCR - degenerated oligonucleotide primer polymerase chain reaction

E12 - 12 day-old embryo

EDC - epidermal differentiation complex

EM - electron microscopy

EMANIAC - EM-assisted nucleosomes interacting capture

FC - fibrillar centres

FISH - fluorescent in situ hybridisation

FLG - profillagrin

FRET - fluorescence resonance energy transfer

GC - granular centres

GC -guanine cytosine

HDAC - histone deacetylase

HMT - histone methyltransferase

ICD - interchromatin model

ICN - inter-chromosomal network model

IF - intermediate filaments

IGC - interchromatin granule clusters

INM - inner nuclear membrane

INV - involucrin

KO -knockout

LCE - late cornified envelope proteins

LMNA - lamin A

MAR - matrix attachment region

NOR - nuclear organising region

NPC - nuclear pore complex

NS - nuclear speckles

NT - nick translation

ONM - outer nuclear membrane

OR - odorant receptor

PcG - polycomb bodies

PCR - polymerase chain reaction

PKC - protein kinase C

PML - promyelocytic leukaemia

RNAi - RNA interference

RNP - ribonucleoprotein

RT - room temperature

snRNP - small nuclear ribonucleoprotein

SPRR - small proline rich protein

TA - transactivation domain

List of Figures

List of Tables

Appendix

1. Introduction

Development of multicellular organisms is a very complex process requiring sophisticated regulation and coordination of gene expression and resulting in differentiation of the progenitor cells into specialized cell types. Many mechanisms involved in this complicated enterprise are controlled at different levels, including the DNA regulatory sequences (response elements, silencers, enhancers etc.), epigenetic modifications of DNA and histones, posttranscriptional control by different classes of regulatory RNAs (siRNA, miRNA, antisense transcripts and others) or control at the level of translation (Chen and Rajewsky, 2007).

Studies on the nuclear architecture performed within the last two decades demonstrated a complex structure of the eukaryotic nucleus including organisation of interphase chromosome territories, functional significance of different types of nuclear bodies or mechanisms of anchoring of genomic DNA within the distinct intra-nuclear compartments (Sadoni *et al.*, 1999). Growing understanding of the nuclear complexity and increasing amount of the molecular biology data along with improvements in techniques like three dimensional fluorescent in situ hybridisation (3D-FISH) and bioimaging led to the discovery of novel mechanisms involved in the control of gene expression which includes three dimensional compartmentalization of the genomic domains, gene clustering and changes of intra-nuclear localization of gene loci (Sadoni *et al.*, 1999).

This PhD thesis presents the results of analysis of tissue-specific remodelling of the higher-order structure of the genomic locus containing epidermal

differentiation complex (EDC) during mouse skin development associated with the changes in the expression of its genes. Results obtained from the analysis of EDC distribution during the development of the epidermis in wild-type and p63 knock-out mice strongly suggest that changes of the intra-chromosomal and intra-nuclear position of EDC are important for facilitating gene expression in this locus and are crucial for the establishment of a fully functional multilayered epidermis. Furthermore, analysis of the EDC conformation demonstrates an important role of Satb1 as a p63 target in the regulation of gene expression within the EDC.

The thesis is divided into 5 chapters: Introduction, Materials and Methods, Results, Discussion, Conclusions and Future directions. In the Introduction, literature relevant to this area of research was reviewed comprising the contemporary knowledge on the structure of the eukaryotic nucleus and functional significance of the mechanisms controlling skin morphogenesis and structure of the EDC locus. In the Material and methods section, techniques and methodology used in this research project were described. The Results chapter is devoted to the presentation of the data generated, which are discussed in the following chapter. At the end, conclusions and future research plans are presented.

1.1 Epidermal morphogenesis and its genetic regulation.

The epidermis is the outermost layer of the skin separated from the underlying dermis by the basal membrane which consists of proteins secreted by epidermal keratinocytes and by dermal fibroblasts. Its main function is to protect the body from a number of environmental stressors including thermal insults,

mechanical injuries, infections, UV irradiation, as well as to prevent water loss. The epidermis and dermis function cooperatively and their continuous interactions give a rise to epidermal appendages, such as hair follicles and sweat glands. The matured multilayered epidermis develops as a result of a complex highly coordinated process which lasts in mice around 10 days (Koster and Roop, 2007b).

1.1.1 Epidermal morphogenesis.

In mice, epidermal development begins when the cells of the surface ectoderm covering a whole embryo become committed to the epidermal fate at E8.5 (day of embryonic development 8.5). This process leads to the formation of fully functional multilayered epidermis at E18.5 (M'Boneko and Merker, 1988).

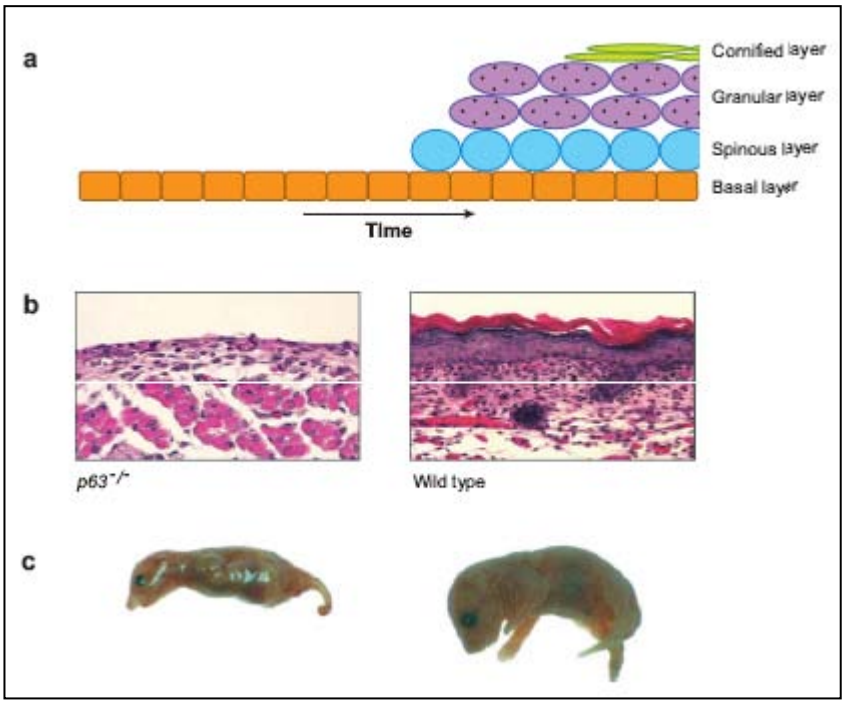

Figure. 1.1 Epidermal morphogenesis in wild type mouse and p63 knock out mouse. After commitment to epidermal fate, the basal layer cells give rise to periderm that sheds in later stages, subsequently the intermediate layer of cells appears between them which undergoes maturation into spinous cells. Spinous cells differentiate into the granular layer and eventually cornified layer. The whole process of epidermal stratification leads to the establishment of the epidermal barrier which is inevitable for vitality of mouse. p63 knock out mouse dies shortly after birth from dehydration and often abnormalities (Koster and Roop, 2007b).

Cells of the surface ectoderm express keratins K8 and K18, while after commitment to the epidermal fate they begin to express K5 and K14 (Byrne *et al.*, 1994). Tissue recombination experiments proved that the signal required for epidermal specification comes from the dermis, however its nature is not clear (Ferraris *et al.*, 2000). It is known that this process correlates with the increase of Wnt/β-catenin signalling and induction of p63 expression, which plays a role as a master regulator of epidermal development (Koster and Roop, 2007b).

The p63 gene contains two promoters and gives rise to two groups of isoforms: the ones with transactivation (TA) domain and the others lacking this domain (ΔN) (Yang *et al.*, 1998). Expression of TAp63 appears first and it is responsible for induction of K14, however it does not do it directly but through activation of factor AP-2γ known to regulate the K14 expression (Koster *et al.*, 2006). Oppositely to TAp63, ΔNp63 is able to induce directly K14 but it starts being expressed after epidermal stratification so it rather plays a role in maintaining K14 expression (Barbieri and Pietenpol, 2006; Koster and Roop, 2007b).

In addition to keratin genes, p63 regulates a large number of genes including ATP-dependent chromatin remodelling enzymes Brg1 and Mi-2α/β (Fessing et al., 2011). Ablation of the Brg1 leads to the alterations in epidermal barrier formation (Indra *et al.*, 2005). Mi-2α/β is also required for proper keratinocyte differentiation in mice (Kashiwagi *et al.*, 2007).

After initial commitment step, keratinocytes of the basal layer give a rise to a second layer of cells (the periderm), which is shed with the acquisition of the epidermal barrier function(Smart, 1970). Asymmetric division of basal cells leads to the development of the intermediate epidermal layer (Lechler and Fuchs, 2005). Cells of the intermediate layer express K1 and undergo

proliferation until they differentiate into spinous cells. The only known so far difference between the spinous cells and cells of intermediate layer is the ability to proliferate. Differentiation of the basal cells into intermediate layer cells and later spinous cells is regulated by ΔNp63. Genes involved in the control of differentiation of intermediate layer cells into spinous cells also include IKKα, IRF6, 14-3-3σ and Ovo1. Mutants with depletion of expression in one of these genes fail to develop spinous cell layer and develop extended areas of keratinocytes expressing K1 (Koster and Roop, 2007b).

Further differentiation of keratinocytes into granular cells is triggered by the increase of Ca^{2+} concentration. In mature epidermis, increasing gradient of Ca^{2+} from basal layer up to the cornified layer was shown by many investigators (Menon *et al.*, 1992). Increased levels of Ca^{2+} activate protein kinase C (PKCα and PKCη) which downregilates K1 and K10 expression and induces the expression of Loricrin, Filaggrin and transglutaminase, which serves as the markers of granular layer keratinocytes (Koster and Roop, 2007b).

The cells of the cornified layer of the epidermis form cell envelopes composed of the proteins cross-linked into a rigid scaffold and of lipids covalently attached to the exterior surface (Segre, 2006a). Regulation of the epidermal barrier formation requires further investigation, and so far a few transcription factors involved in the control of this process have been identified: Klf4, Grlh3/Get1, Brg1 and Arnt (Geng *et al.*, 2006; Hoffjan and Stemmler, 2007; Indra *et al.*, 2005; Segre *et al.*, 1999).

It has been proposed that during formation of the cornfied structure, the structural proteins involucrin, envoplakin and periplakin are sequentially cross-linked to form an initial scaffold. This process is catalyzed by epidermal

transglutaminases which promote establishing of the disulphide and (γ-glutamyl) lysine isopeptyde bonds. Later proteins such as loricrin, small proline-rich (SPRRs) and late cornified envelope proteins (LCE) are added to form envelope (Marshall *et al.*, 2001). At the end, the lipids (i.e. ceramids) are synthesized in lamellar granules that are extruded into the extracellular space, establishing a lipid envelope that further reinforces the epidermal barrier (Hoffjan and Stemmler, 2007).

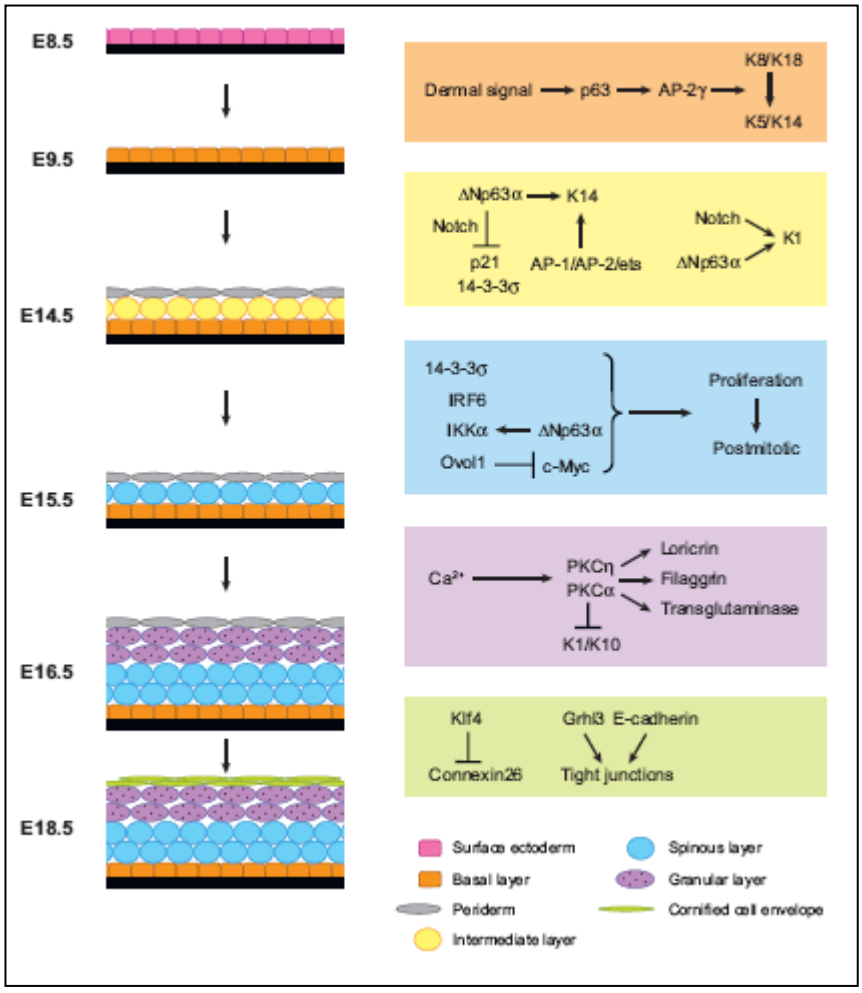

Figure 1.2 Skin morphogenesis and its regulation. Explanation in the text (adapted from Koster and Roop, 2007)

The epidermal barrier is indispensible for survival of the newborn mice. p63 knockout mice that fail to establish epidermal stratification die shortly after birth from dehydration (Mills, Zheng et al. 1999). The barrier function of the epidermis

is maintained during postnatal life. This process is mediated by epidermal stem cells residing in the basal epidermal layer and hair follicle (Lechler and Fuchs, 2005; Mills *et al.*, 1999).

Since cornified cells are being constantly replenished and damaged, basal layer cells have to maintain their proliferative activity and supply progenitors to form new terminally differentiated keratinocytes. The mechanism preventing stem cells of the epidermal basal layer from differentiation are still not clear; however, there is evidence that ΔNp63 is also involved in the control of this process (Parsa *et al.*, 1999). P63 inhibits the expression of p21 and 14-3-3σ which are involved in controlling epidermal terminal differentiation (Dellambra *et al.*, 2000). In addition, it inhibits p21 by downregulating Notch signalling which is an upstream regulator of p21. It was found that ΔNp63 is also involved in promoting differentiation of basal layer cells by inducing of K1 expression. This suggest that ΔNp63 has different influence on distinct subsets of basal layer cells (Barbieri and Pietenpol, 2006; Koster and Roop, 2007b).

1.1.2 Structure of the epidermal differentiation complex.

Epidermis-specific genes are clustered in the genome into at least three different loci: keratin type I and II loci located on mouse chromosomes 11 and 15, respectively, as well as in the epidermal differentiation complex (EDC) located on chromosome 3. In the human genome, these loci are located on chromosomes 12,17 and 1 respectively.

EDC occupies a region of approximately 3.1 Mb on mouse chromosome 3, which contains a number of genes that fulfill important functions in epidermal

differentiation (Rothnagel *et al.*, 1994; Song *et al.*, 1999). EDC is homologous to the corresponding locus on human chromosome 1q21 (Martin *et al.*, 2004a; Mischke *et al.*, 1996; Volz *et al.*, 1993). So far more than 40 genes have been identified within EDC. Some of them encode the proteins involved in the formation of the cornified envelope (CE), including Loricrin, Involucrin, Flaggirin, Trichohyalin as well as Small proline-rich and Late cornified envelope protein families. Other genes encode calcium binding proteins of the S100a family (Hoffjan and Stemmler, 2007; Martin *et al.*, 2004a; Presland and Dale, 2000).

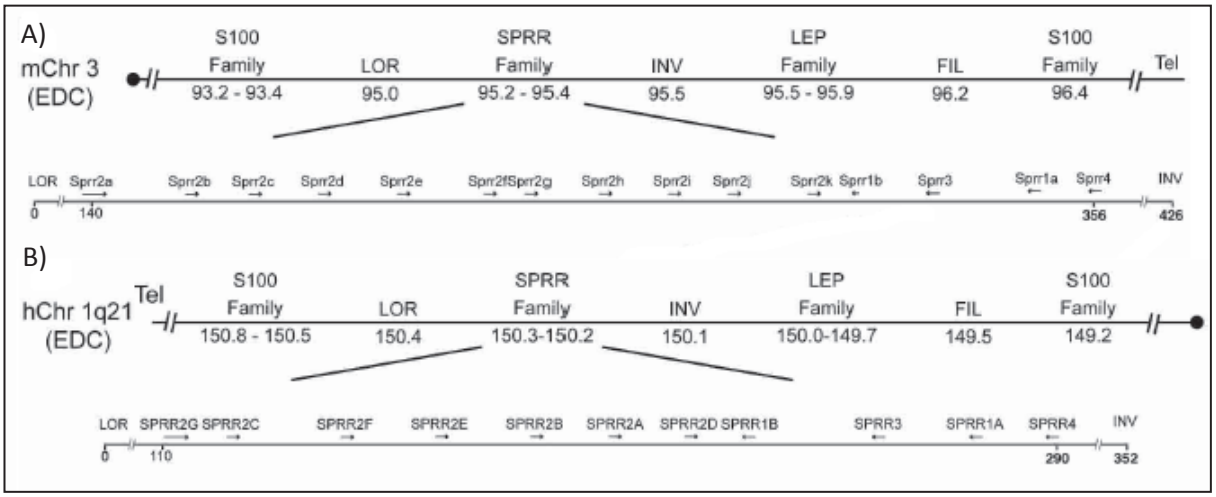

Figure. 1.3 Structure of the EDC in mouse (A) and in human (B). EDC contains many genes involved in establishing cornified cell envelope . Structure of this loci in mouse is similar to the EDC structure n humans (adapted from (Martin *et al.*, 2004a).

Structure of the EDC in mice and human is quite similar: the central 1.2 Mb domain contain genes encoding structural proteins: Loricrin, Involucrin, the families of small proline-rich (Sprr) and the late envelope proteins (LPE). This central region of the EDC is flanked by the genes from the S100 family (Martin *et al.*, 2004a).

1.1.3 Major EDC components and their role in the control of terminal keratinocyte differentiation

Most of the genes from the EDC locus are expressed in the epidermis and play distinct roles in keratinocyte differentiation, however some of them are expressed also in other tissues (i.e., S100 family proteins). Major EDC genes comprise: S100 family genes, Loricrin, small proline reach protein family genes (SPRR), Involucrin, late cornified envelope family genes (LCE) and profillagrin (FLG).

S100 proteins are members of multigene family of 21 proteins which have different functions in a wide variety of cell types and tissues. They are characterized by low molecular weight (9-13 kDa) and the presence of two calcium binding EF motives (Eckert *et al.*, 2004) and exert their functions by binding and modulating of the activity of other proteins. Fourteen S100 protein genes are located within the EDC and 13 of them are expressed in normal and/or diseased epidermis (Eckert *et al.*, 2004). Some of S100A (i.e. S100A2, A7, A8, A9, A15) are more upregulated in a number of skin diseases like cancer, psioraris or imflamation of the skin (Hoffjan and Stemmler, 2007).

Loricrin is the major component of the cornified envelope and it constitutes about 70% of its mass (Hohl *et al.*, 1991; Steinert and Marekov, 1995). It is absent in most of the internal epithelia, with an exemption of the mouse forestomach (Hohl *et al.*, 1993). Loricrin accumulates in the granules of epidermal granular layer (termed L-granules to differentiate them from profillagrin-containing F-granules) before it is integrated into the cornified envelope (Bickenbach *et al.*, 1995; Steven *et al.*, 1990). Mouse Loricrin consists of 481 amino acids and is enriched in glycine (55%), serine (22%) and cystein

(7%) (Mehrel *et al.*, 1990). It contains tandem repeats of amino acids forming the “glycine loops” which are belived to confer flexibility to the protein and cornified envelope (Hohl *et al.*, 1991). However, Loricrin knockout mice revealed only minor reduction of the stability of the stratum corneum and mutant mice were more susceptible to ultrasound fragmentation. In Loricrin knockout mice, the skin phenotype disappeared 4-5 days after birth. This study suggests that loricrin functions may be compensated by other proteins, most probably SPRRs and repetin (Jarnik *et al.*, 2002; Koch *et al.*, 2000).

SPRR proteins are coexpressed with Loricrin and serve as molecular cross-linkers during formation of the cornified envelope (Steinert *et al.*, 1998). Up to now, 17 different SPRRs are known, which are divided into 3 subfamilies (SPRR1, SPRR2 and SPRR3), showing strong sequence homology to Loricrin and Involucrine (Gibbs *et al.*, 1993; Zimmermann *et al.*, 2005). The mass ratio of the Loricrin and SPRR proteins differs among the epithelial tissues, for example it equals 100:1 in new-born mouse epidermis and 3:1 in in the forstomach. It was suggested that this ratio may determine the biochemical properties of the cornified envelope (Jarnik *et al.*, 1996).

Involucrin is thought to serve as a scaffold for the other cornified envelope components (Steinert and Marekov, 1997). It is synthesized in the outer living layers of terminally differentiating keratinocytes of all stratified squamus epithelia (Banks-Schlegel and Green, 1981) and together with two other proteins (envoplakin and periplakin) is incorporated into the cornified envelope serving as a substrate for transglutaminase. Involucrin knockout mice are developed normally and have normal skin, most probably due to compensation by the envoplakin and periplakin (Djian *et al.*, 2000). However, triple-knockout

mice deficient in involucrin, envoplakin and periplakin have delayed embryonic barrier formation and postnatal hyperkeratosis with abnormal cornified envelope structure (Sevilla *et al.*, 2007). Mice deficient in only one of these proteins do not show any major abnormalities which proves their ability to compensate a loss by each other (Aho *et al.*, 2004; Maatta *et al.*, 2001).

Eighteen different genes of the **Late Cornified Envelope (LEP)** family are located as a subcluster of EDC. Structurally they are related to SPRR proteins and are also cornified envelope precursors and have protein crosslinking functions (Marshall *et al.*, 2001). They can be divided into three groups based on homology and position within EDC. Members of two of these groups are expressed at relatively high levels in the epidermis, while the third one is expressed at low levels also in other epithelia (Jackson *et al.*, 2005).

Profillagrin is encoded by the FLG gene which serves as the main component of the keratohyalin granules within epidermal cells. During epidermal terminal differentiation the 400 kDa profillagrin polyprotein is dephosphorylated and rapidly cleaved by serine proteases to form monomeric fillagrin (37 kDa; (Rothnagel and Steinert, 1990), which binds to and condenses the keratin cytoskeleton and thereby contributes to the cell compaction process required for squam biogenesis (Sandilands *et al.*, 2009). Loss of profillagrin or fillagrin leads to a poorly formed stratum corneum (ichthyosis) which is also prone to water loss (xerosis). The “flaky tail mouse is a spontaneous mutant with dry flaky skin which express the aberrant form of profillagrin. This mutated profillagrin cannot be proteolitically processed and as a consequence flaky tail mice are deprived of functional fillagrin. They lack keratohyalin granules (Presland *et al.*, 2000) and exhbit greatly increased percutaneous antigen transfer (Fallon *et al.*, 2009).

Human genetic studies suggest that malfunction of skin barrier function as a result of decreased flagirin expression may lead to a number of human skin diseases including ichtyosis vulgaris (Smith *et al.*, 2006) and eczema (Sandilands *et al.*, 2007).

FLG gene is also a member of other EDC family genes which include **flaggirin2, trichohyalin, trichohyalin2, repetin, cornulin and hornerin**. These proteins are associated with the keratin intermediate filaments and are partially cross-linked to the cornified envelope (Segre, 2006b).

1.2 Nucleus as a centre of developmentally regulated genetic programs.

The nucleus is the site of the storage, retrieval and replication of genetic information dynamically responding to the signals from the inside and outside of the cell. All these processes are highly complex, dynamic and require coordinated action of many molecules and molecular complexes. In addition, all of them are dependent on the information contained in the genomic DNA, whose length is measured in meters, while dimensions of the nucleus is measured in micro meters. All these facts suggest that DNA and chromatin are highly compacted in three-dimensional nuclear space and is the subject of intensive investigation in recent years (Woodcock and Ghosh 2010).

The nucleus is an organelle of eukaryotic cells originating probably from archeobacteria acquired by pre-eucaryotic ancestors via endosymbiosis (Embley and Martin, 2006; Lopez-Garcia and Moreira, 2006). It is separated from the cytoplasm by a characteristic double membrane (nuclear envelope)

studded with large proteinaceus pores. A typical diploid human nucleus is a spheroid with a volume of about 500 μm^3 containing approximately 6 Gbp of genomic DNA distributed among 46 chromosomes (Carmo-Fonseca *et al.*, 1996; Handwerger and Gall, 2006). Mouse genome is slightly smaller - it comprises of 5 Gbp distributed into 40 chromosomes (Waterston *et al.*, 2002). Nucleus is usually positioned within the cell to the specific location controlled by means of interaction between the nuclear envelope (NE) and three major components of the cytoskeleton – microtubules, actin filaments and intermediate filaments (Starr, 2007).

During interphase most of the nuclear volume is filled with a chromatin consisting of the genomic DNA, histones and other proteins which can be divided into two major fractions: more relaxed and transcriptionally active euchromatin and compacted heterochromatin characterized by relatively low levels of gene expression. Genomic DNA is distributed among the chromosomes which are highly condensed and visible as a separated “thick sticks” during the metaphase and decondense in the interphase retaining their individuality and occupying spatially limited volume in the nucleus with average diameter about 2μm (Cremer and Cremer, 2001; Cremer and Cremer, 2010). Some observations suggest that nucleus also contains a structure called nuclear matrix which is believed to constitute scaffolding for nuclear suborganelles (Pederson, 2000), however its existence has not been proved so far (Woodcock and Ghosh 2010).

Chromosomes occupy distinct territories in the interphase nucleus while inter-chromosomal compartments are filled by a number of subnuclear organelles (subnuclear foci, nuclear bodies) differing remarkably with their appearance, biochemical features and functions (Cioce and Lamond, 2005; Taddei *et al.*,

2004; Tsutsui *et al.*, 2005). The most visually prominent subnuclear foci are nucleoli, however there is a number of other nuclear bodies such as nuclear speckles, Cajal bodies and PML bodies (Handwerger and Gall, 2006). Other nuclear bodies include: gems, paraspeckles, clastosomes and polycomb bodies (Spector, 2006).

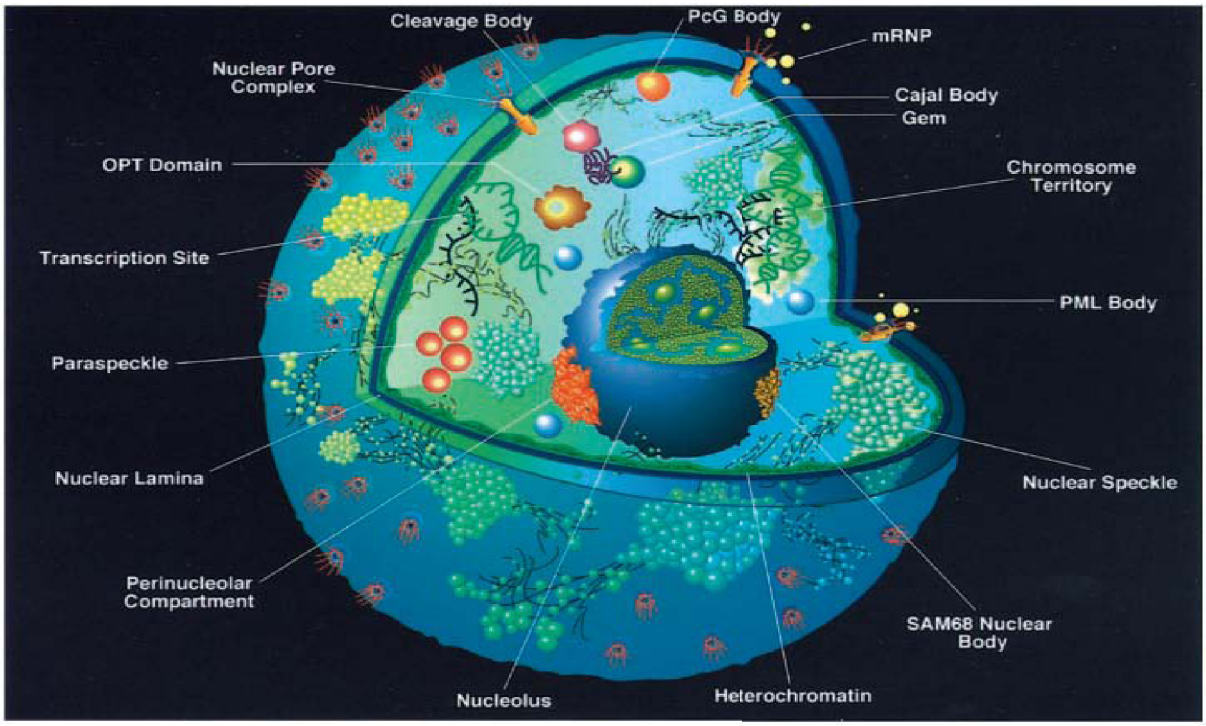

Figure 1.4 Nucleus and its suborganelles (Spector, 2003). Nucleus is a complex organelle of eukaryotic cells storing and processing genetic information, participating in ribosome biogenesis and in many other processes. It is filled with chromosome territories occupying individual spaces. Also, there are plethora of nuclear bodies differing in their properties and functions seen between the chromosome territories.

1.2.1 Nuclear size and shape

Maintaining the proper size and shape of eukaryotic cells and their nuclei is highly important for their survival. There is marked variability in the size and shape of the nuclei in different cells. Despite this variability (Umen, 2005) most

of the cells within distinct cell-types, have similar “karyoplasmic ratio” (ratio of the nuclear to cellular volume (Huber and Gerace, 2007).

Nuclear shape and size depend on the nuclear lamina and different elements of the cytoskeleton (Brandt *et al.*, 2006; Huber and Gerace, 2007; Melcer and Gruenbaum, 2006). The nuclear lamina is a network of lamin polymers and lamin-associated proteins which are present in the inner nuclear membrane. Mutations in lamins cause abnormalities in the nuclear shape and result in diseases called laminopathies (Gruenbaum *et al.*, 2005; Melcer and Gruenbaum, 2006). Lamina together with microtubules control size and shape of the nuclei but there are also other proteins involved like Kugelkern and Kurzkern which colocalize with lamins at the inner nuclear membrane and are indispensible for the proper control of nuclear shape (Brandt *et al.*, 2006).

1.2.2 Nuclear envelope (NE) separates genetic material and participates in its organization

The nuclear envelope (NE) surrounds the whole nucleus separating it from the cytoplasm and regulating the traffic of high molecular complexes. The NE contains a large number of different proteins that have been implicated in chromatin organization and gene regulation (Hetzer 2010; Wilson and Berk 2010; Akhtar and Gasser, 2007). The NE consists of two concentric lipid membranes, the inner nuclear membrane (INM) and the outer nuclear membrane (ONM). These two layers fuse in the places of nuclear pore complexes’ (NPC). NPC controls trafficking of high molecular particles to and from the nucleus. They are highly organized proteinaceus complexes comprising of 30 different proteins called nucleoporins (Hetzer; Lim and

Fahrenkrog, 2006). The lumen between two nuclear membranes referred to as perinuclear space is approximately 50 nm wide and is a continuation of the lumen of the endoplasmatic reticulum (ER).

INM and ONM interact with distinct protein structures, which is crucial for the structure and integrity of the nucleus. INM contacts the underlying nuclear lamina and regions of the chromatin and contains a set of characteristic integral proteins responsible for the interactions with the nuclear lamina. These include LEM-domain-containg LAP2, emerin or MAN1, or lamin B which is thought to target heterochromatin to some specific areas of the INM. Nuclear lamina are an important element of nuclear structure (Prunuske and Ullman, 2006; Schirmer and Gerace, 2005). They create a perinuclear meshwork of intermediate filaments (IF), however they are also dispersed throughout the nucleoplasm possibly forming a thin fibrillar network. In addition, lamina also play a role in the control of transcription, DNA replication, and signalling cascades (Taddei *et al.*, 2004). ONM ensures the proper localization of the nucleus by interactions with cytoskeltal proteins as well as with the centrosome and has similar proteins to those present in the peripheral ER, however some of them appeared to be ONM-specific (Prunuske and Ullman, 2006).

1.2.3 Nuclear Matrix– scaffold of chromatin and nuclear bodies

The nuclear matrix consists of an insoluble aggregate of many different proteins and RNA. It is defined as a structure that remains after applying DNAse I digestion followed by salt extraction. There is evidence that it has at least partially fibrillar structure. Presence of the nuclear matrix explains many observations made in different cells during replication, transcription or splicing,

however some researchers suggest that matrix is only an artifact caused by unphysiological conditions applied to the nucleus (Pederson, 2000; Woodcock and Ghosh 2010). Some researchers distinguish two different compartments in the nuclear matrix: a network-like internal nuclear matrix (INM) and a nuclear shell (or nuclear lamina) that connects INM to the inner and outer membranes (Mika and Rost, 2005; Tsutsui *et al.*, 2005). INM consists mainly intermediate filaments such as lamins, NuMa and hnRNP proteins. Nuclear matrix also plays role in chromatin organization – DNA attaches to nuclear markers structures with specific AT-rich sequences referred to as matrix attachment regions (MAR) (Anachkova *et al.*, 2005) which is mediated by specific proteins like special AT-rich binding protein 1 (Satb1) or scaffold attachment factor-B1 (Safb1).

1.2.4 Chromatin organizes DNA and is responsible for establishing transcriptional microenvironment

Genomes of the eukaryotes are packed into a nucleoprotein complex known as chromatin, which influences most of the processes involving DNA and transcription (Rando and Chang, 2009). The chromatin consists of the genomic DNA, histone and nonhistone proteins structured in the way which allow to pack DNA of the length almost 2 m into the nuclear space of the diameter usually not bigger than 10 μm. Genomic DNA is wrapped on nucleosomes which are protein complexes consisting on average of 147 bp of DNA looped in 1.7 left-handed turn around an octamer of the core histones encompassing 4 dimers: H2A, H2B, H3 and H4 (Horn and Peterson, 2006). Each histone has specific domains for histone-DNA and histone-histone interactions as well as N-terminal and C-terminal ends outstanding radially from the nucleosomal core. These

"tails" undergo many different post-translational modifications (Horn and Peterson, 2006; Rando and Chang, 2009).

The degree of the chromatin compression depends on many factors such as cell cycle phase, cell type, physiological stimuli, and it can range from the naked DNA fibre to the highly compressed chromatin of metaphase chromosomes. The structure of the chromatin on the level higher then nucleosomes has not been fully described up to now. Results of the in situ electron microscope analyses deliver surprisingly little information, and chromatin in ultrathin sections in these studies looks amorphous (Woodcock and Ghosh 2010). These observations may suggest that nucleosomes interdigitate leading to the amorphous appearance. Studies of the chromatin isolated from the nucleus or reconstituted in vitro were much more informative. Chromatin isolated from the nucleus at low ionic strength has an electron microscopic appearance of the "beads-on-a-string" structure corresponding to the histone-DNA complexes of 11 nm in diameter. In a solution of physiological salt concentration (0.15 mM KCl) chromatin forms condensed fibre of 30 nm in diameter referred as " a solenoid" or "30 nm fibre" (Carmo-Fonseca *et al.*, 1996; Horn and Peterson, 2006). Interpretation of the first electron microscopic studies of isolated compact 30-nm fibres as a simple solenoidal organization with linker DNA followed the helical trajectory is now considered as incorrect. Studies of crystallized tetranucleosomes suggested the zigzag structure with contacts between the nucleosomes 1 and 3 and between 2 and 4 (Schalch *et al.*, 2005). Computer modelling as well as studies using the technique EMANIC (EM-assisted nucleosomes interacting capture; nucleosomal arrays are lightly fixed with parafolmaldehyde, dispersed in low salt solution and the links between them

analysed) suggested 30 nm fibre as a heteromorphus structure with the zigzag arrangement interrupted by solenoidal structure (Grigoryev *et al.*, 2009).

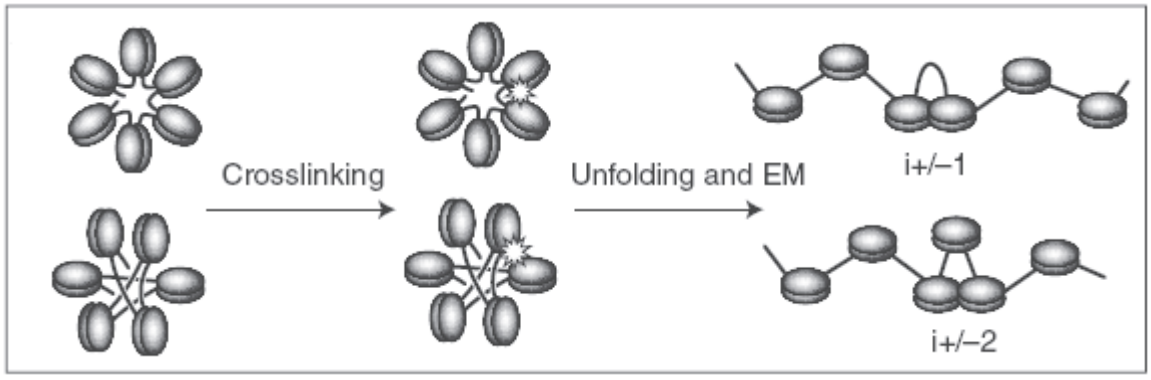

Figure 1.5. Chromatin fibre is a mix of zigzag and solenoid structure – scheme of EMANIC experiment (Woodcock and Ghosh).

The way in which chromatin is organized at the level "above the 30 nm fibre" is also not entirely understood and is described in the subchapter on chromosome territories.

Traditionally, on the basis of cytogenetic and electro-microscopic observations, chromatin is divided into heterochromatin and euchromatin (Dillon, 2004; Heitz, 1928; Horn and Peterson, 2006). However, now these terms are used more widely extending the definition of "heterochromatin" also to a silent chromatin even if it does not have other heterochromatic features. Euchromatin consists of non-folded nucleosomal fibres and is invisible under the light microscope and contains most of the transcriptionally active genes.

Heterochromatin is a part of chromatin that remains condensed, visible under the light microscope and consists of a regular nucleosome arrays (Grewal and Jia, 2007). Its main physical features are cytological visibility, condensation, compartmentalization and spreading (Craig, 2005).

The reason of the cytological identifiability of heterochromatin is probably its higher condensation compared to the euchromatin. The length of the linker region between the nucleosomes is reduced and the length of linker protected from the micrococal nuclease digestion is increased by 10 bp. It is thought that changes in nucleosomal structure are the major reason for formation of the higher order structure of the heterochromatin (Dillon, 2004). This can be divided into two parts. Constitutive heterochromatin remains in the compact state during the whole cell cycle, whereas formation of some other regions referred as "facultative heterochromatin" is dependent on the developmental regulation (for example Barr bodies in mammalian female cells) and appears only in some cell types and/or at different developmental stages (Dillon, 2004; Heitz, 1928). Most of the constitutive heterochromatin is pericentromeric and consists of tandem repeats of satellite sequences varying in size from 7 in *Drosophila* to more than 1900 found in *Arabidopsis*. This feature causes relatively uniform sequence composition which probably is significant for heterochromatin formation (Dillon, 2004).

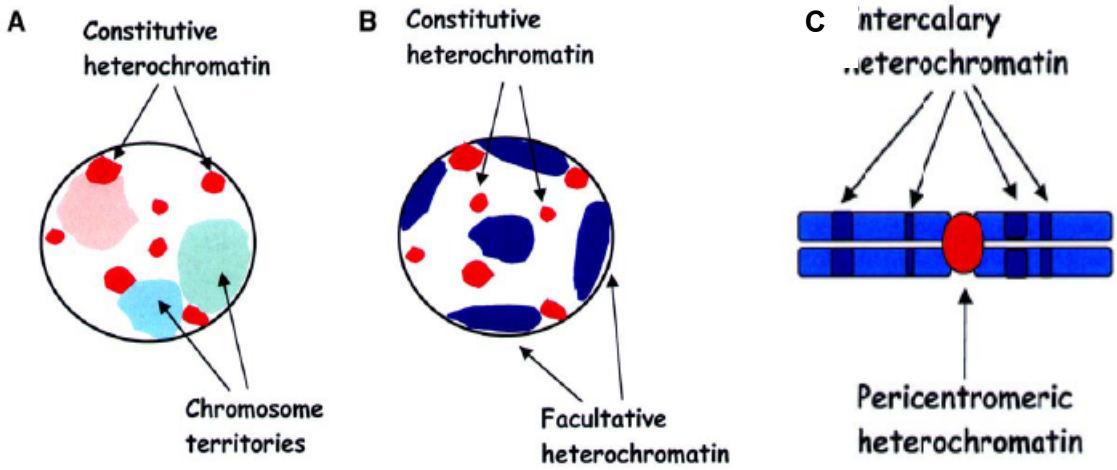

Figure 1.6 Organisation of heterochromatin in the nucleus. (A) Schematic illustration of the interphase nucleus of a mouse B cell. Condensed clusters of pericentromeric heterochromatin, each containing several centromeres. (B) In differentiated post-mitotic cells such as plasma cells and glial cells, much of the genome becomes condensed into facultative heterochromatin. The detailed organisation of this type of heterochromatin remains unknown. (C) Regions of intercalary heterochromatin have been described on the long arms of Drosophila chromosomes (Dillon, 2004).

Constitutive heterochromatin is usually constrained to an irregular rim located at the nuclear periphery and around the nucleolus and also in patches throughout the nucleoplasm (Carmo-Fonseca *et al.*, 1996).

The other difference between heterochromatin and euchromatin is that the first one shows extensive CpG methylation of DNA, both in vertebrates and plants (Gaszner and Felsenfeld, 2006).

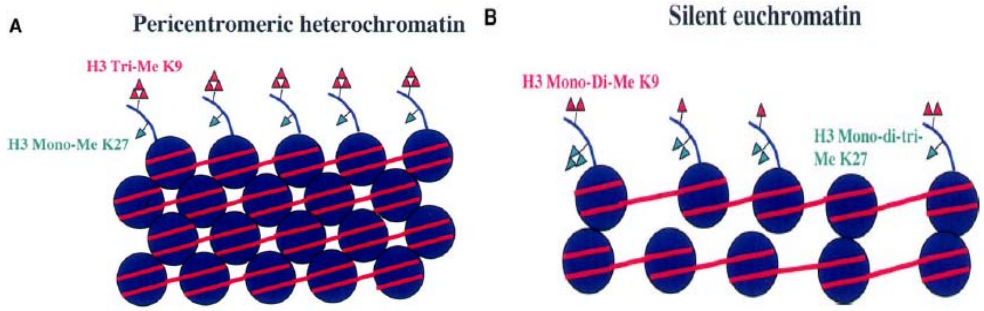

Figure 1.7 The organization of pricentromeric hetrochromatin (A) and silent euchromatin (B) Pericentromeric heterochromatin is marked by the presence of tri-methyl lysine 9 and mono-methyl lysine 27residues of histone H3. The major histone modifications in silent euchromatin are mono- and di-methyl H3 lysine 9 and mono-, di- and tri-methyl H3 lysine 27 (Dillon, 2004).

One of the major characteristics of heterochromatin is its ability to propagate in a region-specific and sequence independent manner, which serves us the additional mechanism of transcriptional gene silencing in the nucleus (Grewal and Jia, 2007). Some of the genes localized near heterochromatin sites are protected from silencing by the insulators, a specific DNA sequences recruiting euchromatin-promoting enzymes: HATs – histone acetylotransferases, H3K4 and H4R3 histone methylases (HMTs), as well as ATP-dependent chromatin - remodelling enzymes (Gaszner and Felsenfeld, 2006). Besides the linear spreading, also nonlinear, three-dimensional extension of the heterochromatin has been suggested (Branco and Pombo, 2007).

Formation of heterochromatin depends, as already mentioned, on the methylation of H3 lysines 9 by histone methyltransferase (HMT) encoded by the

Su(Var)39H gene. This specific methylation is recognized by HP1 protein that binds to methylated residues and could direct compaction of DNA by dimerization of its particles (Cheutin *et al.*, 2003; Dillon, 2004; Jenuwein, 2001; Maison and Almouzni, 2004). Lysine residues are subject to mono-, di- and tri-methylation, which involves different type of enzymes mediating these distinct methylation patterns and also some specimens of euchromatin are also methylated at H3K9. Eventually, it was shown that pericentromeric heterochromatin is enriched with H3K9 tri-methylation and H3 K27 mono-methylation (dependent on Suv39H HMTase). Compared to mono- and di-methylated H3K9 methylated species of euchromatin (dependent on G9a HMTase; Dillon, 2004; Peters *et al.*, 2003).

Heterochromatin plays an important role in the control of gene expression control as a transcriptional suppressor, as well as the genome guard protecting it from illegitimate recombination of the dispersed repetitive DNA elements and as organizer of the inter-nuclear space (Grewal and Jia, 2007). It was believed that due to the compact structure of the heterochromatin, access of transcriptional machinery to DNA is limited, resulting in silencing of gene expression. Many arguments such as huge amount of the repetitive sequences, silencing of euchromatic genes replaced into heterochromatic region or into its neighborhood also support this opinion. However, image of a heterochromatin as a stable, transcriptional inactive structure seems to be oversimplified now (Grewal and Jia, 2007; Horn and Peterson, 2006; Yasuhara and Wakimoto, 2006). Recently, a few hundreds of heterochromatic genes in Drosophila, plants and mammals have been discovered. In the case of Drosophila the gene density in heterochromatin was estimated to be six times lower compared with euchromatin. It is known so far that at least some of them are transcriptionally

active. It was estimated that heterochromatin is only 1.4 times more condensed than euchromatin (Young *et al.*, 2001) and, in contrast to initial opinions, it provides no diffusion barriers for large macromolecules, such as transcription factors (Fedorova and Zink, 2008). Up to date, evidence indicates that factors that are responsible for gene silencing and chromatin condensation in euchromatin (like HP1) protein have an opposite influence on heterochromatic genes. (Grewal and Jia, 2007; Horn and Peterson, 2006; Yasuhara and Wakimoto, 2006). It was recently shown that besides some repetitive sequences are also expressed in heterochromatin which seems to be crucial for the maintenance of heterochromatin structure (Grewal and Elgin, 2007; Grewal and Jia, 2007; Horn and Peterson, 2006).

1.2.5 Chromosomes – the largest subunits of functional genomic organization.

The whole genome is organized into separate entities - the chromosomes. Chromosomes are long linear double stranded DNA molecules linked with histones and other proteins. Their level of compaction differs depending on the cell cycle phase, GC/AT content, as well as on gene density and transcriptional activity. In metaphase, they are visible under the light microscope as separate entities because of the high level of DNA compaction. Chromosomes consist of a centromere, a place of the formation of kinetochore, which anchors the fibre of the mitotic spindle, pericentromeric area rich in repetitive sequences, arms and telomers **(Fig.1.9)**. During interphase, chromosomes are partially decondensed and except for some heterochromatin aggregates, invisible under the light microscope. Fluorescent in situ hybridization (FISH) using chromosome specific DNA probes revealed that chromosomes sustain their individuality and occupy autonomous, to high degree separate spaces in the nucleus referred as

chromosomal territories (CT) (Cremer and Cremer, 2001). Other experiments showed that not only do chromosomes preserve their individuality but also the same is true about their subdomains (Teller *et al.*, 2007).

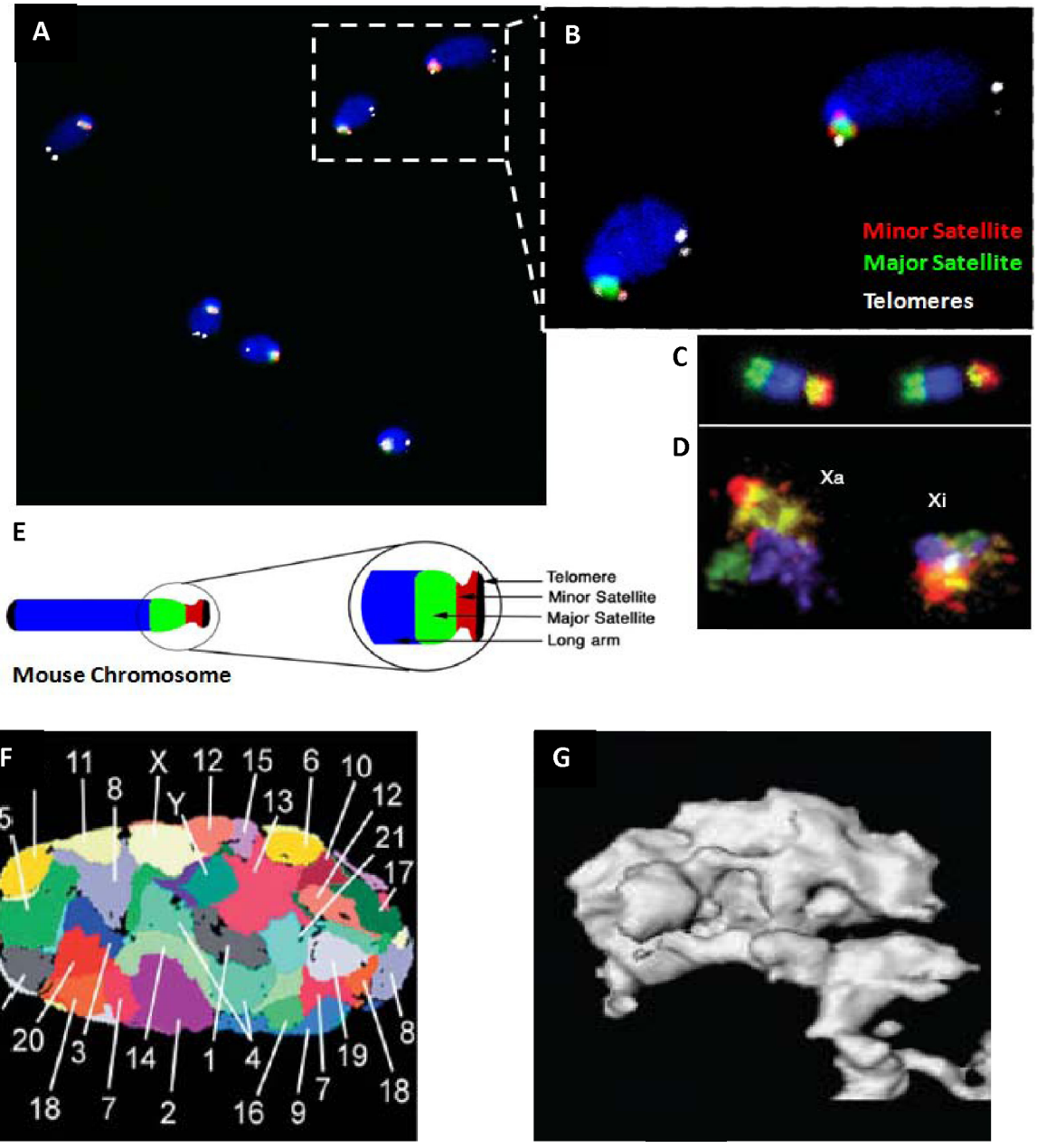

Figure 1.8 Chromosome structure in metaphase (A,B,C,E) and interphase (D,F,G). A,B,E – structure of mouse metaphase chromosomes pericentromeric repetitive sequences (Major and Minor satellite repeats) and telomeres detected by FISH; C,D – distribution of 4 different chromosome regions in human metaphase (C) and interphase (D) X chromosomes; F,G – interphase chromosome territories of human G0 fibroblast and example of single chromosome territory; interphase chromosomes occupy individual spaces within the nucleus. Their shape is irregular and may be approximated as an ellipsoid with diameter of about 2 μm (Bolzer *et al.*, 2005).

There are many open questions regarding the organization of chromosomes within the nucleus (Branco and Pombo, 2007; Spector, 2003; Taddei *et al.*,

2004). However several models, explaining some phenomena associated with chromosome territories, have been proposed: Interchromatin model (ICD), chromosome territory-interchromatin compartment model (CT-IC) and inter-chromosomal network model (ICN) (Branco and Pombo, 2007).

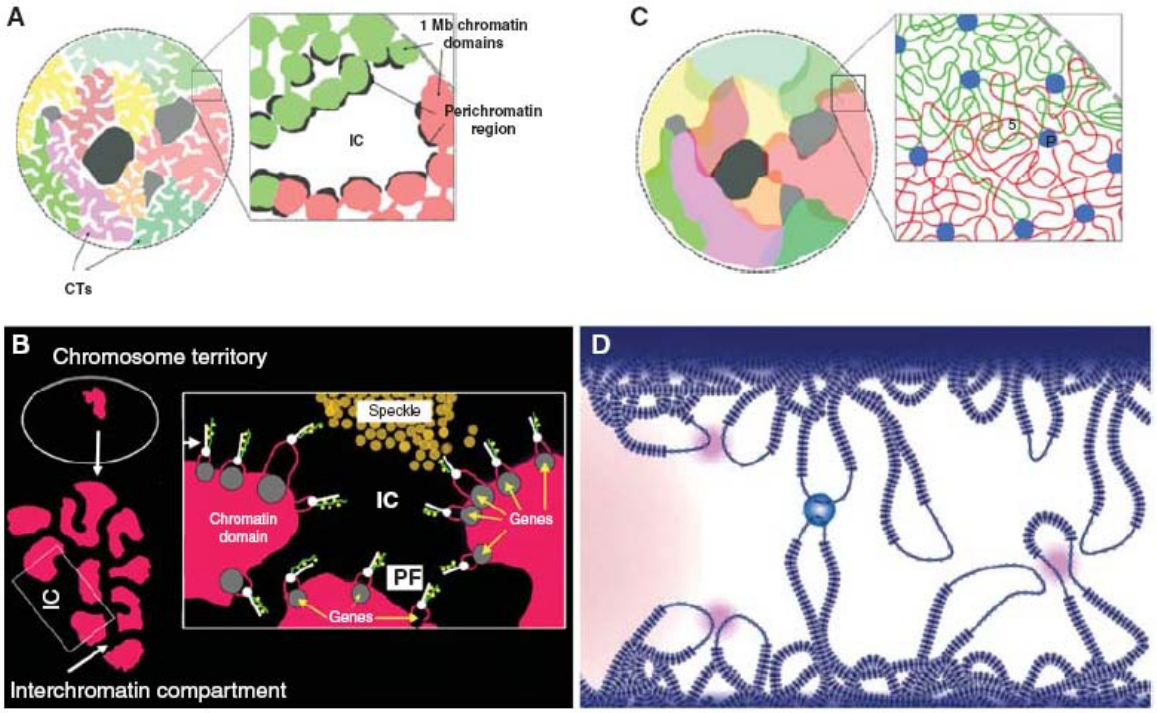

Figure 1.9 Different models explaining the distribution and organization of chromosomes within the interphase nucleus. A - interchromatin domain model (ICD) – impenetrable for high molecular mass particles chromosome territories are separated by DNA free "interchromatin domain"; B - chromosome territory – interchrimatin compartment (CT-IT) – modification of the previous model, which assumes that chromosomes are intersected by channels and the invaginations of the surface of chromosome territories; C,D - interchromosomal network model (ICM) – chromosome territory is a network occupying some particular space but intermingling with neighboring chromosome territories(Branco and Pombo, 2007).

Interchromatin domain model was proposed as a first after discovery that interphase chromosomes do not spread over the whole nucleus but occupy relatively compact individual spaces - chromosomal territories. Model was supported by observations that many active genes are localized on the surface of the chromosome territory, whereas intergenic DNA tends to cluster in its internal parts. Discovery of the genes transcribed inside of the chromosome

territories led to modification of this model, and instead CT-IT model was proposed. It was assumed that chromosome territory CT was divided into 1 Mbp domains, built up of the rosettes of small loops called “100 kbp chromatin domains”. Active genes had to be located at distal parts of this loops. So far there is no proof of existence of such structures. Recent studies did not confirm that either chromosome or even heterochromatin domains can provide diffusional barriers for large macromolecules. Three dimensional in situ hibridisation followed by confocal microscopy revealed a high level of intermingling of the chromosome territories. These findings were further confirmed by In situ hybridization followed by electron microscopy. These new discoveries led to the development of interchromosomal network model. ICM assumes that intra-chromosomal associations will favor chromosomal discreteness, whereas interchromosomal ones will favor intermingling. Chromosome territory is according to ICM a heterogeneous chromatin network of different chromatin density, GC and gene content (Branco and Pombo, 2007).

Chromosome territories exhibit nonrandom positioning in the nucleus, while patterns of their distribution are probabilistic. Several principles ruling the establishment of this pattern were discovered. First, usually larger chromosomes are located more peripherally than smaller ones (Sun *et al.*, 2000). Second, bioinformatical analysis of the full genomic sequences showed that gene clustering is rather a rule than an exemption. In particular housekeeping genes have a tendency for clustering, however examples of tissue-specific gene clusters are also known (epidermal differentiation complex is one of them) (Hurst *et al.*, 2004; Lercher *et al.*, 2002) . It was found that chromosomes with higher gene density are located more internally than the

gene-poor chromosomes. Gene richness/ poorness correlates with the GC/AT content in DNA sequences, which may also play an important role in the chromosome territory positioning. Sequencing data revealed that particular chromosomes are highly heterogenic in terms of the gene density and GC/AT content, which also leads to remarkable differences in the localization of chromosomal subregions (Costantini *et al.*, 2009; Zhang and Zhang, 2003; Zhang *et al.*, 2004). It was shown that gene-rich regions known to contain high percentage of GC pairs (which corresponds with R-bands depicted by Giemsa staining) and replicated early during S phase of the cell cycle tend to localize in the nuclear interior. Gene-poor and AT-rich subregions, replicated later during S phase (G band) usually cluster in the perinuclear or perinucleolar space. This heterogeneity leads to polarization of the structure of chromosome territory with gene-poor regions clustered at the nuclear periphery, whereas gene-rich regions are in the nuclear interior (Shopland *et al.*, 2006).

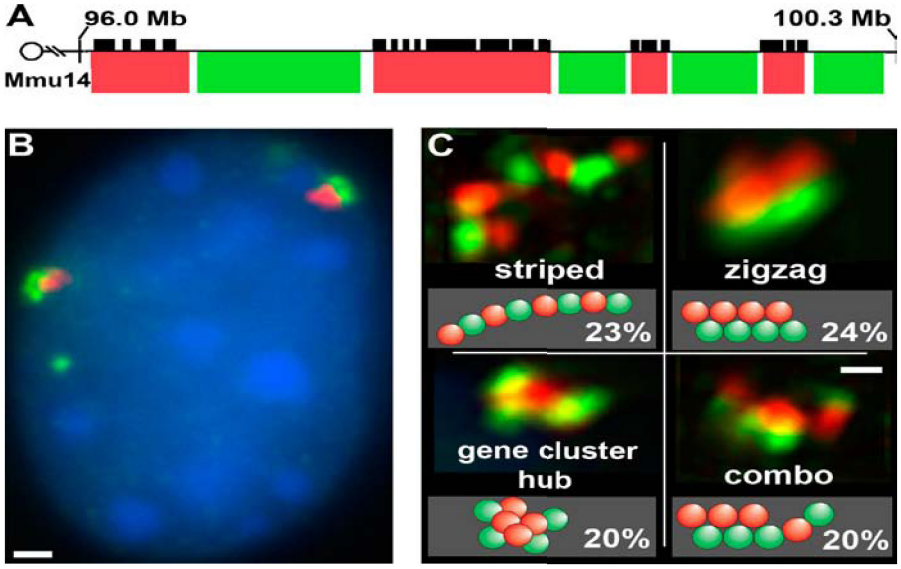

Figure 1.10 Different configurations of the region on mouse chromosome 14 comprising 4.3 Mbp (Shopland *et al.*, 2006). a) Linear model of loci b) Pool of BAC-probes containing gene clusters was labelled with rodamine (red) the other pool containing "genomic desert" was labelled by fluoresceine (green). Gene-rich regions of studied DNA tend to gather in nuclear interior oppositely to gene poor regions clustering at nuclear periphery c) different chromatin configurations.

1.2.6 Nucleolus is a site of the ribosome synthesizes and also plays an important role in chromatin organization

Nucleolus is a well-defined structure of the nucleus, where ribosomal RNAs (rRNAs) are synthesized, processed and assembled with ribosomal proteins (Hernandez-Verdun, 2006). As other nuclear suborganelles, it is not surrounded by the lipid membrane but contrary to them nucleoli have a unique density and robust structure which makes them one of the easily visualized subnuclear structures to visualize and purify (Lam *et al.*, 2005). Nucleolar size and structure are strongly correlated with rDNA transcription and reflect metabolic activity of the cell. Cells with high intensity of translation growing cells have larger nucleoli (Derenzini *et al.*, 2009; Hernandez-Verdun, 2006; McKeown and Shaw, 2009), which is also true for rapidly proliferating cancer cells (Derenzini *et al.*, 2009; Derenzini *et al.*, 1998).

Despite its robustness, the nucleolus is a very dynamic structure with a high rate of protein trafficking which was shown with FRET experiments. Its size and structure, as well their number depend on the actual metabolic state of the cell, as well as on the cell cycle (Hernandez-Verdun, 2006).

Nucleoli are disintegrated during mitosis and reconstitute around specific DNA loci referred as Nucleolar Organising Region (NOR) after the cell division. NORs consists of multiple copies of rRNA genes (rDNA coding for 18S, 5.8S, 28S, controlled by common promoter) arranged in head to tail tandem repeats (Hernandez-Verdun, 2006; Lam *et al.*, 2005). Usually, only part of the NORs are active and only part of the rRNA genes in each active NOR participates in transcription (McKeown and Shaw, 2009). Studies in HELA and primary LEP cells showed that there are some cell-type specific differences in the distribution

of the competent and non-competent NORs among the specific NOR-bearing chromosomes (Smirnov *et al.*, 2006).

Number of rDNA loci varies among the species, among the distinct cell populations as well as among the individuals, so does the number of rDNA genes, which may underlie phenotypic variability (Veiko *et al.*, 2007). In mice, number of rDNA genes differ from 105 to 310 depending on the strain and individual (Veiko *et al.*, 2007), and it was estimated to be about 230 copies for C57Bl/6J mice (Gaubatz *et al.*, 1976; Gaubatz and Cutler, 1978).

Different organisms have a different number of NOR loci: from 1 in yeast up to 10 in humans (Hernandez-Verdun *et al.* 2006). Laboratory strains of mice have rDNA clusters within the centromeric regions of chromosomes 12, 15, 16, 18 and 19, however some wild-type Asian strains have them also on several other chromosomes (Dev *et al.*, 1977; Ito *et al.*, 2008; Kurihara *et al.*, 1994). Due to the linear proximity, centromeres of NOR-bearing chromosomes associate with nucleoli, moreover also chromosomes devoid of rRNA genes also have their centromeres associated with the nucleolus at the frequency more than it is expected from a random distribution (Carvalho *et al.*, 2001). The number of nucleoli varies, but usually there are 1 up to 6 nucleoli in the nucleus. Nucleoli assemble only around active NORs and additionally have a tendency to fuse (Hernandez-Verdun, 2006; McKeown and Shaw, 2009; Sullivan *et al.*, 2001).

During the cell cycle, the multiple small nucleoli around invidual active NORs fuse into one or a few larger nucleoli (nucleolar fusion Anastassova-Kristeva, 1977). There are two main hypothesis with regards to mechanism of the nucleolar fusion. The first hypothesis assumes that nucleoli have a tendency to merge and non active NORs would be mainly outside of the nucleolus. The

second hypothesis explains fusion as an outcome of intrinsic merge tendency of the NOR bearing chromosomes. Experimental data support the second hypothesis due to the fact that most inactive NORs are associated with the nucleolus, while fusion is an effect of the combined merge tendencies of NOR bearing chromosomes and nucleoli (Sullivan *et al.*, 2001).

Some NORs are mostly inactive and can be found outside of the nucleolus (Weipoltshammer *et al.*, 1996), however most of them, including non-active NORs, are located inside of the nucleolus (Kalmarova *et al.*, 2007). Interestingly, certain intranucleolar NORs (supposedly non-competent) are situated on elongated chromatin protrusions which connect nucleoli with chromosome territories located distantly from the nucleoli (Kalmarova *et al.*, 2007). Studies on replicating cells revealed that associations of the distinct NORs (and corresponding chromosomes) with nucleoli can be conserved through the mitosis (Kalmarova *et al.*, 2008).

It was shown by electron microscopy that nucleoli are usually associated with heterochromatin (Testillano *et al.*, 1991) and the nucleolar surrounding is believed to promote gene silencing. In addition, loci at nucleoli or nucleolar periphery are significantly less mobile, while disruption of the nucleoli increases the mobility of nucleolar associated loci (Chubb *et al.*, 2002).

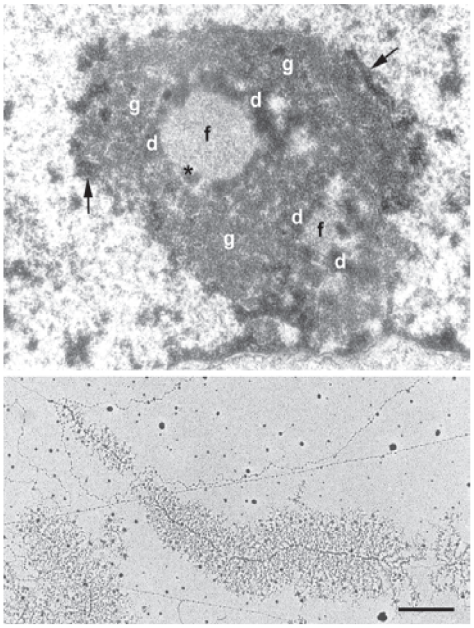

Figure 1.11 Nucleolus. Electron micrograph of a nucleolus fixed in situ and spread of the nucleolar chromatin from mouse cells. (a) Thin-sectioned nucleolus from a mouse cell. Black arrows indicate perinucleolar condensed chromatin, and the asterisk shows dense fibrillar components (DFCs) clump in fibrillar centers (FCs). f, d and g correspondto FC, DFC and granular components (GCs), respectively. (b) Spread CT (Christmas tree structure, 4 μm long) from a mouse cell is shown at the same magnification as (a) (Raska, 2003).

The most important function of the nucleolus is ribosomal RNA (rRNA) synthesis, processing and assembly of the ribosomal subunits. In metabolically active somatic cells rRNA synthesis accounts for about one-half of the total cellular RNA production, however most of the r-genes are inactive (Raska *et al.*, 2006).

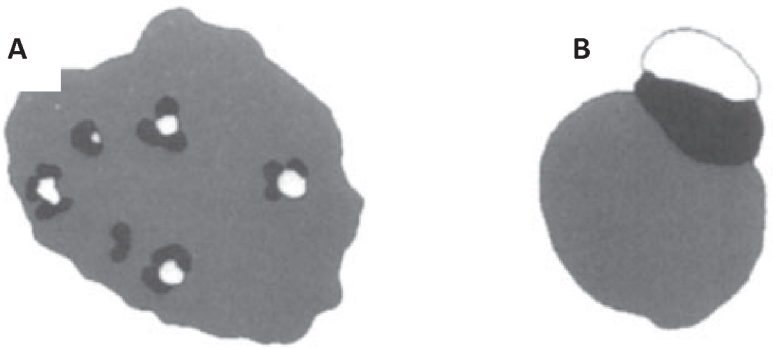

Figure 1.12 Nucleoli from cells of different degree of transcriptional activity. Diagrams of ultrastructural features observed in EM thin sections. A) "Typical" nucleolus from a human cultured fibroblast B) Typically segregated pattern of inactive nucleolus(Raska, 2003).

Besides of the RNA processing and ribosomal subunits assembly, nucleolus is thought also to have many “non-canonical functions”, such as virus infection control, maturation of non-nucleolar RNAs or RNPs, senescence and regulation of the telomerase function, regulation of the cell cycle, tumour suppressor activity, cell stress sensing and signalling (Raska *et al.*, 2006). Nucleolus also serves as a domain of sequestration of molecules that normally operate outside this organelle, mainly in the nucleoplasm (i.e. phosphatase cdc 14) (Sirri *et al.*, 2008).

1.2.7 Centromeric clusters and their role in tethering chromosomes together in the interphase nucleus

Centromeres frequently associate together and form clusters, which may be considered as nuclear bodies having their own individuality and significance. As already mentioned, centromeres are heterochromatic regions of DNA to which the mitotic spindle attaches during mitosis (Aleixandre *et al.*, 1987; Choo, 2001). They consist mainly of different types of DNA repeats and may be detected by a pancentromeric FISH probe which hybridises to α-satellite repeats located in the central centromere domain of all human chromosomes and to major satellite repeats of mouse chromosomes (Mitchell *et al.*, 1985). It is known that centromeres tends to cluster and usually the number of pancentromeric signals within the cell is much lower versus the total number of chromosomes (Alcobia *et al.*, 2000; Haaf and Schmid, 1991). Centromere merging may have a significance for the nuclear structure and most probably for the regulation of transcription of some loci.

There are several studies investigating the distribution and clustering of centromeres in the interphase nuclei. In human and mouse quiescent

lymphocyte nuclei (G0), most centromeres were found at the nuclear periphery (Weierich *et al.*, 2003). Centromeres in many cycling cells behave according to the following scheme: many of the centromeres are located in the nuclear interior during the early G1. In late G1 and early S phase, centromeres migrate to the nuclear periphery and fuse into clusters. In late S and G2, centromeres partially de-cluster and move towards the nuclear interior. Peripheral location and clustering of centromeres are the most pronounced in non-cycling, quiescent cells (G0) and cells which are terminally differentiated (Solovei *et al.*, 2004b).

It was shown that peripheral location of centromeric clusters is determined at least partially, by the direct or indirect interactions with the nuclear lamina. Protein LBR is an example of such interactions. It binds to the nuclear lamina and can bind directly to DNA and also protein HP1 is associated - histone H3 methylated on Lysine 9 which is a heterochromatic marker (Gruenbaum *et al.*, 2005; Hoffmann *et al.*, 2002; Holmer and Worman, 2001). Fibroblasts from Hutchinson–Gilford progeria syndrome (HGPS) patients which is caused by mutation in lamin A (LMNA) are almost entirely deprived of peripheral heterochromatin (Goldman *et al.*, 2004) similarly to LMNA-knockout mice (Nikolova *et al.*, 2004) which confirms importance of lamin-hetrochromatic interactions.

It is also known that in quiescent normal human hematopoietic cells and primary quiescent fibroblasts that centromere clustering is not random and that it is cell type specific. Different combinations of the probes specific to particular centromeres showed that some of centromeres are clustered together in more than 60% of cells. This chromosomes turned out to be NOR bearing which

could explain their association, but there were also striking associations of centromeres which did not contain a NOR region and were found together in 56% of peripheral blood monocytes (Haaf and Schmid, 1991).

Another study investigated the association of centromeric clusters and nucleoli in postmitotic Purkinje Cells. Specific patterns of these associations were observed to be dependent on the level of cell maturation. In newborn mice the relative volumes of heterochromatin associated with nucleoli and nuclear border were equal. However, during maturation the amount of the clusters associated with nucleolus increased up to 84 %. In addition, the number of clusters decreased from 7.6 to 5.2, as well as the number of nucleoli decreased and they changed their positions from peripheral to more internal (Solovei *et al.*, 2004a).

1.2.8 Nuclear Speckles (NS) as facilitators of splicing

Nuclear speckles, referred also as “splicing speckles”, “domains SC35” or “splicing factors compartments” (SFCs), are nuclear bodies distributed in between the chromosome territories and are enriched in splicing factors. They appear as a structures of irregular shape containing high concentrations of the splicing snRNPs as well as other splicing-related proteins such as poly-A^+ RNA and also RNA polymerase II. Speckles were recognized under electron microscope as a Interchromatin Granule Clusters (IGC) and are defined as a IGC containing splicing-factors (Lamond and Spector, 2003). They are often associated with paraspecles (Xie *et al.*, 2006).

Normally, 25-50 speckles can be observed in the mammalian interphase nucleus (Lamond and Spector, 2003). Their size ranges from one to several micrometers and they are composed of 20-25 nm granules connected by a thin

fibril, which results in a beaded chain appearance. Speckles occupy approximately 5-10% of the nucleoplasmic volume (Xie *et al.*, 2006). According to the electron microscopy speckles are located in the regions of the nucleoplasm that contain little or no DNA (Lamond and Spector, 2003). In contrast to to nucleolus, they do not form assembly around specific chromatin loci, however they are often found closely located to the highly active transcription sites. In mammalian cells, the intracellular localization, composition and shape of speckles respond to changes in mRNA transcription and protein phosphorylation (Handwerger and Gall, 2006). With the decrease of transcription, speckles get enlarged and show a rounded shape (Xie *et al.*, 2006).

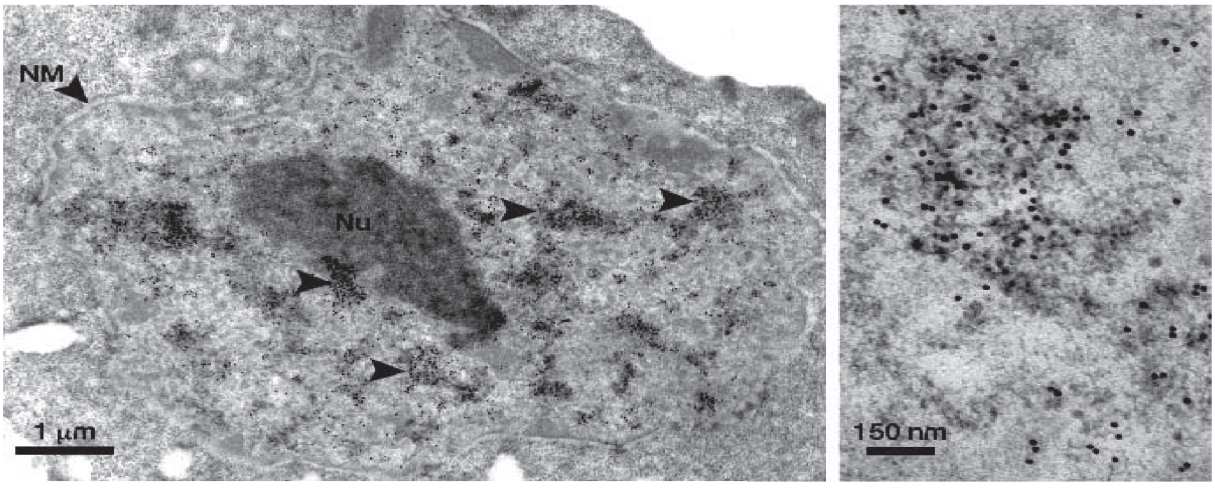

Figure 1.13 Speckles: Immuno-electron microscopic localization of pre-mRNA splicing factors. Splicing factors localize to interchromatin granule clusters (IGCs/speckles; left panel, arrowheads) and perichromatin fibrils (transcription sites). IGCs are composed of a series of particles measuring 20-25 nm in diameter that are connected in places by a thin fibril, resulting in a bead chain appearence (right panel). Sections are immunolabelled with 3C5 antibody, which recognizes the SR family of pre-mRNA splicing factors, and 15-nm gold-conjugated secondary antibody. NM, nuclear membrane; Nu, nucleolus (Xie *et al.*, 2006).

Speckles contain many proteins involved in splicing like splicing factors, transcription factors, 3'-end RNA-processing factors, the eucaryotic translation factor eIF4E, protein involved in translational inhibitions and some structural

proteins (Lamond and Spector, 2003). Also, there are several kinases (CLK/STY, PRP4 or PSKH1) and phosphatases (protein phosphatase 1;PP1) that can phosphorylate or dephosphorylate the components of the splicing machinery in speckles. Some of this particles have very tentative relationship to the domain structure like ASF/SF2, the other ones like SC35 seem to provide its structural component (however the signal obtained from anti-SC35 antibodies probably depicts only the core of the speckles) (Hall *et al.*, 2006). Speckles also contain a population of the serine-2-phosphorylated form of the RNA polymrase II (Pol II), however they are not enriched in this molecule and transcription does not take place within this nuclear suborganelle (Hall *et al.*, 2006; Xie *et al.*, 2006). For some of the speckle components amino acid targeting sequence has been indentified – the arginine/serine rich domain (RS domain). Additionally, a population of poly(A)$^+$RNA has been loclized near the speckles. It is not known whether these RNAs encode proteins or represent non-coding RNAs. The amount of splicing factors in speckles exceeds 5-10 fold their diffusive nucleoplasmic distribution, which allows to visualize them by immunofluorescence by using anti-splicing-factors antibodies (i.e. Y12, SC35) (Lamond and Spector, 2003).

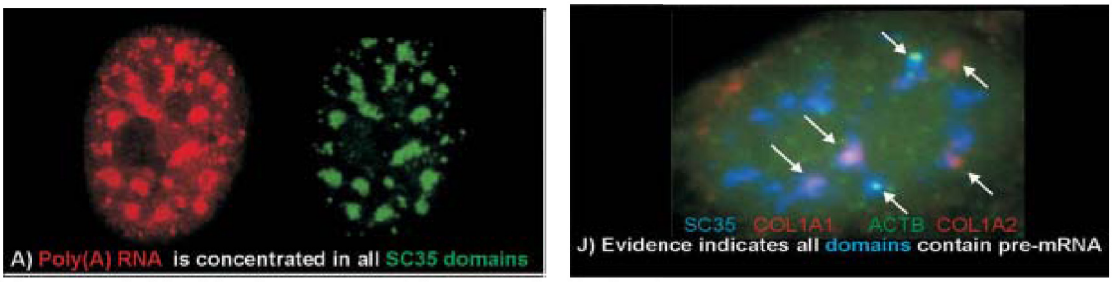

Figure 1.14 Nuclear speckles and their RNA visualized by fluorescent microscopy (Lamond and Spector, 2003). A) Comparison of the distribution of Poly(A$^+$) RNA and SC35 domains B) Colocalization of SC35 domains and the mRNAs of collagen 1A1 (COL1A1), collagen 1A2 (COL1A2) and beta actin (ACTB))

Speckles are thought to localize at the functional centre of a local euchromatic neighborhood, around which many active genes tends to cluster (Hall *et al.*, 2006). However some actively expressed genes do not require close proximity of speckles. Clustering of active genes near speckles may be caused by nucleation by splicing factors associated with the gene being transcribed. Presence of unspliced mRNA and its further accumulation upon splicing inhibition implies that they are involved in gene expression and splicing of pre-mRNA for which it is not completed cotranscriptionally. Additionally presence of the Ser^2P pol II, whose CTD domain is known to be required for splicing and to promote assembly of spliceosomes, support this opinion (Xie *et al.*, 2006). The fact that most of the splicing in speckles occurs at the outer edge of the domain and that localization of various factors implicated in mRNA export (REF/Aly, breast cancer linked protein MLN51) have been reported within the domain suggests that postsplicing steps linked to screening for defective transcripts and export could also take place there (Hall *et al.*, 2006). Uridine labelling studies showed that concentration of splicing factors within speckles is in great excess to splicing factors bound to even the most abundant individual pre-mRNA found there. This finding led to the hypothesis that the concentration of various mRNA metabolic factors in domains facilitates a rapid recycling and/or reassembly of macromolecular complexes required for efficient expression of highly active genes (Hall *et al.*, 2006).

1.2.9 Other nuclear bodies

There is a set of other nuclear bodies whose functions in the nucleus has been to some degrees recognised. Some of them are described below.

Cajal bodies referred to also as coiled bodies are ubiquitous subnuclear organells that occur both free in the nucleoplasm and are physically associated with histones and snRNA gene loci. Gems are in many ways similar to CBs and some scientists suggest that they are just another manifestation of Cajal Bodies (Matera and Frey, 1998). CBs were firstly described in 1903 by Ramon y Cajal as a “nucleolar accessory bodies” due to their frequent association with nucleolar periphery in neurons (Cajal, 1903; Cioce and Lamond, 2005). Both nuclear bodies seem to be a storage and maturation places of different splicing factors and are possibly involved in regulation of gene expression.

Gems or Gemini bodies are nuclear structures that have size and shape similar to those of CBs, containing a high concentrations of SMN protein (Matera and Frey, 1998) and associated factor Gemin2. SMN is present in cytoplasm and nucleus where it is highly enriched in Gems. Depletion of SMN by means of the RNAi in living HeLa PV cells lead to the disappearance of Gems, which suggests tat SMN is their main building block, however not in all cells expressing SMN one can detect gems (Feng *et al.*, 2005; Gubitz *et al.*, 2004).

*Promyelocytic leukaemia (*PML) *nuclear bodies* referred also as a Krener bodies or nuclear domain 10 (ND 10) are proteinaceous structure tightly bound to the nuclear matrix and one can often find them juxtaposed to other nuclear bodies like splicing speckles, gems and Cajal Bodies (Bernardi and Pandolfi, 2007; Dellaire and Bazett-Jones, 2004). They are spherical or ring-shaped with little

mass of protein inside. NBs are probably involved in many different cellular processes including gene transcription regulation, apoptosis or antiviral response, however they may be also only a storage place for excessive amount of some proteins(Bernardi and Pandolfi, 2007). The number of PML bodies varies from 3 to 30, but on average is 10 (Nuclear Domain 10 - origin of their name), and their size range from 0.3 μm to 1 μm in diameter. Similarly to other nuclear bodies their number and size change significantly during the cell cycle. There are few PML NBs in G_0 but their number increases during G_1 and is maximal in G_2. Besides difference of the number of PML NBs related to cell cycle, there are also difference responding to cell and tissue type. For example, there are remarkable changes of the number of these structures in different prostate compartments (Dundr and Mistel)2010).

Paraspeckles are a distinct class of nuclear bodies recognized as a discrete foci in the interchromatin nucleoplasmic space containing Paraspeckle Protein 1 (PSP1), Paraspeckle Protein 2 (PSP2) and p54/nrb (Fox *et al.*, 2002; Lamond and Sleeman, 2003; Lamond and Spector, 2003). They may be involved in gene expression regulation and splicing. Typically 10-20 paraspeckles are present in the interchromatin nucleoplasmic space in all analyzed human cells. Their distribution seems to be non-random therefore they probably are associated with certain chromatin domains. Paraspeckles resemble splicing speckles, to which they are often located adjacent, but do not contain snRNPs or protein splicing factors (Fox *et al.*, 2002).

Polycomb bodies (PcG) is a prominent subnuclear organelle containing proteins belonging to polycomb repressive complex 1 (PGC1) involved in gene repression (Hernandez-Munoz *et al.*, 2005). PcGs are of a round or irregular

shape and size of 0.3 – 1 μm localized in the neighborhood of heterochromatin. Usually one can be found 12 to 16 PcGs, larger of them are found near the centromeres. They seems to be non randomly distributed. Unlike the other nuclear bodies polycomb bodies remain stable associated with its loci throughout mitosis, which may be responsible for the inheritance of gene repression among distinct cells (Saurin *et al.*, 1998). They can be detected by antibodies against Ring1, Bmi1 or Pc2 proteins (Spector, 2006).

1.3 Levels of epigenetic regulation of gene expression.

Chromatin can be divided into two basic compartments: relatively decondensed euchromatin which tends to be located in internal parts of the nucleus and compact heterochromatin which mostly gathers in the proximity of nuclear envelope and the nucleolus. Euchromatin is thought to be transcriptionally active compared to heterochromatin, however this is not true for all genes and there are many exemptions out of this rule. The current view regarding this euchromatin/ heterochromatin issue is that the local "transcriptional environment" is favorable for expression of some set of genes whereas repress the others (Fedorova and Zink, 2008).

1.3.1 DNA methylation and hydroxymethylation

DNA methylation in plants and vertebrates is a post-replication modification resulting in adding the methyl group at the C5 position of cytosine to form 5-methylthytocyne (5mC). In vertebrates, this modification occurs predominantly at CpG dinucleotides (Razin and Kantor, 2005; Rottach *et al.*, 2009).

Approximately 60-70% of CpG sites are methylated in the mammalian genome. Exceptions are represented by a relatively short regions with high CpG density called CpG islands mainly located in the promoters and first exons of many housekeeping genes (Rottach *et al.*, 2009). CpG sites are often differentially methylated in a cell and tissue specific fashion at the gene regulatory regions beyond the proximal promoters, and, in particularly in recently discovered CpG island shores, located at about 2 kb from the transcription start sites or even further (Irizarry *et al.*, 2009). DNA methylation is usually associated with gene repression and inheritable cell specific pattern of this modification is the best characterized truly epigenetic mechanism regulation of gene expression (Klose and Bird, 2006). DNA methylation is catalyzed by DNA methyltranfarases (Dnmts). In mammals Dnmt1 is the major maintenance methyltransferase that methylates cytosine within hemi-methylated CpG sites after DNA replication (Pradhan and Esteve, 2003). Such maintenance modification is the major mechanism of epigenetic inheritance of cell specific DNA methylation. Importantly, the DNA methylation pattern is significantly remodelled during specific developmental stages (in germ cells and pre-implantation embryos) (Reik *et al.*, 2001). Dnmt3a and Dnmt3b are the major vertebrate de novo DNA methylases (Goll and Bestor, 2005; Rottach *et al.*, 2009). DNA methylation patterns are also changed during differentiation of adult somatic cells and it is important epigenetic mechanisms in establishing gene specific programs driving tissue development and homeostasis (Fouse *et al.*, 2008; Meissner *et al.*, 2008; Mohn *et al.*, 2008). Moreover, the defects in maintaining the appropriate cell-type-specific DNA methylation status are associated with different diseases, including cancer. However, our knowledge of mechanisms controlling DNA

methylation remodelling and their specific role in gene expression remains very limited.

DNA methylation could repress gene expression through inhibiting some transcription factor binding to DNA (Bird, 2002). But such mechanisms are not generally employed (Kass *et al.*, 1997). Instead, methylated DNA is recognized by methyl-DNA binding proteins that target repressive chromatin remodelling complexes to the methylated genome regions (Jaenisch and Bird, 2003; Rottach *et al.*, 2009). Interestingly, DNA methylation is required for induction of the subset of C/EBPα target genes by creating new binding sites from half-CRE sequences for this transcription factor (Rishi *et al.*, 2010), thus demonstrating its role in activation of gene expression.

The sensitivity of the keratinocyte gene expression program to the changes in the global DNA methylation level has been earlier demonstrated by using DNA methyltransferase inhibitor 5-aza-cytidine (Elder and Zhao, 2002b). Paul Khavari lab has recently demonstrated the essential role of the DNMT1 in maintenance of the gene expression status in the epidermal progenitor cells and the epidermal tissue renewing using regenerated human skin produced from DNMT1 deficient keratinocytes and transplanted onto the immuno-deficient mice (Sen *et al.*, 2010b), severe defects in cell proliferation and caused their spurious differentiation and ultimately resulted in loss of the tissue self-renewal (Sen *et al.*, 2010b). Importantly, analysis of changes in gene expression program after DNMT1 depletion in epidermal progenitor cells showed induction of genes associated with cell cycle arrest and epidermal differentiation.

The hydroxylation of the 5 methyl-cytosine in DNA into 5-hydroxymethylcytosine (5hymC) by TET proteins has recently been demonstrated in vitro and in vivo

(Ito *et al.*, 2010; Tahiliani *et al.*, 2009). 5hydroxymethylcytosine was identified in the DNA of mouse embryonic cells (Ito *et al.*, 2010), as well as in Purkininje neurons (Kriaucionis and Heintz, 2009) and other somatic cells (Szwagierczak *et al.*, 2010). DNA hydroxymethylation has distinct gene regulatory properties from the DNA methylation which remain mainly unknown (Tahiliani *et al.*, 2009). Moreover, hydroxylation of 5mC within DNA could lead to its rapid conversion into non-modified C and remodelling of the DNA methylation patterns (Ito *et al.*, 2010). It would be interesting to explore a potential role of DNA hydroxymethylation and TET proteins in the control of gene expression in the epithelial progenitor cells during skin development and renewal.

1.3.2 Histone modifications

Histone proteins may be subject to methylation, phosphorylation, ubiquination and ADP-ribosylation of particular amino acid residues (Dillon, 2004; Shilatifard, 2006). Significance of these markings has been recognized only partially. Additionally histones have different variants which are in part cell type specific and also affect the functional properties of chromatin. Modifications of histones are referred sometimes as the “histone code” because some of them encode instructions for efector proteins or change histone properties influencing in this way chromatin structure. Histone postsynthetic modifications may be devided into three categories – those which create binding sites for other proteins, those which alter the charge on the histone and some modifications seem not to have any functional meaning being only a trace after the presence of enzymatic complex. An example of modification which establishes binding site is the methylation of H3 at lysine 9 which creates the binding site for the protein HP1 associated with heterochromatization. Histones associated with active

chromatin are in many cases hyperacetylated and because of that have reduced positive charge on them (i.e. acetylation of H4 at lysine 16). Charge on the histone decides on the strength and extent of the interaction with DNA and lowered positive charge causes weaker association and less compact chromatin structure. In silent pericentromatic chromatin histones H3 and H4 are relatively underacetylated compared to euchromatin. So far more than 100 different histone modifications have been described and many of them correlate with transcription or transcriptional repression, even though they do not necessarily have functional meaning. Trimethylation of H3 at lysine 4 in yeast is an example. H3K4 is methylated by the enzyme Set1p which is associated with initiating from of RNA polymerase phosphorylated on the Serine 5. H3K4me3 is typically present at 5' ends of transcribed genes, however elimination of H3K4me3 by deletion of SET1 is well tolerated by yeats. Another factor affecting chromatin structure is nucleosomes positioning. Growing evidence suggests that nucleosomes at least in some part of the genome are positioned in DNA sequence specific manner. There are sequences which promote Nucleosome Free Regions (NFR). NFRs are present usually in enhancers and at the start site of transcription.

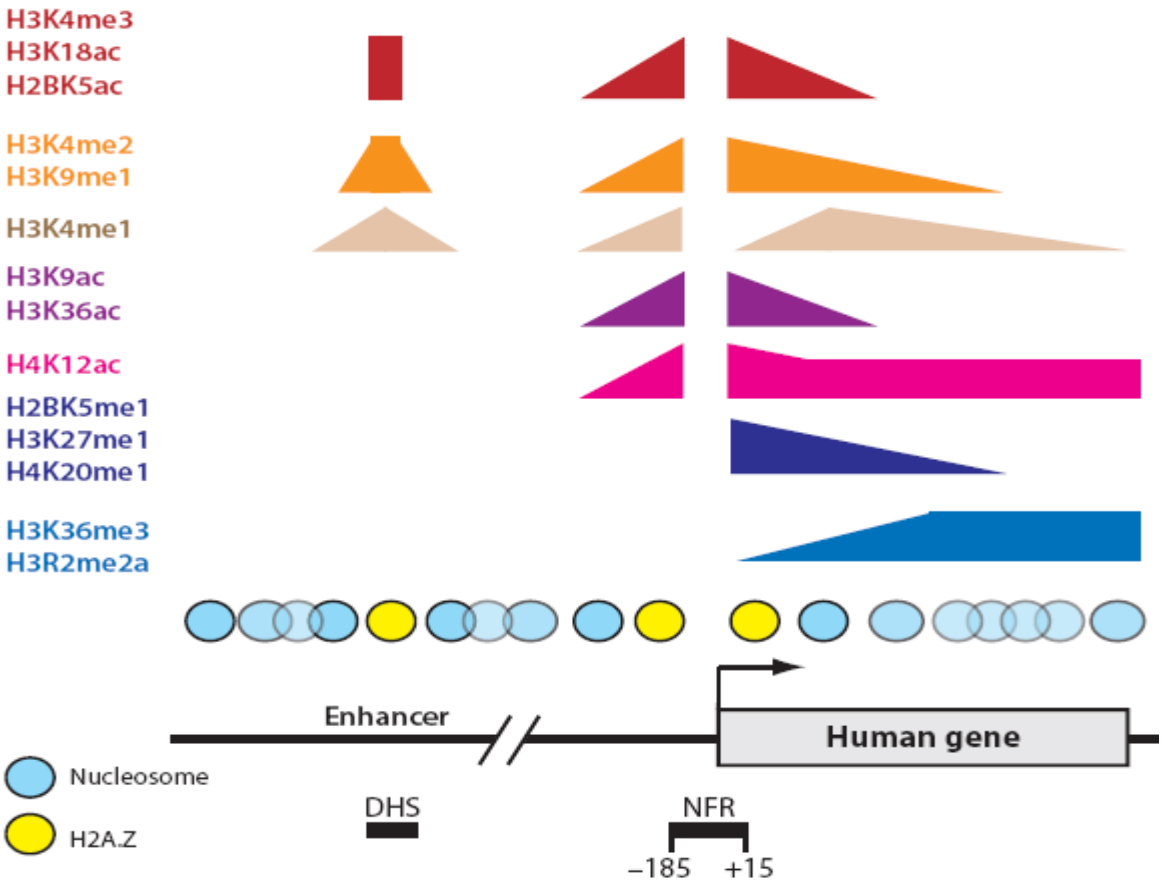

Figure 1.15. Typical epigenetical marks of active mammalian promoter (Rando and Chang, 2009). Explanation in text.

1.3.3 ATP-dependent chromatin remodelling

ATP-dependent chromatin remodelling complexes alter DNA-histone interactions using an energy of the ATP hydrolysis (Clapier and Cairns, 2009; de la Serna *et al.*, 2006). Their activity could lead to the changes of the nucleosome translational positioning and/or nucleosome conformation and could also facilitate eviction and deposition of the nucleosomes. The molecular mechanisms underlying the ATP-dependent chromatin remodelling are a subject of intensive investigations using different chromatin substrates in cell-free systems (Bowman, 2010; Gangaraju and Bartholomew, 2007), while analysis of these mechanisms in vivo remains technologically very challenging. ATP-dependent chromatin remodelling is mediated by multi-subunit complexes

containing core ATPase. The additional subunits modulate the activity of the core ATPase, facilitate the targeting of the complexes to the specific genomic regions and may interact with other proteins (Hogan and Varga-Weisz, 2007). The chromatin remodelling enzymes belong to the SNF2 superfamily of ATP-dependent ATPases and all have a helicase-like domain. Based on the presence of additional domains, are divided into several groups. The best studied remodellers belong to the SWI/SNF, ISWI and CHD groups (Clapier and Cairns, 2009; de la Serna *et al.*, 2006).

ATPases of the SWI/SNF group contain the bromo-domain which binds to acetylated histone tails. In mammals, SWI/SNF group ATPases include Brg1 (also known as Smarca4 and Snf2β) and closely related Brm protein (also known as Smarca 2 and Snf2α Tang *et al.*, 2010). In addition to Brg1 or Brm, mammalian SWI/SNF complexes contain other subunits called BAFs. Chromatin remodelling by SWI/SNF complexes is required for gene activation and repression depending on contest (Tang *et al.*, 2010). The genetics studies demonstrated a crucial role of Brg1 in early embryonic development, as well as in organogenesis including skin morphogenesis (de la Serna *et al.*, 2006; Indra *et al.*, 2005), while Brm appeared to be mostly dispensable (Reyes *et al.*, 1998).

The essential role of Brg1 in regulation of gene expression in the epidermis has been demonstrated by tissue-specific inactivation of this gene in mice (Indra *et al.*, 2005). Brg1 deficiency did not cause severe defects in proliferation or early keratinocyte differentiation, but led to defects in late stages of keratinocye differentiation leading to formation of a non-functional barrier.

ATP-dependent chromatin remodellers from the CHD group contain 2 chromo-domains in their N-terminal part (Marfella and Imbalzano, 2007). These

domains could directly bind to DNA, RNA and methylated histone H3. The remodellers of CHD group are further sub-divided into several subgroups based on the presence of additional protein domains. One of such subfamilies include Chd3 (also known as Mi-2a) and Chd4 (also known as Mi-2β proteins in mammals. These proteins harbor paired PHD (plant homeo domain) domains in their N-terminus. These domains involved in chromatin remodelling and binding to methylated histone peptides. Chd3 and Chd4 protein were found in multi-subunit complexes that posses both histone deacetylase and ATP-dependent chromatin remodelling activities. These complexes were called NURD (nucleosome remodelling and histone deacetylase). NURD contains several proteins usually associated with transcriptional repression: HDAC1 and HDAC2, Rba48 and Rba46, MTA1, MTA2 and MTA3, and MBD3 (Denslow and Wade, 2007). Chd4 was also found in association with proteins involved in transcription activation (Williams *et al.*, 2004), suggesting its complex role in gene regulation.

Inactivation of Chd4 gene demonstrated its essential role in early embryonogenesis and development of several tissues including skin (Kashiwagi *et al.*, 2007; Marfella and Imbalzano, 2007; Williams *et al.*, 2004). Epidermal specific inactivation of Chd4 demonstrated its crucial role for several aspects of epidermal development (Kashiwagi *et al.*, 2007). Early (E10.5) depletion of the protein in the developing ventral epidermis leads to reduction of its supra-basal layers and ultimate depletion of the basal layer. Loss of Chd4 at E13.5 in dorsal epidermis did not cause any significant changes, in the structure of the epidermis, however, was accompanied by impaired induction and development of the hair follicles.

1.3.4 Higher-order chromatin remodelling and nuclear compartmentalization of the genomic loci

It is well-accepted now that gene positioning in 3D-nuclear space is not random and that nuclear compartmentalization of the transcriptional machinery is highly important for the control of gene expression.

There are several examples of the cell-type specific localization of the distinct genomic loci in the nucleus associated with cell differentiation and tissue development.

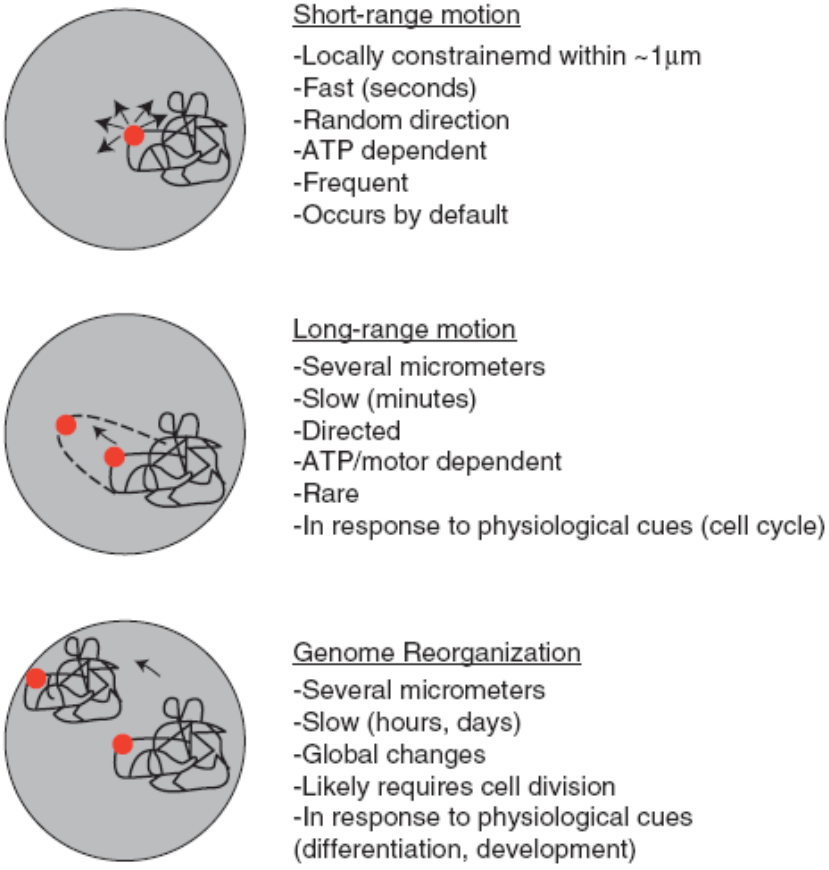

Figure1.16. Different types of chromatin movements (Misteli, 2007).

Cell-differentiation-associated relocation of the genomic loci was observed in several cell types including keratinocytes induced to differentiation by Ca^{2+} in vitro. Epidermal differentiation complex was frequently observed externally to the chromosome territory 1 (CT1), while in lymphoblast cells in which EDC genes are silenced, EDC was located inside of the chromosome territory (Williams *et al.*, 2002b).

Similar outlooping of the gene loci relatively to the corresponding chromosome territory was reported for Hoxb gene cluster in mouse embryonic stem cells (ES). After induction of the Hoxb genes expression by retinoic acid, the levels histone modifications associated with transcriptional activity increased, followed by the loci decondensation and extrusion out of the chromosome territory (Chambeyron and Bickmore, 2004; Chambeyron *et al.*, 2005).

Distinct positioning of the loci in 3D nuclear space is also important for the control of expression of some hepatocyte specific genes like Afm, Cyp2j5 or Pah activated by the transcriptional activator Hnf1α. Activated genes are positioned internally in the domains enriched in methylated histone H3K4 and RNA polymerase II. In hepatocytes isolated from Hnf1α -/- mice, locus containing gene targets of Hnf1α were positioned preferentially at the nuclear periphery and exhibited increased levels of trimethylated histone H3K27 and reduced H3K4 methylation (Luco *et al.*, 2008).

Gene outlooping is also shown for major histocompatibility complex II loci (MHC II) expressed in human B-lymphoblastoid cells. Additionally MRC5 fibroblast cells treated with IFN-γ which is known for induction of MHC II genes showed increase in extrachromosomal location of the MHC II loci (Volpi *et al.*, 2000).

Immunoglobin loci activated for transcription and rearrangements during B lymphocyte development are another example of the loci repositioning correlated with increase of gene expression. It was shown that Ig heavy (H) and Igk loci are preferentially located at the nuclear periphery in pro-T cells and hematopoietic progenitors, whereas take more internal position in pro-B cells (Kosak *et al.*, 2002).

Pro-neural regulatory gene Mash1 is an example of transcription-related loci repositioning associated also with changes in the time of replication. It is known that before commitment of embryonic stem cells to the neural lineage it is repressed. Analysis of mouse embryonic stem cells showed that in this state Mash1 loci are located at the periphery within chromatin domains that show low levels of H3K9 acetylation and enhanced H3K27 trimethylation. After induction of its transcription by retinoic acid, Msh1 locus relocates from nuclear periphery towards the interior. (Williams *et al.*, 2006).

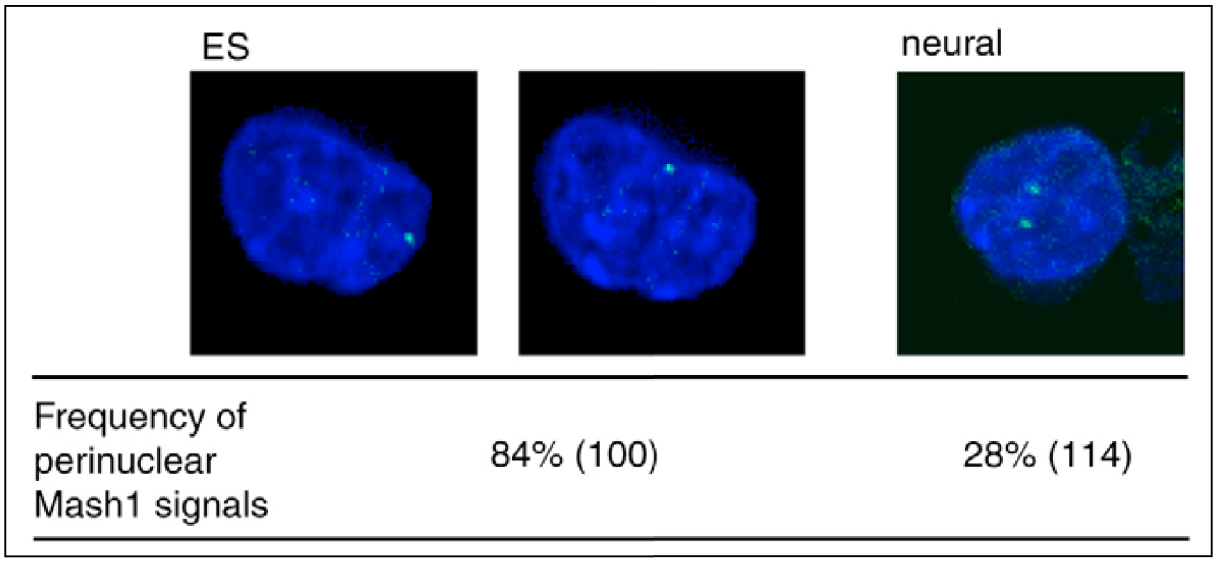

Figure 1.17 Mash1 locus in mouse embryonic stem cells (ES) and in neural cell. Mash1 is positioned peripherally in embryonic cells, after neural induction associated with 100-fold upregulation their localization changes to internal (Williams *et al.*, 2006).

This Information supports the hypothesis that gene relocation is likely to be driven by the transcription activation. Study of the CFTR loci does not completely contradict this opinion, however shows that decrease of transcription does not have to be accompanied by the return of loci to the previous location. Although CFTR loci in several different human cell lines relocates from nuclear periphery towards interior upon activation when its transcription was blocked it remained in the internal part of chromosome territory with the euchromatic markings typical for active loci (Zink *et al.*, 2004).

1.3.5 Long-range intra- and inter-chromosomal interactions

Using chromosome conformation capture (3C) and related techniques allowing reliable detection of the chromatin interactions, it was shown that some genomic regions may form associations with distantly located regions within one chromosome territory or even between different chromosome territories and that these interactions have functional significance (Fraser and Bickmore, 2007).

One of the most spectacular observations regarding such associations was done using 3C technique for analysis of the mouse olfactory neurons. It was shown that one active enhancer element H (second, homological loci is methylated) on chromosome 14 has ability to colocalize with multiple odorant receptor (OR) promoters on different chromosomes. Eventually it associates with one OR promoter and as a result only one from 1300 receptors is expressed in each distinct olfactory neuron (Lomvardas *et al.*, 2006).

The other study described the large scale intra-chromosomal interactions in the region spanning over 120 kb which is important for cytokine gene regulation during the differentiation of naive $CD4^+$ T cells to T_H1 or T_H2 cells. A strong association between the promoter region of the IFNγ gene on chromosome 10 and the regulatory regions of the T_H2 cytokine locus on chromosome 11 has been reported, however functional significance of these interactions remains to be defined (Spilianakis *et al.*, 2005).

1.4 Mechanisms that control the positioning of genes and chromosomes.

During the last few years, some general mechanisms that control intranuclear gene positioning have been proposed (Brown *et al.*, 2008; Fedorova and Zink, 2008; Misteli, 2007).

It is well accepted now that chromatin is non randomly anchored to the nuclear scaffold (nuclear matrix). In addition, distinct chromosomes are attached directly or indirectly to peripheral nuclear lamina and/ or nucleolus. It is known that special AT rich sequences like MAR and SAR have an affinity for the nuclear matrix and are responsible for the anchoring of the distinct chromatin domains. These associations are mediated at least in part by Satb1 or Safb1 proteins (Ottaviani *et al.*, 2008). It was shown that Satb1 provides cage-like architecture in thymocyte nucleus and also that it has the ability to recruit several chromatin

remodelling enzymes to activate or repress transcription. Moreover, lamins and other proteins associated with the nuclear envelope bind chromatin as well as a variety of transcriptional repressors like HA95 or HDAC3. As an outcome of these and many unknown so far interactions, chromosome structure is organized in semi-deterministic way (zig-zac structure, see subchapter on chromosomes), likely due to the local differences in the AT/GC contents, different types of specific sequences and interactions between them and nuclear lamina and/ or nuclear matrix (Ottaviani *et al.*, 2008).

Some researchers suggest that positioning of the chromosome or loci is dependent on the number of actively transcribed genes in the region. It was suggested that loci gather in the proximity of speckles due to nucleation of splicing factors associated with the transcribed genes. A similar mechanism may act in case of the loci recruitment near the concentration of transcription factors (Brown *et al.*, 2008; Ottaviani *et al.*, 2008).

Positioning of the distinct loci may be also related to the positioning of the transcription factories which are distributed as discrete loci (around 2000 in Hela cells). Many facts support the model in which DNA is recruited into the transcription factory oppositely to the previously proposed model assuming that RNA polymerase relocates towards the transcribed loci. It may also additionally enhance relocation of the chromatin towards speckles, since transcription factories are remarkably more frequent in the direct neighborhood of speckles (Iborra *et al.*, 1996; Osborne *et al.*, 2007; Wei *et al.*, 1999).

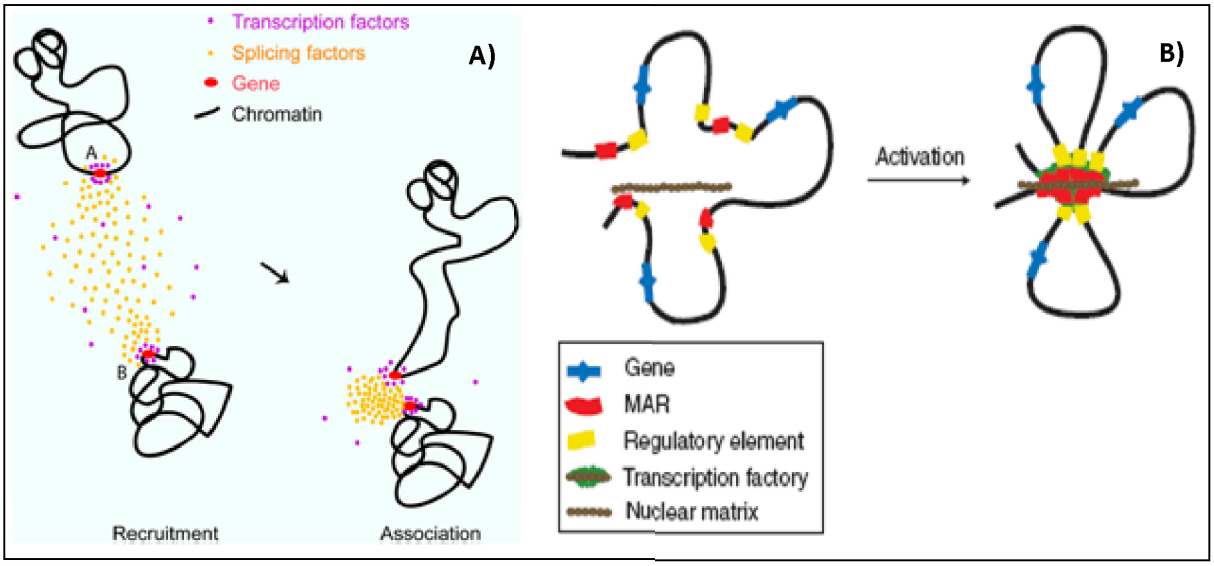

Figure 1.18 Recruitment of loci to the speckle (A) and to the transcription factory (B). A- Genes in the process of transcriptional elongation accumulate splicing factors; nucleation of splicing factors associated with genes into speckles may cause association with other genes (Brown *et al.*, 2008). B- Activation of transcription is accompanied by the anchoring of MARs to the nuclear matrix. Interaction of MARs with the nuclear matrix brings together gene coding sequences, regulatory DNA elements and the transcription factory (Ottaviani *et al.*, 2008).

Nuclear architecture may also be influenced by specific interactions between distinct chromosomes, and associations with nuclear bodies. The most striking example of influence of the nuclear body on the genome organization is the nucleolus. The nucleolus is assembled around the specific sequences (nucleolar organizing regions - NORs), which are present in several distinct chromosomes and most probably affect chromosomal location. Moreover, nucleoli tend to fuse, which brings also NOR bearing chromosomes together (Chubb *et al.*, 2002; Kalmarova *et al.*, 2007). Beside nucleolus also Cajal bodies and PML bodies have been reported to associate with chromatin (Fedorova and Zink, 2008).

In addition, also long-range movements driven by actin/ myosin ATP-dependent movement have been reported (Chuang *et al.*, 2006).

In conclusion, despite the tremendous achievement in understanding the role of higher-order chromatin remodelling in the control of gene expression, many aspects of the spatial and molecular organization of the expression of tissue-specific genes in the nucleus remain to be explored. In this study, skin will be used as a model to study the mechanisms that control higher-order chromatin remodelling during development and differentiation. In particular, the role of the p63 transcription factor and genome organizer Satb1 in the control of higher-order remodelling of the EDC locus in keratinocytes will be investigated.

2. **Aims**

Recent studies showed that gene positioning may be one of the mechanisms regulating gene expression, especially for the genes involved in tissue differentiation and development. I will test the hypothesis that higher-order chromatin remodelling of tissue-specific EDC locus in epidermal progenitor cells during skin development is regulated by the p63 transcription factor and genome organizer Satb1.

To test this hypothesis, I propose the following specific aims:

1.) To describe the changes in nuclear architecture during epidermal differentiation
2.) To characterize the remodelling of higher-order chromatin structure of the EDC locus at distinct stages of epidermal development..
3.) To characterize the role of p63 in the control of higher order chromatin remodelling of the EDC locus using p63KO mice as a model.
4.) To characterize the role of Satb1 in the control of EDC conformation during epidermal development.

3. Materials and methods

The experimental work has been performed in 3 phases. First, Fluorescent in Situ Hybridisation (3D FISH) was performed on the mouse skin with 3D preserved nuclear structure, then the resulting FISH signals were detected and collected using laser scanning confocal microscopy followed by the three dimensional analysis of obtained image stacks Finally, the results were analyzed statistically.

3.1 Fluorescent in Situ Hybridisation of the nuclei with 3D preserved structure (3D FISH).

In order to label loci of interest as well as chromosome territory 3, FISH was performed on the nuclei with a 3D preserved structure in mouse skin at defined stages of development (3D FISH) (Solovei *et al.*, 2002) was performed. Briefly, the cryosections of the mouse skin with the 3D preserved nuclear structure were prepared. Also, 3D FISH probes were designed and DNA for their synthesis was amplified: the DNA of mouse chromosome 3 by DOP-PCR (Telenius *et al.*, 1992) and the DNA of the selected Bacterial Artificial Chromosome (BAC) DNA with the GenomiPhi V2 Amplification Kit (GE Health care Ltd, Little Chalfont, UK; (Dean *et al.*, 2001)). Subsequently, probes were labelled by DOP-PCR labelling (chromosome 3) and by nick translation (BAC DNA;(Rigby *et al.*, 1977). Specificity and efficiency of labelling were checked by FISH (2D FISH) on the metaphase spreads previously prepared newborn

mouse primary fibroblasts. Probes after validation were used in 3D FISH experiments.

3.1.1 Collection and processing of the mouse skin for the 3D FISH experiments. Preparation of cryosections.

All animal experiments were performed under Project Licence of Prof. Vladimir Botchkarev. Blocks with mouse tissues were prepared by Dr. A. Mardaryev and Dr. M.Fessing (University of Bradford) as follows: the whole embryos were collected at E11.5, E16.5 and E18.5 and skin tissue was collected from neonatal animals at p10 or 6 month old animals. p63 -/- mice have been previously described (Mills *et al.*, 1999; Yang *et al.*, 1999). p63 -/- and p63 +/+ control embryos at E16.5 were obtained by breeding p63 +/- animals purchased from Jackson Laboratories (Bar Harbor, MN, USA). The embryonic genotype was determined using PCR as recommended by the supplier. For each developmental stage, 4-7 samples were collected. For FISH and immuno-fluorescent analysis of 3D preserved nuclei the samples were frozen after fixation with formaldehyde and gradual equilibration in buffered sucrose solutions (Solovei *et al.*, 2009). Briefly, the embryos or tissues were fixed in 4% formaldehyde at 4^{o} C overnight, than incubated in 50 mM ammonium chloride solution at room temperature for 5 min followed by washes with 0.1M phosphate buffer (pH 7.0). Then the samples were consecutively incubated in 5% and 12.5% sucrose solution in the phosphate buffer for 1 hour at room temperature followed by overnight incubation in 20% sucrose solution at 4^{o} C. Finally the samples were frozen and embedded in OCT medium (Raymond A Lamb – Laboratories) using ethanol/dry ice bath. 20 µm cryosections on the positively charged microscope slides were prepared using cryostate Microm.

3.1.2 Labelling of BAC probes.

DNA probes for the specific locus detection were generated using the Bacterial Artificial Chromosomes (BACs). BACs were chosen using a Clone Finder (tool available on the website of the National Centre for Biotechnology Information) and ordered by Dr M. Fessing (The University of Bradford) from mouse genomic library kept in the BAC/PAC Resource Centre (BPRC) at Children's Hospital Oakland Research Institute in Oakland, California, in the United States (Osoegawa *et al.*, 2000). The following BAC clones were used in the study:

Probe	BAC name	Featured gene	BAC start	BAC end	Featured gene start	Featured gene end
EDC	RP24-318N12	**S100a6**	90284072	90451873	90416816	90418336
	RP24-61G19	**Lor**	91716002	91899804	91884193	91887064
	RP24-248L10	**Ivl**	92215201	92392463	91887064	92377637
	RP24-341I21	**Lce3c**	92634255	92806759	92748408	92749652
	RP23-425P7	**S100a10**	93215624	93411886	93359039	93368567
EDC distal 5'-flank	RP24-209B20	**Tdo2**	81643088	81823587	81762334	81779650
EDC distal 3'-flank	RP23-157O24	**RhoC**	104460046	104652045	104591970	104597377
Rps27	RP23-480F10	**Rps27**	89997746	90169775	90016591	90017569

Table 3.1. Description of BACs used for probes synthesis.

BACs were shipped as a bacterial LB agar stab culture and streaked to single colonies on a LB agar plate with 12.5 µg/ml chloramphenicol. Glycerol stocks for long term storage in -85°C were prepared.

DNA isolation from BAC clones.

First, the following solutions were prepared:

P1 solution (4°C):
50 mM tris, pH 8
10 mM EDTA

P2 (RT):
0.2 M NaOH
1% SDS

P3 (4C):
3M NaOAc,
pH 5.5

2ml of LB media containing 12.5 µg/ml of chloramphenicol was placed in 15 ml Falcon tube and inoculated with a single isolated bacterial colony using a sterile pipette tip. Bacteria were grown overnight at 37°C shaken at 225-300 rpm. Tips were removed with a forceps and solutions with bacteria were spun at 3000 rpm. Supernatants were discarded, pellets resuspended in 0.3 ml of P1 solution and the bacterial suspension was transferred to 1.5 ml Eppendorf tube. Next, 0.3 ml of P2 solution was added, the contents the tube were gently mixed and incubated in RT for about 5 minutes. Afterwards, slowly 0.3 ml of P3 was added and the tubes were placed on ice for at least 5 minutes. Next, tubes were centrifuged at 15,000 g for 10 minutes at 4°C. Tubes were removed from the centrifuge, placed on ice and the supernatant were transferred to a new 1.5 ml Eppendorf tube with 0.8 ml ice-cold isopropanol. Contents of the tubes were mixed and left on ice for 5 minutes and then spun in the centrifuge at 15,000 g for 15 min at 4°C. The supernatant was removed and 0.5 ml of 70% ethanol was added to wash the pellet. After inverting the tubes several times they were spun at 4°C. The supernatant was removed and the pellet air dried at 37°C. After ethanol evaporation, DNA was resuspended in 20 µl of TE buffer.

Amplification of BAC DNA – Genomiphi V2

BAC DNA isolated from E.Coli was amplified with Genomiphi V2 DNA Amplification Kit (GE Health care Ltd, Little Chalfont ,UK; (Dean *et al.*, 2001)). The kit contains hexamer pimers, the **DNA polymerase** of Bacillus subtilis phage **phi29,** nucleotides and buffers**.** Isothermal DNA amplification at 30**°C**

yields products of a size from a few hundred bp to above 10 kb. Results of amplification were checked by electrophoresis in the 1% agarose gel.

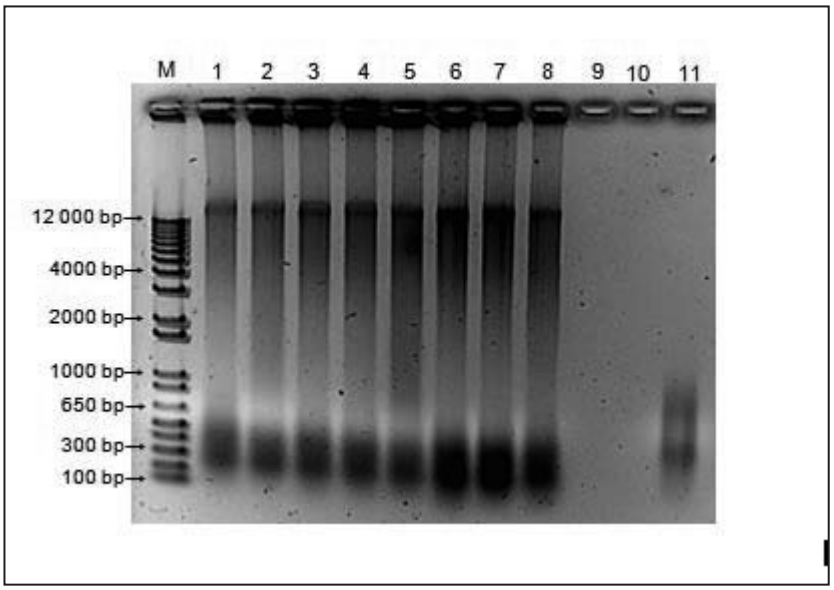

Figure. 3.1 Example of electrophoregram of amplified BAC DNA and amplified DNA of chromosome 3. M- marker ("1 kb plus DNA Ladder", Invitrogen), lines 1-8 contain 2 µl of different BAC DNA amplified with GenomiPhi Amplification Kit, line 11 contains DNA of chromosome 3 amplified by DOP-PCR.

Labelling of BAC probes for FISH analysis

Labelled dUTPs (FITC-dUTP, Cy3-dUTP, Bio-dUTP, Dig-dUTP) have been provided by Dr M.Fessing, additionally FITC-dUTP was synthesized.

FITC-dUTP synthesis

10 mg of FITC (fluorescein-5-EX, succinimidyl ester, Molecular Probes, Inc., T-6134) was dissolved in 417 µl DMSO so as to obtain 40 mM FITC. Then 10 µl H_2O, 10 µl 0,2 M bicarbonate buffer and 10 µl 40 mM FITC were mixed and incubated for 4 hours at 26°C. After the incubation 2 µl of 2 M glycine (pH 8.0), 4 µl of 1 M Tris-HCl (pH 7.75) and 154 µl of water were to obtain 200 µl of 1 mM FITC – dUTP.

Nick translation is a method of DNA labelling combining 5'→3' polymerase, 5'→3' exonuclease activities of *Escherichia coli* DNA polymerase I and random damage of one of DNA strands by Deoxyribonuclease I (DNase I) resulting in single strand breaks (nicks; (Rigby *et al.*, 1977)). If a nick or single strand break with a 3 hydroxyl terminus is present in a duplex DNA molecule, the enzyme translocates it, removing nucleotides ahead of it by 5′→3′ exonuclease activity and synthesizing the new DNA strand behind it (Kelly *et al.*, 1970) with labelled nucleotides using 5′→3′ polymerase activity .

First, the following solutions were prepared:

a) dNTP mixture:

100 µl	2mM dATP
100 µl	2mM dGTP
100 µl	2mM dCTP
20 µl	2mM dTTP
80 µl	H2O

b) 10xNT – buffer:

50 ml	1M Tris-HCl pH 7.5
5 ml	1M MgCl2
50 mg	BSA
45 ml	H_2O

c) 0.1M Mercaptoethanol

d) DNase I (grade II, from bovine pancreas, Roche, Cat.No:104 159, 100mg)

1mg/ml in 0.15M NaCl in 50% glycerol

e) Stop Mixture:

50mg	Bromphenolblue
250mg	Dextranblue
1ml	5M NaCl
2ml	0.5M EDTA pH8
1ml	1M Tris-HCl pH 7.4

Afterwards, the following reaction solution in 200µl tubes on ice was prepared:

2µl	DNA (GenomPhi BAC amplification)
5µl	NT buffer
5µl	0.1M Mercaptoethanol
5µl	dNTP mixture
1µl	labelled dUTP

Next DNase I from stock solution was diluted 1:200 with water and 1 µl was added to the tube as well as 1 µl of DNA-polymerase I (5 U/ul) (Roche Diagnostics GmbH, Penzberg, Germany). Tubes were incubated in a thermocycler at 15°C for 2 hours. Finally 50 µl of Stop Mixture was added. Probes were stored at -20°C.

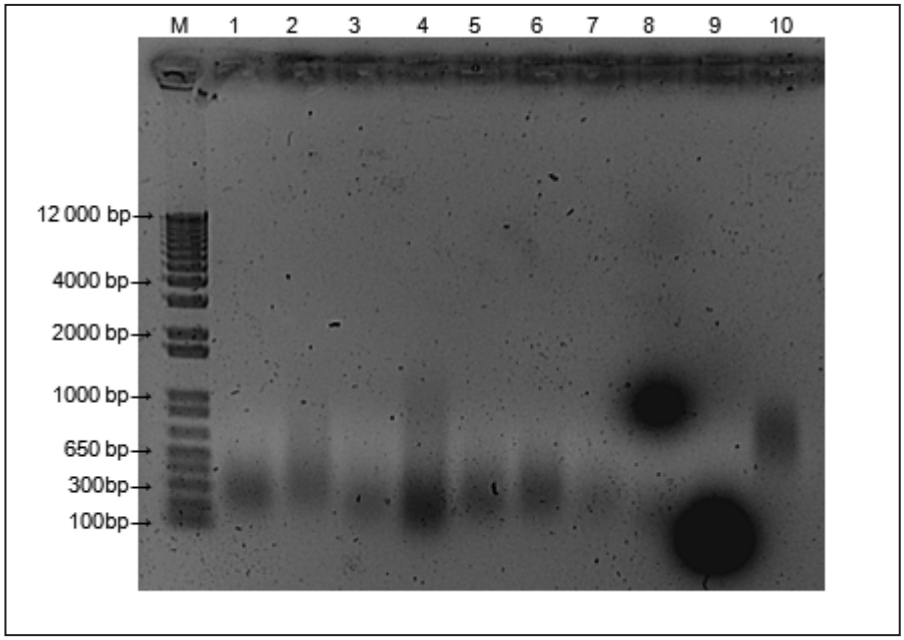

Figure. 3.2 Example of electrophoregram of labelled BAC probes and chromosome 3. M- marker ("1 kb plus DNA Ladder", Invitrogen), lines 1-9 contain 2 µl of different BAC probes labelled by nick translation with: lines 1-7 digoxegenin, line 8 Texas Red, line 9 FITC; line 10 contains DNA of chromosome 3 labelled by DOP-PCR with biotin.

3.1.3 Chromosome painting

The DNA of mouse chromosome 3 (second amplification of flow- sorted chromosomes, obtained from Prof. T. Cremer, Munich University, Germany) was amplified by DOP-PCR method in which DNA is amplified by PCR reaction with degenerated 6MW primers (Telenius *et al.*, 1992). The same method with slightly changed reaction parameters was then applied for labelling of DNA with biotinylated dUTPs.

Chromosome amplification with DOP-PCR

The DNA of chromosome 3 was amplified by DOP-PCR utilizing degenerated 6MW primer: 5'- CCGACTCGAGNNNNNNATGTGG - 3' (Eurofins MWG GmbH, Ebersberg, Germany). Amplification was performed via the following steps: 2μl of chromosome 3 secondary amplification, 10μl of 10x PCR buffer (Invitrogen), 4 μl of 50 mM $MgCl_2$ (Invitrogen Ltd, Paisley, UK), 2 μl of 100 μM 6MW primer (Eurofins MWG GmbH, Ebersberg, Germany), 8 μl of 2.5 mM dNTPs (Invitrogen Ltd, Paisley, UK) and 72 μl of water was mixed on ice. Next 2 μl of Taq polymerase (Roche Diagnostics GmbH, Penzberg, Germany) was added and whole solution was gently mixed. Tube was placed in thermocyler and the following parameters of amplifications were set: initial denaturation at 94°C for 3 minutes 35 cycles of 94°C for 1 minute, 56°C for 1 minute and 72°C for 2 minutes. After the last cycle, the tube was incubated for 5 minutes in 72°C. Finally, 2 μl of solution was checked by electrophoresis in 1% agarose gel.

Chromosome labelling with DOP-PCR

Amplification was performed as follows: 2μl of chromosome 3 amplification, 10μl of 10x PCR buffer (Invitrogen Ltd, Paisley, UK), 4 μl of 50 mM $MgCl_2$ (Invitrogen Ltd, Paisley, UK), 2 μl of 100 μM 6MW primer (Eurofins MWG GmbH, Ebersberg, Germany), 5 μl of 2mM ATP, GTP, CTP mix (Invitrogen Ltd, Paisley, UK), 8 μl of 1 mM TTP (Invitrogen Ltd, Paisley, UK), 6 μl of biotynylated UTP (Bio-UTP) and 62 μl of water was mixed on ice. Next 2 μl of Taq polymerase (Roche Diagnostics GmbH, Penzberg, Germany) was added and the whole solution was gently mixed. A tube was placed in the thermocyler and the following parameters of amplifications were set: initial denaturation at 94°C for 3 minutes 40 cycles of 94°C for 30 seconds, 56°C for 1 minute and 72°C for 30 seconds. After the last cycle tube was incubated additionally for 5 minutes in 72°C. Finally, 2 μl of solution was checked by electrophoresis in 1% agarose gel.

3.1.4 Synthesis of the mouse major satellite repeat probe.

To detect mouse centromeres mouse major satellite sequences were amplified and later labelled by nick translation. The following primers were used for PCR reaction (Horz and Altenburger, 1981):

Forward primer: 5'-GCG AGA AAA CTG AAA ATC AC
Reverse primer: 5'-TCA AGT CGT CAA GTG GAT G

As a template, mouse genomic DNA was used. Annealing temperature of the thermocycler programme was set at 56°C.

3.1.5 Check of prepared probes – 2D FISH

Preparation of nuclei from newborn mouse primary fibroblasts.

1 million cells were seeded in each of 4 Petri dishes with complete cell culture medium containing FBS and were grown for 2 days. Next, cells were incubated for 30 minutes in the medium containing 0.1 µg/ml of colcemid at 37°C. Afterwards, cells were rinsed with prewarmed to 37°C 1xPBS and incubated in 2 ml of trypsin (2.5g/L) for 3-5 minutes. After all these steps cells were detached from the substratum into 4ml of medium. Cells were pippetted up and down to obtain a single cell suspension, transferred to 15 ml falcon tubes and centrifuged at 1000rpm at RT for 6 minutes. Around 80-90% of supernatant was removed, leaving 1-3 ml and the rest was mixed. Afterwards, 10 ml of hypotonic 0.56% KCl solution prewarmed to 37°C was added dropwise, while the solution was being vortexed. Then tubes were filled up to 15 ml with hypotonic solution and incubated at 37°C for 25 min. The cell suspension was centrifuged at 1000 g at RT for 6 minutes and the supernatant was decanted. After this step the nuclei were gently resuspended with a wide-bore plastic Pasteure pipette in 2ml of fixative (ice cold methanol : acetic acid 1:3) and transferred to a new 15 ml Falcon tube. The tube was filled with fixative and centrifuged at 1000 g at RT for 6 minutes, then decanted, filled with the fixative, resuspended and incubated at RT for 10 minutes. Next, it was again centrifuged at 1200 g at RT for 6 minutes, decanted and the pellet was washed with 14 ml of fixative. It was repeated 10 times. Finally 2ml of the fixative was left in the tube over the cell pellet, resuspended and stored at -20°C.

Metaphase spreads

Metaphase spreads were prepared according to recommendations of Cheung et al. (1995). Previously prepared mouse primary fibroblasts (MPFs) were centrifuged at 1600 rpm. Fixative was decanted and the new one added (methanol: acetic acid 3:1), up to the level left after previous usage to keep the same concentration of the nuclei. A metal tray was placed on the surface of water in the water bath. The water was warmed up to 55°C and its level was adjusted to reach the ratio of water surface to the air volume under the water bath cover of 0.23. A microscope slide was placed on the tray and two drops of MEFs suspension were applied on its opposite sides. Water bath was covered for a couple of minutes till the total evaporation of the fixative, and the slide was checked under the phase contrast microscope. If at least 3 metaphase spreads were observed, the microscope slide was placed in Coplin jar with 70% ethanol and kept overnight. The same procedure was repeated to obtain around 20 microscope slides with metaphase spreads. On the next day 70% ethanol was changed and then slides were transferred to absolute ethanol solution and incubated for 10 minutes. Afterwards, they were air dried and kept for a one week in the closed box at RT. Next, they were incubated at 60C for 2 hours. Shortly before the end of incubation, pepsin solution were prepared: 50 µl of 10% pepsin stock solution was added to pre-warmed to 37°C 0.01 HCl. After incubation at 60°C microscope slides were placed in a Coplin jar with previously prepared Pepsin solution and incubated for 10 minutes at 37°C. Next, slides were washed 3 times for 5 minutes in PBS solution, then placed in 70% ethanol,

additionally dehydrated in 100% ethanol and dried at RT. Finally they were placed in plastic box and stored at -20°C.

2D FISH

In order to check the probes specificity and labelling efficiency, 2D FISH with probes was performed on slides with MPF metaphase spreads: 7 µl of labelled with Bio-dUTP chromosome 3 DNA (chromosome paint), 25 µl of BAC probe (from 1 up to 3 BACs labelled with different fluorophores , biotin or digoxigen), 1 µl Salmon Sperm DNA, 10-25 µl Cot1 DNA (depending on the BAC's DNA amount) and ethanol in the amount of 2.5 total volume of the rest of ingredients were mixed and placed for 30 minutes at -80°C. Afterwards, the tubes were spun down at 14000 rpm for 15 min at 4°C. The supernatant was discarded. The pellet was air dried and dissolved in 2.5 µl of deionized formamide at 55°C. Next, 2.5 µl of 20% dextran sulphate in 4x SSC was added and the solution was mixed. Places with the highest density of metaphase spreads on the microscope slides were marked and mounted with the probe and 15x15 mm cover slip. Cover slips were sealed with rubber cement and dried for 15-20 minutes. Chromosome and probe DNA were denatured by incubating slides at 75°C for 2 min and hybridization were carried out at 37C for two days. After hybridisation, slides were washed three time at 2xSSC for 10 min at 37^{o}C followed by washing in 0.1xSSC for 10 min at 60 ^{o} C. For detection of chromosome paints, slides were incubated with avidin-Alexa488 (Invitrogen, Carlsbad, CA) and or streptavidin-Cy5 (Rockland Laboratories, Gilbertsville, PA). BAC probes were detected similarly or by using two layer protocol. If Bio-dUTP were used slides were incubated with avidin-Alexa488 followed by incubation with goat antibody against avidin conjugated to FITC. In the case of

the probe labelled with Dig-dUTP, mouse anti-Digixogenin antibody conjugated to Cy3 was used and secondary goat anti-mouse antibody also conjugated to Cy3 was applied. DNA was stained with DAPI (Sigma, St Louis, USA) and slides were embedded using VectraShield medium (Vector Laboratories, Burlingame, CA) and sealed with nail polish. Finally, the result was analyzed using the epifluorescent microscope or were scanned using Zeiss LSM510M microscope confocal microscope described above.

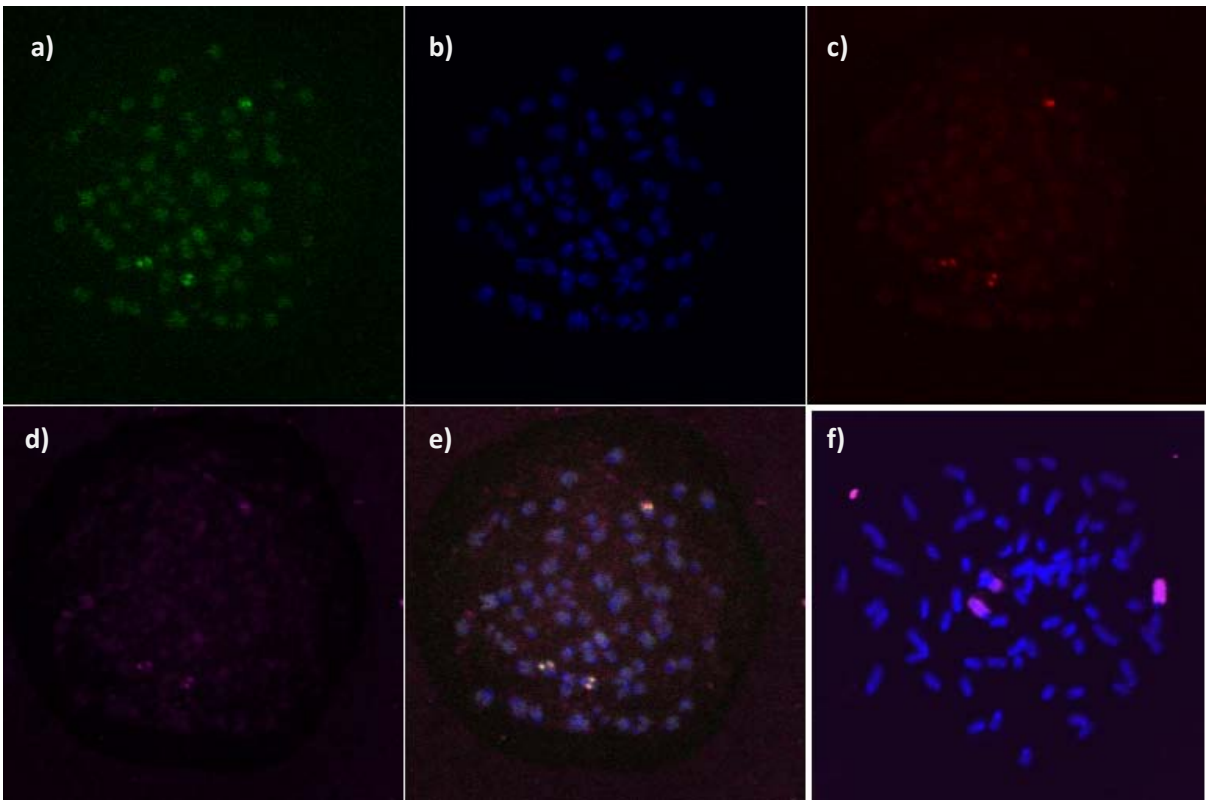

Figure.3.3 2D FISH – BAC probes (a-e) and chromosome 3 on metaphase spread (f). a) the intercontig - DNA linking Loricrin and Rps27, labelled directly by nick translation with FITC b) all metaphase chromosomes stained with DAPI c) BAC containing Rps27 labelled directly by nick translation with Cy3 d) BAC containing Loricrin labelled by nick translation with biotin and detected with streptavidin conjugated with Cy5 e) overlay of all images showing localization of all signals on the same chromosome f) chromosome 3 labelled by DOP-PCR with biotin and detected with streptavidin conjugated with Cy5; Image acquired with 63x oil apochromat objective using Zeiss LSM 510 confocal microscope.

3.1.6 3D-FISH

Slides with cryosections were dried at RT for 30 minutes and then placed in a Coplin jar in 10mM sodium citrate (pH 6.0) for 5 minutes. Next they were heated up to boiling point in a microwave and placed in a water bath at 90°C for 10-30 minutes (depending on the probes, chromosome territory requires 30 minutes incubation, while for BAC probes 10 minutes is enough). Afterwards slides were transferred into the Coplin jar with 2x SSC for 5 minutes at RT and finally into the 50% formamide in 2x SSC for at least 2 hours at 4°C.

The DNA probe mixture was prepared as follows: 100 μl of chromosome paint or BAC probe (125 μl in the case when pool of different BACs covering one loci was used), 25- 80 μl of mouse Cot1 DNA (depending on the amount of DNA – 10 μl for the first 25 μl of probe + 5μl for each next 25 μl of probe), and ethanol in the amount of 2.5 total volume of the rest of ingredients were mixed and placed for 30 minutes at -80°C. Afterwards, the tubes with probes were spun down at 14000 rpm from 20 min at 4°C. The supernatant was discarded. The pellet was air dried and dissolved in 2.5 μl of formamide at 55C. Next 2.5 μl of 20% dextran sulphate in 4x SSC was added and the whole solution was mixed. The probe mixtures were placed on the skin cryosections under glass chambers. Genomic and probe DNA were denatured by incubating slides at 85^{o}C for five minutes and hybridisation was carried out at 37^{o}C for two days. After hybridisation slides were washed three time at 2xSSC for 10 min at 37°C followed by one wash in 0.1xSSC for 10 min at 60^{o}C. When biotinylated probes were used the slides were incubated with avidin-Alexa488 (Invitrogen, Carlsbad, CA) or streptavidin-Cy5 (Rockland Laboratories, Gilbertsville, PA).

DNA was stained with DAPI (Sigma, St Louis, USA) and slides were embedded using VectraShield medium (Vector Laboratories, Burlingame, CA).

3.2 Confocal microscopy, image processing and analysis.

FISH slides were scanned through the whole depth of cryosection using confocal microscope and three dimensional images (image stacks, scans) of mouse skin were obtained. Scans were corrected for chromatic shift which appeared due to differences in emission light wavelengths of used fluorophores. Effects of spherical aberrations on the analysis was found to have minor importance and neglected for this stage of experimental work. Finally, analysis of the loci position in relation to chromosome territory 3, analysis of radial positions and intergene distances were performed following the recommendations published previously (Ronneberger *et al.*, 2008).

3.2.1 Microscopy

Microscope slides with FISH samples were scanned using confocal laser scanning microscope Zeiss LSM 510 Meta equipped with UV laser (Enterprise, emitting light of 351nm, 364 nm wave lengths) and VIS lasers: Argon (458 nm, 477 nm, 488 nm, 514 nm), HeNe1 (543 nm) and HeNe2 (633nm). Stacks of the confocal images were acquired with a 63x/1.4 plan-apochromat oil objective and a voxel size of 100nm x 100 nm x 200 nm.

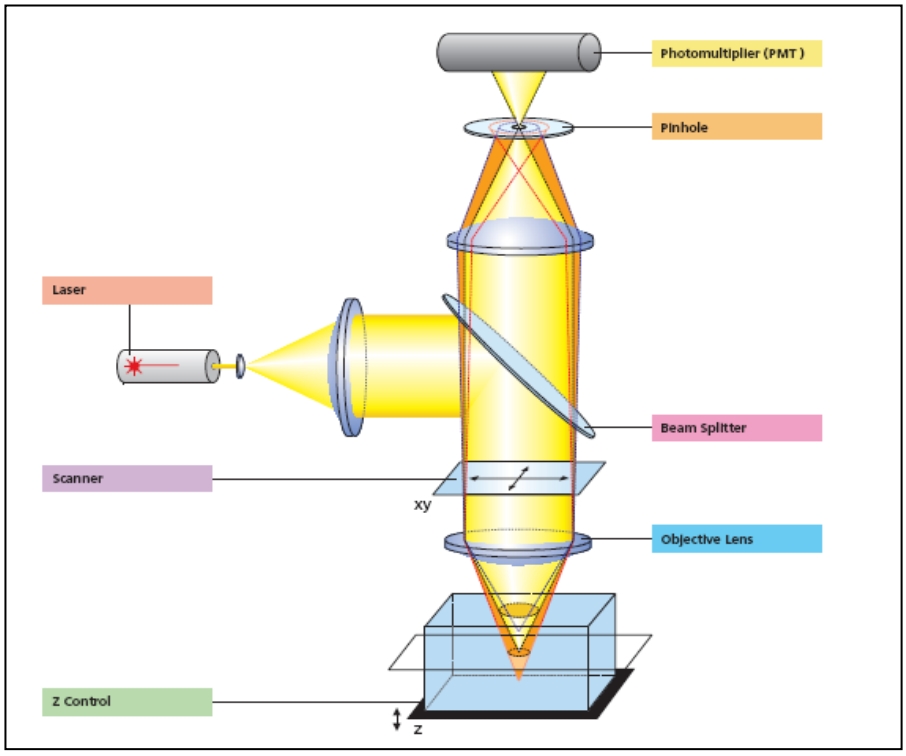

Figure. 3.4 Scheme of the light path in the confocal microscope. In conventional widefield microscope the in-focus image information is mixed with out of focus image information from planes outside the focal plane, which reduces the image contrast and increases the share of stray light detected. In confocal microscope, the pinhole (confocal aperture) greatly reduces the out of focus light enables obtaining high quality images from optical sections scanned in different depths of relatively thick specimens.

Usually 3 to 4 different fluorophores with the emission peaks far enough from each other and excited efficiently with the lasers available were used for labelling: 4',6-diamidino-2-phenylindole (DAPI, blue nuclear counter stain), Fluorescein isothiocyanate (FITC, green), Indocarbocyanine (Cy3, red) and Indodicarbocyanine (Cy5, infra red). Images were recorded in separate channels responding to the corresponding flurophores (filter settings; Luger et al. 1997, Anachkova et al. 2005).

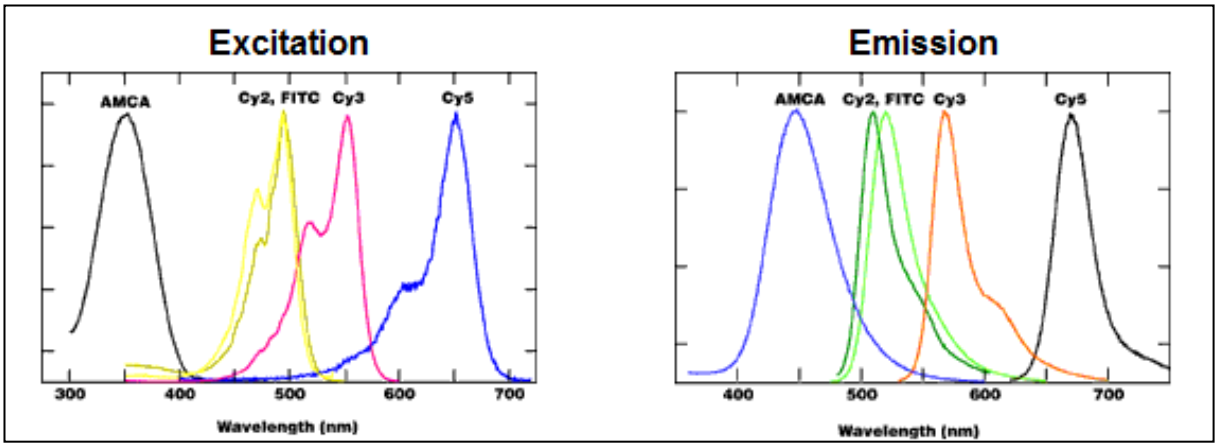

Figure. 3.5 Excitation and emission spectra of used flurophores. Four different fluorophores were used for labelling of DNA: DAPI (maximal absorbtion/excitation at 358 nm light wave length, maximal emission at 461 nm wave length; spectrum of DAPI is similar to AMCA), FITC (492 nm ,510 nm), Cy3 (550 nm, 570 nm) and Cy5 (650 nm, 670 nm) (Source: http://www.jacksonimmuno.com/technical/f-cy3-5.asp)

Scans of the sections from the 20 µm cryosections were acquired and saved as a three dimensional image stacks for further analysis.

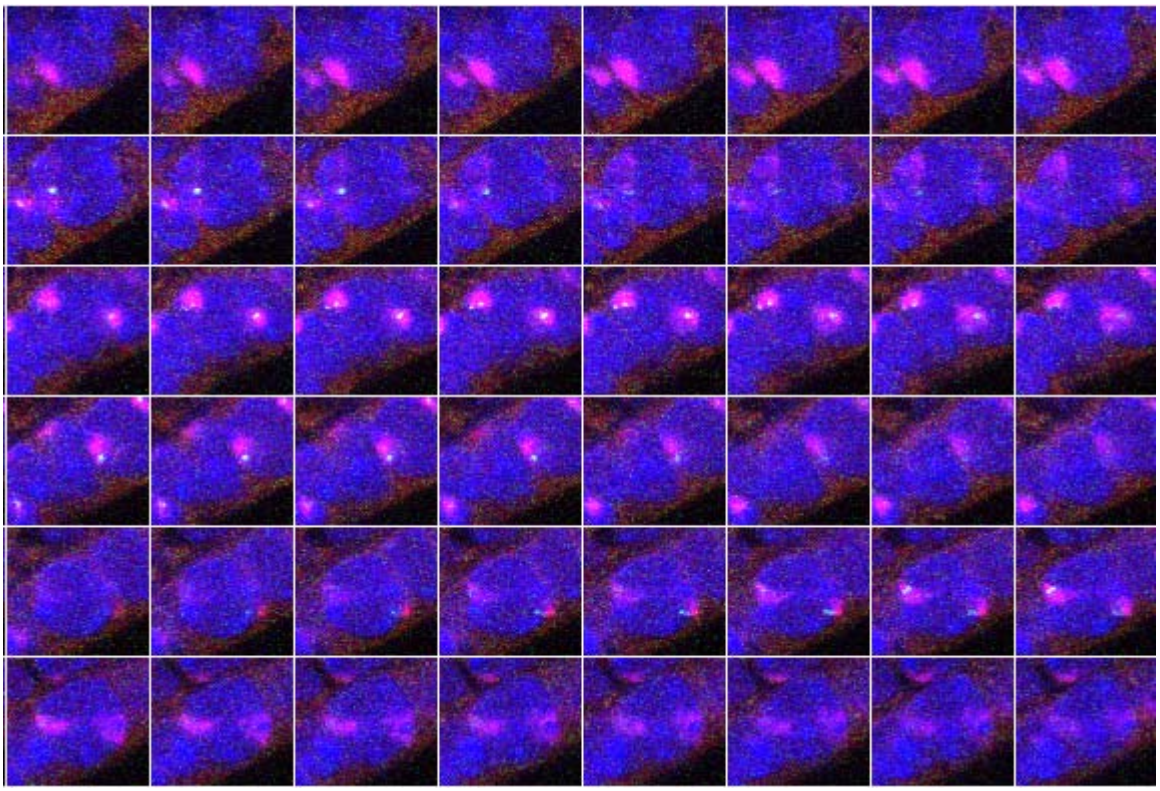

Figure. 3.6 Example of optical section series acquired by Zeiss LSM 510 M confocal microscope.

3.2.2 Optical aberrations and their correction.

Chromatic aberration

Chromatic aberration is a wave-length dependent image deformation caused by the fact that refraction index (η) of every optical glass is dependent on the light wave length (λ). As a result of focusing of different light wavelengths at different focal points, a chromatic shift appears between the channels recording signals from different fluorophores. Aberration is observed mainly in axial direction and in addition, lateral chromatic shift due to the optical system misalignment may appear (North, 2006).

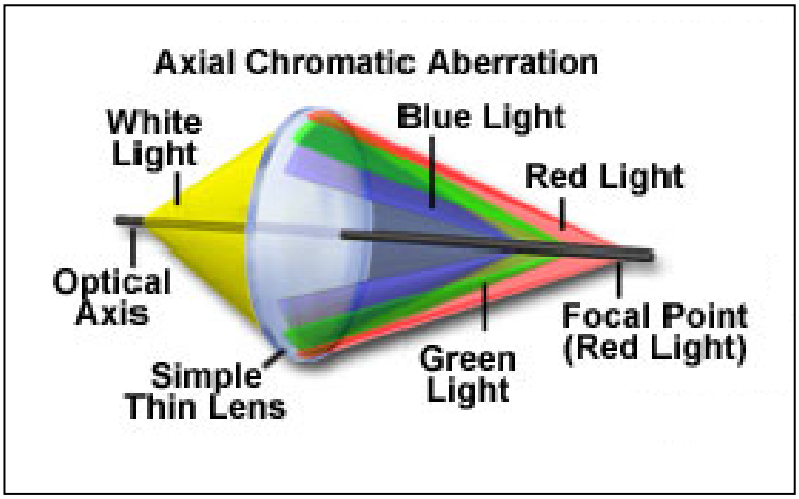

Figure. 3.7 Scheme of chromatic aberration. Rays of light of different wave lengths are refracted differently and as a result they focus in different places which is observed as a chromatic shift. (Source: http://www.olympusfluoview.com/theory/confocalobjectives.html)

In order to correct the chromatic shift the, microscope slides with 0.5 um Tetraspeck Beads (Invitrogen Ltd, Paisley, UK) were scanned. Scans were transferred to ImageJ program, where centroids of at least 20 beads in each of 4 channels were calculated and 3D chromatic shift between them was estimated in "Syncmeasure 3D" plugin (Walter *et al.*, 2006). Measurements

were averaged and shifts were corrected in two steps: first channels were moved pixelwiese in Zeiss Image Browser (correction in xy direction). Subsequently, they were transferred back to ImageJ where corresponding number of optical slices from the beginning or the end of the stacks containing data from different channels was removed (z-axis correction). The procedure was applied initially to the scans of TetraSpeck beads, and the results of the correction were checked by measurements in “Syncmeasure 3D” plugin.

Alternatively, in the case of the radial position and distance measurements, only data in Excel file were corrected.

Shift correction measurements				Shift after correction		
Channel	Shift x	Shift y	Shift z	Shift x	Shift y	Shift z
Ch 1 (blue)	0	0	0	0	0	0
Ch 2 (green)	201.962	478.72	236.204	-12.059	14.337	112.414
Ch 3 (red)	265.708	394.199	354.862	-58.151	21.109	116.997
Ch 4 (far red)	266.365	393.575	353.869	-15.343	12.838	63.145

Table. 3.2 Example of shift correction measurements before and after the correction. Chromatic shift was measured relatively to the blue channel.

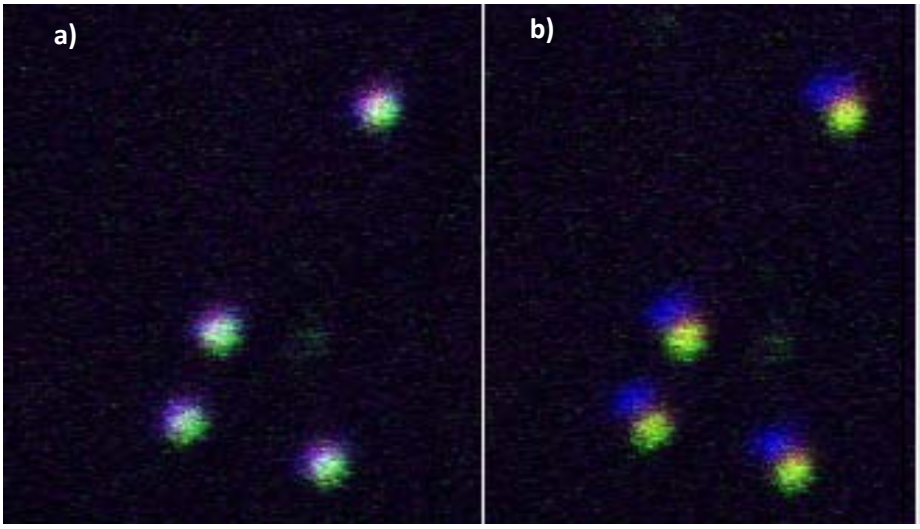

Figure. 3.8 Scan of TetraSpeck fluorescent beads after correction (a) and before (b). Beads were stained throughout with four different fluorescent dyes, yielding beads that each display four excitation/emission peaks — 365/430 nm (blue), 505/515 nm (green), 560/580 nm (orange) and 660/680 nm (far red) which are similar to excitation/emission peaks of used fluorophores.

Spherical aberration

Spherical aberration is a phenomenon whereby light rays passing through the lens at different distances from its centre are focused to different position in the z-axis. It is caused by the refraction indices (ŋ) mismatch. Refraction indices of immersion oil and cover glass as well as of objective lens are matched almost perfectly so the aberration usually is caused by different ŋ of embedding medium (Vectashield, Vector Laboratories Inc., Burlingame, CA ,USA) or specimen itself (Visser *et al.*, 1992).

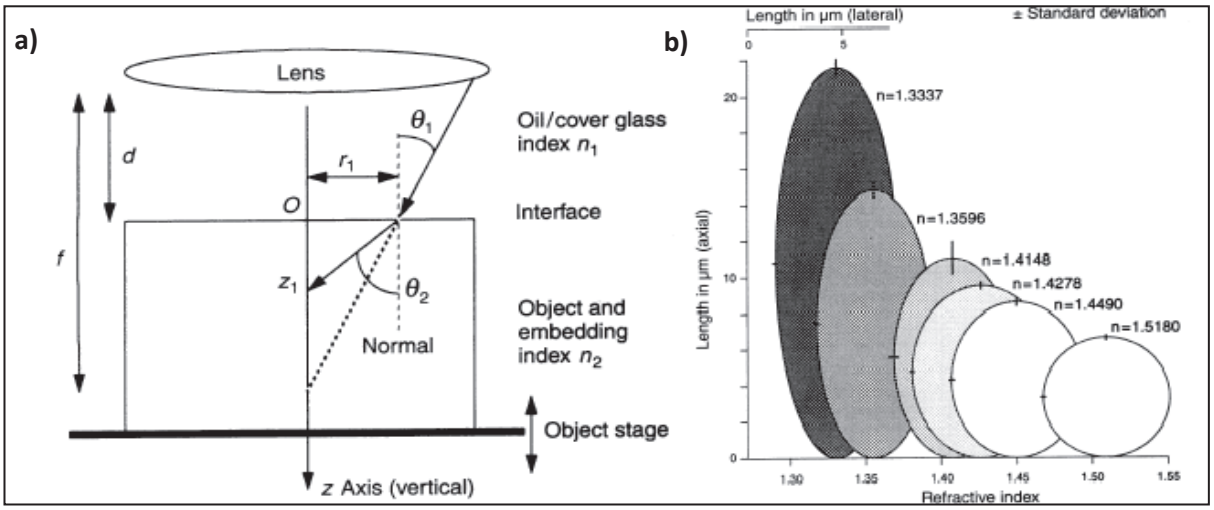

Figure 3.9 Scheme of spherical aberration (a) and its results in imaging of the 6 µm spheres mounted with different type of mounting media (b). Due to the differences in refraction indices of cover slip and mounting media light rays are refracted. The degree of the refraction depends on the place on the lens through which particular ray crosses it (a). Spherical aberration can cause geometrical distortions manifested mostly by z-axis extension, severity of this distortions depends on the size of the difference between the refraction indices (Visser T D *et al.*, 1992).

Spherical aberration has been measured on the scans of 4 µm TetraSpeck beads (Invitrogen Ltd, Paisley, UK) attached to the microscope slide surface and mounted with the medium used during the scaning of the FISH slides. Z-axis extension was estimated to be on average 1.2. To asses influence of this distortion on measurements Z-coordinates for a sample of data sets were corrected in the Microsoft Excel program after chromatic shift corrections.

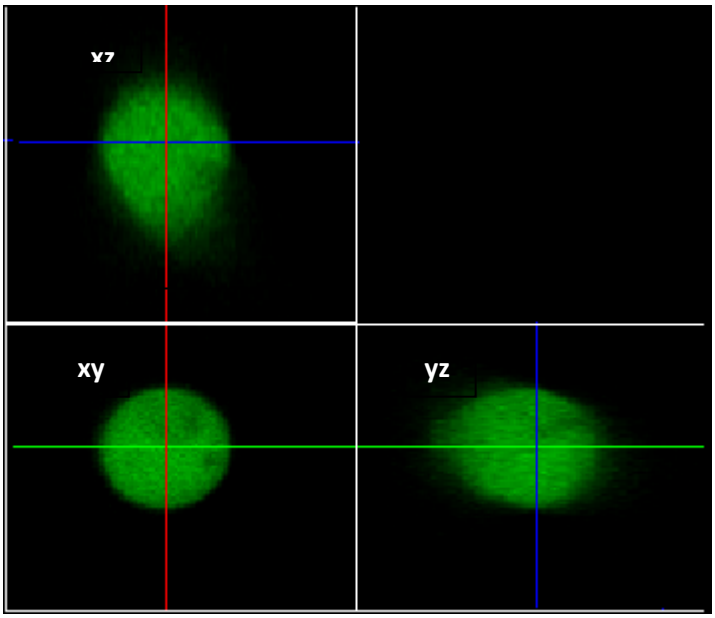

Figure 3.10 Scan of 4 µm TetraSpeck bead in xz, xy and yz planes showing z-axis extension. Fluorescent beads were attached to the surface of microscope slide and scanned. Their dimensions in both axes were measured and showed 1.25 z-axis extension.

	Intergene distances			Radial positions in [nm] and normalized						
e16	L-G	R-G	R-L	Loricrin (L)		Rps27 (R)		Gabpb2 (G)		radius
				[nm]	%	[nm]	%	[nm]	%	
e16	1082	1038	893.8	3259	81.2	2947	73.8	3001	74.8	4021
corrected	1028	995	829.9	3125	81.6	2800	73.4	2866	74.8	3839
difference	5.3%	4.4%	7.7%	4.3%	0.4%	5.3%	0.5%	4.7%	0.0%	4.7%

Table. 3.3 Example of the z-axis extension correction. Influence of z-axis stretching was examined - all loci and nuclear z-coordinates were corrected in Excel (multiplied by 0.8). Calculations showed that stretching of z-axis has minor effect on normalized radial positions, however it may have significant effect on non- normalized distances.

Corrections showed that z-axis distortion had minor influence on the values of normalized radial positions, however it may have some effect on intergenic distances measurements.

3.2.3 Analysis of localisation of the loci relatively to the chromosome territory 3.

In the scans of FISH slides with DOP-PCR labelled chromosome territory 3 position of the loci relatively to this territory were assessed via the following steps. Optical section containing centroid of particular loci was selected in the ImageJ program. Two dimensional image of the chromosomal territory in this section was divided in to three parts: internal that was closer to nuclear centre, medium and peripheral (closer to nuclear border). This analysis was possible because the chromosome territory 3 in almost all nuclei was located in very close proximity to the nuclear border. In each case, 50 nuclei (100 loci) were assessed. Positional data were summarised, the information was compared to the measurements from other cell types and analyzed statistically.

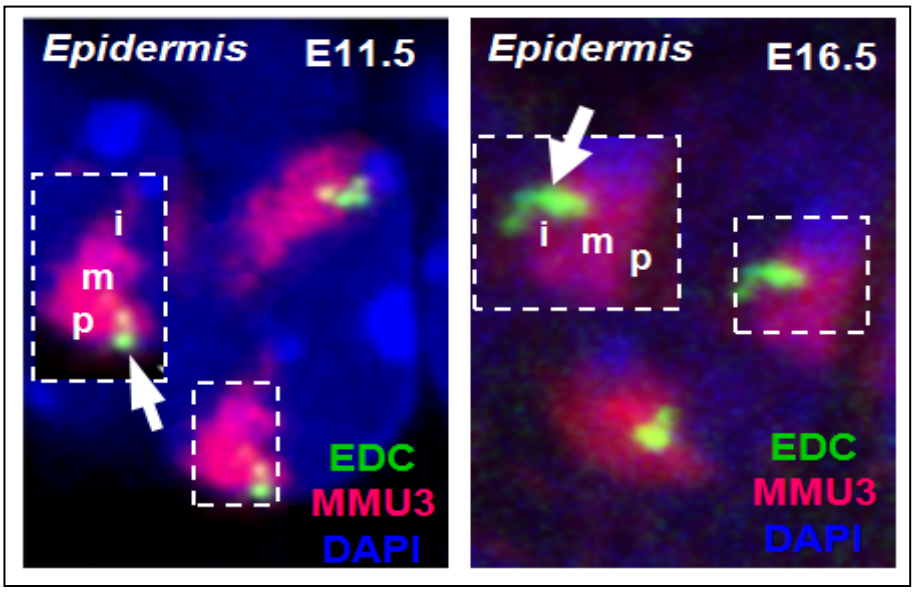

Figure 3.11 Analysis of the loci position relatively to the chromosome territory 3. Chromosome territories were divided into three parts relatively to the nuclear centre: internal, medium and peripheral. Positions of the loci were described relatively to each part of the chromosome territory.

3.2.4 Radial positions of the loci and measurements of distances between them.

Confocal image stacks were imported to the image processing programme ImageJ. Coordinates of a few hundreds of random points from the nuclear surface depicted by DAPI counterstain were acquired and exported to Microsoft Office Excel where the nuclear geometric centre was calculated by means of coordinate averaging. The average nuclear radius for each nucleus was calculated as a mean of distances from the nuclear geometric centre to all surface points. Centroids of the FISH signals corresponding to the particular loci were calculated in the plugin of ImageJ – the Centre Finder and exported to Excel. They were corrected for chromatic aberration. Distances between the nuclear centre and loci were calculated and related to the average nuclear radius (Ronneberger *et al.*, 2008).

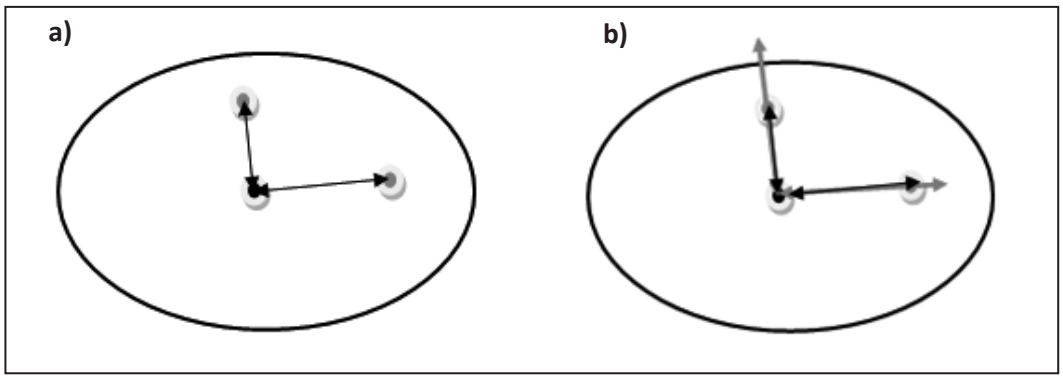

Figure 3.12 Radial position (a) and radial position normalized by average nuclear radius (b). Comparison of plain distances between loci and nuclear centres between different cell types may be misleading due to differences in the nuclear size therefore radial positions should always be normalized.

3.2.5 Measurement of the volume of the central domain of EDC

In case of the 3D-FISH covering the EDC central domain, the volumes of the signals were measured after adjusting the threshold to the level above the intensity of 99% percent of voxels in each stack by the 3D object counter plugin of ImageJ program. Further, the real volume of the central domain was calculated based on the comparison with the volume of the signal of multicolor beads of distinct size (100nm, 500 nm, 4 μm TetraSpeck, Invitrogen), measured in the similar way (**Table 3.4**).

Beads were dryed on the slide, mounted with Vectashield and scanned (for 500 nm and 4um usually used voxel size 100x100x200 nm, for 100 nm beads 20X20X100 nm – some researchers advice larger oversampling for the point spread function measurements). For the 100 nm beads, the DAPI channel was used, while for the 500 nm and 4 um beads the red channel was used. Measurements were done with ImageJ plugin - 3d object counter. In measurements 1,3 and 4 threshold automatically set up by the plugin was chosen, which seemed to include all voxels with the intensities above the background level related to the fluorescent signal. In measurements 2 and 5, about 160% of the suggested threshold was chosen (**Table 3.4**).

Measurement no	1	2	3	4	5
Bead size	100 nm	100 nm*	500 nm	4 um	4 um*
voxel volume [um3]	0.00004	0.00004	0.002	0.002	0.002
theoretical (real) sphere volume [um3]	0.000523	0.000523	0.0654	33.49	33.49
measured sphere volume [um3]	0.106	0.01582	1.45	61.52	38.05
measured/real ratio	202.55	30.23	22.24	1.84	1.14

Table 3.4. Comparison of theoretical and measured signal volumes from TetraSpeck multifluorescent beads

3.2.6 Radial positions and volumes of the centromeric clusters and nucleoli.

Centroids of centromeric clusters and nucleoli as well as their volumes were calculated by the 3D object counter plugin of ImageJ program. In addition, coordinates of 200-400 points from the surface of the nucleus were retrieved with ImageJ. For calculation of radial positions of centromeric clusters and nucleoli, script was written in R (The R foundation for statistical computing) according to following algorithm: 1.) 5 closest points to the particular point of interest (centroid of cluster or nucleolus) were found 2.) the average from the distances between the point of interest and the points in the surface were calculated 3.) average of measurements for all centromeric clusters or nucleoli in the nucleus were calculated. In each experiment 30 nuclei from the basal, spinous and granular layer were analysed. The significance of the differences of mean values between the layers were assessed by the T-test (see below). In addition, mean values were compared to the average of measurements obtained from the corresponding computer model nuclei (see next subchapters).

3.2.7 Measurements of the nuclear volume and shape.

Retrieved coordinates from the surface of the nuclei were used for calculation of the nuclear volume and shape. Volume was calculated by the script written in R (The R foundation for statistical computing) according to the following alogorithm: 1.) calculate the surface of optical slice “i” 2.) calculate the surface

of optical slice “i+1” 3.) calculate average of surfaces “i” and “i+1” 4.) sum all averages within the nucleus 5.) multiply by the distance between optical sections.

The surface coordinates were used subsequently for fitting of the ellipsoid equation and retrieving of the axis sizes of the best fitted ellipsoid by publically available MATLAB (Mathworks) script “minVolellipse” using the least square algorithm.

3.2.8 Mathematical models of nuclei.

Observed changes in the distribution of nucleoli and centromeric clusters can be caused by factors actively or passively controlling their positions, however they may be also potentially explained by constraints imposed by changes in the shape and volume of nuclei from particular layers.

To answer the question about specificity of changes in the radial positions mathematical modelling based on previous measurements was performed. Model nucleus had the average size of the nuclei from distinct epidermal layers, average number of nucleoli and centromeric clusters which were also of average size characteristic for distinct layer. Distribution of nucleoli and clusters was restricted by the nuclear surface and other nucleoli/clusters was randomized. After generation of nuclei radial positions were calculated and averaged in sets of 30. At the end, radial positions from the model were compared with radial position from experiment with the T-test.

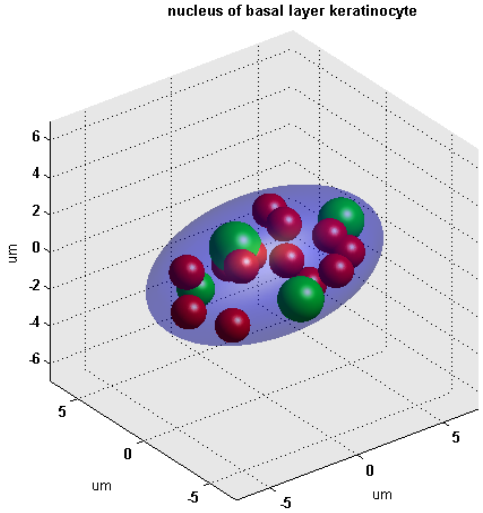

basal	
volume [um3]	324
long axis [um]	6.36
short axis [um]	3.41
number of nucleoli	4.16
average size of nucleoli [um3]	5.26
st dev of size of nucleoli [um3]	2.28
radial position of nucleoli	0.54
number of clusters	13.33
average size of cluster [um3]	2.28
st dev of size of cluster [um3]	1.29
radial position of clusters	0.72

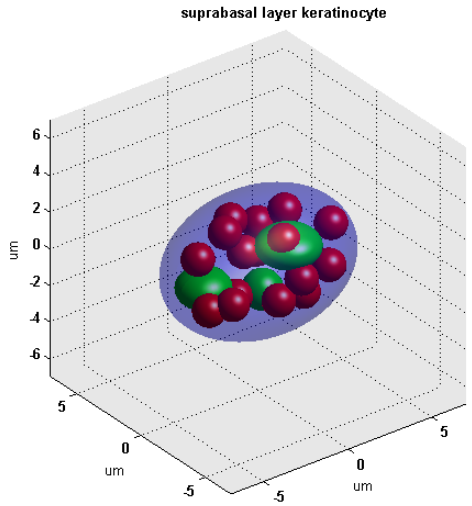

suprabasal	
volume [um3]	264
long axis [um]	5.23
short axis [um]	3.61
number of nucleoli	3.21
average size of nucleoli [um3]	11.14
st dev of size of nucleoli [um3]	6.7
radial position of nucleoli	0.42
number of clusters	16.57
average size of cluster [um3]	1.94
st dev of size of cluster [um3]	2.28
radial position of clusters	0.76

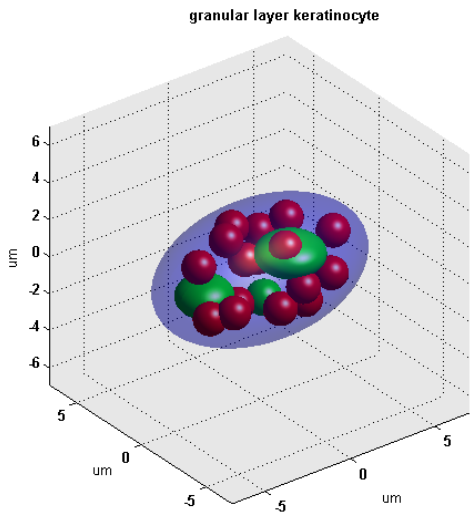

granular	
volume [um3]	257
long axis [um]	5.88
short axis [um]	3.4
number of nucleoli	2.82
average size of nucleoli [um3]	12.07
st dev of size of nucleoli [um3]	9.21
radial position of nucleoli	0.43
number of clusters	16.1
average size of cluster [um3]	1.64
st dev of size of cluster [um3]	0.65
radial position of clusters	0.69

Figure. 3.13 Parameters and visualization of mathematical model of epidermal nuclei.

3.2.9 3D reconstruction of the keratinocyte nucleus.

To investigate spatial association between the centromeric clusters and nucleoli the nucleus of basal epidermal keratinocyte Data was chosen for detailed 3D reconstruction. Information from each channel was reconstructed separately and assembled together after a chromatic shift correction. The reconstruction was done based on manual retrieving of the surface points followed by triangulation and visualization in the MATLAB (Mathworks) program.

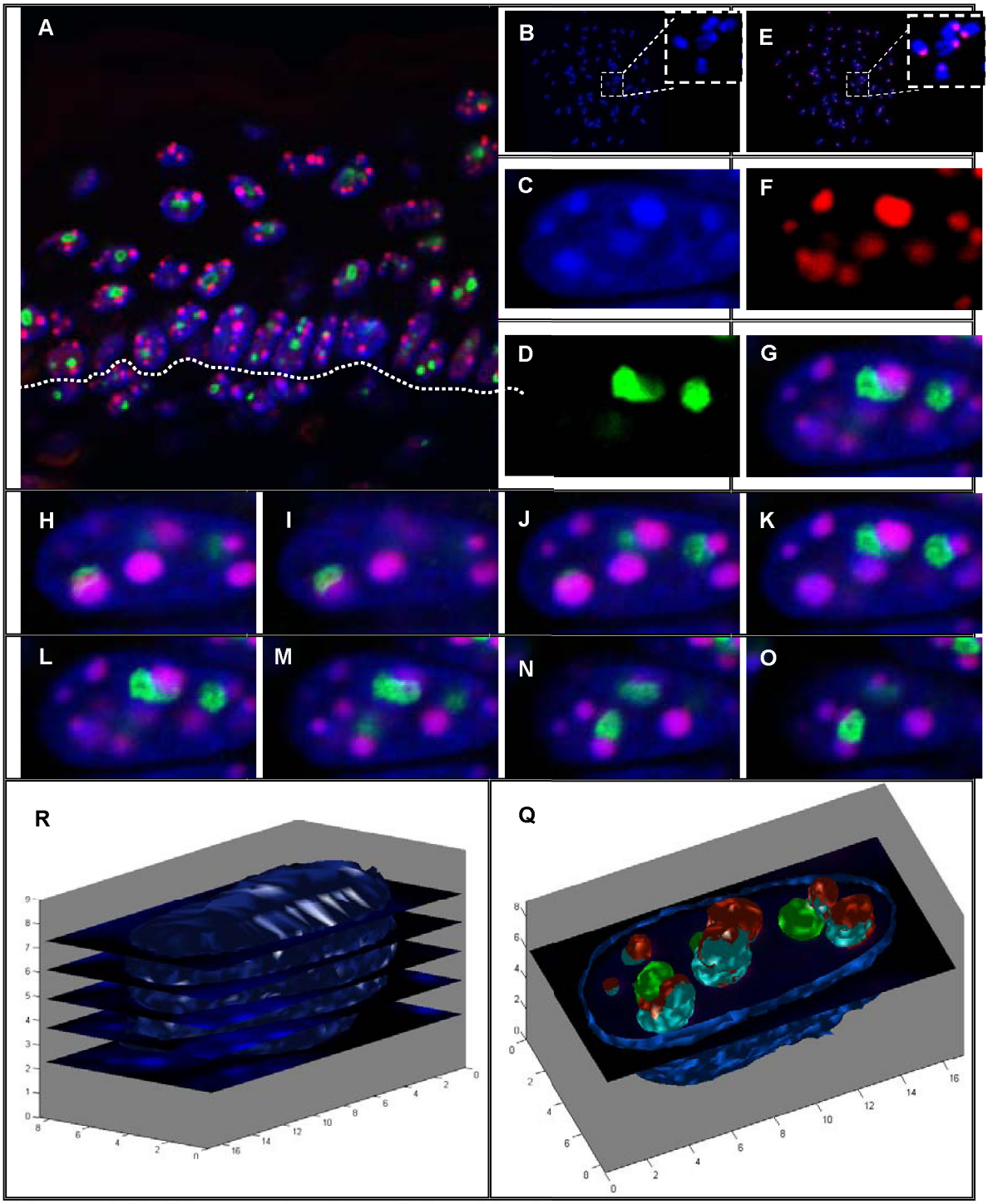

Figure. 3.14 3D reconstruction of the data from 3D confocal scan of FISH with immunostaining for nucleoli on mouse footpad. A- Footpad epidermis hybridized with mouse major satellite probe (red), C,D,F,G – magnified basal layer nucleus; B,E- mouse metaphase spreads hybridized with mouse major satellite probe – centromers localized in subtelomeric positions; H-O – chosen optical sections from nucleus presented in C,D,F,G; R- illustration of 3D-shape reconstruction from confocal scans; Q-reconstruction of nuclear interior presenting: nuclear surface (marine blue), DAPI chromocentres (light blue), mose centromeric clusters (mouse major satellite (red) and nucleoli (green).

3.3 Statistical analysis

Obtained data were analyzed statistically in Excel and its Add-ins. Categorical data were analyzed by the chi-square test of “r x k contingency tables” (Quinn and Keogh, 2002; Samuels and Witmer, 2003a) and data on radial position as well as data on intergene distances were analyzed with analysis of variances (ANOVA) followed by the Newman-Keuls procedure or with T-test for the comparison of the means (Samuels and Witmer, 2003b).

3.3.1 Statistical analysis of the position of loci within the chromosome territory 3.

In analysis of position of loci in relation to chromosome territory 3 (CT3) spatial localizations of FISH signals were assessed and ordered into one of three following categories: peripheral, middle and internal reflecting parts of chromosome territory. Typically 50 nuclei were examined and as outcome frequencies (proportions) of localization of 100 loci in particular positions were obtained.

95% confidence intervals for these proportions were calculated so as to estimate their relation to the real proportion in the population. Distribution of frequencies were assumed to be normal and confidence intervals were computed (Samuels and Witmer, 2003c).

First estimate of the proportion (describing the ratio of observations that fall into particular category to the total number of observations) ṕ - “p tilde”, was calculated:

$$\acute{p} = \frac{y + 2}{n + 4}$$

ṕ - estimate of the proportion, “p tilde”
n- number of observations
y- the number of observations out of n, that fell into category in question

Than standard error of ṕ was estimated:

$$SE_{\acute{p}} = \sqrt{\frac{\acute{p}(1 - \acute{p})}{n + 4}}$$

ṕ - estimate of the proportion, “p tilde”
$SE_{\acute{p}}$ - standard error of ṕ (for a 95% Confidence interval)

Finally 95% Confidence intervals for proportion (frequency) were obtained:

$$\acute{p} \pm 1.96 SE_{\acute{p}}$$

ṕ - estimate of the proportion (“p tilde”, centre of confidence interval)
$SE_{\acute{p}}$ - standard error of ṕ (for a 95% Confidence interval)

Calculations were repeated for each category in each data set.

Localization of loci within CT3 was analyzed in nuclei of different tissues and the aim of this part of the study besides of analysis of distribution of loci within one cell type was also to compare the distribution of loci in different tissues and in different cell types. To investigate the relation between distributions of loci in different cell types statistical analysis by means of Chi-square test (X^2) of “r x k contingency tables” sets was performed. “r x k contingency table” contains

specifically ordered data where “r” stands for raw, data record consisting of the distribution of one loci within chromosome territory 3 in one tissue and “k” means column, represented position: peripheral, middle or internal.

Null hypothesis (H0) on equality of each pair of data sets (data on particular loci in particular tissue) were tested separately assuming probability of wrongly rejection of the H0 (Type I error) below 0.05.

The chi-square statistic (X^2) was calculated from the following formula:

$$X^2 = \sum \frac{(O - E)^2}{E}$$

X^2-chi-square statistic
O – observed frequency
E- expected frequency

Values of expected frequencies were derived each time from the r x k contingency table:

$$E = \frac{(Raw\ total) * (Column\ total)}{Grand\ Total}$$

E- expected frequency

Finally values of chi-square statistics were compared with the critical values for the Chi-square test with 2 degrees of freedom (df) and the level of significance α=0.05:

$$df = (r-1)(k-1)$$

df- degrees of freedom
r - raw
k - column

When 3 or more data sets were compared in one time Bonferroni adjustment was applied so as to avoid the increase of the risk of the Type I error due to summing of risks from particular pair comparisons.

$$\alpha_B = \frac{\alpha}{N}$$

α_B – significance level for a pair of data after Bonferroni adjustment.
α – required final significance level (0.05)
N – number of compared data sets ($N \geq 3$)

3.3.2 Statistical analysis of the radial positions and intergene distances.

Arithmetic means of measurements of either 60 or 80 normalized radial positions of loci and distances between them as well as their confidence intervals were calculated. Than the measurements were compared pairwise by means of T-test and in cases when three means were compared by one-way ANOVA followed by the Newman-Keuls procedure.

So as to be able to use T-test values of the measurements from the sample have to: (1) be similar (not significantly different from) to the normal distribution and (2) have equal variations. Therefore, at the beginning normality of the distribution was checked. First, the data were plotted on the histogram, second, the Lilliefor's normality test was performed (Lilliefors , 1967). Equality of the variances was checked usingLevene's test (Levene , 1960). Both Lilliefor's

and Levene's test calculations were performed using the Excel's Add-in Gerry's stat tools. Additionally independence of the measurements has been assumed.

Confidence Intervals have been calculated in the following way:

$$\acute{y} \mp t_{.025} \frac{s}{\sqrt{n}}$$

ý – mean of the sample
s - standard deviation
$t_{.025}$ – critical value of Student's distribution
n – number of measurements (sample size)

For pair-wise analysis of sets of measurements two-tailed T-test for comparison of data sets with equal variances built in Microsoft Excel2007 were used.

In many cases there was a need for simultaneous comparison of three data sets. In such situation the null hypothesis (H_0) on equality of all three means were tested by f analysis of the variations (one way ANOVA). If H_0 was rejected than further investigation was conducted utilizing Newman-Keuls procedure.

In ANOVA, the means of measurements within the groups and the grand mean were calculated as follows:

$$\acute{y}_{i\blacksquare} = \frac{(y_{i1} + y_{i2} + \cdots + y_{in_1})}{n_i} = \frac{\sum_{j=1}^{n_i} y_{ij}}{n_i}$$

$$\acute{y}_{\blacksquare\blacksquare} = \frac{\sum_{i=1}^{I} \sum_{j=1}^{n_i} y_{ij}}{n^*}$$

$$n^* = n_1 + n_2 + \cdots + n_I = \sum_{i=1}^{I} n_i$$

y_{ij}- observation j in group i
I - number of groups
n_i- number of observations in group i
$\acute{y}_{i\blacksquare}$- group mean for group i
n^*- total number of observations
$\acute{y}_{\blacksquare\blacksquare}$- grand mean, the mean of all observations

Further Sum of Squares (SS, difference between the data record and appropriate mean) between the groups, SS within the groups, mean square as well as degrees of freedom between the groups and within them were calculated as follows:

ANOVA Quantities with formulas			
Source	df	SS(Sum of Squares)	MS (Mean Square)
Between groups	I-1	$\sum_{i=1}^{I} n_i (\acute{y}_{i\blacksquare} - \acute{y}_{\blacksquare\blacksquare})^2$	SS/df
Within Groups	n*-I	$\sum_{i=1}^{I} \sum_{i=1}^{n_i} (y_{ij} - \acute{y}_{i\blacksquare})^2$	
Total	n-1	$\sum_{i=1}^{I} \sum_{j=1}^{n_i} (y_{ij} - \acute{y}_{\blacksquare\blacksquare})^2$	

Table 2.4 Formulas for basic ANOVA quantities.

Finally the null hypothesis (H_0) on means' equality was tested by F test with two parameters: numerator degrees of freedom equal to df(between) and denominator degrees of freedom equal to df(within) and the significance level α=0.05. The F statistic were calculated as follows:

$$F_S = \frac{\mathrm{MS(between)}}{\mathrm{MS(within)}}$$

If the value of statistic was higher than the critical value from F distribution table, H_0 is rejected and data sets underwent the Newman-Keuls procedure.

In the Newman-Keuls procedure sample means were arranged in the arrays of increasing order. Next critical values were calculated:

$$R_i = q_i \sqrt{\frac{MS(within)}{n}}$$

R_i- critical value
q_i-constrant (taken from the table for critical constrants for the Newman-Keuls procedure)
MS(within) – mean square calculated during ANOVA analysis

The critical values (R_i) were than compared with the differences between sample means. If the respective R_i was smaller than the difference between the samples than the hypothesis was rejected, which means that means of the sample are significantly different.

4. Results

4.1 Changes in the three-dimensional nuclear organization and chromatin structure during terminal keratinocyte differentiation in epidermis.

4.1.1 Changes in the shape of the nucleus during terminal keratinocyte differentiation.

For proper comparison of the size and shape of nuclei from different layers of the epidermis, 3D measurements of the nuclei from 80 μm thick cryosections of the foot pads from newborn mice scanned with confocal microscope were performed. Quantitative data along with the MATLAB reconstruction of the cryosections of footpad epidermis stained with antibody against Ki67 are shown in **Figure 4.1**.

Topography of the nuclei in the mouse foot pad epidermis, as well as nuclear shape generated by the reconstruction based on 3D confocal scan are shown in **Fig. 4.1A**. The area of the epidermis of approximately 77 μm x 73 μm selected for analysis consisted of 120 cells: 62 basal layer keratinocytes, 44 spinous layer keratinocytes forming three layers of cells (23, 18 and 3 cells) and 14 of granular layer keratinocytes (**Fig4.1B**).

The most striking and easily recognized difference was a change in the orientation of the longest axis (dimension) of epidermal cell nuclei. In the basal layer, the longest axis was oriented perpendicularly to the basal membrane, whereas nuclei in spinous and granular layers were oriented parallel to the

basal membrane and perpendicularly to the longest axis of the nuclei in basal layer.

To assess quantitatively changes in the shapes of nuclei from different epidermal layers nuclear shapes were approximated with MATLAB by fitting ellipsoids into the sets of points from the nuclear surface depicted by nuclear dye (DAPI), followed by a comparison of the ratios of the long axis to the average of 2 shorter axes (ratio E, **Fig.4.1B**). Nuclei from the basal and granular layers were significantly more elongated (E ratio = 1.87 and 1.76 respectively) than nuclei from the spinous layer (1.46, p-value<10^{-3}).

Nuclei from the basal epidermal layer had an average volume of 361.15 ± 98.6 μm^3 and were about 25% larger (p-value < 10^{-7}) than nuclei from spinous and granular layers with average volumes of 257.21 ± 66.2 (**Fig. 4.1C**). Since first volume measurements of volume of basal layer nuclei showed considerable variability, we performed additional measurements on cryosections stained with antibodies against Ki67 which depicts proliferating cells, especially cells in S and G2 phases of cell cycle. It turned out that Ki67 positive basal keratinocytes had nuclei of about 12 % larger (384.64 ± 116.4 $\mu m^{3)}$ versus Ki67 negative basal keratinocytes (337.66 ± 70.9 $\mu m^{3;}$ p-value=0.046; **Fig. 4.1C**).

Proliferating (Ki67 positive) cells were present only in the basal layer (14 Ki67 positive nuclei; 22.5% of all basal layer keratinocytes), while they were absent in the upper (spinous and granular) epidermal layers.

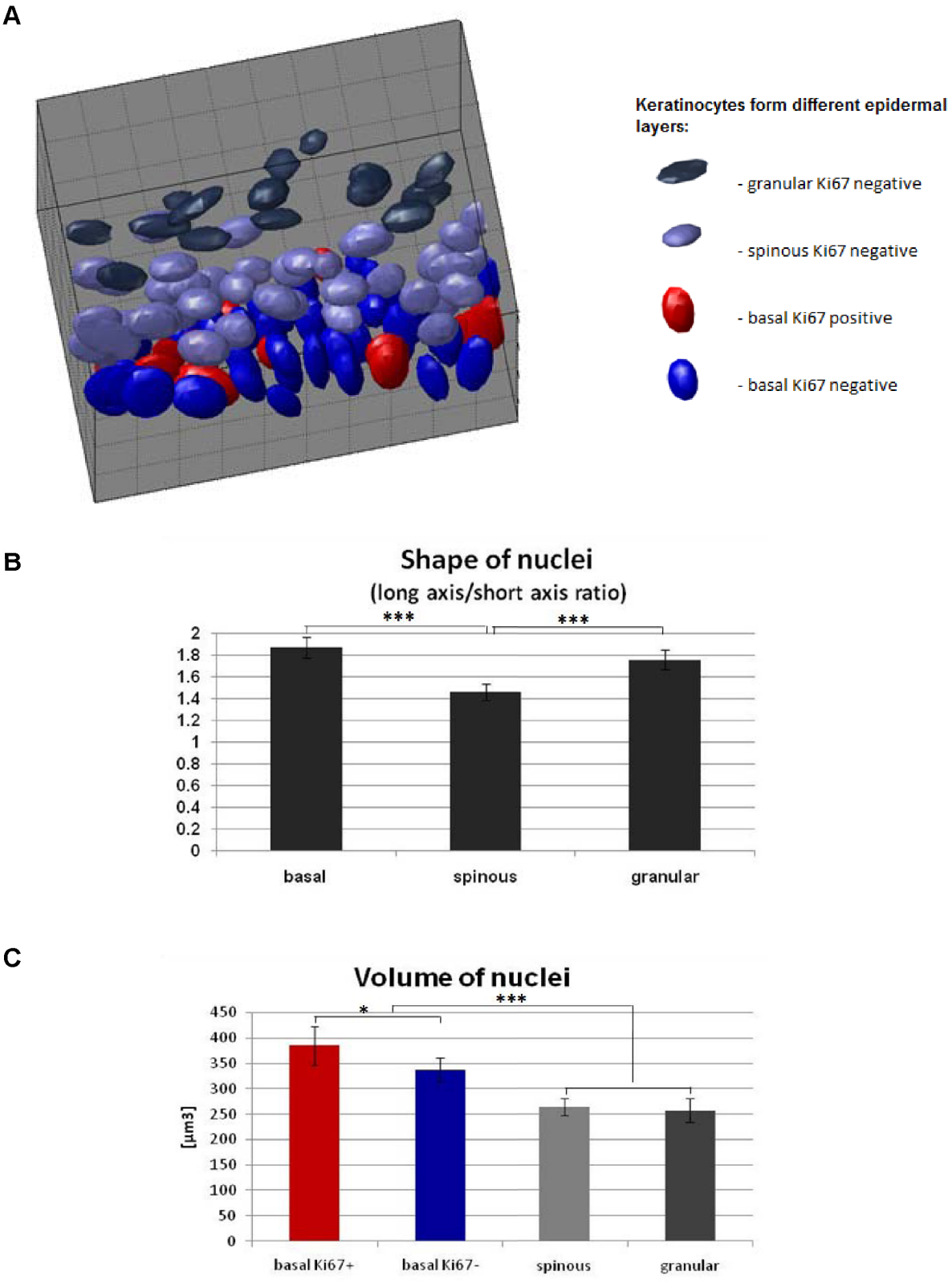

Figure 4.1. Remodelling of nuclar size and shape during terminal differentiation of keratinocytes in murine epidermis. A – Nuclei in mouse footpads epidermis stained with marker of proliferating cells antibody against Ki67 and DAPI – 3D reconstruction of confocal stack images, B – Remodelling of shape of nuclei during epidermal differentiation, C- decrease of the nuclear volume during keratinocyte differentiation.

4.1.2 Transcriptional activity in keratinocytes increases in the spinous layer and decreases in the granular layer of the epidermis.

Transcriptional activity of the epidermis was evaluated by immunofluorescence with established markers of active euchromatin – trimethylated on Lysine 4 histone H3 (H3K4trimet; **Fig. 4.2A**) and distinct forms of RNA polymerase II (Pol II; **Fig.4.2B -4.2C**). Immunostaining with antibody against H3K4trimet showed high levels of expression in the basal and first/second layers of spinous cells and then significantly decreased in the granular layer. Immunostaining with the antibody against total CTD domain of RNA Pol II (**Fig. 4.2B**) and with antibodies against CTD domain of Pol II phosphorylated on serine 2 (elongating pol II, **Fig.4.2C**) showed strong expression in the basal layer and even stronger in the spinous layers, while it was decreased significantly in the granular layer. Thus, keratinocyte differentiation in the epidermis is accompanied by the increase of expression of the markers of “active chromatin” in the spinous layer followed by marked decrease of expression in the granular layer.

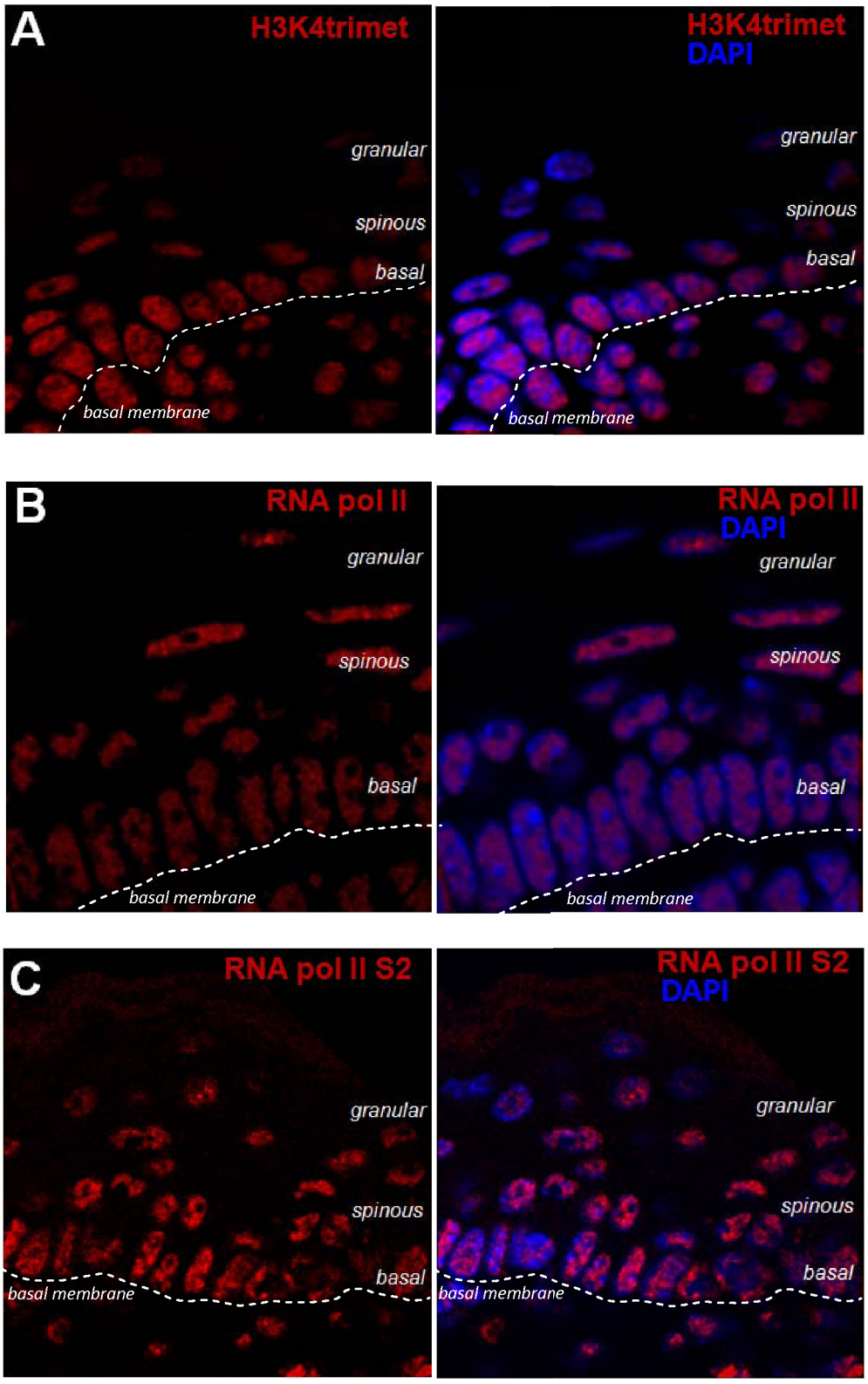

Figure 4.2. Decrease in expression of markers of transcriptionaly active chromatin during terminal keratinocyte differentiation. Markers of active chromatin are strongly expressed in basal and spinous layers, while showing a remarkable decrease in their expression in the granular layer. A - H3K4trimet; B – RNA Pol II (active and inactive); C phospho-serine-2 RNA Pol II (elongation of transcription);

4.1.3 Decrease of the number of nucleoli and increase of their volume in terminally differentiated keratinocytes.

Nucleoli are the largest nuclear bodies and they are formed only around active NOR regions of the distinct chromosomes. Nucleoli tether different NOR bearing chromosomes together thus having an influence on the 3D nuclear structure. To describe the patterns of distribution of nucleoli in different layers of epidermis, an immunofluorescent detection of nucleolar marker nucleophosmin (B23) was performed. The nucleoli number and their volumes were calculated (**Fig. 4.4A, 4.4C**) as well as radial positions (**Fig.4.4B**) were measured. Results were visualised by generating 3D models of the average nucleoli from different epidermal layers (**Fig. 4.3B-D**).

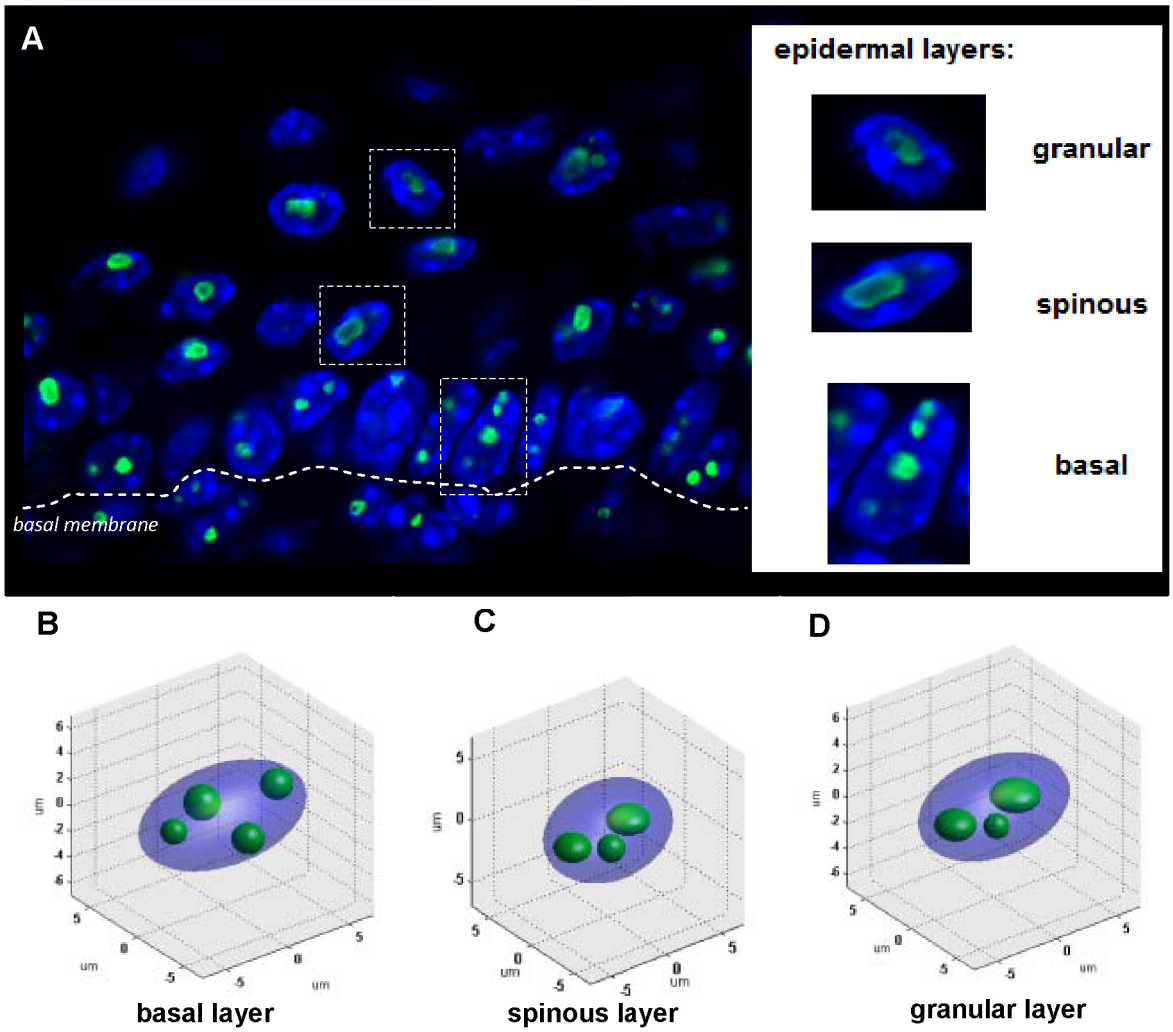

Figure 4.3. Remodelling of nucleoli during terminal differentiation of keratinocytes in murine epidermis – immunostaining and nuclear models. A- Differences in the number, size and distribution of nucleoli demonstrated by immunofluorescence with antibody against nucleophosmin (B23). B-D Mathematical modelling of the average keratinocyte nucleus from the distinct epidermal layers: basal (B), spinous (C), granular (D).

Quantitative analyses showed that nuclei of the epidermal basal cells have significantly more nucleoli (4.16 ± 0.96 per nucleus, **Fig. 4.4A**) compared to the nuclei of more differentiated spinous layer cells (3.21 ± 0.8; p-value=0.0021), which in turn was more than in the granular layer (2.82 ±1.02; p-value=0.0186). Interestingly, the number of nucleoli in the granular layer was similar to the number of nucleoli in dermal fibroblasts (2.78 ± 0.77).

Despite a significantly decreased number of nucleoli in the spinous layer, their total volume per nucleus (29.2 ± 10.6 μm^3 and 11.3 % of the volume of the nucleus, **Fig. 4.4C**) was significantly increased and was on average 25% bigger than in the basal layer (20.8 ± 8.3 μm^3 and 7% of the nuclear volume). In the granular layer the volume of the nucleoli decreased compared to the spinous layer, however, it was still larger than in the basal layer (24.7 ± 9.8 and 9.6% of nuclear volume). The average size of individual nucleoli increased in more differentiated cells – the smallest nucleoli were seen in the basal layer (5.26 ± 2.28 μm^3, **Fig.4.3C**), while the volume of nucleoli in spinous and granular layers was increased more than twice (11.4 ± 6.7 μm^3 and12.7 ± 9.21 μm^3 ,respectively). In addition, in more than 10% of nucleoli in the spinous and granular layers, unusually big nucleoli with the volume exceeding 10% of the volume of nucleus were seen. Thus these data suggest that during terminal keratinocyte differentiation, the number of nucleoli is decreased, while their volume is increased, perhaps due to their fusion.

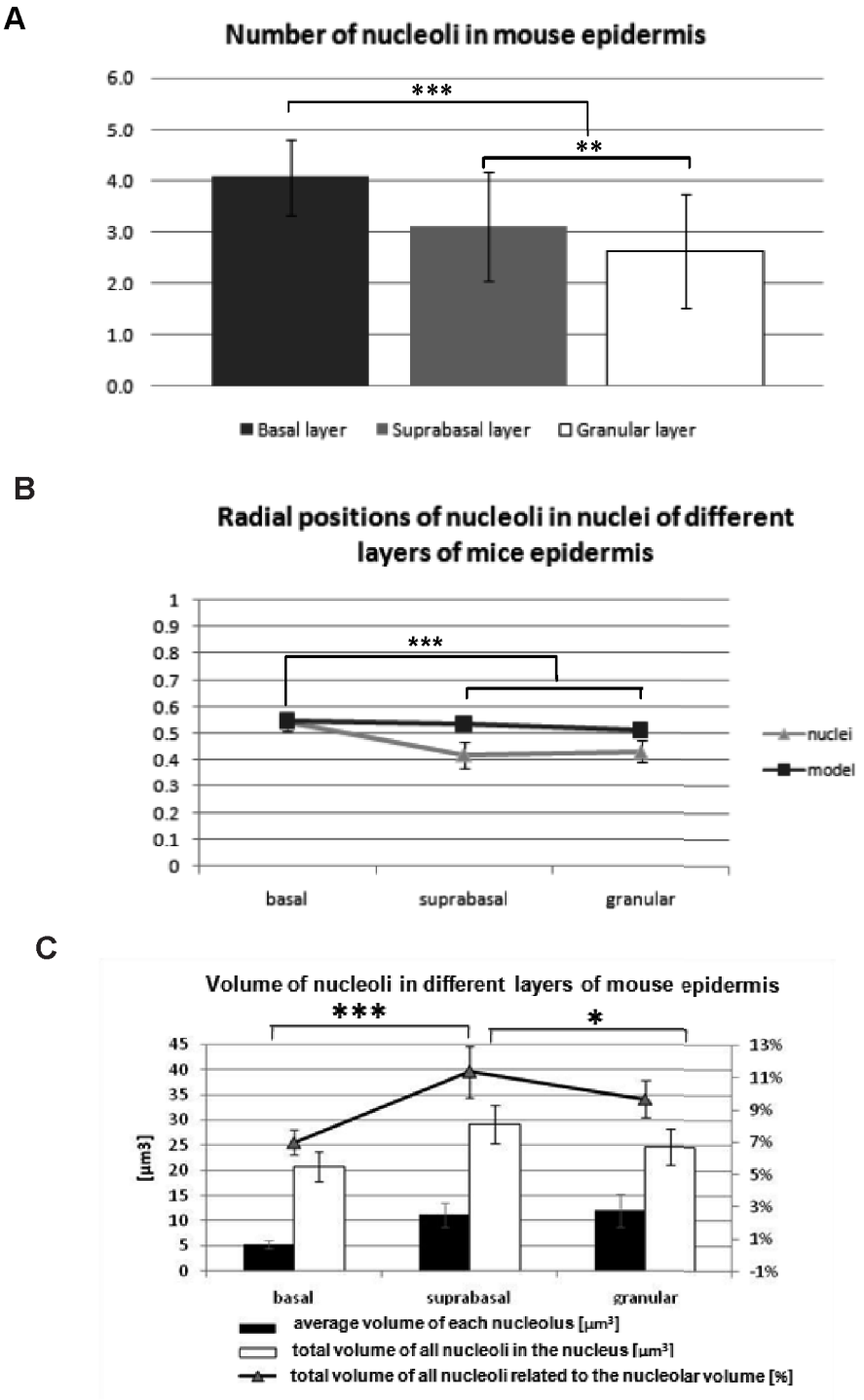

Figure 4.4. Remodelling of nucleoli during terminal differentiation of keratinocytes in murine epidermis –quantitative analysis. A- Changes in the number of nucleoli during epidermal differentiation. B- Distribution of nucleoli in different layers of the epidermis compared with random mathematical model. C- Increase in the volume of the nucleoli in the spinous and granular layers versus basal epidermal layer. (Average size of nucleoli, average of sum of volumes of nucleoli (VS) in the nuclei and VS related to nuclear volume are presented).

Decrease in the number of nucleoli in upper layers of epidermis was associated with repositioning of the nucleoli into more internal positions. In the basal layer, the average radial position of nucleoli (distance from nuclear centre related to the length of the radius coming through the centroid of the nucleolus) was 54.3 ±9.8% while in the spinous layer (**Fig. 4.4B**) it was more than 10% lower (42.2 ±14.1%), similarly to the granular layer (43.4 ±11.7%; p-value<10^{-3}).

To determine whether changes in the nucleolar positioning in epidermal cells are the result of pure geometrical constraints or other factors including changes in gene expression may also be involved in the mathematical model of average nuclei from every epidermal layer that was designed. Each model nuclei has the average size and shape characteristic for a particular layer, and also the average number and volumes of nucleoli and centromeric clusters (based on measurements of nuclei dimensions and quantification of number and size of nucleoli and centromeric clusters described before). The distribution of nucleoli and clusters was random and restricted by two conditions: 1.) they have to be within the nucleus and 2.) they cannot overlap.

Radial positions of nucleoli in the model are not significantly different and within the range of 55-57%. In the spinous and granular layers radial positions from the experiment were more than 20% below the model which allows us to conclude that the more internal position of nucleoli in these layers is not only the outcome of geometric changes, but also some additional forces such as biochemical changes associated with cell differentiation are involved.

4.1.4 Terminal keratinocyte differentiation is associated with an increase of the number of centromeric clusters and with changes in their position to more peripheral versus un-differentiated cells.

Centromeres due to their fusions and association with nuclear border or nucleoli are, together with nucleoli, probably the most important factors responsible for determining 3D nuclear organization. They consist mainly of different DNA repeats which form the heterochromatin (**Fig. 4.6C**) visualised with an antibody against histone H3 trimethylated on lysine 9 which marks all centromeric clusters and is an established marker of heterochromatin.

The distribution of centromeric clusters was analysed in a way similar to the nucleoli (except for the volumes) based on the FISH signal from the mouse pancentromeric probe (**Fig.4.5A**). This probe hybridises with mouse major satellite repeat which is located in the central domain of each mouse centromere. Results were visualized in the 3D models generated as an average nucleus from different epidermal layers (**Fig. 4.5B-D**).

The analysis showed that the number of centromeric clusters increases from 13.33 ±3.7 in basal layer to 16.57 ±3.15 and 16.10 ±3.13 in spinous and granular layers respectively (p-value< 10^{-3}, **Fig.4.6A**).

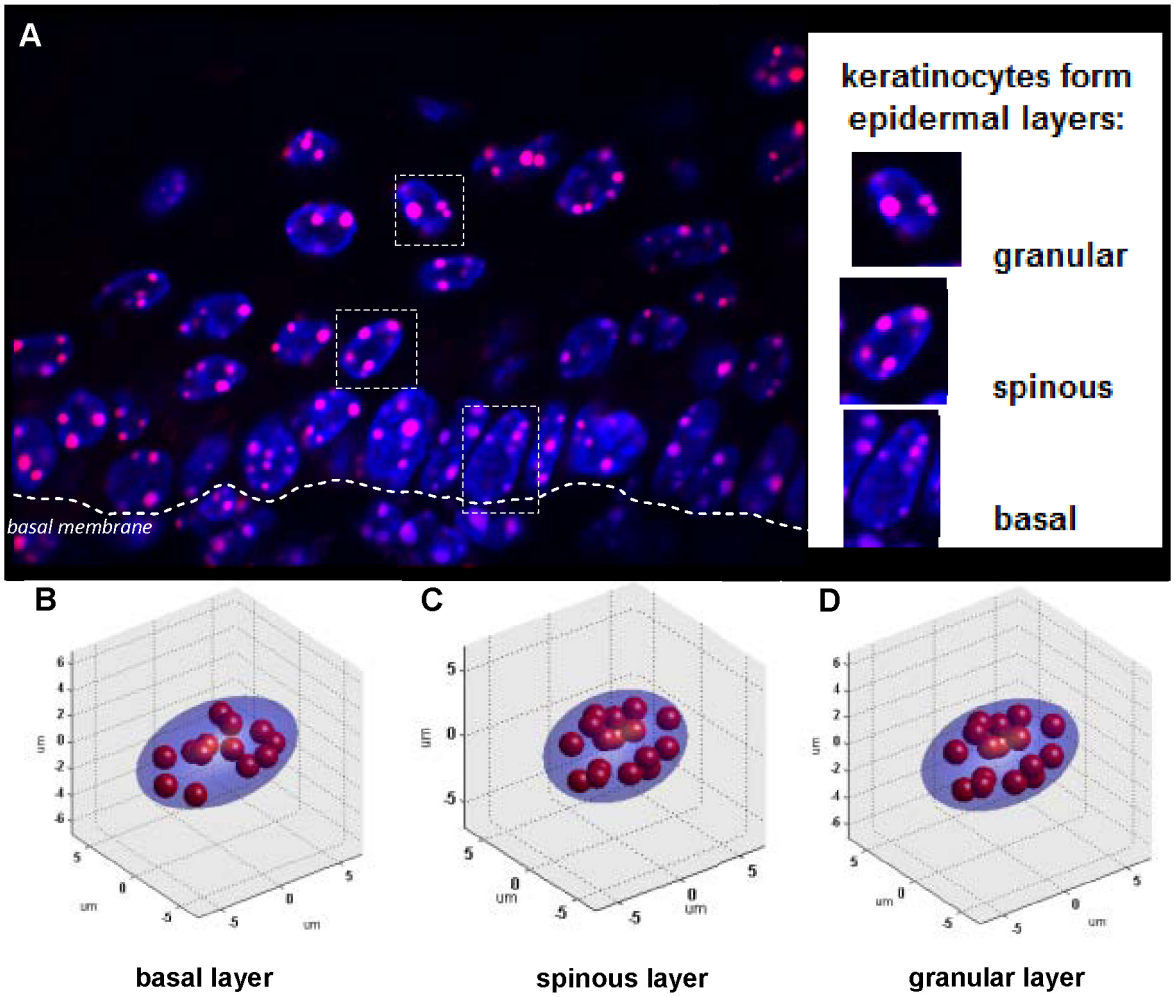

Figure 4.5. Remodelling of heterochromatic clusters during terminal differentiation of keratinocytes in murine epidermis – immunostaining and nuclear models. A- Differences in the number, size and distribution of nucleoli demonstrated by immunofluorescence by FISH with mouse pancentromeric probe. B-D Mathematical modelling of the average keratinocyte nucleus from the distinct epidermal layers: basal (B), spinous (C), granular (D).

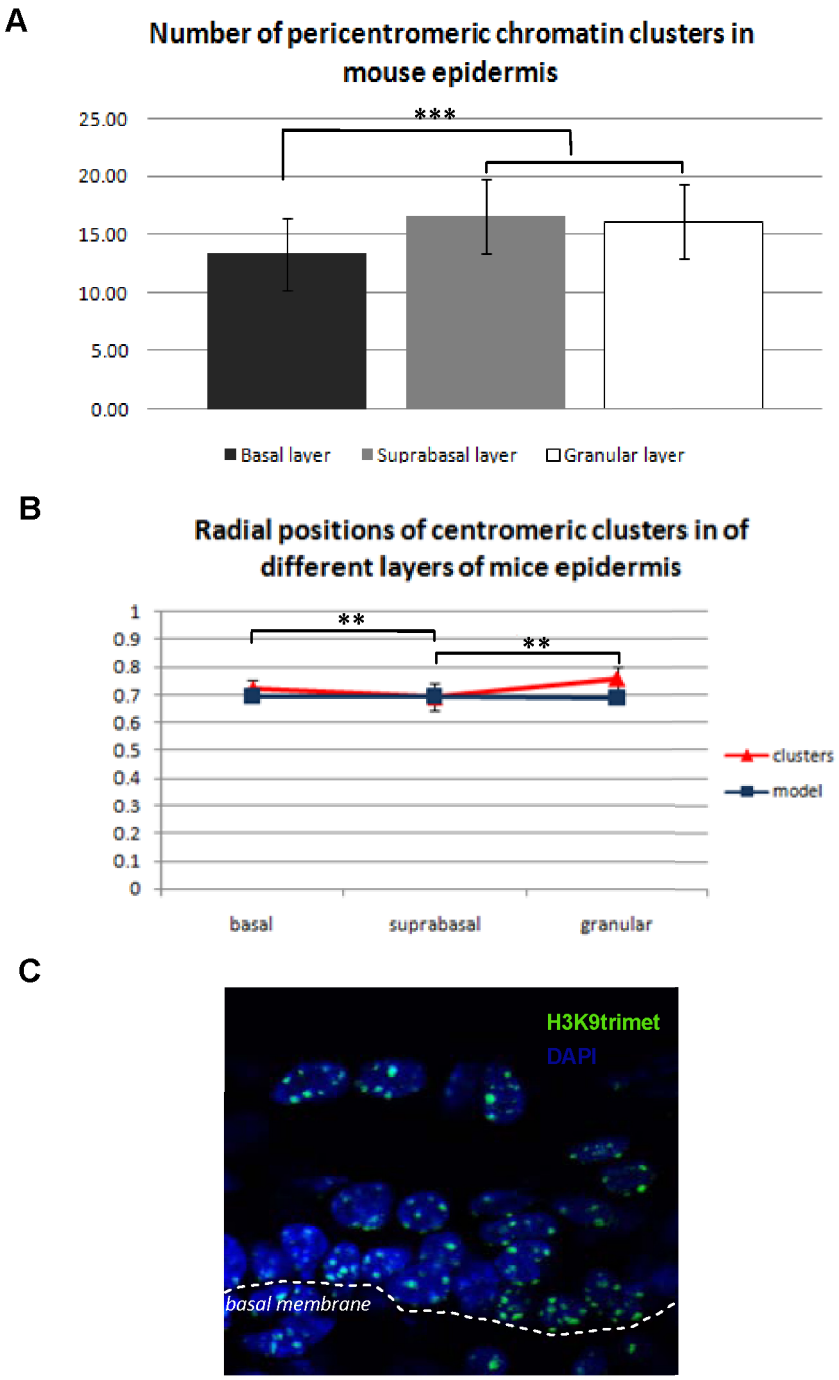

Figure 4.6. Remodelling of heterochromatic clusters during terminal differentiation of keratinocytes in murine epidermis quantification. A - Changes in the number of clusters during epidermal differentiation. B- Distribution of heterochromatic clusters in different layers of the epidermis compared with a random mathematical model. C- Heterochromatic marker histone 3 trimethylated on Lysine 4 detected by immunofluorescence marks the same spaces as pancentromeric probe.

Average radial positions of centromeric clusters increased from 72 ±4% in basal layer up to 76 ±4% in spinous layer (p-value< 10-2,**Fig.4.6B**) and decreased in the granular layer to 69 ±7% (p-value< 10-4).

Comparison of the experimental radial positions with the radial positions from the mathematical model indicated that in granular layer repositioning of centromeric cluster cannot be fully explained by geometrical changes of the nuclear shape and is likely to be subject of influence of other factors.

These data suggest that terminal keratinocyte differentiation in the epidermis is accompanied by re-distribution of heterochromatic centromeric clusters, which are increased in number and are getting more dispersed in the nucleus of terminally differentiated cells.

4.1.5 Centromeric clusters and nucleoli contact each other creating three dimensional structural network of constrains, which changes during terminal keratinocyte differentiation.

Centromeres as well as nucleoli tether together different chromosomes in the interphase nuclei (homologous chromosomes fuse together rarely).

To visualise the interactions between centromeric clusters and nucleoli, a model reconstructing the nucleus from epidermal basal layer with centromeric clusters detected by DAPI and pancentromeric probe as well as with nucleoli depicted by antibody against nucleophosmin was prepared. This reconstruction is presented in **Figures 4.7A-E**, exposing different details separately and all together.

In **Fig.4.7G** we isolated nucleoli and only those centromeric clusters which interact with nucleoli. It was found that 5 centromeric clusters out of 14 were associated with nucleoli, whereas three nucleoli were associated with one centromeric cluster and one with two clusters.

Comparison of fluorescent signals coming from nucleoli and centromeric clusters demonstrated that centromeric clusters and nucleoli are localized very closely to each other and partially fuse during keratinocyte differentiation (**Fig.4.7H-M**). Quantification of these interactions showed that in the nuclei of epidermal basal layer cells these associations are more frequent (**Fig 4.7N**), compared to spinous and granular layers.

Thus terminal keratinocyte differentiation in the epidermis is accompanied by dynamic changes in:

1.) the distribution of transcriptionally active chromatin;

2.) volume and number of nucleoli;

3.) number and inter-nuclear localization of centromeric clusters;

4.) number of associations between the nucleoli and centromeric clusters.

These data suggests that 3D-architecture of the nucleus shows marked re-arrangements during transition of the nucleus from very active state (basal and spinous epidermal layers) to inactive state (granular layer).

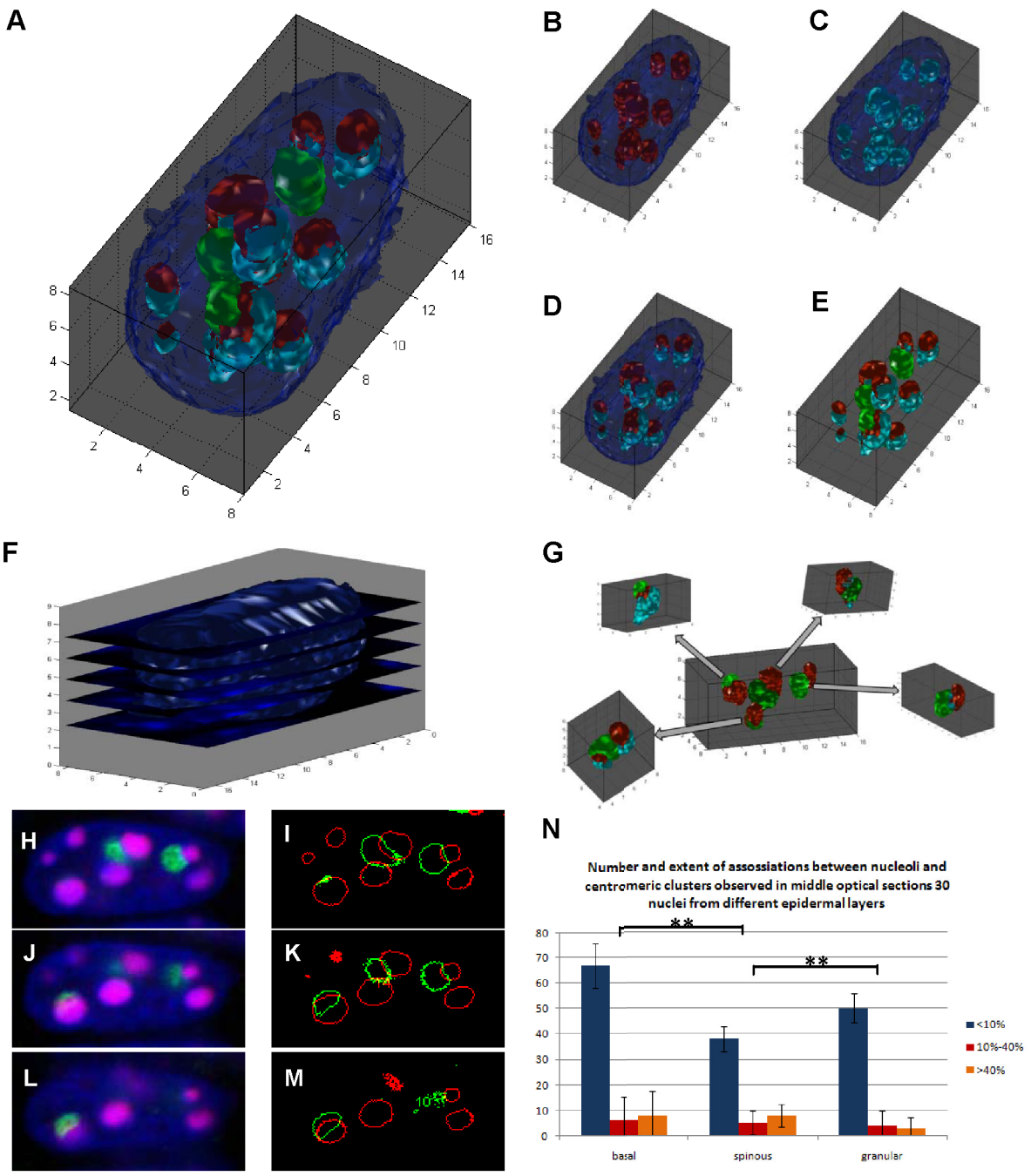

Figure 4.7. Interactions between the nucleoli and heterochromatic clusters in basal epidermal keratinocytes. A - 3D-reconstruction of basal epidermal keratinocyte nucleus including the nucleoli and hetero-chromatic clusters depicted by anti-B23 antibody, pancentromeric murine 3D-FISH probe and DAPI. B-E,G – Only some elements of the model are visualised: heterochromatic clusters detected with pancentromeric probe (B), heterochromatic clusters detected with DAPI (C), overlay of pancentromeric and DAPI signals show differences (D), heterochromatic clusters and nucleoli (E), nucleoli and only these clusters which interact with them. F- 3D map visualising optical sections showed below (H-M). H-M – heterochromatin within nucleoli shown in different optical sections. N-Nucleoli interact with centromeric clusters more frequently in basal layer, in spinous layer number of interactions is smaller than in basal and granular, but spinous layer nuclei have more big "overlaps" between clusters and nucleoli than in granular layer.

4.2 Remodelling of the higher-order chromatin structure of the epidermal differentiation complex (EDC) during skin morphogenesis in mice.

Epidermal differentiation complex (EDC) and Loricrin relocate from the nuclear periphery towards centre during normal skin development.

Because of the remarkable changes in the nuclear architecture occurring during terminal keratinocyte differentiation in adult epidermis, the next step of the work was focused on the analyses of higher-order chromatin organization of tissue-specific gene loci in epidermal cells during development. For further analyses epidermal differentiation complex (EDC) was chosen, which is located on mouse chromosome 3 and contains large number genes activated during terminal keratinocyte differentiation and epidermal barrier formation.

It was shown that there are remarkable changes in the nuclear positions of EDC in the epidermal basal cells of 16 day-old mouse embryo (E16.5) compared with 12 day-old embryo (E11.5). 3D FISH showed that epidermal differentiation complex (EDC) loci were located at the periphery close to the nuclear membrane at E11.5, whereas at E16.5 the majority of the loci had a more internal position. These findings were confirmed by further analysis of the Loricrin gene as a part of EDC, which was selected because of the high increase of its expression during skin development. Such a big shift in the position was not observed for analysed control loci either from the genomic neighbourhood close to EDC - Rps27, Gabpb2 (0.3 Mb and 1.5 Mb distant from 5'- and 3'- flank regions of EDC) or more distant neighbourhood - Tdo2 (EDC 5' distal flank, the loci) and RhoC (8 Mbp and 11Mb distant from from 5'- and 3'- flank regions of EDC). Positions of the loci were analyzed in three different

ways. First they were related to the distinct parts of chromosome territory 3 (internal - closest to the nuclear interior, middle and peripheral closest to nuclear border). Frequencies of their localization relative to the distinct parts of chromosome territory were summarized and presented in the figures. To confirm the positional changes of the loci observed their radial positions and intergene distances were measured. Finally, calculated intergene geometrical distances were related to the distances between the loci expressed in base pairs of the DNA length.

4.2.1 EDC and Loricrin relocate from the nuclear periphery towards the centre between E11.5 and E16.5.

4.2.1.1 EDC and Loricrin relocate from the nuclear periphery in E11.5 towards interior and retain their positions in later developmental stages.

Positions of EDC in nuclei of the epidermal basal layer nuclei of 12 days old embryo (E11.5) are at least 3 times more frequent on the peripheral part of chromosome territory 3 than in more developmentally advanced epidermis. Loricrin as a part of EDC, takes similar positions at E11.5 and E16.5, and is found less frequently in the middle position at p10.

Inter-nuclear EDC positions were analysed by 3D-FISH in the epidermal basal cell nuclei at the following stages of development: 12 day- old embryo (E11.5), 16 day-old embryo (E16.5), 17.5-days old embryo (E17.5) and 10 day-old mice (P10, **Fig.4.8B**). In case of Loricrin, the epidermal basal layer cells were examined in E11.5 and E16.5 embryos, as well as in 10 day-old mice (P10, **Fig.4.9B**).

A

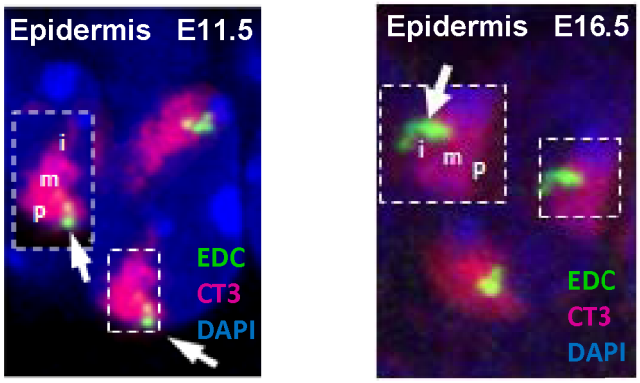

B

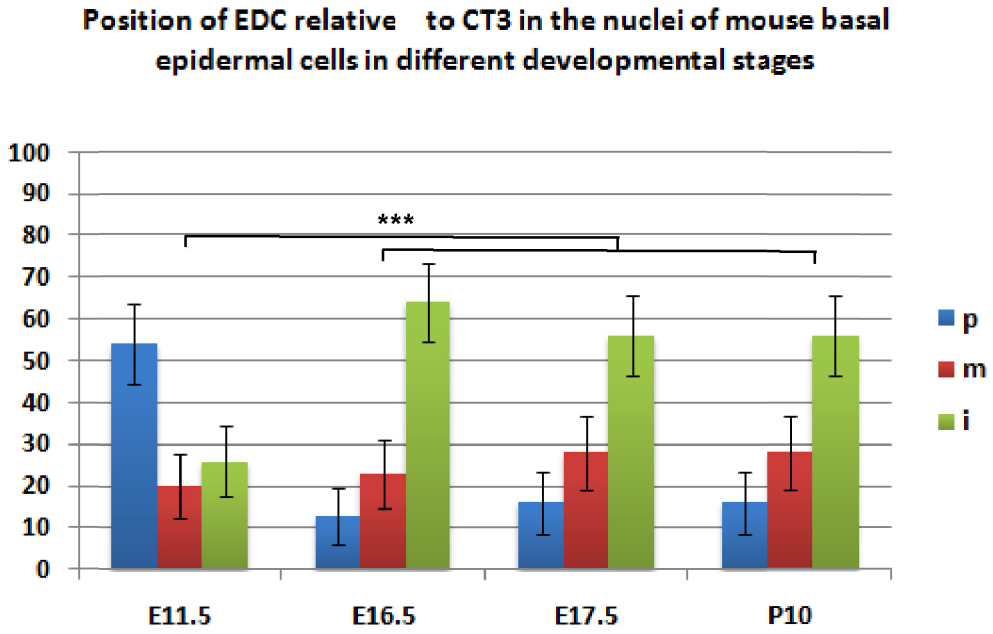

Figure 4.8. Position of the epidermal differentiation complex (EDC) relative to chromosome territory 3 (CT3) in nuclei of the epidermal basal layer cells of the wild type mouse. 50 nuclei (100 loci) of epidermal basal layer cells of 12 days old embryo (E11.5), 16 days old embryo (E16.5.5), 17.5 days old embryo (E17.5) and 10 days old mouse (P10) were assessed. The number of loci in particular chromosome parts are shown on the figure.

It was shown that there is significant difference (p-value $<10^{-7}$) in the distribution of EDC between the nuclei at E11.5 and more developmentally-advanced stages (**Figure 4.8B**). 54% of the loci at E11.5 showed peripheral positions, while 26% were located internally. At E16.5, E17.5, P10 the percentage of loci at the peripheral positions decreased and varied from 13% to 16%, whereas 56% to 64% of the loci showed internal positions.

Since EDC occupied 3 Mbp domain on chromosome 3 to improve the precision of analysis and check if the distinct points of the EDC behave in the same manner as the whole locus, the intra-nuclear position of the Loricrin gene was analyzed as well.

Similarly to the whole EDC, Loricrin showed a similar nuclear localization in the nuclei of epidermal cells at all developmental stages (**Fig. 4.9B**). In particular, Loricrin loci were significantly more frequent at the peripheral position at E11.5 (p-value $<10^{-5}$; peripheral 55%, 26% internal) versus E16.5 (12% peripheral, 52% internal) and P10 (27% peripheral, 60% internal). These observations supported the hypothesis that the relocation of the EDC and Loricrin towards the interior is required for efficient transcription.

A

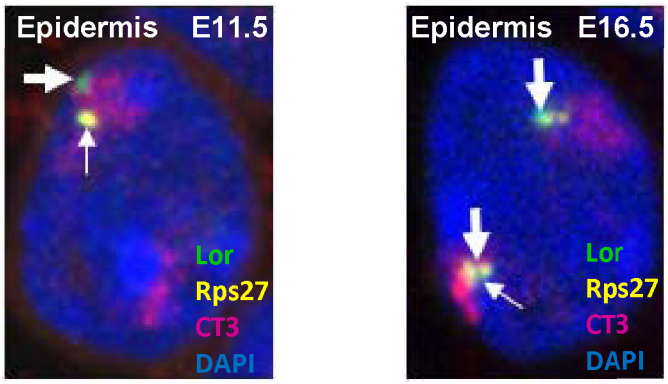

B

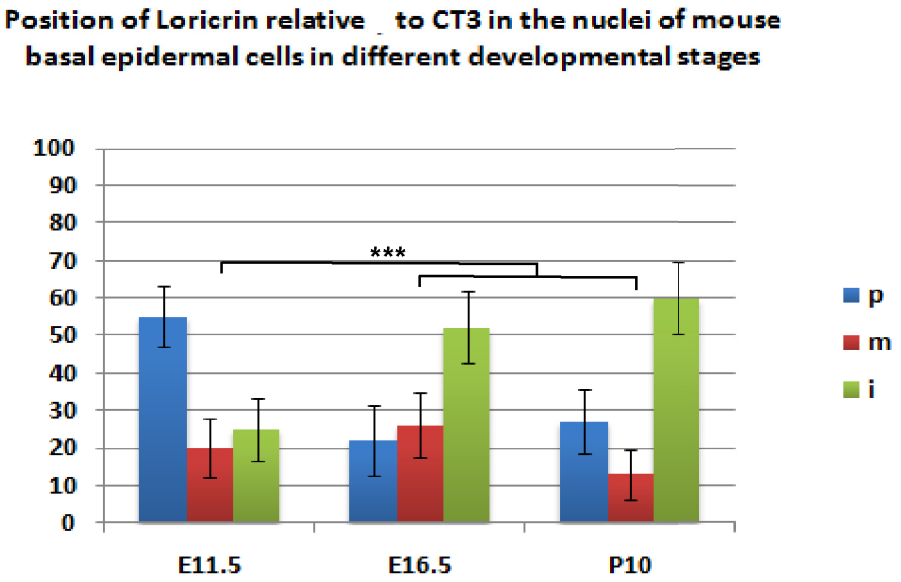

Figure 4.9 Position of Loricrin relative to chromosome territory 3 (CT3) in the nuclei of the wild type mouse epidermal basal layer cells. Nuclei of the epidermal basal layer cells of the 11.5 day-old embryo (E11.5), 16.5 day-old embryo (E16.5.5) and 10 day-old mouse (P10) were assessed.

However, the position of the Loricrin at E16.5 and P10 were not changed which further proves that relocation of the Loricrin towards the nuclear centre is a permanent process required for maintenance of high levels of its expression.

4.2.1.2 In contrast to the EDC, intra-nuclear position of the control loci in epidermal progenitor cells change moderately or do not change at all between the distinct developmental stages.

All control loci had mostly internal positions in E11.5 which supports the hypothesis on specificity of changes in the position between E11.5 and E16.5 for EDC and Loricrin. More than 60% of Rps27 loci at E11.5 were located in the internal part of chromosome territory 3 and this was significantly higher at E16.5 and p10. Gabpb2 was also located mostly internally, however there were no significant changes in the internal position of the Gabpb2 loci between e17.5 and E11.5. Tdo2 and RhoC showed more internal positions than Loricrin and EDC at E11.5 but had similar distribution to them at E16.5.

In order to assess specificity of the observed relocation of the Loricrin and EDC from the nuclear periphery at E11.5 into the nuclear interior, distributions of the control neighbouring loci Rps27 (**Fig.4.10**), Gabpb2 (**Fig.4.11**) and two more distant (10 Mbp) loci Tdo2 and RhoC (**Fig.4.12**) were examined.

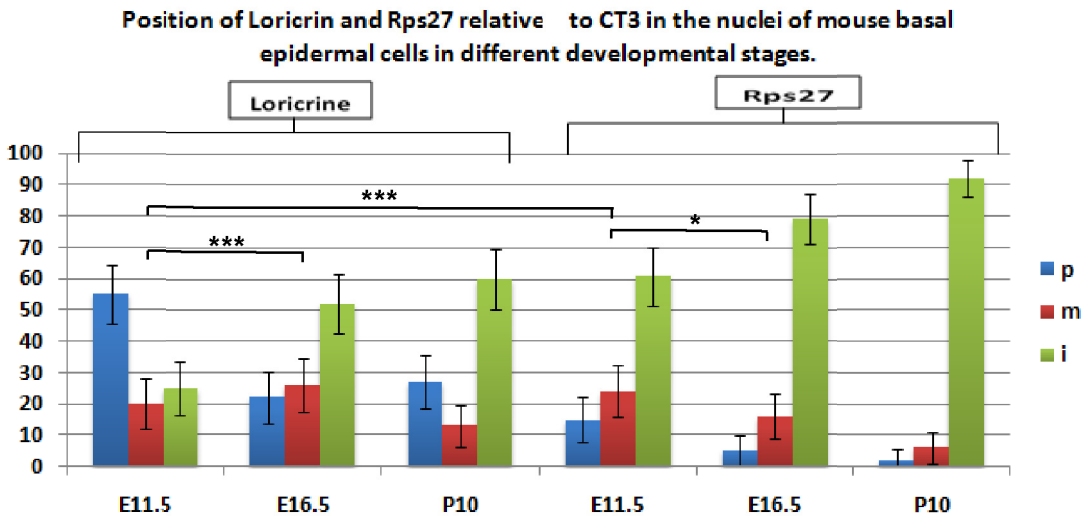

Figure 4.10. Position of Loricrin and Rps27 relative to chromosome territory 3 (CT3) in the nuclei of the wild type mouse epidermal basal layer cells. Nuclei of the epidermal basal layer cells of the 11.5 days old embryo (E11.5), 16.5 days old embryo (E16.5) and 10 days old mouse (P10) were assessed.

In contrast to Loricrin and EDC, positions of the Rps27 in relation to CT3 at all examined developmental stages were mostly internal which supports the hypothesis about the specificity of the movement of Loricrin in epidermal progenitor cells (**Fig.4.10**).

Analysis also showed that there is significant increase in the number of loci in internal position at E16.5 (79%) compared to E11.5 (61%, p-value=0.012), and at P10 (92%) versus E16.5 (79%, p-value = 0.033; significant for this pair however not fulfilling condition of Bonferroni adjustment). This relocation may be due to the close proximity of Rps27 to EDC (0.3 Mb).

Compared to the Loricrin and EDC, Rps27 was seen significantly more frequently in the internal part of CT3 at all developmental stages. The most pronounced differences were seen in 12 day-old embryo when most of the Loricrin and EDC loci were located peripherally and Rps27 loci were located mostly internally.

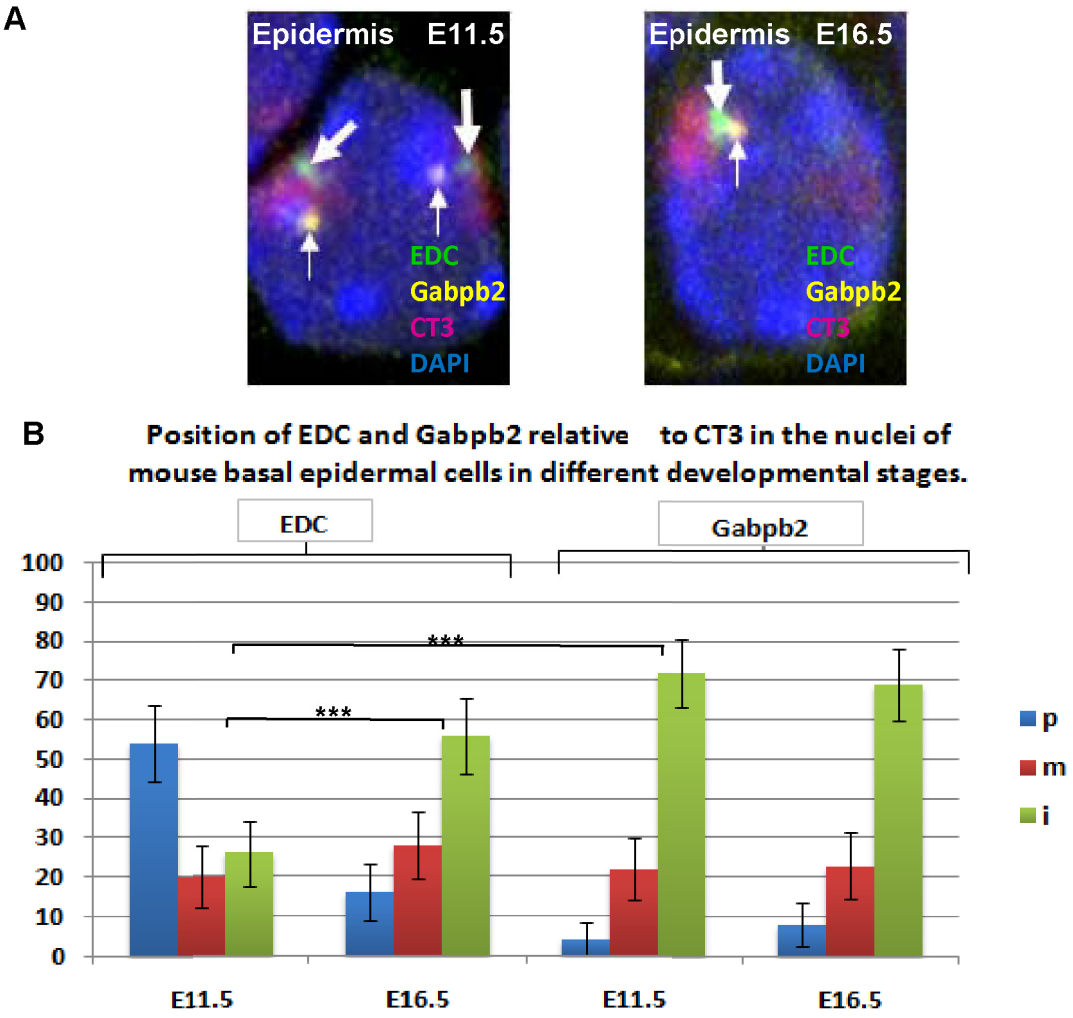

Figure 4.11 Position of EDC and Gabpb2 in relation to chromosome territory 3 (CT3) in the nuclei of the wild type mouse epidermal basal layer cells. Nuclei of the epidermal basal layer cells of the 11.5 days old embryo (E11.5), and 16.5 day-old embryo (E16.5) were assessed.

Gabpb2 positioning was also located more internally compared to EDC and Loricrin at E11.5 (72% versus 26% for EDC; **Fig.4.11**). However, at E16.5 there were no significant differences between the positioning of the Gabpb2 and EDC. Although, Gabpb2 was located slightly more internally (peripheral 4%, internal 72%, p-value=0.025) at E11.5 versus Rps27 (peripheral 15, internal 61%), there were no significant differences between the positions of the Gabpb2 and Rps27 at E16.5.

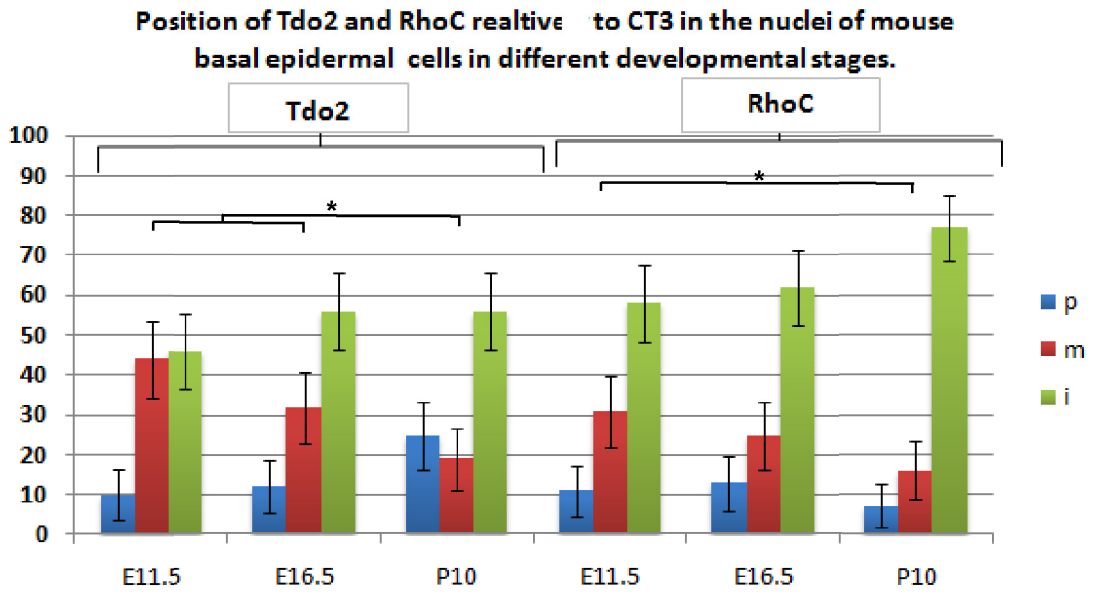

Figure 4.12. Position of Tdo2 and RhoC in relation to chromosome territory 3 (CT3) in the nuclei of the wild type mouse epidermal basal layer cells. Nuclei of the epidermal basal layer cells of the 11.5 day-old embryo (E11.5), 16.5 days old embryo (E16.5) and 10 days old mouse (P10) were assessed.

Intra-nuclear distribution of the distant controls Tdo2 and RhoC was also different from the positioning of Loricrin at E11.5. Both Tdo2 and RhoC loci showed rather internal than peripheral positions in the nuclei of epidermal basal cells in all examined developmental stages (**Fig.4.12**).

According to these observations and statistical analysis, distribution of the Tdo2 loci was not changed between E11.5 and E16.5, whereas at p10 loci were significantly more frequent in the internal position than in the earlier stages of development.

Positioning of the RhoC was not significantly different between E11.5 and E16.5 and there was no difference in their distribution between E16.5 and p10. However RhoC at p10 was significantly more internal than at E11.5.

4.2.2 Developmentally-regulated relocation of the EDC towards nuclear interior is cell-type specific.

EDC in dermal fibroblasts of E16.5 occupied more peripheral position (63%) in contrast to basal and suprabasal epidermal cells. There was no significant difference in distribution of Gabpb2 loci between the epidermal and dermal cells, in which Gabpb2 always showed more internal positioning versus the EDC.

Expression of Loricrin and most of the other genes within EDC is restricted to the epidermis. To check if changes of their positions during development are specific to the epidermis the localization of the EDC in dermal fibroblasts was compared with keratinocytes of basal and suprabasal epidermal layer (**Fig.4.13**).

A

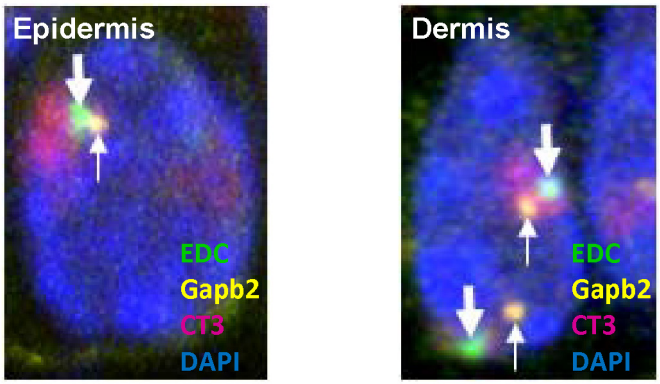

B

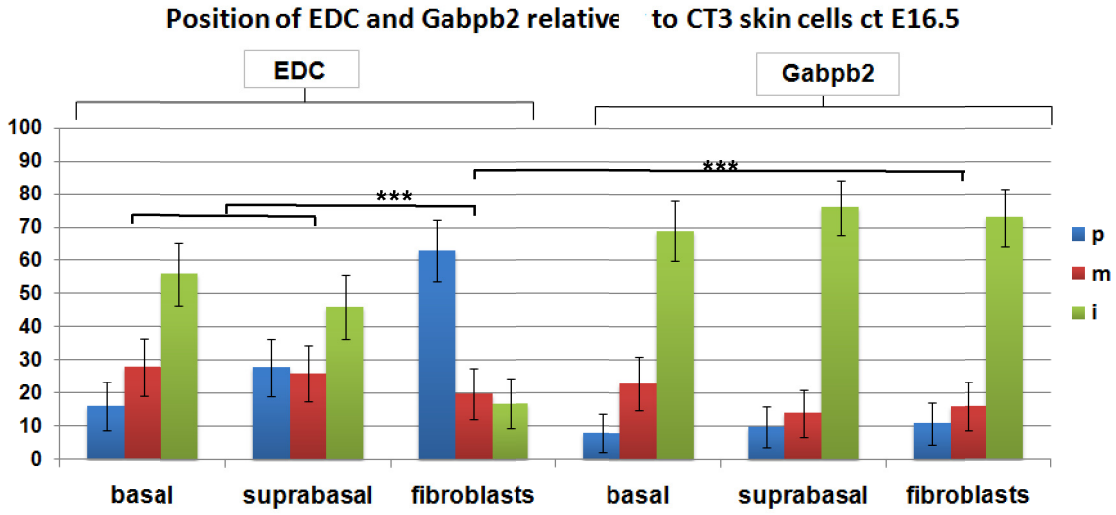

Figure 4.13 Position of epidermal differentiation complex and Gabpb2 relative to chromosome territory 3 (CT3) in the nuclei of different cell layers in wild type mouse. Nuclei of dermal fibroblasts, and of the epidermal basal and suprabasal layers were assessed.

Analysis showed that nuclear positioning of the EDC in dermal fibroblasts is remarkably different from its distribution in the epidermal cells. EDC loci in the nuclei of fibroblasts of 16 day-old embryos were at least three times more frequently seen in the peripheral part of chromosome territory 3 versus the nuclei of basal epidermal cells (p-values $<10^{-5}$). However, basal and suprabasal epidermal cells at E16.5 did not show any significant differences in the EDC location.

In contrast to the EDC, there was no significant difference in distribution of Gabpb2 in the nuclei between dermal and epidermal cells. Gapbb2 was approximately four times more frequently seen in the internal position (73%) than EDC in fibroblasts at E16.5 (17%).

4.2.3 Radial positions of Loricrin and as well as the intergene distances between the loci confirm data on the dynamics of its intra-chromosomal positions.

To confirm data on the intra-chromosomal loci positions, radial positions and relative radial positions (radial positions normalized to average nuclear radius) of the Loricrin, Rps27 and Gabpb2 in basal epidermal cells were calculated. In addition, intergenic distances were measured and subsequently related to the intergenic distances expressed in DNA base pairs in order to further characterize the movement of loci. In general, obtained data were consistent with the results of analysis of the dynamics of the intra-chromosomal gene localization during epidermal development.

4.2.3.1 Radial positions and intergene distances of the Loricrin, Rps27 and Gabpb2 in epidermal cells.

Variability of the radial positions and intergene distances between the loci was assessed by histograms (histogram examples in **Fig.4.14A-C**).

A

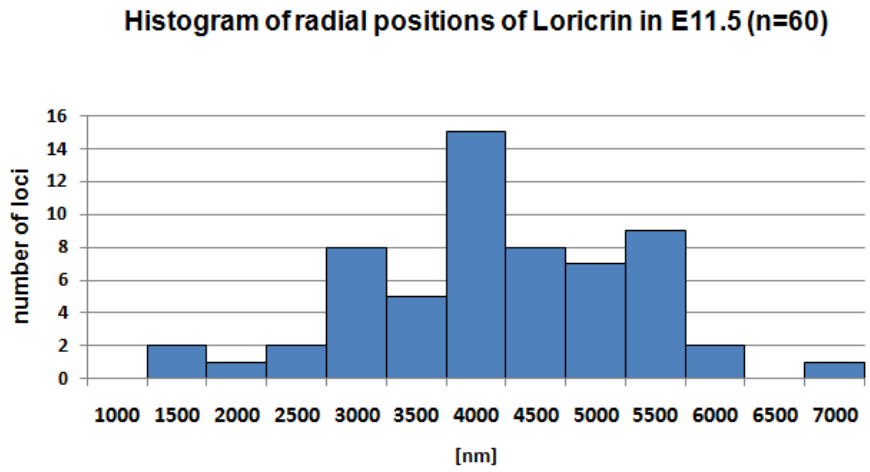

B

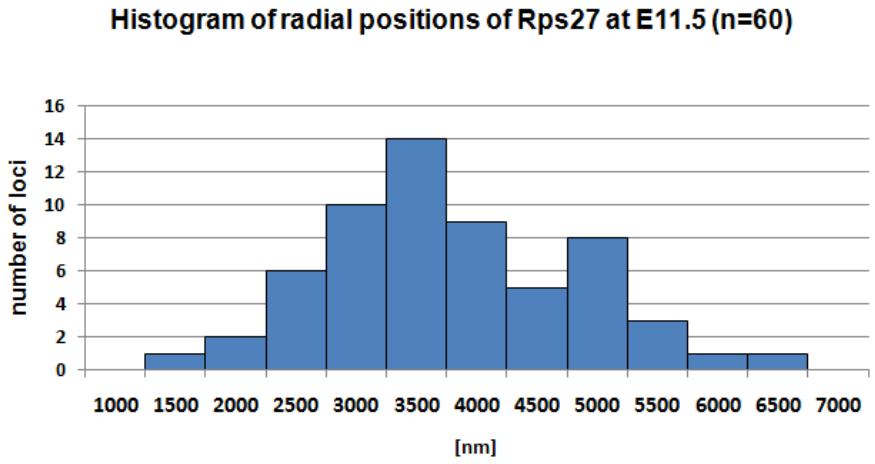

C

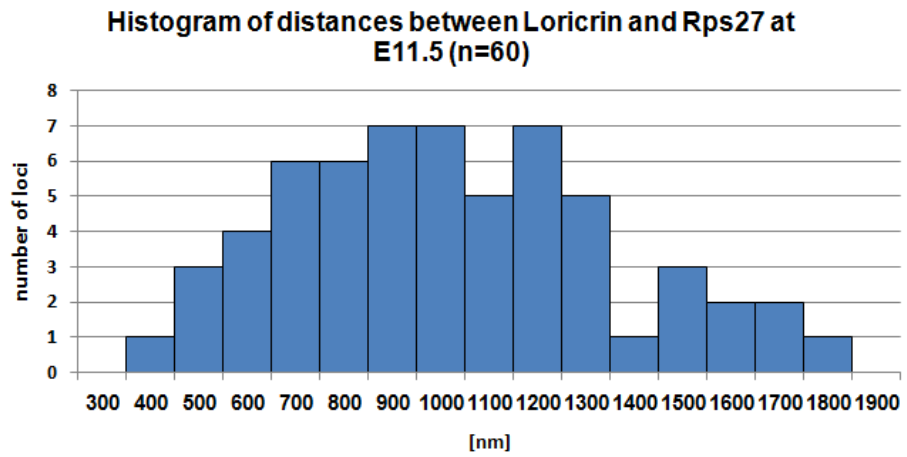

Figure 4.14 Histograms of radial positions of Loricrin and Rps27 and distance between them at E11.5. Radial positions of Loricrin (A) and Rps27 (B) in 30 nuclei of the epidermal basal layer as well as distances between them (C) were measured (60 loci), depicted on the histogram and tested for normality of distribution at E11.5.

Significant variability in radial gene positioning and intergene distance was observed. At E11.5, distance of Loricrin from the nuclear centre varied from 1300 nm to 6700nm with the average of 3962 nm (**Fig.4.14A**), while the

distance between Loricrin and Rps27 spread from 350 up to 1870 with the average of 974 nm (**Fig.4.14C**).

To further characterize these data sets, Lilliefor's test for the normality and Levene's test for equality of variances were performed. These tests showed that distribution of the values may be considered as not significantly different from the normal distribution and that condition of the variance equality had been fulfilled which allowed us to analyze them statistically using Student and ANOVA tests.

4.2.3.2 Dynamics of the radial positions of gene loci are consistent with their positioning versus the chromosome territory 3.

Nuclei at E11.5 were significantly larger than other examined nuclei. Loricrin localization was more peripheral at E11.5 versus Rps27 and Gabpb2, whereas not different from them at E16.5. Rps27 showed more internal position at E16.5, while Gabpb2 was distributed similarly in assessed tissues. Distances between Loricrin and Rps27 as well as between Loricrin and Gabpb2 were shorter in E16.5 than in E11.5.It is likely that DNA linking Loricrin and Gabpb2 is more condensed than fragment linking Loricrin and Rps27 and that loci are more condensed at E16.5 than at E11.5 and E16.5p63KO.

Radial positions were calculated as distances from the loci to the nuclear centre on the basis of coordinates extracted from the confocal scans. To avoid the influence of changes in the nuclear volume on the measurements, the average radii of the epidermal cell nuclei were calculated and compared between E11.5 and E16.5. It was shown that nuclei of basal epidermal cells of 12 day-old embryo are significantly bigger than in other examined cell types (P-value<0.001). Average radii of nuclei of other analysed skin samples were not significantly different. Distances between the loci and nuclear centres (radial positions in nm) were considered as raw data and only radial positions normalized to the average nuclear radius were analyzed in detail to avoid the influence of the nuclear size on the result of analysis (**Fig. 4.16**). Subsequently,

intergenic geometrical distances between the loci were measured (**Fig.4.18**) and converted into the corresponding intergenic distances expressed in the DNA base pairs (**Fig.4.19**).

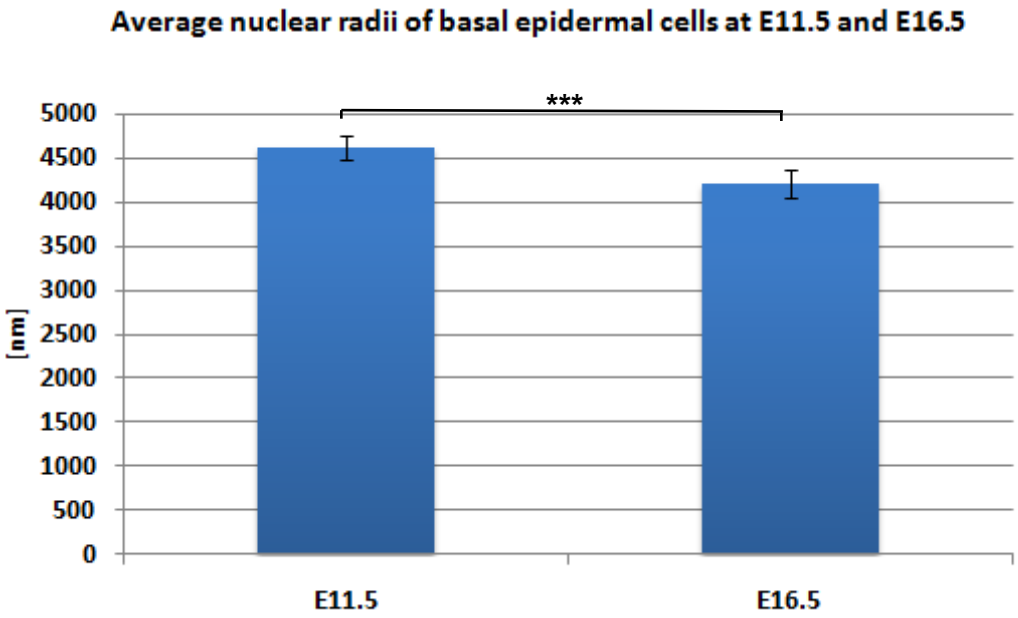

Figure 4.15. Average nuclear radii in different cell types of mouse epidermis. Average nuclear radius for each nucleus was calculated on the basis of arithmetic mean from a few hundreds of random radii. Average for all nuclei assessed in the sample depicted on the figure.

Statistical comparisons of the differences between average of radial positions were performed within one distinct cell type (different loci, **Figure 4.17C**) or within distinct type of the loci (different tissues, **Fig. 4.17A**).

A

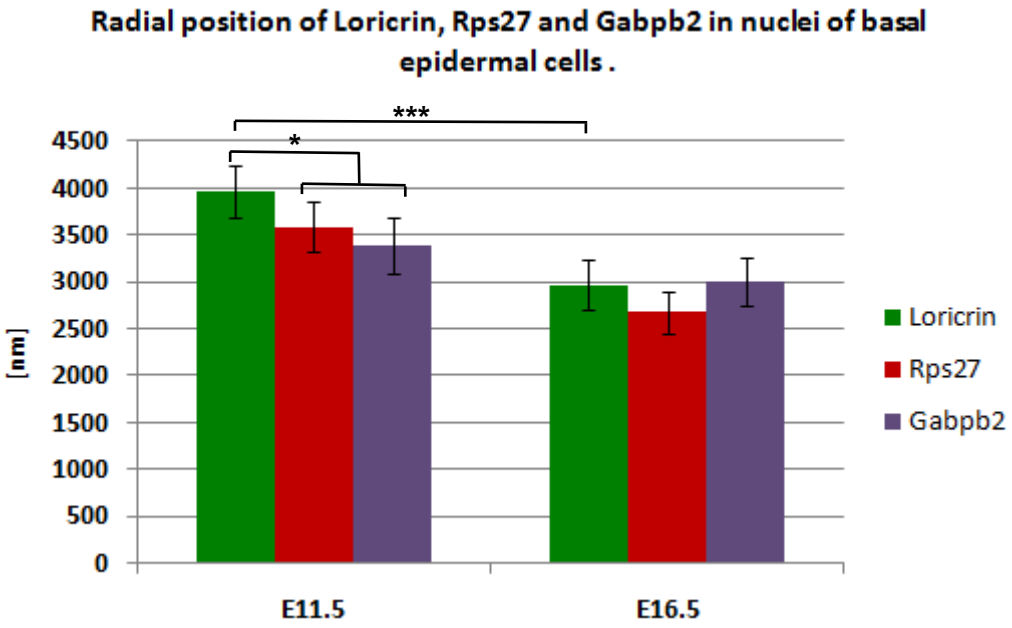

B

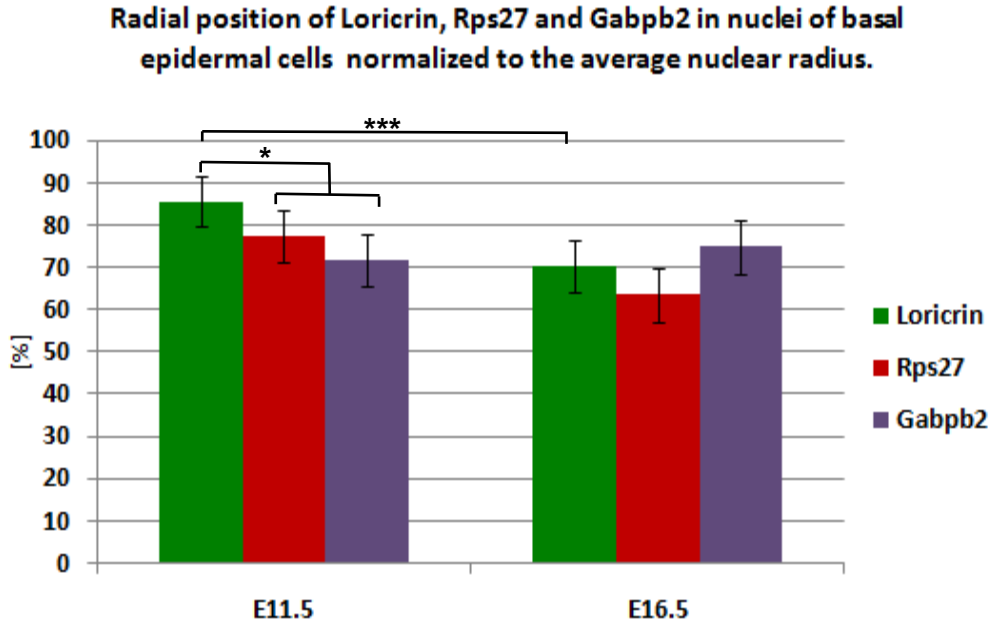

Figure 4.16. Radial positions of Loricrin, Rps27 and Gabpb2 in the nuclei of epidermal basal cells at E11.5 and E16.5. A- Radial positions (distances from loci to nuclear surface) of Loricrin, Rps27 and Gabpb2 in 30 nuclei of epidermal basal layer of E11.5 are shown (60 loci); **B-** Radial positions of Loricrin, Rps27 and Gabpb2 were normalized to the average nuclear radius.

In general, the analysis of the normalized radial positions of the loci in the developing epidermis confirmed the results of intra-chromosomal analysis. In the E11.5 epidermis, Loricrin showed significantly more peripheral localization (3962 nm, 86%; **Fig. 4.16A** and **Fig.4.16B**, summary of statistics in **Fig. 4.17**)

than both Rps27 (3582nm, 77%) and Gabpb2 (3387 nm, 72%). At E16.5, the the position of Loricrin was not significantly different from positions of control loci. Loricrin showed significantly more internal position at E16.5 (70%) compared to E11.5 (85.5%), while Rps27 and Gabpb2 loci showed similar radial.

A

	Relative radial positions	
	E11.5	E16.5
Lor-Rps	↓	-
Lor-Gabpb2	↓	-
Rps-Gabpb2	-	↑

B

↑ - significantly bigger
↓ - significantly smaller
- no significant difference
p-value <0.01
p-value<0.05

C

	Relative radial positions			Intergenic distances	
	Loricrin	Rps27	Gabpb2	Lor-Rps	Lor-Gabpb
E11.5-E16.5	↓	↓	-	↓	↓

Figure 4.17 Statistical comparison of normalized radial positions and intergenic distances of Loricrin, Rps27 and Gabpb2 (One-way ANOVA followed by Newman-Keuls procedure). Hypothesis on equality of the means of normalized radial position of all three loci in the particular tissue (a) or one locus in all three tissues (b) were tested and if hypothesis were rejected means were subject to Newman-Keuls procedure leading to further assessment of the significance differences between radial positions; intergenic distances were analyzed in similar way (c on the right). Symbols in the table are explained in the legend (b). In the first column of the table the pairs of analyzed loci in particular tissue (a) or pairs of tissues (c) are displayed. Indications of changes in the main part of the table describe relation of the loci (or tissue) in the second position of the pair to the tissue (or loci) in the first position.

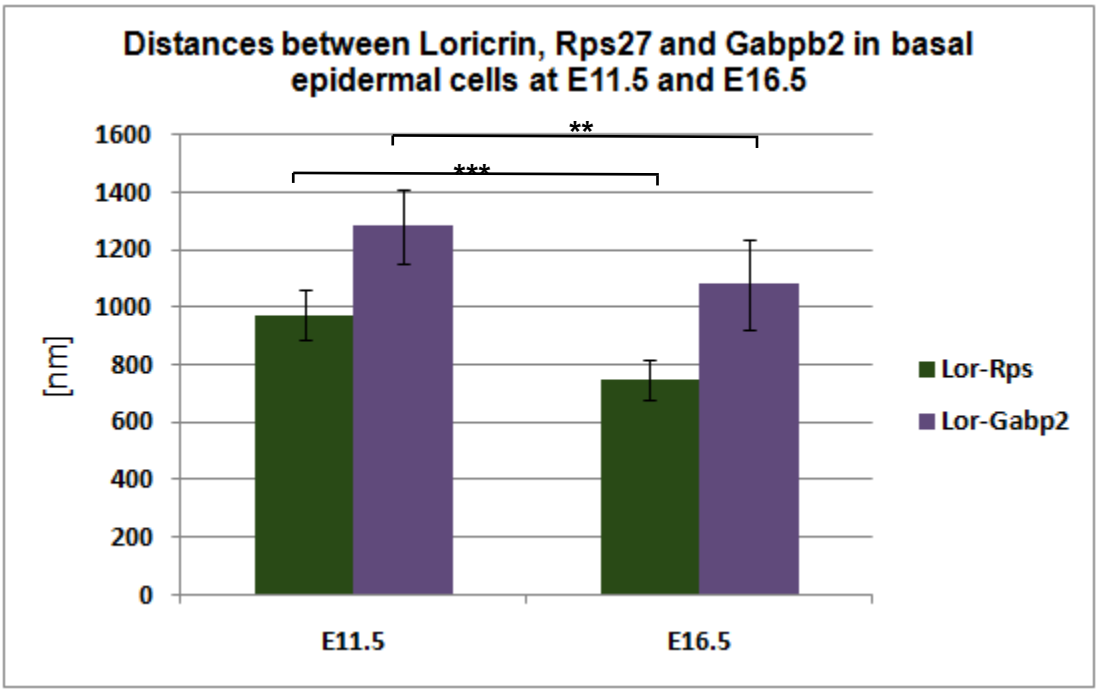

Figure 4.18 Distances between Loricrin, Rps27 and Gabpb2 in nuclei of epidermal basal layer. Distances between Loricrin, Rps27 and Gabpb2 were measured in 30 nuclei (60 pairs of loci in 3 combinations) of epidermal basl layer cells in E11.5 and E16.5.

Assessments of the intergene distances between the Loricrin and Rps27 as well as between the Loricrin and Gabpb2, confirmed the observed changes in the radial positions of Loricrin between E11.5 and E16.5. At E11.5, distances between the Loricrin and Rps27 (974 nm, **Fig.4.18**) and the Loricrin and Gabpb2 (1282nm) were significantly higher than at E16.5 (Lor-Rps 747nm and Lor-Gabpb2 1081 nm). These data were consistent with previous results since Loricrin moves towards the internal part of chromosomal territory 3 occupied also by Rps27 and Gabpb2.

Intergenic distances between the loci of interest expressed in DNA base pairs (bp) were related to these geometrical distances which gave the ratio bp/nm that can be considered as a one of the criteria of chromatin condensation (**Fig.4.19**).

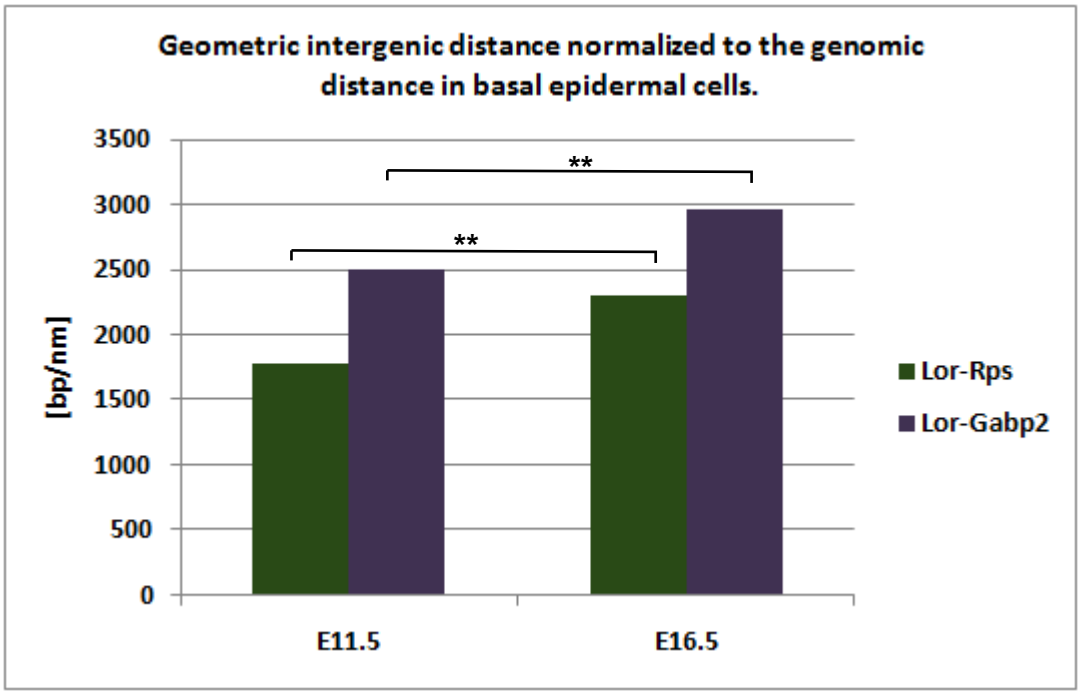

Figure 4.19 Relation of distances between Loricrin, Rps27 and Gabpb2 in nuclei of epidermal basal layer normalized to the genomic distance. Distances between Loricrin, Rps27 and Gabpb2 as a ratio of physical measured distance to genomic distance expressed in of base pairs/ nanometres.

	Intergenic distances					
	Lor-Rps [nm]	Lor-Rps [bp/nm]	Lor-Gabpb [nm]	Lor-Gabpb [bp/nm]	Rps-Gabpb [nm]	Rps-Gabpb [bp/nm]
E11.5	974.3	1769.6	1281.7	2495.6	-	-
E16.5	747.2	2307.5	1080.8	2959.5	1037.8	4743.4

Table 4.1. Summary of distance measurements between Loricrin, Rps27 and Gabpb2 in nuclei of basal epidermal cells.

Based on the data shown in **Fig.4.19** and **Tab.4.1** DNA domains between the Rps27 and Loricrin are less condensed compared domains between Loricrin and Gabpb2 at E11.5 and at E16.5 and that DNA fragment spanning from the Rps27 up to Gabpb2 is more condensed at E16.5.

Thus, these data suggest that during development of the epidermis 5Mbp chromatin domain on mouse chromosome 3 containing EDC shows remarkable remodelling of the higher order structure. In particular, EDC and Loricrin relocate from the peripheral part of the chromosome territory 3 to the internal

part of the territory. This results in shortening of the distances between the Loricrin and control genes Gabpb2 and decrease of radial positioning of the EDC and Loricrin (**Fig.4.20**).

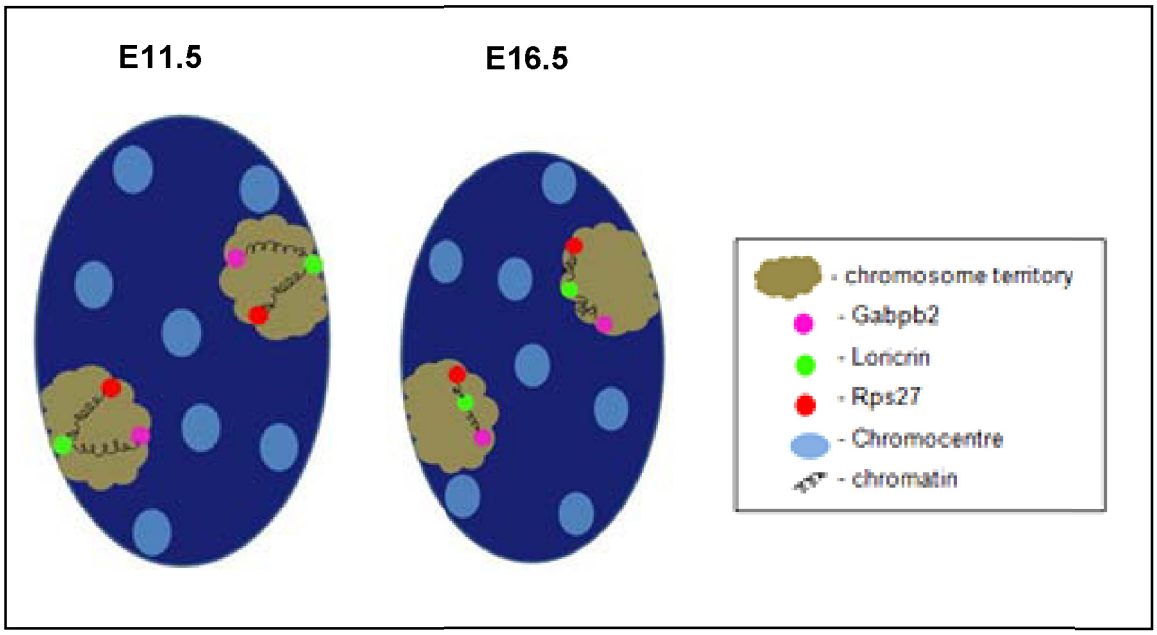

Figure 4.20. Repositioning of EDC in mouse epidermis during morphogenesis. EDC which is represented on the figure by Loricrin is located at E11.5 at the periphery of chromosome territory 3 oppositely to control loci Rps27 and Gabpb2 from its neighbourhood. At E16.5 most EDC loci are located in the internal part of the nucleus as well as control loci. Distance between EDC and control loci decreas.

4.3 Role of p63 in EDC organization and epidermal differentiation – analysis of p63KO mice

EDC and Loricrin loci in epidermal cell nuclei of the E16.5 p63 knock-out mice showed significant differences to age-matched wild-type mouse.

To further understand mechanisms involved in the control of developmentally regulated relocation of the EDC and Loricrin towards nuclear interior in epidermal progenitor cells, we hypothesized that p63 transcription factor serves as a master regulator of epidermal development plays a role in the control of changes in higher order chromatin remodelling and EDC relocation.

To address this hypothesis, analysis of the skin of 16 day-old embryo of p63 KO mice which failed to develop stratified epidermis and showed low levels of the Loricrin expression was performed.

4.3.1 Analysis of the intra-chromosomal position of EDC, Loricrin and control loci in E16.5 p63 knock-out and wild-type mice.

In the epidermal layer of E16.5 p63 knock-out mice Loricrin and EDC were located more frequently in the peripheral part of the chromosome territory 3 which was similar to its distribution in the nuclei of basal layer of wild-type mice at E11.5 and different from the distribution in the nuclei of wild-type at E16.5. Position of Rps27 was also less internal at E16.5 p63KO mice compared to the nuclei of basal cells of E16.5 wild-type mice. Distribution of Gabpb2 in basal epidermal cell nuclei was not different in p63KO versus wilde-type mice. Distribution of the EDC as well as Gabpb2 was not significantly different in fibroblasts of E16.5 p63KO mice from their distributions in the nuclei of wild type mice at E16.5.

Analysis of the positions of the EDC, Loricrin, Rps27 and Gabpb2 relative to chromosome territory 3 were performed in the nuclei of the basal epidermal

layer at E16.5 p63KO mice (**Fig.4.21** and **Fig.4.22**) as well as in dermal fibroblasts of p63KO mice (**Fig.4.23**).

A

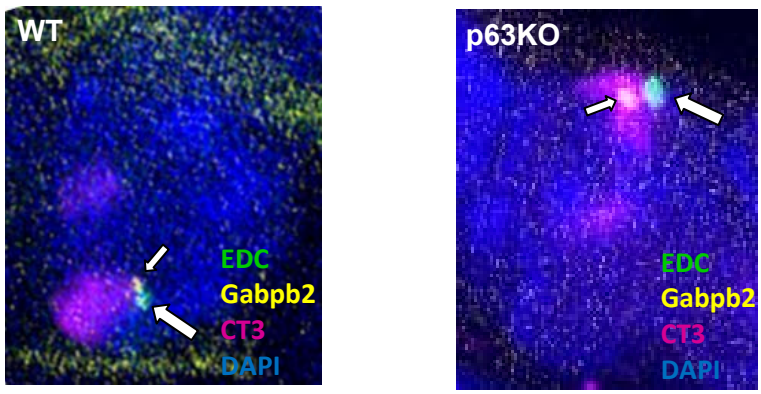

B

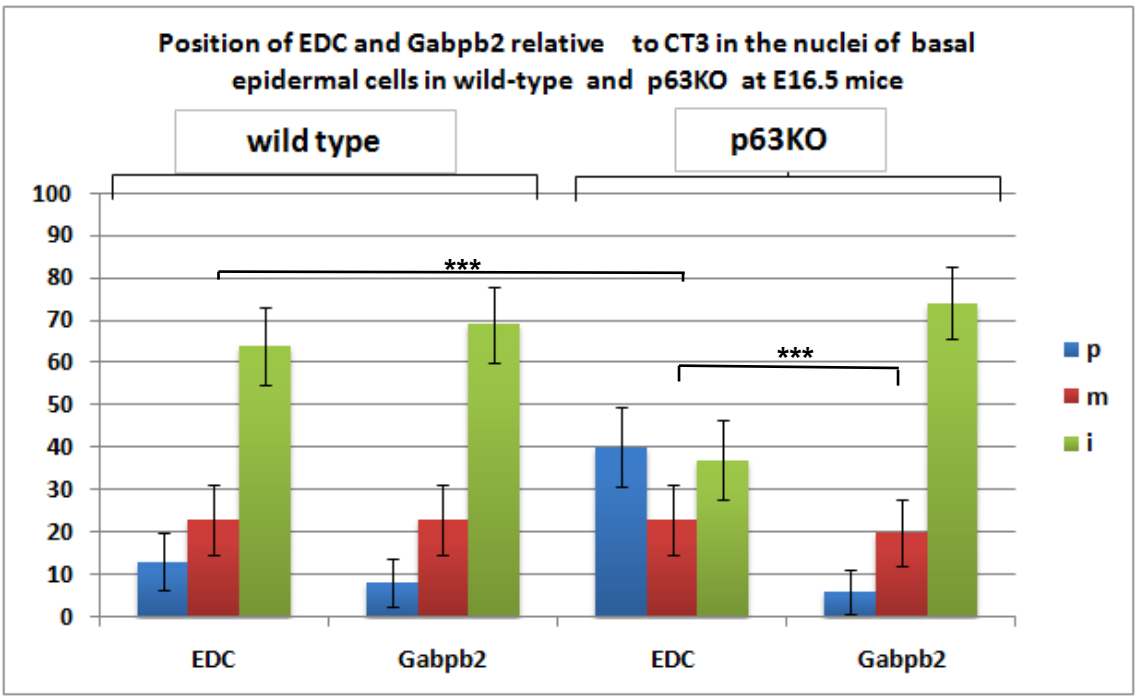

Figure 4.21. Position of EDC and Gabpb2 relative to the chromosome territory 3 (CT3) in the nuclei of the basal epidermal cells of the skin of 16 days old wild type and p63KO embryo.

Analysis showed that distribution of the EDC and Loricrin in epidermis of the E16.5 p63KO mice was significantly different from the E16.5 wild-type mice and was quite similar to the E11.5 wild-type mice, thus supporting a hypothesis that changes in a position of Loricrin were functionally linked to the changes of its

expression during epidermal development and differentiation (**Fig.4.21**). In addition, it was shown that positioning of the control loci were almost not affected (Rps27; **Fig.4.22**) or their distribution was not different from the wild-type embryonic epidermis at all (Gabpb2;**Fig. 4.21**).

Specifically, EDC in p63KO mice showed significantly more peripheral localization (peripheral 40%, internal 37%, p-value<10^{-5}) than in wild-mice at E16.5 (peripheral 16%, internal 56%). It is also worth noticing that location of the EDC in p63KO mice was not significantly different from its location at 12 day-old wild-type embryo.

A

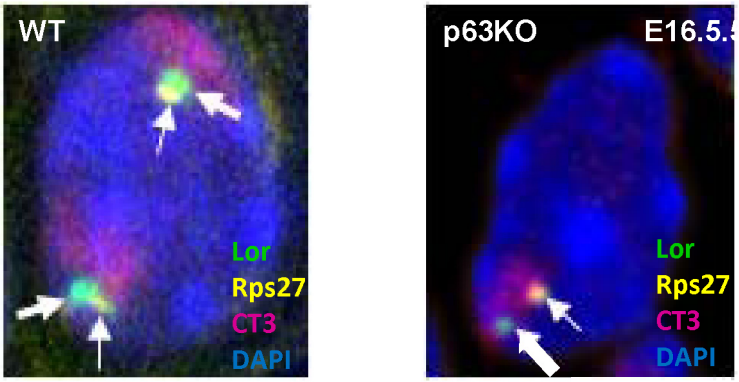

B

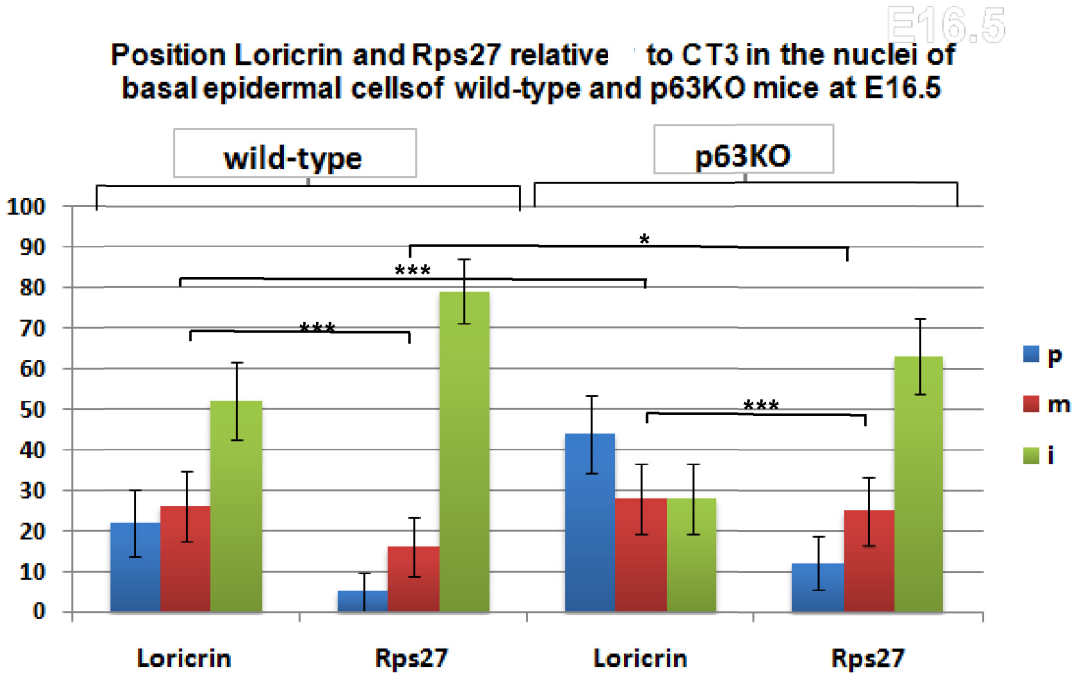

Figure 4.22. Position of Loricrin and Rps27 relative to chromosome territory 3 (CT3) in the nuclei of the skin epidermal basal layer cells of the of 16 days old wild-type and p63KO embryo.

Loricrin gene showed significantly more peripheral position in p63KO mice (44% peripheral, 28% internal, p-value=0.0007) than in wild-type mice (22% peripheral, 52% internal; **Fig. 4.22**).

Intra-nuclear location of Rps27 and Gabpb2 in p63KO mice is not significantly different from its location in wild-type mice.

In both p63KO and wild-type mice, the location of Loricrin was similar to positions of EDC.

A

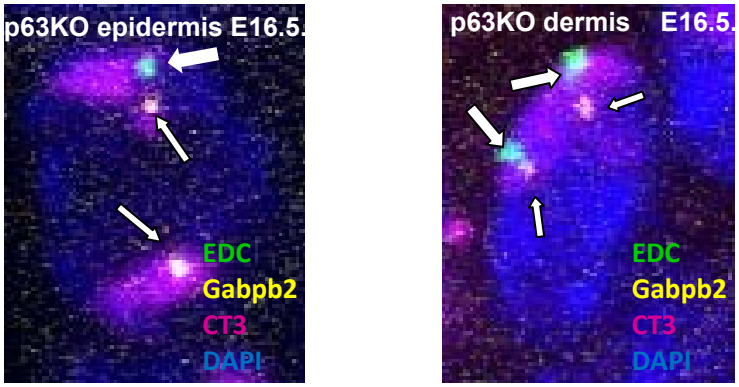

B

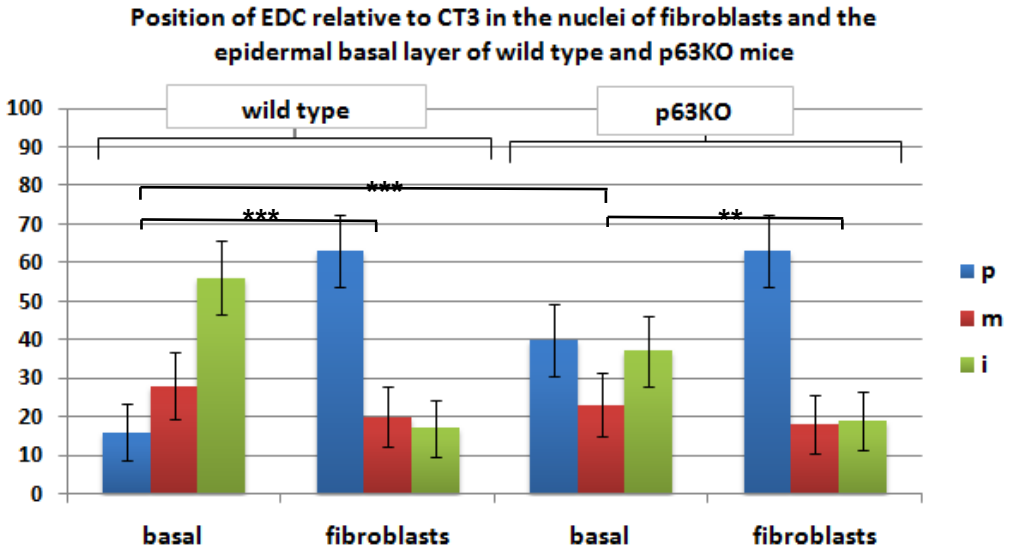

C

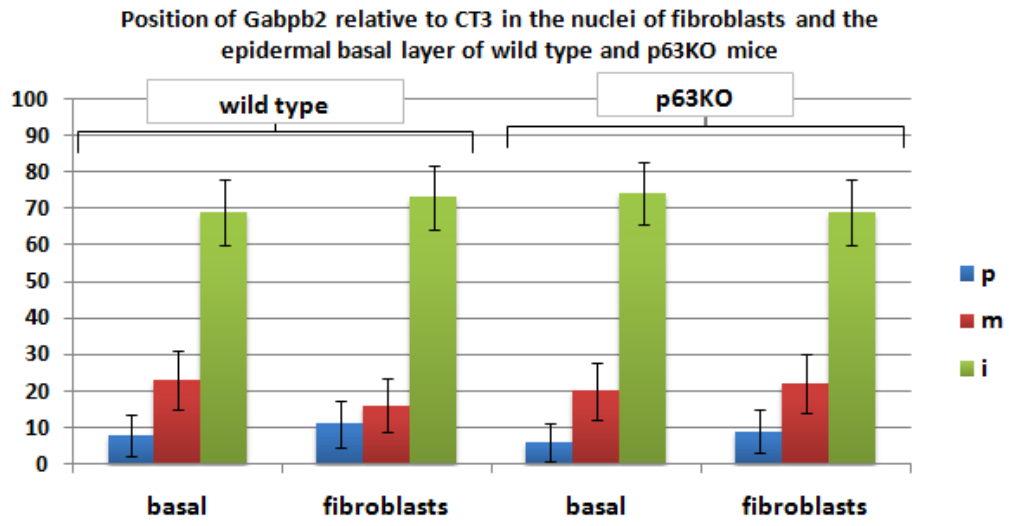

Figure 4.23 Position of EDC and Gabpb2 relative to chromosome territory 3 (CT3) in the nuclei of epidermal basal layer cells and fibroblasts of 16 day-old wild-type and p63KO embryo.

In contrast to epidermal cells, position of the EDC in the nuclei of fibroblasts of the E16.5 p63KO embryo were significantly more peripheral (63%, p-value=0.0031) versus basal epidermal cells (40%, **Fig.4.23B**).

There was no significant differences in the distribution of EDC between the E16.5 p63KO fibroblasts and wild-type fibroblasts, thus suggesting that changes in the positioning of the EDC and Loricrin in epidermal progenitor cells in p63KO mice were indeed tissue specific.

This was supported by the data showing a lack of significant differences in the location of Gabpb2 relatively to the chromosome territory 3 between the fibroblasts and basal epidermal cells in E16.5 p63KO mice (**Fig.4.23C**).

Also, there were no differences in distribution of Gabpb2 between the E16.5 fibroblasts of wild-type mice and p63KO mice.

4.3.2 Measurements of the radial positions and intergene distances between the Loricrin and control loci in the nuclei of the E16.5 p63 KO mice.

In addition to the analyses of teh distribution of the loci relatively to the chromosomal territory 3, radial positions and intergene distances between the Loricrin and control gene loci in the epidermis of E16.5 p63KO mice were calculated and compared to the corresponding parameters from wild type mice.

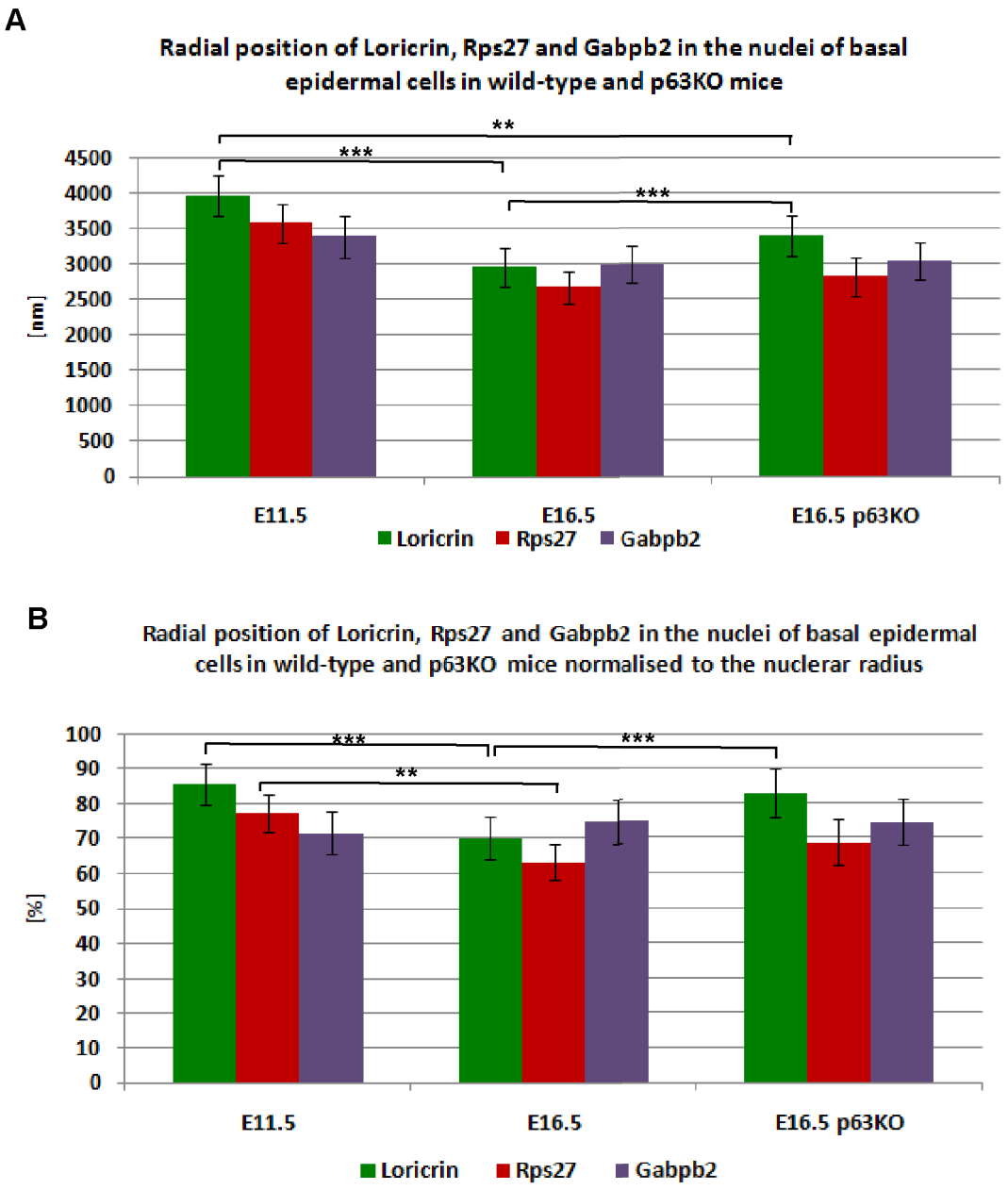

Figure 4.24. Radial positions of the Loricrin, Rps27 and Gabpb2 in the nuclei of basal epidermal cells in wild-type mice at E11.5 and E16.5 and at E16.5 in p63KO mice. A- Radial positions of Loricrin, Rps27 and Gabpb2 were normalized by average nuclear radius of their particular nuclei. **A-** Radial positions (distances from loci to nuclear surface) of Loricrin, Rps27 and Gabpb2 in 30 nuclei of basal epidermal cells at E11.5 and E16.5 in wild-type mice and at E16.5 in p63Ko mice. **B-** Radial positions of Loricrin, Rps27 and Gabpb2 were normalized to the average nuclear radius.

In general, results of the radial position analyses of the loci in E16.5 p63KO mice were consistent with the results of the analyses of intra-chromosomal loci positions **(Fig.4.24)**. In E16.5 p63KO mice, position of the Loricrin was more perpheral (83%) than in wild-type mice (70%). Positions of Rps27and Gabpb2

in E16.5 p63KO mice were not significantly different from the E11.5 and E16.5 wild type mice.

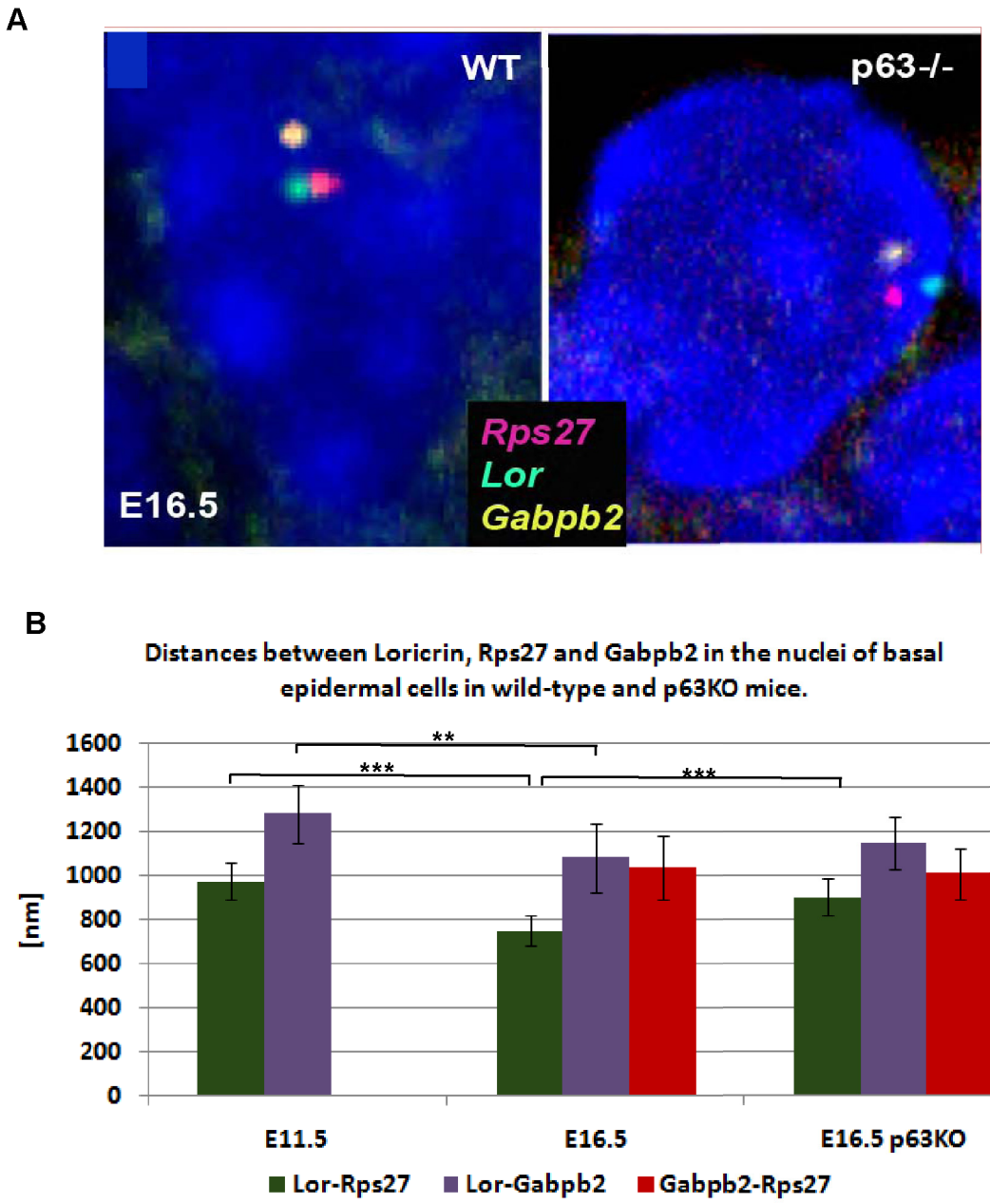

Figure 4.25. Distances between Loricrin, Rps27 and Gabpb2 in nuclei of basal epidermal cells. Distances between Loricrin, Rps27 and Gabpb2 were measured in 30 nuclei (60 pairs of loci in 3 combinations) of epidermal basal layer cells at E11.5, E16.5 and E16.5 p63KO and compared.

Data obtained on the radial positions were further confirmed by examining the intergene distances between the loci (**Fig 4.25**). Distances between the Loricrin and Rps27 (974 nm) and the Loricrin and Gabpb2 (1281 nm) were not

significantly different between the wild-type mice at E11.5 and at E16.5 in p63KO mice, while in wild-type mice such distances were significantly different.

A

	Relative radial positions		
	E11.5	E16.5	E16.5p63KO
Lor-Rps27	↓	-	↓
Lor-Gabpb2	↓	-	-
Rps-Gabpb2	-	↑	-

B

↑ - significantly bigger
↓ - significantly smaller
- no significant difference
p-value <0.01
p-value<0.05

C

	Relative radial positions			Intergenic distances	
	Loricrin	Rps27	Gabpb2	Lor-Rps27	Lor-Gabpb2
E11.5-E16.5	↓	↓	-	↓	↓
E11.5-E16.5p63KO	-	-	-	-	-
E16.5-E16.5p63KO	↑	-	-	↑	-

Figure 4.26. Statistical comparison of normalized radial positions and intergenic distances of Loricrin, Rps27 and Gabpb2 (One-way ANOVA followed by Newman-Keuls procedure). Hypothesis on equality of the means of normalized radial position of all three loci in the particular tissue (a) or one locus in all three tissues (b) were tested and if hypothesis were rejected means were subject to Newman-Keuls procedure leading to further assessment of the significance differences between radial positions; intergenic distances were analyzed in similar way (c on the right). Symbols in the table are explained in the legend (b). In the first column of the table the pairs of analyzed loci in particular tissue (a) or pairs of tissues (c) are displayed. Indications of changes in the main part of the table describe relation of the loci (or tissue) in the second position of the pair to the tissue (or loci) in the first position.

Intergene distances between the loci of interest expressed in DNA base pairs (bp) were similar to geometrical distances which gave the ratio bp/nm that can be considered as a criterium of chromatin condensation (**Fig.4.27**).

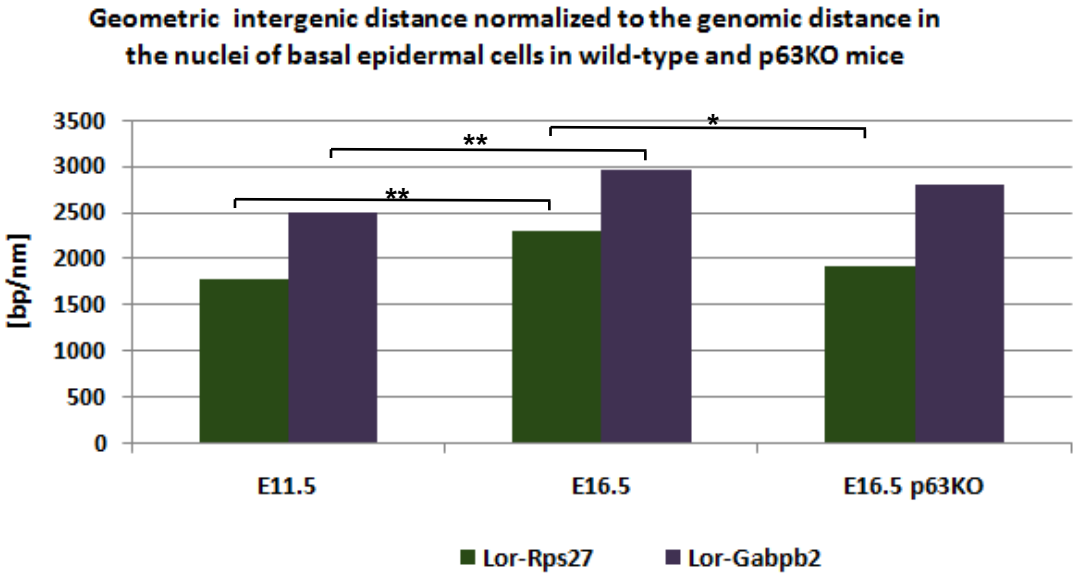

Figure 4.27. Relation of distances between Loricrin, Rps27 and Gabpb2 in the nuclei of basal epidermal cells in base pairs to geometrical distances. Distances between Loricrin, Rps27 and Gabpb2 in expressed in bp/nm.

Based on the data from Fig.3.26 and Tab.1 we can suggest that DNA domains between the Rps27 and Loricrin were more condensed than domains between the Loricrin and Gabpb2 in E16.5 p63KO mice, similarly what was seen in E11.5 and E16.5 wild type mice.

	Intergenic distances					
	Lor-Rps [nm]	Lor-Rps [bp/nm]	Lor-Gabpb [nm]	Lor-Gabpb [bp/nm]	Rps-Gabpb [nm]	Rps-Gabpb [bp/nm]
E11.5	974.3	1769.6	1281.7	2495.6	-	-
E16.5	747.2	2307.5	1080.8	2959.5	1037.8	4743.4
E16.5 p63KO	902.8	1909.8	1144.8	2307.5	1007.1	4887.8
fpads	908.0	1898.8	-	-	-	-
fpads SATB1KO	774.3	2226.7	-	-	-	-

Table 4.2. Summary of distance measurements between Loricrin, Rps27 and Gabpb2 in nuclei of basal epidermal cells.

Thus these data suggest that developmentally regulated process of the EDC and Loricrin relocation to nuclear interior in epidermal progenitor cells is significantly altered in p63KO mice versus wild-type mice. This suggest a role

for p63 in the control of higher-order chromatin remodelling in the EDC locus during epidermal development (**Fig.4.28**).

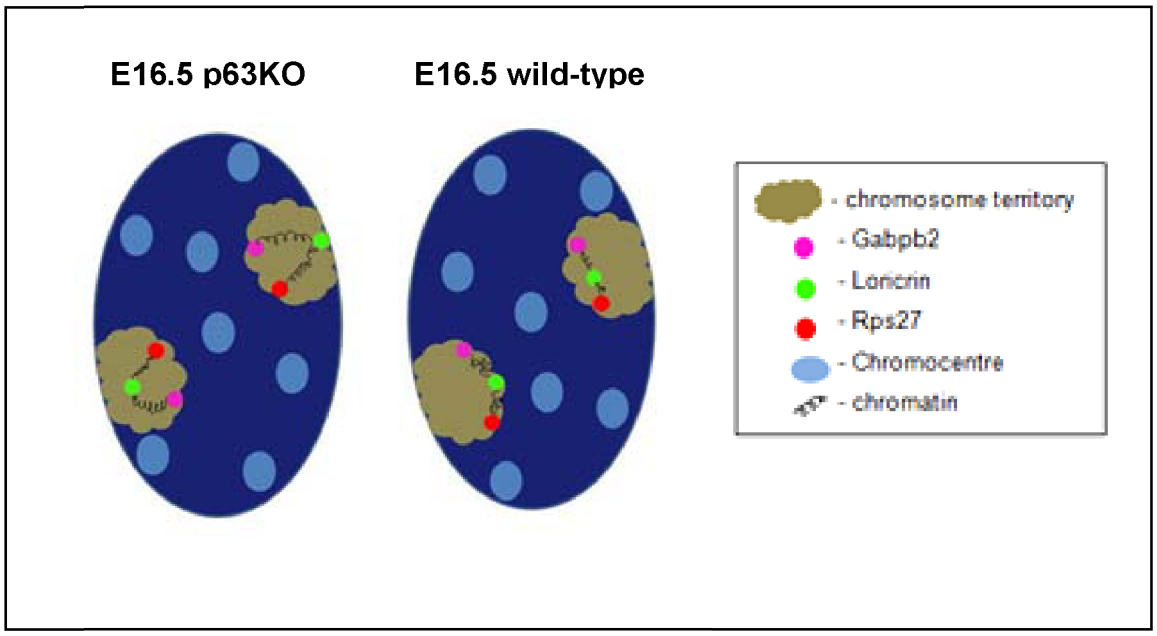

Figure 4.28. Repositioning of EDC in wild type and p63KO mice at E16.5. EDC which is represented on the figure by Loricrin, oppositely to wild-type, is located at E16.5 at the periphery of chromosome territory 3 oppositely to control loci Rps27 and Gabpb2 from its neighbourhood, which is similar to the distribution of these loci at E11.5. At E16.5 most EDC loci are located in the internal part of the nucleus as well as control loci. Distance between EDC and control loci decreas.

4.4 Role of Satb1 in EDC organization – analysis of Satb1KO mouse skin.

Satb1 is a protein known for DNA binding and chromatin organising properties and direct target for p63 in keratinocytes (Fessing et al. 2011). Thus we decided to test a hypothesis that Satb1 mediates the effects of p63 on higher-order chromatin remodelling of the EDC locus during development. To address this question positions of Loricrin and control loci Rps27 and Gapb2 as well as conformation of central part of EDC was analysed by 3D FISH. Additionally skin morphology was characterized. Data obtained suggest that Satb1 remodels chromatin architecture at the tissue-specific EDC gene locus, by establishing specific higher-order chromatin conformation of the central domain of this locus where epidermis-specific genes are clustered.

4.4.1 Satb1KO mice have impaired epidermal morphology and barrier formation

To assess the role of Satb1 protein in the control of epidermal differentiation, haematoxylin staining was performed on footpad skin of P0.5 Satb1Ko and wild-type mice. Satb1 -/- mice at P0.5 show a significant decrease ($p<0.01$) of the epidermal thickness, as well as a thinning of the granular epidermal layer compared to wild-type mice, more pronounced in the foot pads versus dorsal skin (**Fig. 4.29 A, B**). In addition, Satb1 -/- mice showed significantly ($p<0.05$) decreased epidermal proliferation compared to wild-type controls (**Fig. 4.29 C**).

Consistently with microarray and RT-PCR data that show marked decrease in expression of a large number of genes involved in terminal keratinocyte differentiation in Satb1 -/- mice compared to wild-type controls (Fessing et al., 2011), immunofluorescence analysis revealed markedly reduced expression of the Loricrin in Satb1-null epidermis versus the controls (**Fig. 4.29 D**). These data indicate that *Satb1* as downstream target for p63 is indeed involved in the control of epidermal development, terminal keratinocyte differentiation and epidermal barrier formation.

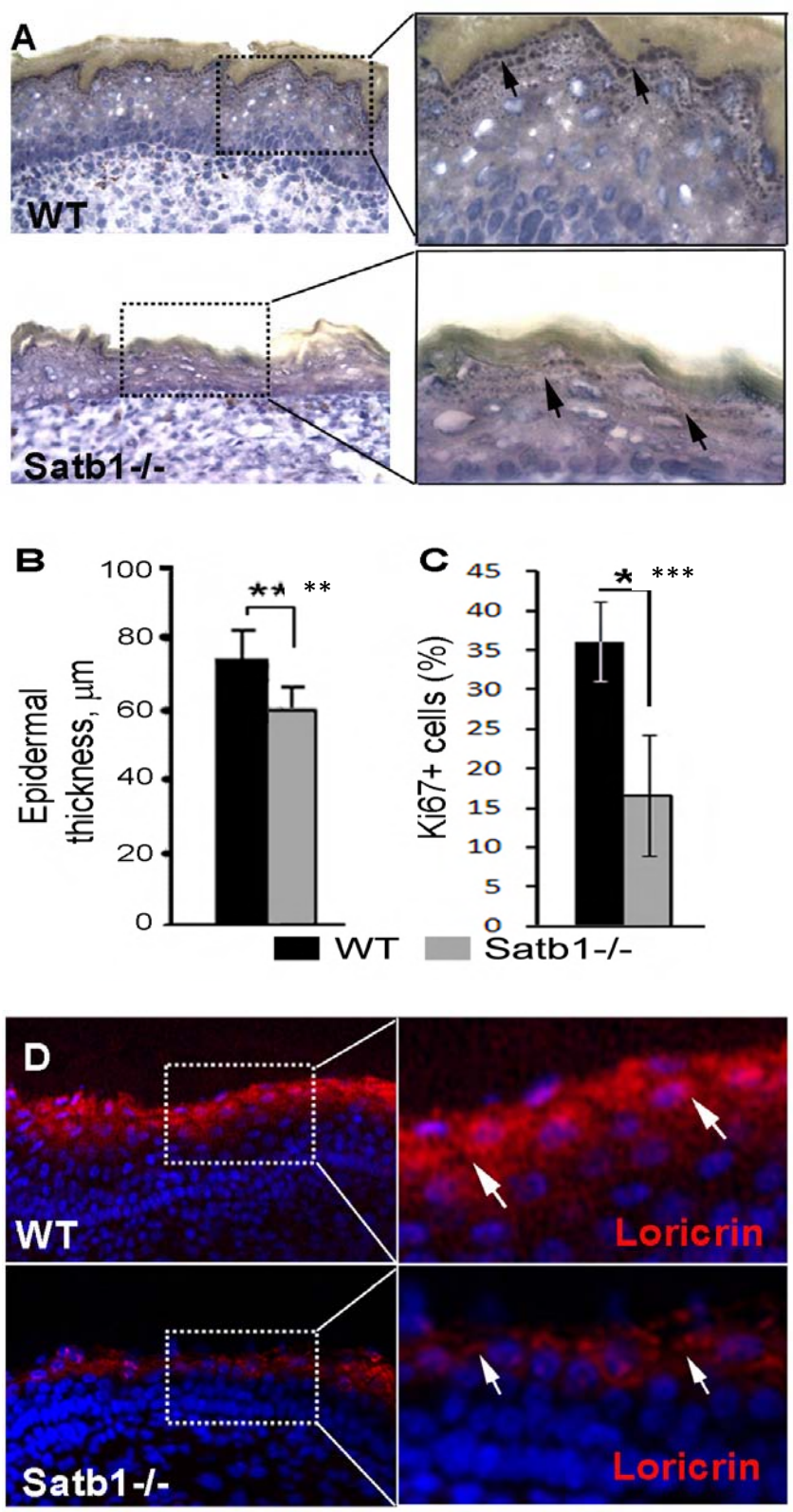

Figure 4.29. Satb1 knockout mice show alterations in the epidermal structure and Loricrin expression. A-C: Alterations in the structure of granular layer (A, arrows) and significant ($p<0.05$) decrease of the epidermal thickness (B) and cell proliferation (C) in newborn Satb1-/- mice versus WT controls: Decrease of Loricrin expression in the epidermis of Satb1-/- versus WT mice.

4.4.2 Radial positions of Loricrin are more internal in the nuclei of basal epidermal cells in Satb1KO mice compared to wild-type mice.

4.4.2.1 ***Analysis of the intra-chromosomal position of Loricrin and Rps27 did not exhibit significant differences between footpad epidermis of Satb1KO and wild-type* mice.**

There was no significant difference in the Loricrin distribution in epidermal cells between Satb1 KO and wild-type mice. There was no significant difference in the distribution of Rps27 in the skin of Satb1KO and wild type mice.

Positions of Loricrin and Rps27 in relation to chromosome territory 3 were analysed. Cells of basal and suprabasal epidermal layer and fibroblasts in Satb1KO mice (**Fig.4.30**) were examined.

A

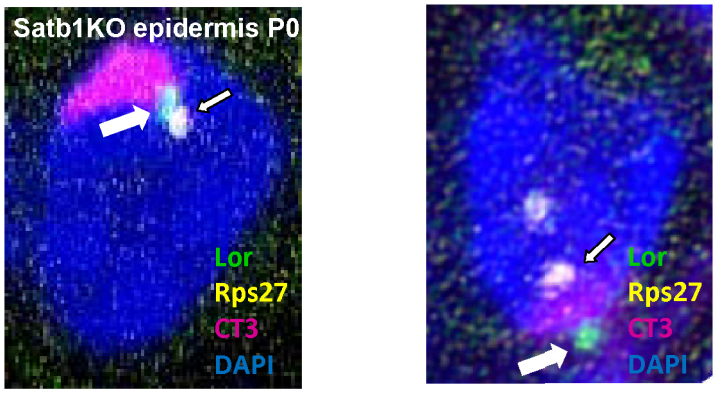

B

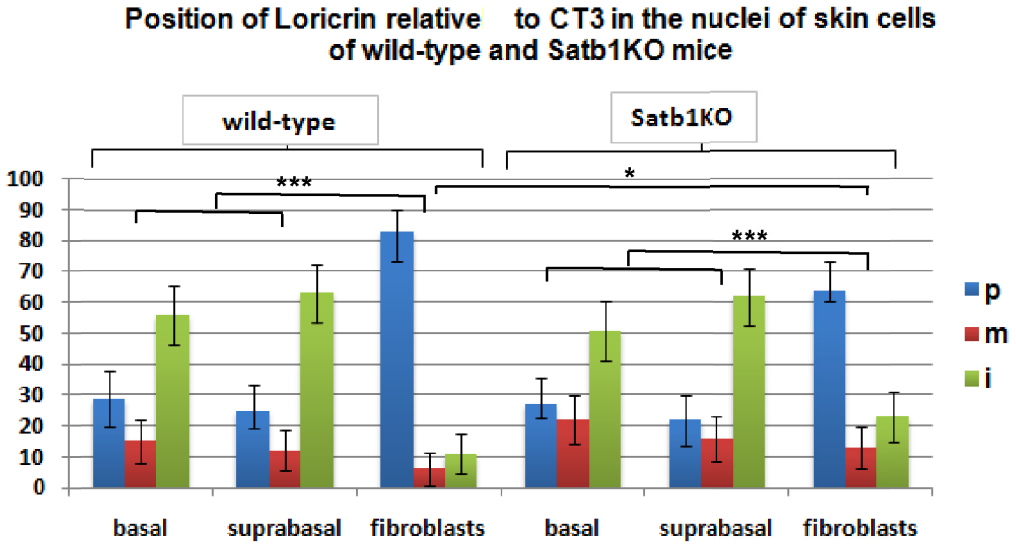

C

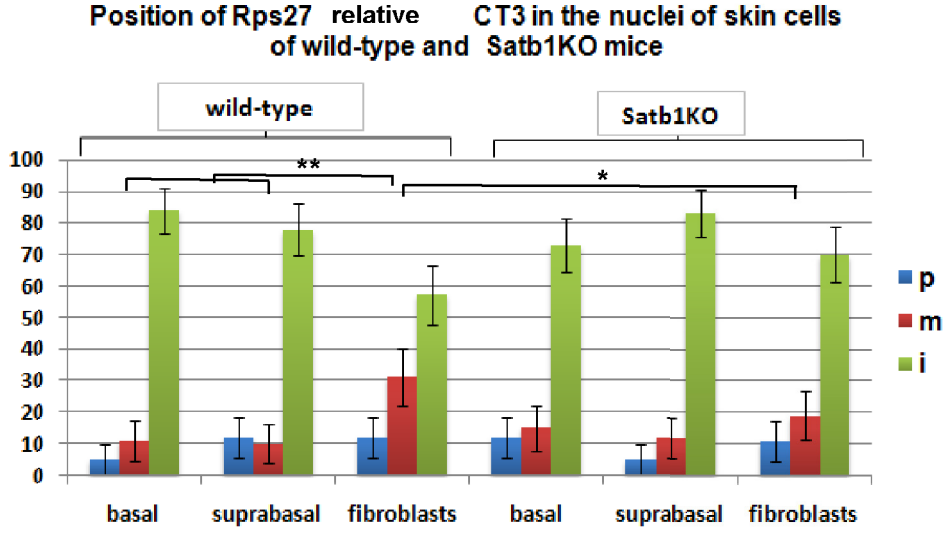

Figure 4.30 Position of Loricrin in relation to chromosome territory 3 (CT3) in the nuclei of different cell layers in p0 footpads of Satb1 KO mice. Nuclei of dermal fibroblasts and of the epidermal basal and suprabasal layers were assessed.

No significant differences in the position of Loricrin between basal and spinous epidermal layers of wild-type and Satb1KO mice were found, however Loricrin was located significantly more peripheral in fibroblasts of wild-type mice (83%, p-value=0.0097) than in Satb1KO mice (64%).

However, no significant differences in the positions of Rps27 were found between epidermal or dermal cells of wild-type and Satb1KO mice.

4.4.2.2 Loricrin positions are more internal in Satb1 KO mice compared to wild-type mice according to the measurements of its radial positions.

Loricrin showed more internal positions in the epidermis of Satb1KO mice compared to wild-type mice, whereas Rps27 retained its position in both strains. Intergenic distances between these two loci were significantly smaller in Satb1KO mice. Thus it was likely that DNA domains linking Loricrin and Rps27 was more condensed in Satb1KO mice versus wild-type controls.

Radial positions, normalized radial positions and intergenic distances were calculated for wild type and Satb1KO mice in the footpad epidermis (**Fig. 4.30-32**).

A

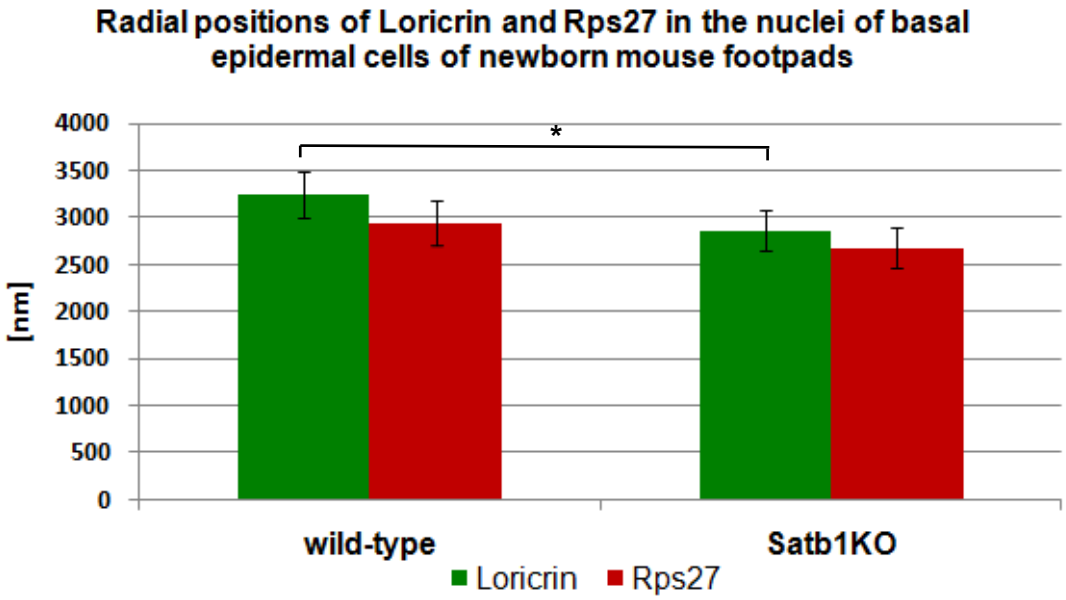

B

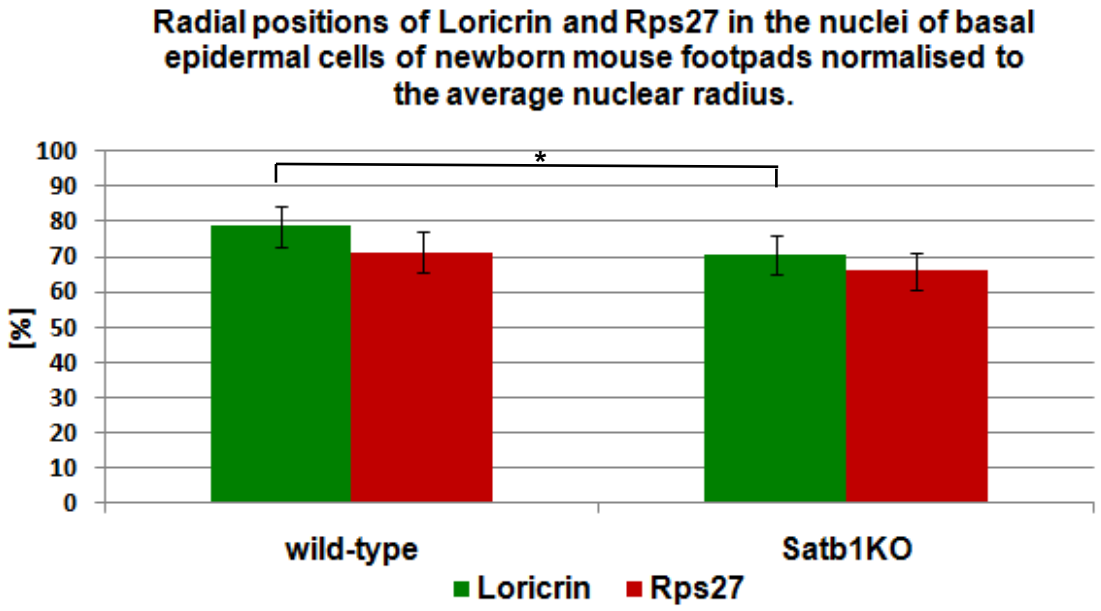

Figure 4.31 Radial positions of Loricrin and Rps27 in the nuclei of basal epidermal cells in wild type and SATB1KO mice normalized to the average nuclear radius. Radial positions of Loricrin, Rps27 were normalized by average nuclear radius of their particular nuclei.

In contrast to the lack of changes in the intra-chromosomal positions of Loricrin, radial positions showed that its distribution in Satb1 KO mouse is different which suggests that additional experiments should be performed so as to finally answer if whether Satb1 is involved in the control of Loricrin movement and expression.

Loricrin was more internal (79%) in the epidermis of SATB1KO mouse than in wild type (71%, p-value<0.05). Position of Rps27 was similar in both tissues.

4.4.3 Alterations in the conformation of the 5Mb chromatin domain containing EDC in Satb1KO mice.

Conformation of the 5Mb chromatin domain in epidermal progenitor cells determined by 3D-FISH showed changes between Satb1 knockout mice and corresponding wild-type mice: the distances between the Rps27 and Lor genes in Satb1KO mice were significantly ($p<0.05$) increased versus the corresponding controls, while distances between the Lor and Gabpb2 genes did not show any changes between Satb1 mutants and wild-type mice (**Fig. 4.31**). However, lack of significant differences in distances between those genes was seen in dermal cells of the Satb1KO mice and wild-type mice, indicating for the tissue-specific effects of Satb1 on 3D-chromatin structure in keratinocytes (**Fig. 4.31**). Thus, similarity in altered expression of the EDC genes seen in the Satb1 -/- mice were paralleled by similar changes in the conformation of the 5Mb chromatin domain containing EDC.

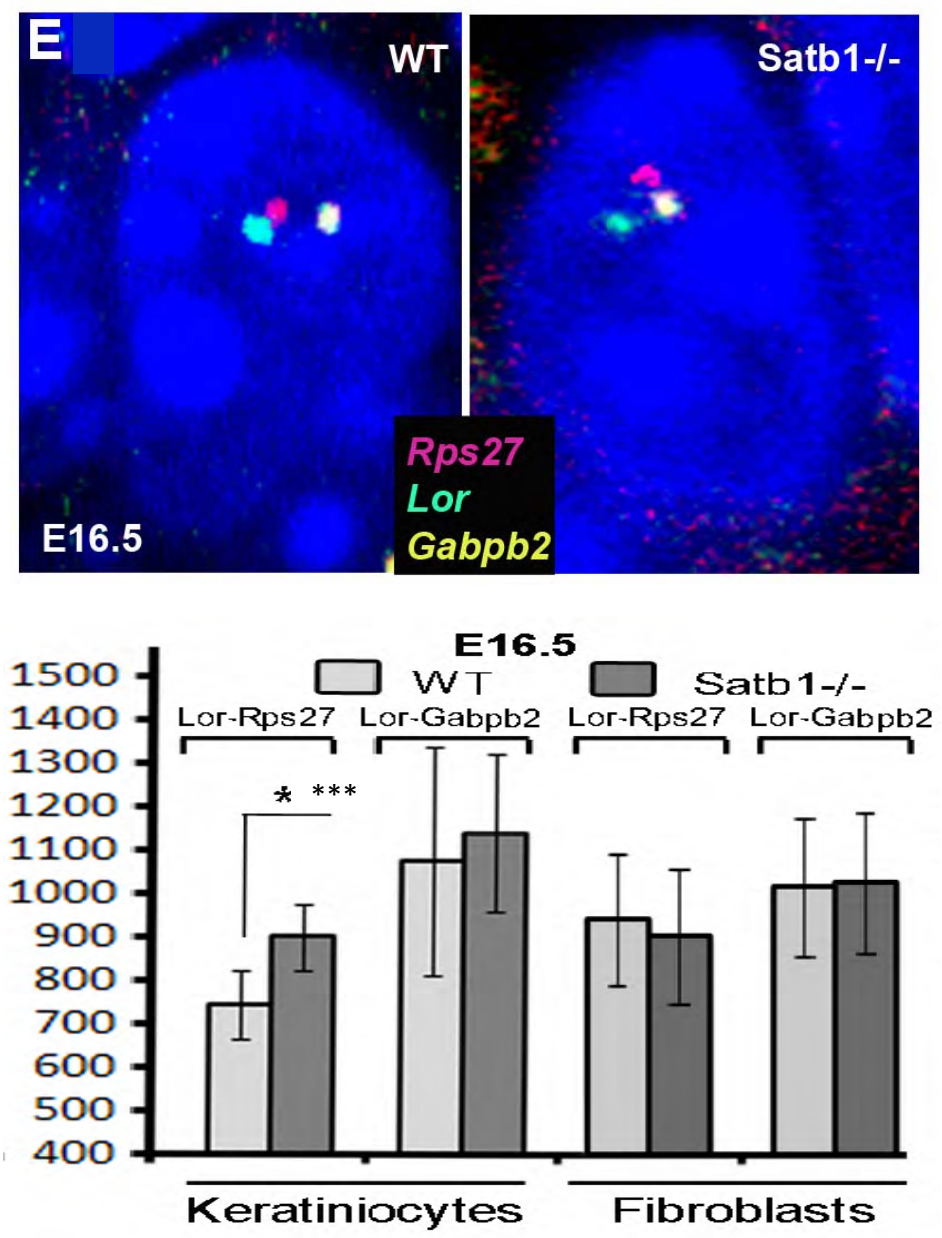

Figure 4.32. Alterations in the conformation of the 5Mb chromatin domain containing EDC in p63-/- and Satb1-/- mice. A - Multi-color 3D-FISH with BACs covering the Rps27, Lor and Gabpb2 in the epidermal cells of p63-/-, Satb1-/- and wild-type mice at E16.5, representative single Z-sections.B - 3D-FISH distances between the Rps27and Lor and the Lor and Gabpb2 in basal epidermal cells Satb1-/- mice and corresponding wild-type mice. Mean+S.E.M, n=60. Pair-wise comparisons – differences between the E16.5 WT versus Satb1 -/- mice are significant ($p<0.01$, Newman-Keuls's test after one way ANOVA test).

4.4.4 Satb1 remodels chromatin conformation of the central EDC domain that contains genes activated during terminal keratinocyte differentiation

To further examine an involvement of Satb1 in chromatin remodelling and execution of gene expression programme in epidermal progenitor cells, 3D-FISH analysis of the chromatin conformation at the EDC locus was performed in the epidermis of E16.5 and P0.5 Satb1 knockout (-/-) and age-matched WT mice. The volume of the central EDC domain, containing a large number of the keratinocyte-specific genes (such as genes belonging to the Sprr and Lce families, as well as *Lor* and *Inv*), significantly increased in the epidermal progenitor cells of Satb1 -/- mice ($p<0.001$) compared to controls. However, in contrast to the epidermal cells, lack of changes in the volume of central EDC domain were seen between dermal cells of Satb1KO and wild-type mice.

The effects of Satb1 ablation on conformation of the central part of the EDC in epidermal cells were domain-specific, since the distances between *S100a6* and *Lor* (5' end of the EDC) or between *S100a10* and Lor (3' end of the EDC) located outside of the central domain remained unchanged in E16.5 Satb1 -/- mice when each of these parameters was compared with those of age-matched WT mice (**Fig. 4.33 A,B**). However, at P0.5, distance between the *Lor* and *S100a6* genes was significantly increased in Satb1 -/- versus wild-type mice, suggesting an involvement of Satb1 in the control of conformation of the 5'- end of the EDC (**Fig. 4.33 B**).

These 3D-FISH data were consistent with microarray and RT-PCR data that show only minor differences in expression of the genes located outside the central EDC domain between Satb1 -/- and wild-type mice (Fessing et al. 2011) and suggest that Satb1 is responsible for the control of gene expression in the central EDC domain via establishing specific chromatin folding specifically at

this region. Therefore, the expression of the genes that constitute the central domain at the EDC locus is tightly linked to its chromatin conformation.

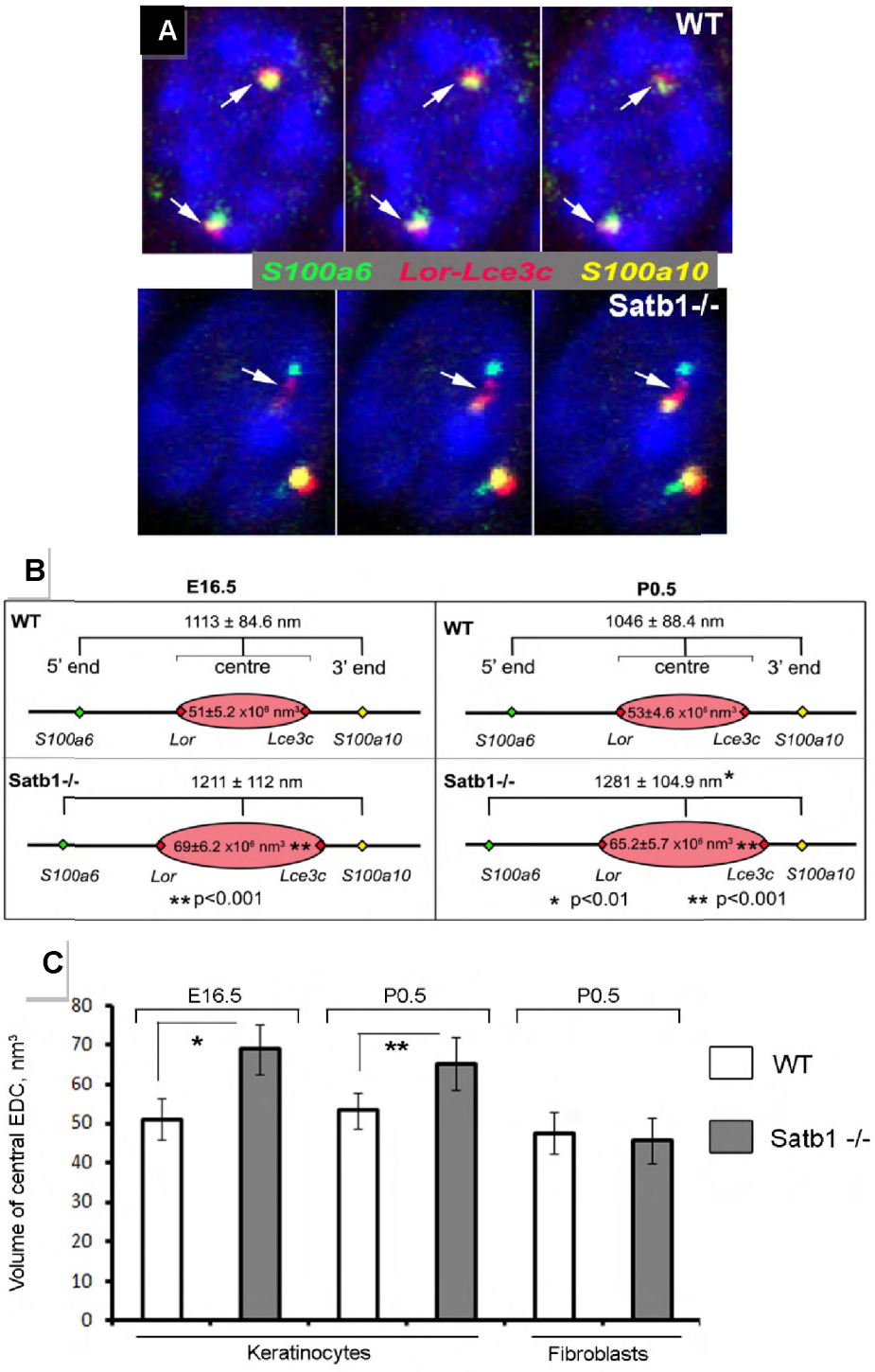

Figure 4.33. Satb1 binds the central EDC domain and regulates its conformation in epidermal cells. A-C: Summary of 3D-FISH analyses with probes detecting the 5'- and 3'-ends of the EDC (S100a6 and S100a10 genes, respectively) and central domain (Lor-Lce3c) in the basal epidermal cells of Stab1-/- and WT mice. Representative single Z-optical sections of newborn WT and Satb1 knockout keratinocyte nuclei are shown (B). Statistical analysis shows significant increase of the volume of central EDC domain in Satb1-/- mice compared to that of WT mice (C, $p<0.001$). Described changes are not observed in dermal fibroblasts (C).

5. Discussion

5.1 Remodelling of nuclear architecture in keratinocytes during epidermal differentiation is associated with changes in their transcriptional activity.

Many studies published in recent years stress the functional importance of nuclear architecture for the control of cell differentiation-associated gene expression programme (Fraser and Bickmore, 2007). It is known that different cell-types characterize with different features of nuclear structure like shape and size of the nucleus (Brandt *et al.*, 2006), number and size of nucleoli, centromeric clusters and others (Dundr and Misteli, 2010). Here, evidence is provided that terminal differentiation of epidermal keratinocytes is accompanied by marked remodelling of their nuclear architecture associated with changes of their transcriptional activity.

5.1.1 Changes in the volume and shape of the nuclei of epidermal keratinocytes reflect their differentiation status and structural organization of the distinct epidermal layers.

Presented data show that nuclei form different keratinocyte layers of the epidermis differ in volume, shape and size (**Fig. 4.1**). Nuclei from basal layer are larger than the ones from the spinous and granular layers, whose volume appear to be similar. It is known that karyo-cytoplasmic ratio is similar in cells of the same type and is essential for the proper tissue structure and functioning. Higher volume of the nuclei of basal keratinocytes may reflect their proliferation/differentiation status (Huber and Gerace, 2007; Umen, 2005) and

may also be due to the fact their population is quite heterogeneous and consists of epidermal progenitor cells, transiently dividing keratinocytes and cells which have stopped dividing (Koster and Roop, 2007b).

Analysis of the shape also shows remarkable differences between the different layers of the epidermis. Basal epidermal keratinocytes and keratinocytes of the granular layer are more elongated compared to cells in the spinous layer. Additionally the long axis of the nuclei in basal cells is oriented vertically in relatively to the dermo-epidermal basal membrane, whereas long axes of the nuclei in spinous and granular layer are orientated horizontally (**Fig. 4.1A-B**). Shape and positioning of the nuclei are controlled by distinct elements of the cytoskeleton and interacting with nuclear envelope and also by the shape of the cell itself (Huber and Gerace, 2007; Melcer and Gruenbaum, 2006). Significance of genetic components in the control of nuclear shape of epidermal cells is unknown, however it was demonstrated that at least in some cell types it is crucial (Brandt *et al.*, 2006). In the epidermis differences in shape and orientation may also reflect structure organization of the distinct layers. Initially In vitro studies suggested that stratification arises as an effect of decrease of contacts with dermo-epidermal basal membrane -epidermal delamination (Vaezi *et al.*, 2002; Watt and Green, 1982), however later studies in situ demonstrated that arising of second epidermal layer is caused by change of the orientation of the plane of division from perpendicular to the basal membrane to paralel (Lechler and Fuchs, 2005). Perpendicular plane of division in basal layer for cells staying in this layer and parallel plain for keratinocytes which passess to spinous layer is very likely to be responsible for changes in long axis orientation between layers of epidermal keratinocytes. In addition, according to our data, keratinocytes of basal layer are packed more densely than in spinous and

granular layer and interact with dermo-epidermal basal membrane. These two features may be at least partially the reason of tthe elongation of basal layer nuclei because vertical direction opposite to the basal layer is the only one available for relatively unrestricted cell growth. The keratinocyte density in suprabasal layers is at least three times lower compared to the basal layer and their positioning seems to be much less restricted – they form 2-3 layers of cells having nuclei on average 25% smaller than in basal layer and with longer axis oriented parallel to the basal membrane (**Fig. 4.1**). This supports the idea that elongation of the long axes of the nuclei from basal layer is likely to be enforced by the association with basal membrane and much higher cell density. In the granular layer nuclei have similar volume as in spinous layer, however they are more elongated (**Fig. 4.1 B-C**). It may again reflect the structural organization of the upper epidermal layers in which cell membrane becomes cornified and cell flattened.

5.1.2 Changes in the transcriptional activity, number and volume of nucleoli are associated with distinct metabolic status of the cells in different epidermal layers

Global levels of transcription and the number and size of nucleoli are tightly coupled with metabolic activity of the cell (Derenzini *et al.*, 2009; McKeown and Shaw, 2009). Analysis of the markers of transcription (**Fig.4.2**) and morphology of the nucleoli (**Fig. 4.3 and Fig. 4.4**) showed significant differences between keratinocytes from different layers of the epidermis.

Transcriptional activity depicted by immunostaining of the active form of RNA polymerase II or trimethylated lysine 4 of histone H3 (H3K4) was high in the

basal layer and increased even more in spinous layers and decreased significantly in the granular layer (**Fig.4.2**). The proliferating epidermal basal layer keratinocytes require a high level of transcriptional activity. In the spinous layer, keratinocytes do not replicate, however, a lot of structural proteins required for epidermal barrier are synthesised at a very high level. In the granular layer, the cell membranes of keratinocytes become cornified, transcription decreases and the cells slowly die becoming a part the cornified cell envelope (Koster and Roop, 2007b).

Nucleoli are largest nuclear bodies and they are formed only around active NORs of the distinct chromosomes. Their most important function is synthesis of rRNA required for ribosome assembly. It was noticed that nucleoli are larger in rapidly dividing cells or in cells with very high metabolic activity(Lam *et al.*, 2005). In the epidermis, there are more nucleoli in the basal layer compared to spinous and granular layers (**Fig. 4.4A**). The number of nucleoli also depends on the metabolic activity of the cell and its differentiation status(McKeown and Shaw, 2009). Less differentiated cells, like basal layer keratinocytes, have a larger number of smaller nucleoli, while in more differentiated cells of spinous and granular layers of the epidermis nucleoli have a tendency to fuse and their number decreases (McKeown and Shaw, 2009; Sullivan *et al.*, 2001) (**Fig. 4.4A**).

Furthermore, the immunofluorescent signal coming from the nucleoli in the granular layer is weaker compared to the spinous layer suggesting that their activity decreased. This correlates well with markers of transcription suggesting that metabolic activity of the cells is high in basal layer, increases in spinous layers and decreases in granular layer (**Fig. 4.2 and Fig. 4.3A**)

5.1.3 Centromeric clusters and nucleoli as structural hubs organizing a global chromatin structure in 3D nuclear space

Centromeres are heterochromatic regions of DNA serving as sites of the attachment of the mitotic spindles during mitosis (Aleixandre *et al.*, 1987; Choo, 2001). The centromere consists mainly of different types of DNA repeats. Centromeres tend to cluster in the nucleus and the number of these clusters visualized after labelling with sub-centromeric probes (pancentromeric in human or major satellite in mouse) is much lower than the total number of chromosomes in the cell (Alcobia *et al.*, 2000; Haaf and Schmid, 1991). The relative simplicity of the detection of centromeres by non-chromosome specific FISH probes suggested the analysis of centromeric clusters as a valuable tool to investigate nuclear architecture.

The data presented demonstrate that the average number of the centromeric clusters per nucleus increases during the epidermal keratinocyte differentiation from about 13 in the basal layer to 16 in spinous and granular layers (**Fig. 4.6A**). This suggests that some centromeric clusters disassemble at least partially during terminal differentiation. In terms of global chromatin organization in the nucleus, it suggests that in the spinous and granular layers only about 2.5 chromosmes form each cluster while in the basal layer each cluster is formed by 3.1 chromosmes. These data suggest that terminal keratinocyte differentiation is accompanied by reorganization of the chromosome positioning and, possibly, their relocation versus each other which may be important for the control of gene expression or silencing. These data, however, are in contrast with other studies describing that in Purkinje cells (Solovei *et al.*, 2004a) or

testis (Scherthan *et al.*, 1996) more differentiated cells show lower number of the centromere clusters. It may suggest that differentiation of keratinocytes is accompanied by distinct patterns of re-organization of 3D nuclear structure compared to other tissues.

Since most centromeric cluster contains centromeres from several chromosomes their intra-nuclear localization may also be of great importance for the genome organization and functioning (Solovei *et al.*, 2004a). According to radial position analysis centromeric clusters have more peripheral positions in the nucleus in the spinous layer than in basal layer and move again towards the nuclear interior in cells of the granular layer (**Fig.4.6B**). Comparison with random mathematical models of the nuclei of the same parameters as experimental allows stating that these positional changes cannot be fully explained by the changes in number and size of clusters or by purely geometrical changes of nuclear size and shape.

Together with centromeric clusters, nucleoli also play a very important role in the genome organization (Solovei *et al.*, 2004a). Because of the nucleoli assembling around the specific loci on 10 chromosomes (5 homological chromosomes in the interphase nucleus) nucleoli show a tendency to form associations with centromeric clusters (Testillano *et al.*, 1991). It is known that most of the NORs are located within the nucleoli (Kalmarova *et al.*, 2007) and therefore, nucleoli can similarly to centromeric clusters tether chromosomes together and restrict their mobility. From this point of view, the observed decrease of the number of nucleoli seen during keratinocyte differentiation also suggests tightening of the network of the special nuclear constrains that could shape the 3D genome organization in epidermal cells.

In addition to the differences in the number of nucleoli in keratinocytes between the distinct layers of epidermis the changes in their nuclear localization have also been observed (**Fig.4.4B**). Nucleoli in the spinous and granular layers of the epidermis had significantly more internal positions than ones in the basal layer. Again, comparison of these data with the mathematical model of random nuclei suggested that these repositioning was specific and cannot be fully explained by changes of geometrical constraints in the nucleus (**Fig.4.4B**). It is likely that more internal positions of nucleoli in the spinous and granular layers is a result of re-organization in the positioning of chromosomes localised in different part of nuclei.

In conclusion, the data presented support the view that the nuclear 3D-structure changes significantly during terminal keratinocyte differentiation and structural differences are accompanied by changes of the global transcriptional and metabolic activity in the cells. Changes at the global genome organization level may have a profound effect on the local gene expression status, especially for the tissue-specific loci regulated by long-range chromatin interactions.

These data also suggest that nucleoli together with centromeric clusters are involved in organization of the 3D nuclear space in a cell-type specific manner and play a role in anchoring of the chromosomes limiting their mobility (**Fig. 5.1**).

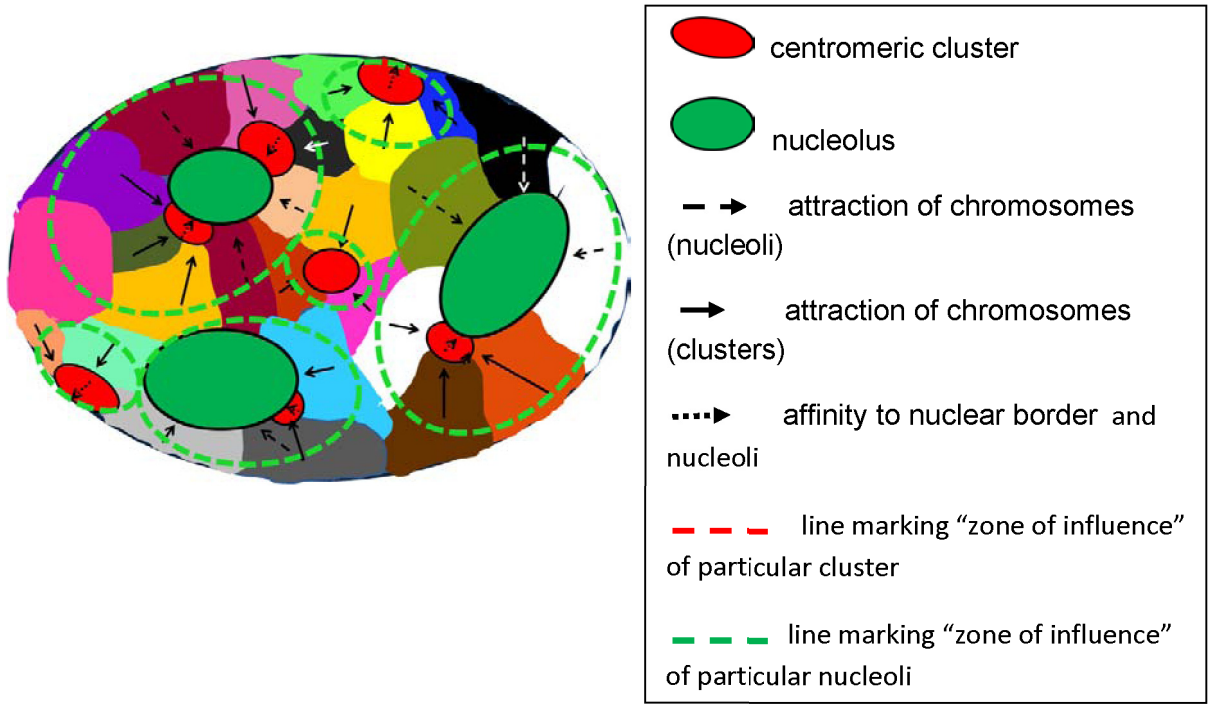

Figure 5.1. Nuclear architecture. Explanation in text.

5.2 The position of the epidermal differentiation complex locus (EDC) within 3D nuclear space is changed during epidermal development.

Several studies published in recent years reported relocation of the loci within 3D nuclear space associated with the changes of gene expression levels and cell differentiation, thus suggesting that gene positioning may be an important factor in the gene expression control (Chambeyron *et al.*, 2005; Kosak *et al.*, 2002; Volpi *et al.*, 2000; Williams *et al.*, 2002b; Zink *et al.*, 2004). It is noteworthy that all these experimental data were obtained in different types of cultured cells and up to now there was no study of these aspects in tissues.

5.2.1 Relocation of EDC in the 3D nuclear space during the murine epidermal morphogenesis.

The data presented in this study show changes in nuclear positioning of the tissue-specific locus involved in the control of epidermal morphogenesis - epidermal differentiation complex (EDC) located on chromosome 3, and, specifically one of its genes (Loricrin), associated with the development of the mouse epidermis. This relocation occurs in the basal keratinocyte nuclei between 11.5 (E11.5) and 16.5 (E16.5) days after gestation and is accompanied by significant upregulatation of the expression of EDC genes . Three different analytical approaches used in this study demonstrate that EDC and Loricrin are localized at the peripheral parts of the nucleus and chromosomal territory in the epidermal keratinocytes at E11.5 (**Fig. 4.8 and Fig. 4.9**). At E16.5 when several epidermal cell layers become visible and gene expression within the EDC is increased. Loricrin and the entire EDC locus moves towards the nuclear interior and internal part of the chromosome territory 3 (**Fig. 4.8 and Fig. 4.9**.).

EDC relocation towards the nuclear interior is cell-type specific and is observed only in the epidermal cells expressing EDC genes, but not in the dermal fibroblasts, where EDC remains at the peripheral position at E16 and later stages similarly to E12.

Behaviour of the highly expressed control loci forming “close genomic neighbourhood” of the EDC - Rps27 and Gabpb2 0.3 Mb and 1.5 Mb of the 5’ and 3’ flank regions of EDC respectively, as well as two control loci from “distant neighbourhood” – Tdo2 and RhoC (8 Mb and 10 Mb from the EDC 5’- and 3’ – flank regions) is very different: these genes either do not change their positions

or change their positions to a much lesser extent compared to the EDC (**Fig.4.12**). These data strongly suggest that relocation of the Loricrin is not merely the result of reorganization of the whole chromosome region, but its movement is locus-specific. At E11.5, the EDC locus has low transcription activity and in contrast to the highly expressed controls is located at the nuclear periphery. At E16.5, Loricrin occupies similar position to these highly expressed genes, which is confirmed by significant shortening of the distances between the Loricrin and Rps27 and the Loricrin and Gabpb2 and correlates with increase of its expression (**Fig 4.16**). These findings are consistent with a widely accepted opinion that many, active genes tend to take more internal nuclear positions in more differentiated cells (Misteli, 2007; Shopland *et al.*, 2006).

5.2.2 Alteration in the higher order chromatin remodelling of the *EDC* locus in p63 deficient mice.

P63 transcription factor serves as a master regulator of epidermal development and regulates a number of tissue specific genes in epidermal keratinocytes. P63 KO mice fail to develop a stratified epidermal barrier – they have only one layer of cells and lack epidermal stratification (Mills *et al.*, 1999; Yang *et al.*, 1999). Our data demonstrate that EDC and *Loricrin* occupy much more peripheral positions within the nucleus and CT3 in skin epithelia of the p63 -/- in comparison to the wild type basal keratinocytes at E16.5. (**Fig.4.21 and Fig.4.22**). This observation suggests the importance of functional relations between the special relocation of the *EDC* locus and the development of the functional epidermis.

Although data presented here provide insights into the basic features of the *EDC* 3D-structure at different stages of epidermal development, there are still many questions regarding its nuclear organization. Measurements of the distances between *Loricrin* and *Rps27* and between *Gabpb2* indicate higher condensation of these domains at E16.5 compared with E11.5 (**Fig.4.25 and Fig. 4.27**). It may indicate that contrary to the *EDC* alone, DNA regions adjacent to the *EDC* locus undergo condensation or that there are some other changes in higher-order chromatin folding. Assuming that 3.1 Mbp EDC region has a form of 30 nm chromatin fibre (packing ratio 1:40) it would measure almost 27 μm whereas according to our measurements it appears to be no longer than 2.5 μm, as a simple string of nucleosomes it would span more than 150 μm. These calculations suggest involvement of some higher-order chromatin organization above 30 nm fibre which possibly allows different types of spatial chromatin reorganization (i.e. looping), not necessarily related to the condensation of the chromatin fibre by itself.

Strong evidence indicates the essential role of the EDC relocation from the nuclear periphery towards nuclear centre for maintenance of the high levels of expression of its genes and for epidermal morphogenesis. Data from our laboratory demonstrate that after relocation into the nuclear interior, EDC becomes associated with nuclear speckles containing large amounts of splicing factors that facilitate high expression of tissue-specific genes. Interestingly, a number of speckles present in the vicinity of the EDC significantly increased at E16.5 versus E11.5. However, the number of the nuclear speckles near *EDC* significantly decreased in p63KO keratinocytes in comparison to the wild type keratinocytes at E16.5 (Fessing et al 2011).

These findings suggest that relocation of *EDC* might be required to facilitate access of its genes to the splicing machinery enriched in speckles. It is also known that transcription factories are distributed more densely around the highly expressed genes, so proximity of speckles may also cause more efficient transcription through easier access to transcription factory sites (Iborra *et al.*, 1996; Osborne *et al.*, 2007). Mechanisms driving the EDC relocation in the epidermal progenitor cells is another important question. Researchers suggest that one of the possible mechanisms responsible for repositioning may be the “nucleation” of loci by domains enriched by transcription or splicing factors (Brown *et al.*, 2008). This mechanism may be involved in the EDC remodelling, since the nuclear speckles containing splicing factors are observed in its vicinity (Fessing et al 2011).

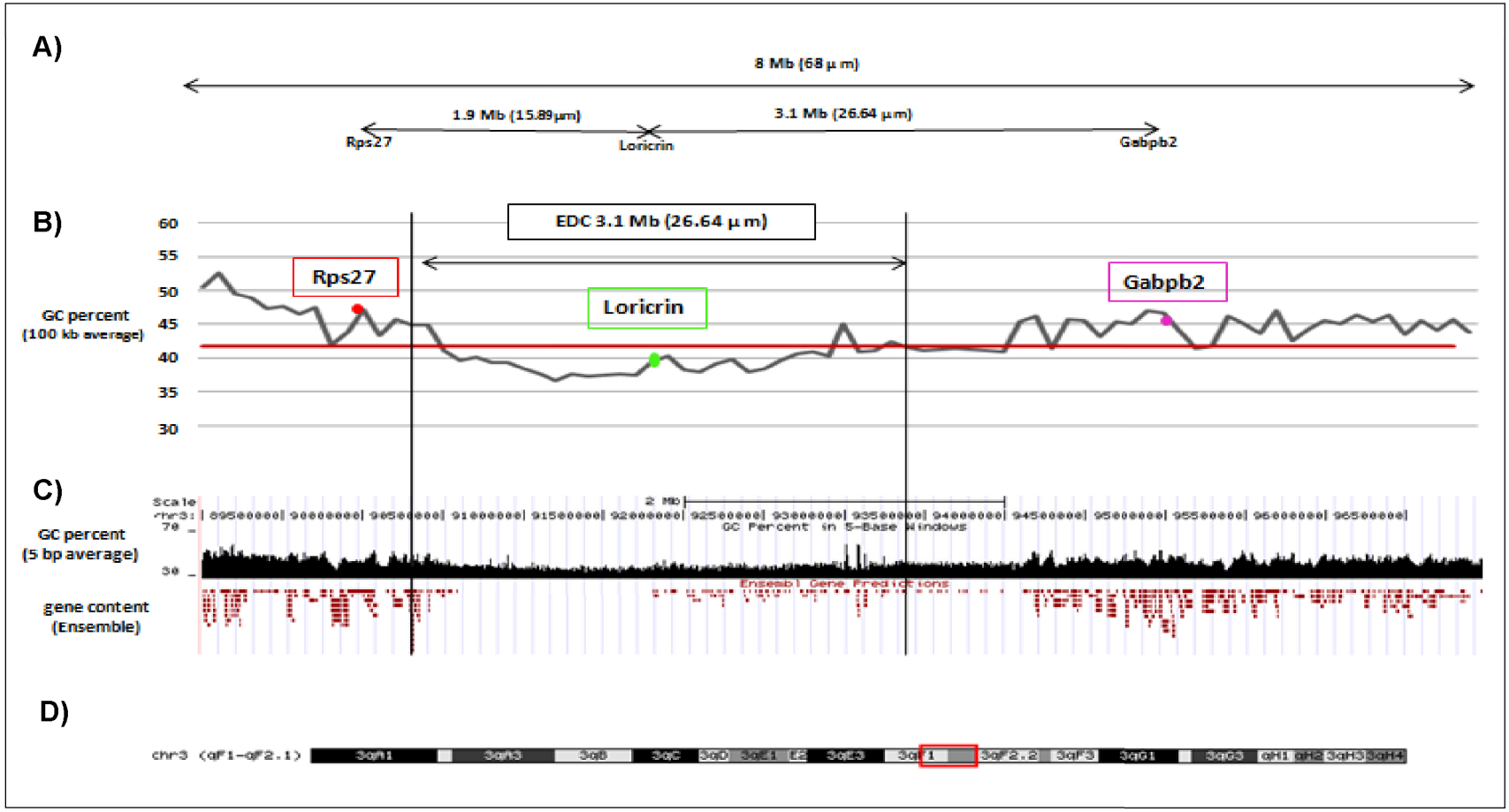

Figure 5.2 Structure and characteristic of epidermal differentiation complex. Figure displays structure and certain features of EDC and its close neighborhood containing control loci Rps27 and Gabpb2 (elaborated on the basis of data from UCSC genome browser (http://genome.ucsc.edu/). A) Distances between the loci in base pairs and (hypothetical length of relaxed chromatin domains is shown bracets). B) GC content of the EDC and its surroundings calculated as an average for 100 kb DNA fragments. C) GC content calculated as an average for 5 base pairs. D) Localization of the loci on chromosome3.

However, there is another possible explanation regarding developmentally regulated relocation of the EDC complex. It is known that genes that tend to cluster in the nucleus are characterized by higher than average GC content, whereas gene-poor genomic regions are AT-rich (Fedorova and Zink, 2008). Linear organization of the *EDC* and its neighborhood based on data from UCSC genome browser (http://genome.ucsc.edu/) is presented in **Figure 5.2**. *EDC* has on both sides the gene-rich and GC-rich neighbourhoods, which, according to the literature should predispose this region to be localized in the nuclear interior. GC-content of the EDC is mostly below average for mouse genome (41,8%), and only relatively short distal 3' and 5' flank regions show higher levels of GC-content. Interestingly 1.3 MB in the 5' part of the EDC is a "gene desert" deprived from any genes which should pull this part towards nuclear periphery. *Loricrin* is one of the first genes on the border of this "gene desert". It is worth mentioning that the regions containing *Rps27* and *Gabpb2* are gene-rich and their GC content exceeds 45%.

This analysis allows the hypothesis that *EDC* has a natural tendency for placement in the peripheral nuclear position due to its low GC content and the presence of the gene poor domain. *EDC* is located at the nuclear periphery in fibroblasts as well as in epidermal keratinocytes at E11.5 when its genes are weakly expressed. After the upregulation of the gene expression within the *EDC* during epidermal development the mechanisms involving nucleation or ATP dependent chromatin remodelling and/or other active mechanisms may pull it towards the nuclear interior, the surface of chromosome territory and inter-chromosome compartment containing speckles. It remains to be determined, however, whether the genomic targets of the p63 transcription factor mediate its effect on the developmentally regulated EDC relocation in the epidermal progenitor cells. It may also be interesting to check

whether EDC changes its positioning in adult epithelial stem cells during their differentiation into epidermal cells.

5.3 Satb1 controls higher order chromatin folding of the EDC locus and is regulated by p63

Satb1 is known as the genome organizer protein that regulates large-scale chromatin folding in many cell types (Agrelo *et al.*, 2009; Cai *et al.*, 2003; Han *et al.*, 2008). In lymphocytes, Satb1 is involved in the remodelling of the higher-order chromatin structure of the T_H2 cytokine locus, and promotes the conformation changes associated with the increase of cytokine gene expression (Cai *et al.*, 2006). Recent data also reveal a role for Satb1 in regulating the expression of stem cell-associated genes and controlling the balance between self-renewal and differentiation (Savarese *et al.*, 2009).

We have shown here that Satb1 binds to the central domain of the tissue-specific *EDC* locus and controls the establishment of its specific conformation in keratinocytes. It has been shown previously that intra-nuclear EDC positioning is cell-type specific, and differs between cultured human keratinocytes and lymphocytes (Williams *et al.*, 2002a). It was also reported that the treatment of isolated human keratinocytes with 5-azacytidine and sodium butyrate promoting the formation of “open” chromatin structure results in an increase of the expression of epidermis-specific genes within the EDC (Elder and Zhao, 2002a). These and other reports suggest that changes in local epigenomic modification at the EDC gene

promoters may also be required for efficient expression of these genes (Ezhkova *et al.*, 2009; Frye *et al.*, 2007; Sen *et al.*, 2010a).

Analysis presented here shows that Satb1 deficiency results in alterations in the conformation of the central EDC domain, which contains a large number of genes involved in the control of terminal keratinocyte differentiation (Brown *et al.*, 2007; Martin *et al.*, 2004b). These alterations, represented by elongation of the central EDC domain, are associated with a marked decrease in expression of the genes involved in the epidermal barrier formation, accompanied by morphological changes in the epidermal structure (thinning of the granular layer, decrease of the epidermal thickness). The lack of similar dynamics in the EDC in the nuclei of dermal cells suggests that the developmentally-regulated remodelling of the higher-order chromatin structure in this locus is associated with an increase of its transcription activity and is indeed a tissue-specific event.

It has been shown that during T_H2 lymphocyte activation, Satb1 promotes the formation of a specific three-dimensional structure of the cytokine locus, in which chromatin is folded into numerous small loops that bring proximal and distal gene regulatory elements together to activate the cytokine gene expression (Cai *et al.*, 2006). Recent data demonstrate that Satb1 also controls the formation of the chromatin loops in the beta-globin locus (Wang *et al.*, 2009). We hypothesize that Satb1 may be involved in the formation of similar loop-like structures within the central EDC domain (Fessing et al., 2011), where cis-regulatory elements of the terminal differentiation-associated genes (Martin *et al.*, 2004b) may be brought in close spatial proximity to form a transcriptionally-active chromatin structure. Specific Satb1 binding was undetected at the *Lor* locus *per se,* and yet it is regulated in the

context of Satb1-dependent three-dimensional transcriptional complex (Fessing et al., 2011). If this hypothesis is correct, the central EDC chromatin domain cannot be properly folded in the absence of Satb1, therefore, this region will remain more decompressed (or elongated) compared to WT cells, and it will not be able to support efficient expression of the terminal differentiation-associated genes. To test this hypothesis, additional studies using the chromatin conformation capture (3C) techniques are required to identify the role of Satb1 in the formation of such chromatin loop-like structures within the EDC locus. However, significant changes in the volume of the central EDC domain shown here provide strong support for this hypothesis.

It was demonstrated by Fessing and colleagues that Satb1 is regulated by p63 by ChIP assay showing that p63 binds upstream to Satb1 transcription site and also by siRNA experiments in showing the absence of Satb1 in the whole E13.5 embryonic skin culture when p63 is silenced. These experiments showed a novel function for the p63 transcription factor, a master regulator of the development of stratified epithelia (Crum and McKeon, 2010; Koster and Roop, 2007a; Truong and Khavari, 2007), in the control of three-dimensional chromatin structure and remodelling in the epidermal keratinocytes during development and terminal keratinocyte differentiation. Genes that control higher order chromatin remodelling, covalent histone modifications and nuclear assembly are likely to represent a previously un-recognized class of the p63 targets and form an important part of the molecular network controlling the complex program of epidermal development and stratification regulated by p63.

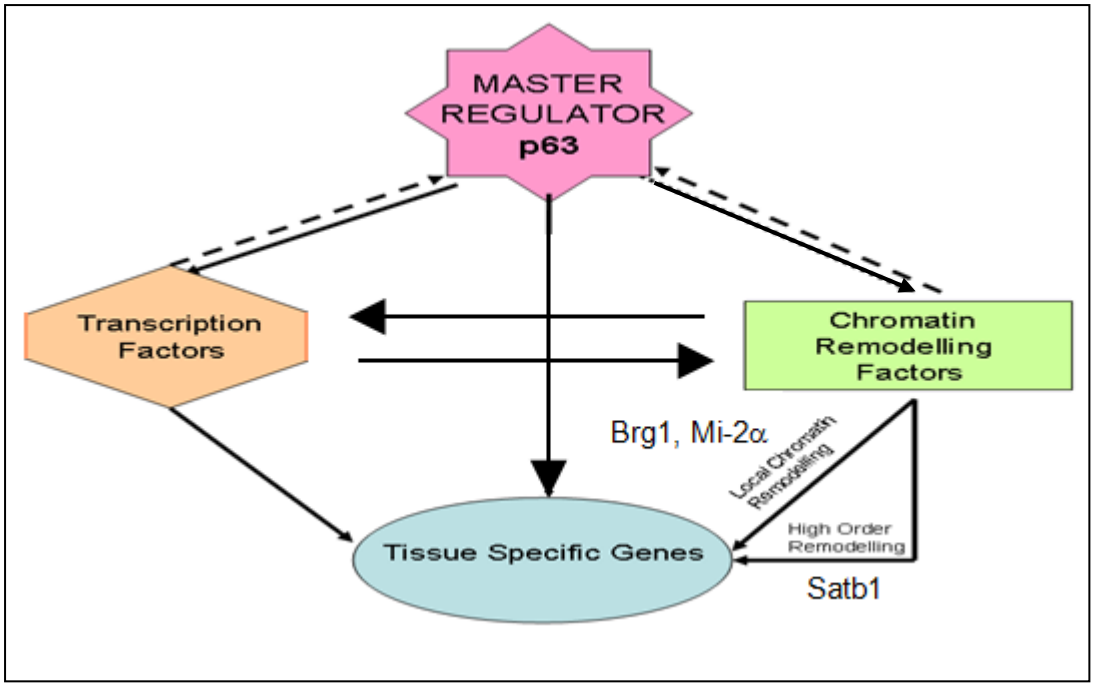

Figure 5.3 Model of regulation of epidermal morphogenesis. Presented study together with other reports indicate that p63 is a master regulator gene acting both directly as a transcriptional factor on tissue specific genes or indirectly via chromatin remodelling factors like SATB1, Brg1 or Mi-2α

6. **Conclusions:**

1. Nuclear architecture of the epidermal keratinocytes undergoes remarkable remodelling during epidermal differentiation, which include changes in the nuclear volume and shape, number, size and distribution of the nucleoli, as well as in the number and distribution of centromeric clusters and frequency of interactions with nucleoli.
2. Changes in the nuclear architecture during terminal keratinocyte differentiation show a correlation with the dynamics of the transcriptional and metabolic activity. In particular, terminal differentiation is accompanied by the decrease of nuclear volume, elongation of its shape, reduction of the number and fusion of nucleoli, an increase in the number of centromeric clusters and a dramatic decrease of the transcriptional activity.
3. Global changes in the nuclear architecture of epidermal keratinocytes are associated with marked remodelling of the higher-order chromatin structure of the EDC locus containing a large number of genes activated during terminal keratinocyte differentiation. EDC is positioned peripherally in the epidermal nuclei at E11.5 when its genes show low expression levels and relocates towards the nuclear interior at E16.5 when EDC genes are markedly upregulated. The EDC relocation during epidermal morphogenesis is cell-type specific and it is not observed in fibroblasts. It is also specific to the EDC locus because genes from its close neighbourhood do not exhibit such pronounced developmentally-regulated movements.

4. The p63 transcription factor serving as a master regulator of epidermal development is involved in the control of EDC relocation in epidermal progenitor cells. The epidermis of E16.5 p63KO exhibits significantly more peripheral positioning of the EDC loci, compared to wild-type mice. This strongly suggests that p63 may control expression of the genes that regulate higher-order chromatin remodelling in epidermal cells during development in developmentally-associated remodelling.
5. The genome organizer Satb1 serving as a direct p63 target controls higher order chromatin folding of the central part of *EDC* and Satb1 knockout mice show alterations of epidermal development and expression of the EDC encoded genes.
6. This study provides a novel fundamental mechanism on how master regulators of tissue morphogenesis control the fate of multi-potent progenitor cells, through establishing tissue- and developmental stage-specific patterns of chromatin organization and remodelling.
7. The programme of epidermal development and terminal differentiation regulated by p63 and other factors include marked remodelling of three-dimensional nuclear organization and positioning of tissue specific loci. In addition to the direct involvement of p63 in controlling the expression of tissue-specific genes, p63 via regulation of the chromatin remodelling factors such as Satb1 promotes establishing specific conformation of the EDC locus required for efficient expression of terminal differentiation-associated genes.

7. Future work

Many questions regarding the functional meaning of nuclear structure, gene positioning and EDC structure require further investigation:

1. It is known that centromere clustering is not random, so extensive FISH analysis of how particular chromosomes cluster could provide much better insights into differences in nuclear structure between keratinocytes in different layers in the epidermis.
2. FISH analysis of the distribution of whole interphase chromosomes as well as LINE and SINE repeats within the nucleus would be desirable since centromeres are specific parts of chromosomes which do not give full information on the chromosome position and conformation.
3. A study of EDC conformation by the chromatin conformation capture assay (3C) and its high-throughput version – carbon copy of chromatin conformation capture assay (5C) in wild-type mice as well as in p63 and Satb1 knockout mice.
4. Charcterization of EDC DNase I hypersensitive sites to describe potential regulatory sequences.
5. Characterization of EDC epigenetic marks – Chip on Chip or Chip-seq for different histone modifications and functional states of RNA polymerase II.

8. **Appendix**

loci	tissue/sample	Position			confidence interval		
		peripheral	middle	internal	peripheral	middle	internal
EDC	e12	54	20	26	9.6%	7.8%	8.5%
	e16	13	23	64	6.8%	8.2%	9.3%
	e17.5	16	28	56	7.3%	8.7%	9.5%
	e17.5 fibroblasts	63	20	17	9.3%	7.8%	7.4%
	e17.5 suprabasal	28	26	46	8.7%	8.5%	9.6%
	p10	16	28	56	7.3%	8.7%	9.5%
	e16 p63KO basal	40	23	37	9.4%	8.2%	9.3%
	e16 p63KO fibroblasts	63	18	19	9.3%	7.6%	7.7%
loricrin	e12	55	20	25	9.6%	7.8%	8.4%
	e16	22	26	52	8.1%	8.5%	9.6%
	p10	27	13	60	8.6%	6.8%	9.4%
	e16 p63KO	44	28	28	9.5%	8.7%	8.7%
rps27	e12	15	24	61	7.1%	8.3%	9.4%
	e16	5	16	79	4.8%	7.3%	8.0%
	p10	2	6	92	3.7%	5.1%	5.7%
	e16 p63KO	12	25	63	6.6%	8.4%	9.3%
gabpb2	e12 B MS-84	4	22	72	4.5%	8.1%	8.7%
	e17.5	8	23	69	5.7%	8.2%	8.9%
	e17.5 fibroblasts	11	16	73	6.4%	7.3%	8.6%
	e17.5 suprabasal	10	14	76	6.1%	6.9%	8.3%
	e16 p63KO	6	20	74	5.1%	7.8%	8.5%
	e16 p63KO fibroblasts	9	22	69	5.9%	8.1%	8.9%
BAC 2.138	e12	10	44	46	6.1%	9.5%	9.6%
	e16	12	32	56	6.6%	9.0%	9.5%
	p10	25	19	56	8.4%	7.7%	9.5%
BAC 2.140	e12	11	31	58	6.4%	8.9%	9.5%
	e16	13	25	62	6.8%	8.4%	9.4%
	p10	7	16	77	5.4%	7.3%	8.2%
loricrin	P0 wt basal	29	15	56	8.8%	7.1%	9.5%
	P0 wt fibroblasts	83	6	11	7.4%	5.1%	6.4%
	P0 wt Suprabasal	25	12	63	8.4%	6.6%	9.3%
	P0 SATB1 KO basal	27	22	51	8.6%	8.1%	9.6%
	P0 SATB1 KO fibroblasts	64	13	23	9.3%	6.8%	8.2%
	P0 SATB1 KO suprabasal	22	16	62	8.1%	7.3%	9.4%
rps27	P0 wt basal	5	11	84	4.8%	6.4%	7.3%
	P0 wt fibroblasts	12	31	57	6.6%	8.9%	9.5%
	P0 wt Suprabasal	12	10	78	6.6%	6.1%	8.1%
	P0 SATB1 KO basal	12	15	73	6.6%	7.1%	8.6%
	P0 SATB1 KO fibroblasts	11	19	70	6.4%	7.7%	8.9%
	P0 SATB1 KO suprabasal	5	12	83	4.8%	6.6%	7.4%
loricrin	e12 bis	59	13	26	9.5%	6.8%	8.5%

Table. A.1 Loci distribution in relation to chromosome territory 3 in different tissues

		edc							loricrine			rps27			Gabpb2					loricrine						rps27						EDC	lor	rps27
		e12 Mu	e16 M	e17.5 B	e17.5 fi	e17.5 s	e16 p63	p10 M	e12 M	e16 M	e16 p63	e12 M	e16 M	e16 p63	e12 B	e17.5 B	e17.5 fi	e17.5 s	e16 p63	P0 wt b	P0 wt fi	P0 wt S	P0 SATI	P0 SATI	P0 SATI	P0 wt b	P0 wt fi	P0 wt S	P0 SATI	P0 SATI	P0 SATI	e16 p63	p10 B	p10B
edc	e12 Munich	0.0	41.3	32.9	2.6	14.6	4.2	32.9	0.0	22.9	2.4	36.5	67.9	42.7	57.1	53.8	51.2	55.8	61.4	19.2	19.8	28.0	17.2	2.5	28.6	73.9	40.7	56.1	49.8	48.6	72.5	1.9	23.9	92.7
	e16 M	41.3	0.0	1.3	60.4	8.6	21.0	1.3	43.2	3.7	31.4	0.2	6.4	0.1	3.1	1.4	2.0	3.6	3.5	8.3	98.5	7.3	6.4	55.9	3.6	10.5	1.6	6.5	2.3	0.8	9.5	57.9	7.8	23.1
	e17.5 B	32.9	1.3	0.0	50.1	4.3	14.7	0.0	34.6	1.2	22.4	0.6	13.0	1.2	5.4	4.5	6.4	9.1	8.4	7.7	89.8	8.8	3.8	48.1	4.5	18.8	0.7	12.7	6.7	4.2	17.4	48.4	8.4	33.9
	e17.5 fibroblasts B	2.6	60.4	50.1	0.0	27.6	12.8	50.1	2.1	38.3	7.4	54.7	90.0	61.7	77.3	74.3	71.8	77.0	82.8	34.1	11.6	44.9	31.5	2.4	45.9	96.5	58.7	77.2	70.2	68.9	95.0	0.2	39.9	116.4
	e17.5 suprabasal B	14.6	8.6	4.3	27.6	0.0	3.3	4.3	15.8	1.1	8.0	6.1	27.1	9.1	17.9	15.9	15.9	19.5	21.6	3.9	61.2	8.0	0.6	26.1	5.5	33.2	8.0	21.8	15.5	13.5	31.8	26.1	6.2	50.4
	e16 p63KO B	4.2	21.0	14.7	12.8	3.3	0.0	14.7	4.9	7.9	1.9	17.3	43.7	21.9	33.8	31.0	29.5	33.6	37.7	7.3	39.1	13.7	4.8	11.6	12.8	49.7	20.5	34.8	28.5	27.0	48.3	11.5	10.8	67.8
	p10 M	32.9	1.3	0.0	50.1	4.3	14.7	0.0	34.6	1.2	22.4	0.6	13.0	1.2	5.4	4.5	6.4	9.1	8.4	7.7	89.8	8.8	3.8	48.1	4.5	18.8	0.7	12.7	6.7	4.2	17.4	48.4	8.4	33.9
loricrine	e12 M	0.0	43.2	34.6	2.1	15.8	4.9	34.6	0.0	24.4	2.7	38.3	70.1	44.6	59.2	55.9	53.3	58.0	63.6	20.6	18.7	29.7	18.6	2.2	30.3	76.2	42.5	58.2	51.8	50.7	74.8	1.5	25.5	95.2
	e16 M	22.9	3.7	1.2	38.3	1.1	7.9	1.2	24.4	0.0	14.6	2.1	18.6	4.0	10.9	9.1	9.6	12.6	13.8	4.1	74.6	6.4	0.9	36.1	3.3	24.3	3.6	15.3	9.4	7.4	23.0	36.6	5.4	40.3
	e16 p63KO M	2.4	31.4	22.4	7.4	8.0	1.9	22.4	2.7	14.6	0.0	26.8	58.6	31.9	44.2	42.7	43.1	48.2	51.0	16.3	33.6	25.1	11.5	9.7	23.5	66.5	28.3	50.4	42.3	39.5	64.7	7.3	21.2	86.7
rps27	e12 M	36.5	0.2	0.6	54.7	6.1	17.3	0.6	38.3	2.1	26.8	0.0	8.9	0.4	4.4	2.6	3.3	5.3	5.5	6.7	92.7	6.5	4.4	50.9	2.9	13.5	1.4	8.2	3.5	1.8	12.4	52.4	6.7	27.0
	e16 M	67.9	6.4	13.0	90.0	27.1	43.7	13.0	70.1	18.6	58.6	8.9	0.0	6.7	4.5	2.6	2.5	1.9	0.7	20.9	125.1	15.7	22.1	81.5	12.8	1.1	11.2	4.3	3.2	3.1	0.7	86.3	18.0	6.8
	e16 p63KO M	42.7	0.1	1.2	61.7	9.1	21.9	1.2	44.6	4.0	31.9	0.4	6.7	0.0	2.2	1.2	2.8	4.5	3.4	10.0	101.2	9.1	7.2	58.0	4.9	11.3	0.9	8.0	3.2	1.2	10.2	59.4	9.6	24.2
Gabpb2	e12 B	57.1	3.1	5.4	77.3	17.9	33.8	5.4	59.2	10.9	44.2	4.4	4.5	2.2	0.0	0.8	5.1	6.4	1.8	19.9	120.1	18.1	16.0	74.3	12.5	9.7	2.8	11.8	6.3	3.3	8.4	75.2	19.1	20.5
	e17.5 B	53.8	1.4	4.5	74.3	15.9	31.0	4.5	55.9	9.1	42.7	2.6	2.6	1.2	0.8	0.0	1.8	2.7	0.7	15.0	113.8	12.5	13.0	69.3	8.2	6.4	3.1	6.5	2.6	0.9	5.4	71.6	13.7	16.9
	e17.5 fibroblasts B	51.2	2.0	6.4	71.8	15.9	29.5	6.4	53.3	9.6	43.1	3.3	2.5	2.8	5.1	1.8	0.0	0.2	1.9	10.4	105.5	6.8	11.6	63.8	4.6	3.9	6.8	1.6	0.1	0.3	3.5	68.4	8.3	13.0
	e17.5 suprabasal B	55.8	3.6	9.1	77.0	19.5	33.6	9.1	58.0	12.6	48.2	5.3	1.9	4.5	6.4	2.7	0.2	0.0	2.1	12.3	109.1	7.8	14.5	67.8	6.1	2.4	9.3	0.9	0.3	1.1	2.1	73.2	9.7	10.1
	e16 p63KO B	61.4	3.5	8.4	82.8	21.6	37.7	8.4	63.6	13.8	51.0	5.5	0.7	3.4	1.8	0.7	1.9	2.1	0.0	18.3	120.9	14.5	17.7	76.4	10.6	3.3	6.6	5.4	2.7	1.6	2.6	79.7	16.3	11.5
loricrine	P0 wt basal layer	19.2	8.3	7.7	34.1	3.9	7.3	7.7	20.6	4.1	16.3	6.7	20.9	10.0	19.9	15.0	10.4	12.3	18.3	0.0	60.1	1.0	1.6	27.1	1.3	23.2	12.6	11.7	9.3	10.1	22.5	31.1	0.4	36.1
	P0 wt fibroblasts	19.8	98.5	89.8	11.6	61.2	39.1	89.8	18.7	74.6	33.6	92.7	125.1	101.2	120.1	113.8	105.5	109.1	120.9	60.1	0.0	69.7	63.5	9.3	75.6	126.7	101.1	104.5	102.7	104.9	126.3	10.9	64.9	140.9
	P0 wt Suprabasal layer	28.0	7.3	8.8	44.9	8.0	13.7	8.8	29.7	6.4	25.1	6.5	15.7	9.1	18.1	12.5	6.8	7.8	14.5	1.0	69.7	0.0	4.3	35.7	0.8	16.4	13.3	6.3	5.6	7.4	16.1	41.2	0.2	27.0
	P0 SATB1 KO basal layer	17.2	6.4	3.8	31.5	0.6	4.8	3.8	18.6	0.9	11.5	4.4	22.1	7.2	16.0	13.0	11.6	14.5	17.7	1.6	63.5	4.3	0.0	28.0	2.5	26.9	7.6	15.9	11.0	9.9	25.7	29.4	3.0	42.4
	P0 SATB1 KO fibroblasts	2.5	55.9	48.1	2.4	26.1	11.6	48.1	2.2	36.1	9.7	50.9	81.5	58.0	74.3	69.3	63.8	67.8	76.4	27.1	9.3	35.7	28.0	0.0	38.7	85.4	57.4	65.9	61.8	62.3	84.5	1.2	31.5	102.2
	P0 SATB1 KO suprabasal layer	28.6	3.6	4.5	45.9	5.5	12.8	4.5	30.3	3.3	23.5	2.9	12.8	4.9	12.5	8.2	4.6	6.1	10.6	1.3	75.6	0.8	2.5	38.7	0.0	14.9	7.9	6.2	3.9	4.4	14.3	42.7	0.9	27.1
rps27	P0 wt basal layer	73.9	10.5	18.8	96.5	33.2	49.7	18.8	76.2	24.3	66.5	13.5	1.1	11.3	9.7	6.4	3.9	2.4	3.3	23.2	126.7	16.4	26.9	85.4	14.9	0.0	17.9	3.2	4.3	5.7	0.0	92.2	19.3	3.1
	P0 wt fibroblasts	40.7	1.6	0.7	58.7	8.0	20.5	0.7	42.5	3.6	28.3	1.4	11.2	0.9	2.8	3.1	6.8	9.3	6.6	12.6	101.1	13.3	7.6	57.4	7.9	17.6	0.0	14.0	7.5	4.3	16.1	57.1	13.2	32.3
	P0 wt Suprabasal layer	56.1	6.5	12.7	77.2	21.8	34.8	12.7	58.2	15.3	50.4	8.2	4.3	8.0	11.5	6.5	1.6	0.9	5.4	11.7	104.5	6.3	15.9	65.9	6.2	3.2	14.0	0.0	1.2	3.3	3.2	72.9	8.5	9.3
	P0 SATB1 KO basal layer	49.8	2.3	6.7	70.2	15.5	28.5	6.7	51.8	9.4	42.3	3.5	3.2	3.2	6.3	2.6	0.1	0.3	2.7	9.3	102.7	5.6	11.0	61.8	3.9	4.3	7.5	1.2	0.0	0.6	3.9	66.8	7.2	13.2
	P0 SATB1 KO fibroblasts	48.6	0.8	4.2	68.9	13.5	27.0	4.2	50.7	7.4	39.5	1.8	3.1	1.2	3.3	0.9	0.3	1.1	1.6	10.1	104.9	7.4	9.9	62.3	4.4	5.7	4.3	3.3	0.6	0.0	4.9	65.8	8.6	16.0
	P0 SATB1 KO suprabasal layer	72.5	9.5	17.4	95.0	31.8	48.3	17.4	74.8	23.0	64.7	12.4	0.7	10.2	8.4	5.4	3.5	2.1	2.6	22.5	126.3	16.1	25.7	84.5	14.3	0.0	16.1	3.2	3.9	4.9	0.0	90.8	18.9	3.7
EDC	e16 p63KO B	1.9	57.9	48.4	0.2	26.1	11.5	48.4	1.5	36.6	7.3	52.4	86.3	59.4	75.2	71.6	68.4	73.2	79.7	31.1	10.9	41.2	29.4	1.2	42.7	92.2	57.1	72.9	66.6	65.8	90.8	0.0	36.5	111.3
lor	p10 B	23.9	7.8	8.4	39.9	6.2	10.8	8.4	25.5	5.4	21.2	6.7	18.0	9.6	19.1	13.7	8.3	9.7	16.3	0.4	64.9	0.2	3.0	31.5	0.9	19.3	13.2	8.5	7.2	8.6	18.9	36.5	0.0	30.9
rps27	p10B	92.7	23.1	33.9	116.4	50.4	67.8	33.9	95.2	40.3	86.7	27.0	6.8	24.2	20.5	16.9	13.0	10.1	11.5	36.1	140.9	27.0	42.4	102.2	27.1	3.1	32.3	9.3	13.2	16.0	3.7	111.3	30.9	0.0

Table A.2. Statistical analysis of differences between loci distribution in different tissues – Chi square test results. Values above $X^2_{(2).05}$ =5.99 mean statistical significance (p=0.05) if pairs are compared. In the table values above $X^2_{(2).0167}$ =8.19 are marked with darker fill, they mean statistical significance when three sets of data are compared (Bonferroni adjustment).

		edc								loricrine			rps27			Gabpbp2					loricrine						rps27						Gabpb2	lor	rps27
		e12 Mu	e12 Bra	e16 M	e17.5 B	e17.5 fi	e17.5 s	e16 p63	p10 M	e12 M	e16 M	e16 p63	e12 M	e16 M	e16 p63	e12 B	e17.5 B	e17.5 fi	e17.5 s	e16 p63	P0 wt b	P0 wt fi	P0 wt S	P0 SATI	P0 SATI	P0 SATI	P0 wt b	P0 wt fi	P0 wt S	P0 SATI	P0 SATI	P0 SATI	e12 B M	p10 B	p10B
edc	e12 Munich	1.0000	0.2832	0.0000	0.0000	0.2758	0.0000	0.1215	0.0000	0.9857	0.0000	0.2970	0.0000	0.0000	0.0000	0.0000	0.0000	0.0000	0.0000	0.0000	0.0001	0.0001	0.0000	0.0002	0.2842	0.0000	0.0000	0.0000	0.0000	0.0000	0.0000	0.0000	0.0000	0.0000	0.0000
	e12 Bradford	0.2832	1.0000	0.0000	0.0001	0.0080	0.0761	0.8891	0.0001	0.2175	0.0047	0.5821	0.0000	0.0000	0.0000	0.0000	0.0000	0.0000	0.0000	0.0000	0.0075	0.0000	0.0000	0.0290	0.0110	0.0003	0.0000	0.0000	0.0000	0.0000	0.0000	0.0000	0.0000	0.0011	0.0000
	e16 M	0.0000	0.0000	1.0000	0.5133	0.0000	0.0135	0.0000	0.5133	0.0000	0.1542	0.0000	0.8886	0.0411	0.9365	0.2123	0.5020	0.3653	0.1646	0.1727	0.0157	0.0000	0.0266	0.0409	0.0000	0.1651	0.0053	0.4426	0.0380	0.3142	0.6649	0.0088	0.0722	0.0202	0.0000
	e17.5 B	0.0000	0.0001	0.5133	1.0000	0.0000	0.1149	0.0007	1.0000	0.0000	0.5572	0.0000	0.7582	0.0015	0.5619	0.0684	0.1049	0.0400	0.0107	0.0152	0.0214	0.0000	0.0124	0.1520	0.0000	0.1041	0.0001	0.6932	0.0017	0.0344	0.1222	0.0002	0.0070	0.0147	0.0000
	e17.5 fibroblasts B	0.2758	0.0080	0.0000	0.0000	1.0000	0.0000	0.0017	0.0000	0.3559	0.0000	0.0248	0.0000	0.0000	0.0000	0.0000	0.0000	0.0000	0.0000	0.0000	0.0000	0.0031	0.0000	0.0000	0.3023	0.0000	0.0000	0.0000	0.0000	0.0000	0.0000	0.0000	0.0000	0.0000	0.0000
	e17.5 suprabasal B	0.0000	0.0761	0.0135	0.1149	0.0000	1.0000	0.1942	0.1149	0.0000	0.5806	0.0182	0.0471	0.0000	0.0107	0.0001	0.0004	0.0003	0.0001	0.0000	0.1388	0.0000	0.0185	0.7374	0.0000	0.0649	0.0000	0.0182	0.0000	0.0004	0.0012	0.0000	0.0000	0.0450	0.0000
	e16 p63KO B	0.1215	0.8891	0.0000	0.0007	0.0017	0.1942	1.0000	0.0007	0.0863	0.0189	0.3816	0.0002	0.0000	0.0000	0.0000	0.0000	0.0000	0.0000	0.0000	0.0257	0.0000	0.0011	0.0920	0.0031	0.0017	0.0000	0.0000	0.0000	0.0000	0.0000	0.0000	0.0000	0.0046	0.0000
	p10 M	0.0000	0.0001	0.5133	1.0000	0.0000	0.1149	0.0007	1.0000	0.0000	0.5572	0.0000	0.7582	0.0015	0.5619	0.0684	0.1049	0.0400	0.0107	0.0152	0.0214	0.0000	0.0124	0.1520	0.0000	0.1041	0.0001	0.6932	0.0017	0.0344	0.1222	0.0002	0.0070	0.0147	0.0000
loricrine	e12 M	0.9857	0.2175	0.0000	0.0000	0.3559	0.0000	0.0863	0.0000	1.0000	0.0000	0.2560	0.0000	0.0000	0.0000	0.0000	0.0000	0.0000	0.0000	0.0000	0.0000	0.0001	0.0000	0.0001	0.3248	0.0000	0.0000	0.0000	0.0000	0.0000	0.0000	0.0000	0.0000	0.0000	0.0000
	e16 M	0.0000	0.0047	0.1542	0.5572	0.0000	0.5806	0.0189	0.5572	0.0000	1.0000	0.0007	0.3463	0.0001	0.1345	0.0043	0.0105	0.0083	0.0018	0.0010	0.1313	0.0000	0.0407	0.6527	0.0000	0.1961	0.0000	0.1645	0.0005	0.0090	0.0246	0.0000	0.0000	0.0667	0.0000
	e16 p63KO M	0.2970	0.5821	0.0000	0.0000	0.0248	0.0182	0.3816	0.0000	0.2560	0.0007	1.0000	0.0000	0.0000	0.0000	0.0000	0.0000	0.0000	0.0000	0.0000	0.0003	0.0000	0.0000	0.0032	0.0079	0.0000	0.0000	0.0000	0.0000	0.0000	0.0000	0.0000	0.0000	0.0000	0.0000
rps27	e12 M	0.0000	0.0000	0.8886	0.7582	0.0000	0.0471	0.0000	0.7582	0.0000	0.3463	0.0001	1.0000	0.0116	0.8245	0.1129	0.2666	0.1930	0.0716	0.0648	0.0343	0.0000	0.0382	0.1103	0.0000	0.2308	0.0012	0.5067	0.0168	0.1751	0.4035	0.0021	0.0252	0.0350	0.0000
	e16 M	0.0000	0.0000	0.0411	0.0015	0.0000	0.0000	0.0000	0.0015	0.0000	0.0001	0.0000	0.0116	1.0000	0.0358	0.1039	0.2692	0.2884	0.3949	0.7051	0.0000	0.0000	0.0004	0.0000	0.0000	0.0017	0.5830	0.0036	0.1180	0.2069	0.2175	0.7153	0.5008	0.0001	0.0330
	e16 p63KO M	0.0000	0.0000	0.9365	0.5619	0.0000	0.0107	0.0000	0.5619	0.0000	0.1345	0.0000	0.8245	0.0358	1.0000	0.3263	0.5610	0.2523	0.1054	0.1792	0.0069	0.0000	0.0104	0.0270	0.0000	0.0852	0.0035	0.6241	0.0181	0.1984	0.5406	0.0061	0.0911	0.0081	0.0000
Gabpb2	e12 B	0.0000	0.0000	0.2123	0.0684	0.0000	0.0001	0.0000	0.0684	0.0000	0.0043	0.0000	0.1129	0.1039	0.3263	1.0000	0.6562	0.0782	0.0414	0.4085	0.0000	0.0000	0.0001	0.0003	0.0000	0.0019	0.0080	0.2452	0.0031	0.0432	0.1909	0.0148	0.5014	0.0001	0.0000
	e17.5 B	0.0000	0.0000	0.5020	0.1049	0.0000	0.0004	0.0000	0.1049	0.0000	0.0105	0.0000	0.2666	0.2692	0.5610	0.6562	1.0000	0.3980	0.2529	0.7154	0.0006	0.0000	0.0019	0.0015	0.0000	0.0169	0.0408	0.2093	0.0393	0.2730	0.6499	0.0659	0.4918	0.0010	0.0002
	e17.5 fibroblasts B	0.0000	0.0000	0.3653	0.0400	0.0000	0.0003	0.0000	0.0400	0.0000	0.0083	0.0000	0.1930	0.2884	0.2523	0.0782	0.3980	1.0000	0.8863	0.3825	0.0056	0.0000	0.0342	0.0030	0.0000	0.1021	0.1390	0.0334	0.4508	0.9628	0.8521	0.1771	0.1212	0.0156	0.0015
	e17.5 suprabasal B	0.0000	0.0000	0.1646	0.0107	0.0000	0.0001	0.0000	0.0107	0.0000	0.0018	0.0000	0.0716	0.3949	0.1054	0.0414	0.2529	0.8863	1.0000	0.3525	0.0021	0.0000	0.0203	0.0007	0.0000	0.0485	0.2972	0.0095	0.6458	0.8708	0.5910	0.3450	0.1077	0.0077	0.0065
	e16 p63KO B	0.0000	0.0000	0.1727	0.0152	0.0000	0.0000	0.0000	0.0152	0.0000	0.0010	0.0000	0.0648	0.7051	0.1792	0.4085	0.7154	0.3825	0.3525	1.0000	0.0001	0.0000	0.0007	0.0001	0.0000	0.0049	0.1886	0.0373	0.0659	0.2565	0.4477	0.2716	0.7700	0.0003	0.0032
oricrine	P0 wt basal layer	0.0000	0.0075	0.0157	0.0214	0.0000	0.1388	0.0257	0.0214	0.0000	0.1313	0.0000	0.0343	0.0000	0.0069	0.0000	0.0000	0.0056	0.0021	0.0000	1.0000	0.0000	0.5941	0.4428	0.0000	0.5225	0.0000	0.0018	0.0029	0.0096	0.0063	0.0000	0.0000	0.8385	0.0000
	P0 wt fibroblasts	0.0001	0.0000	0.0000	0.0000	0.0031	0.0000	0.0000	0.0000	0.0001	0.0000	0.0000	0.0000	0.0000	0.0000	0.0000	0.0000	0.0000	0.0000	0.0000	0.0000	1.0000	0.0000	0.0000	0.0097	0.0000	0.0000	0.0000	0.0000	0.0000	0.0000	0.0000	0.0000	0.0000	0.0000
	P0 wt Suprabasal layer	0.0000	0.0002	0.0266	0.0124	0.0000	0.0185	0.0011	0.0124	0.0000	0.0407	0.0000	0.0382	0.0004	0.0104	0.0001	0.0019	0.0342	0.0203	0.0000	0.5941	0.0000	1.0000	0.1176	0.0000	0.6801	0.0003	0.0013	0.0419	0.0597	0.0248	0.0003	0.0000	0.9093	0.0000
	P0 SATB1 KO basal layer	0.0000	0.0290	0.0409	0.1520	0.0000	0.7374	0.0920	0.1520	0.0000	0.6527	0.0032	0.1103	0.0000	0.0270	0.0003	0.0015	0.0030	0.0007	0.0000	0.4428	0.0000	0.1176	1.0000	0.0000	0.2825	0.0000	0.0220	0.0003	0.0041	0.0069	0.0000	0.0000	0.2183	0.0000
	P0 SATB1 KO fibroblasts	0.2842	0.0110	0.0000	0.0000	0.3023	0.0000	0.0031	0.0000	0.3248	0.0000	0.0079	0.0000	0.0000	0.0000	0.0000	0.0000	0.0000	0.0000	0.0000	0.0000	0.0097	0.0000	0.0000	1.0000	0.0000	0.0000	0.0000	0.0000	0.0000	0.0000	0.0000	0.0000	0.0000	0.0000
	P0 SATB1 KO suprabasal layer	0.0000	0.0003	0.1651	0.1041	0.0000	0.0649	0.0017	0.1041	0.0000	0.1961	0.0000	0.2308	0.0017	0.0852	0.0019	0.0169	0.1021	0.0485	0.0049	0.5225	0.0000	0.6801	0.2825	0.0000	1.0000	0.0006	0.0189	0.0461	0.1444	0.1103	0.0008	0.0000	0.6527	0.0000
rps27	P0 wt basal layer	0.0000	0.0000	0.0053	0.0001	0.0000	0.0000	0.0000	0.0001	0.0000	0.0000	0.0000	0.0012	0.5830	0.0035	0.0080	0.0408	0.1390	0.2972	0.1886	0.0000	0.0000	0.0003	0.0000	0.0000	0.0006	1.0000	0.0000	0.2068	0.1183	0.0591	0.9756	0.0953	0.0001	0.2101
	P0 wt fibroblasts	0.0000	0.0000	0.4426	0.6932	0.0000	0.0182	0.0000	0.6932	0.0000	0.1645	0.0000	0.5067	0.0036	0.6241	0.2452	0.2093	0.0334	0.0095	0.0373	0.0018	0.0000	0.0013	0.0220	0.0000	0.0189	0.0002	1.0000	0.0008	0.0231	0.1192	0.0003	0.0264	0.0014	0.0000
	P0 wt Suprabasal layer	0.0000	0.0000	0.0380	0.0017	0.0000	0.0000	0.0000	0.0017	0.0000	0.0005	0.0000	0.0168	0.1180	0.0181	0.0031	0.0393	0.4508	0.6458	0.0659	0.0029	0.0000	0.0419	0.0003	0.0000	0.0461	0.2068	0.0008	1.0000	0.5583	0.1950	0.1999	0.0127	0.0142	0.0096
	P0 SATB1 KO basal layer	0.0000	0.0000	0.3142	0.0344	0.0000	0.0004	0.0000	0.0344	0.0000	0.0090	0.0000	0.1751	0.2069	0.1984	0.0432	0.2730	0.9628	0.8708	0.2565	0.0096	0.0000	0.0597	0.0041	0.0000	0.1444	0.1183	0.0231	0.5583	1.0000	0.7494	0.1454	0.0696	0.0276	0.0014
	P0 SATB1 KO fibroblasts	0.0000	0.0000	0.6649	0.1222	0.0000	0.0012	0.0000	0.1222	0.0000	0.0246	0.0000	0.4035	0.2175	0.5406	0.1909	0.6499	0.8521	0.5910	0.4477	0.0063	0.0000	0.0248	0.0069	0.0000	0.1103	0.0591	0.1192	0.1950	0.7494	1.0000	0.0848	0.1725	0.0134	0.0003
	P0 SATB1 KO suprabasal layer	0.0000	0.0000	0.0088	0.0002	0.0000	0.0000	0.0000	0.0002	0.0000	0.0000	0.0000	0.0021	0.7153	0.0061	0.0148	0.0659	0.1771	0.3450	0.2716	0.0000	0.0000	0.0003	0.0000	0.0000	0.0008	0.9756	0.0000	0.1999	0.1454	0.0848	1.0000	0.1471	0.0001	0.1535
Gabpb2	e12 B MS-84	0.0000	0.0000	0.0722	0.0070	0.0000	0.0000	0.0000	0.0070	0.0000	0.0003	0.0000	0.0252	0.5008	0.0911	0.5014	0.4918	0.1212	0.1077	0.7700	0.0000	0.0000	0.0001	0.0000	0.0000	0.0008	0.0953	0.0264	0.0127	0.0696	0.1725	0.1471	1.0000	0.0000	0.0022
lor	p10 B	0.0000	0.0011	0.0202	0.0147	0.0000	0.0450	0.0046	0.0147	0.0000	0.0667	0.0000	0.0350	0.0001	0.0081	0.0001	0.0010	0.0156	0.0077	0.0000	0.8385	0.0000	0.9093	0.2183	0.0000	0.6527	0.0001	0.0014	0.0142	0.0276	0.0134	0.0001	0.0000	1.0000	0.0000
rps27	p10B	0.0000	0.0000	0.0000	0.0000	0.0000	0.0000	0.0000	0.0000	0.0000	0.0000	0.0000	0.0000	0.0330	0.0000	0.0000	0.0000	0.0015	0.0065	0.0032	0.0000	0.0000	0.0000	0.0000	0.0000	0.0000	0.2101	0.0000	0.0096	0.0014	0.0000	0.1535	0.0022	0.0000	1.0000

Table A.3 Statistical analysis of differences between loci distribution in different tissues – P-values of Chi square test results. P-values <0.05 are marked with light grey, p-values<0.001 are marked with dark grey fill.

	Radial positions						Intergenic distances			Average nuclear radius
	Loricrin		Rps27		Gabpb2		Lor-Rps	Lor-Gabpb	Rps-Gabpb	
	[nm]	[radius %]	[nm]	[radius %]	[nm]	[radius %]	[nm]	[nm]	[nm]	[nm]
e12	3962.2	85.5	3581.9	77.3	3387.7	71.6	974.3	1281.7	-	4617.3
e16 wt	2961.0	70.2	2675.9	63.4	3000.6	74.8	747.2	1080.8	1037.8	4215.2
e16 p63KO	3399.8	82.7	2816.9	68.8	3047.6	74.4	902.8	1144.8	1007.1	4125.5
fpads wt	3251.4	78.6	2946.8	71.3	-	-	908.0	-	-	4165.8
fpads SATB1KO	2861.5	70.5	2677.4	65.9	-	-	774.3	-	-	4084.4

Table A.4 Radial positions of loci of interest and intergene distances between them. Values of radial positions, normalized radial positions, intergenic distances and average nuclear radii

9. References

Agrelo R, Souabni A, Novatchkova M, Haslinger C, Leeb M, Komnenovic V, Kishimoto H, Gresh L, Kohwi-Shigematsu T, Kenner L *et al.* (2009) "SATB1 defines the developmental context for gene silencing by Xist in lymphoma and embryonic cells". *Dev Cell.* 16:507-16.

Aho S, Li K, Ryoo Y, McGee C, Ishida-Yamamoto A, Uitto J and Klement JF (2004) "Periplakin gene targeting reveals a constituent of the cornified cell envelope dispensable for normal mouse development". *Mol Cell Biol* 24:6410-8

Akhtar A and Gasser SM (2007) "The nuclear envelope and transcriptional control". *Nat Rev Genet* 8:507-17

Alcobia I, Dilao R and Parreira L (2000) "Spatial associations of centromeres in the nuclei of hematopoietic cells: evidence for cell-type-specific organizational patterns". *Blood* 95:1608-15

Aleixandre C, Miller DA, Mitchell AR, Warburton DA, Gersen SL, Disteche C and Miller OJ (1987) "p82H identifies sequences at every human centromere". *Hum Genet* 77:46-50

Anachkova B, Djeliova V and Russev G (2005) "Nuclear matrix support of DNA replication". *J Cell Biochem* 96:951-61

Anastassova-Kristeva M (1977) "The nucleolar cycle in man". *J Cell Sci* 25:103-10

Banks-Schlegel S and Green H (1981) "Involucrin synthesis and tissue assembly by keratinocytes in natural and cultured human epithelia". *J Cell Biol* 90:732-7

Barbieri CE and Pietenpol JA (2006) "p63 and epithelial biology". *Exp Cell Res* 312:695-706

Bernardi R and Pandolfi PP (2007) "Structure, dynamics and functions of promyelocytic leukaemia nuclear bodies". *Nat Rev Mol Cell Biol* 8:1006-16

Bickenbach JR, Greer JM, Bundman DS, Rothnagel JA and Roop DR (1995) "Loricrin expression is coordinated with other epidermal proteins and the appearance of lipid lamellar granules in development". *J Invest Dermatol* 104:405-10

Bird A (2002) "DNA methylation patterns and epigenetic memory". *Genes Dev* 16:6-21

Bolzer A, Kreth G, Solovei I, Koehler D, Saracoglu K, Fauth C, Muller S, Eils R, Cremer C, Speicher MR *et al.* (2005) "Three-dimensional maps of all chromosomes in human male fibroblast nuclei and prometaphase rosettes". *PLoS Biol* 3:e157

Bowman GD (2010) "Mechanisms of ATP-dependent nucleosome sliding". *Curr Opin Struct Biol* 20:73-81

Branco MR and Pombo A (2007) "Chromosome organization: new facts, new models". *Trends Cell Biol* 17:127-34

Brandt A, Papagiannouli F, Wagner N, Wilsch-Brauninger M, Braun M, Furlong EE, Loserth S, Wenzl C, Pilot F, Vogt N *et al.* (2006) "Developmental control of nuclear size and shape by Kugelkern and Kurzkern". *Curr Biol* 16:543-52

Brown JM, Green J, das Neves RP, Wallace HA, Smith AJ, Hughes J, Gray N, Taylor S, Wood WG, Higgs DR *et al.* (2008) "Association between active genes occurs at nuclear speckles and is modulated by chromatin environment". *J Cell Biol.* 182:1083-97.

Brown SJ, Tilli CM, Jackson B, Avilion AA, MacLeod MC, Maltais LJ, Lovering RC and Byrne C (2007) "Rodent Lce gene clusters; new nomenclature, gene organization, and divergence of human and rodent genes". *J Invest Dermatol* 127:1782-6

Byrne C, Tainsky M and Fuchs E (1994) "Programming gene expression in developing epidermis". *Development* 120:2369-83

Cai S, Han HJ and Kohwi-Shigematsu T (2003) "Tissue-specific nuclear architecture and gene expression regulated by SATB1". *Nat Genet.* 34:42-51.

Cai S, Lee CC and Kohwi-Shigematsu T (2006) "SATB1 packages densely looped, transcriptionally active chromatin for coordinated expression of cytokine genes". *Nat Genet.* 38:1278-88. Epub 2006 Oct 22.

Cajal Ry (1903) "Un secillo metod de coloracion seletiva del reticulo protoplasmico y sus efectos en los diversos organos nerviosos de vertabrados e invertabrados.". *Trab. Lab. Invest. Biol.* 2:129-221

Carmo-Fonseca M, Cunha C, Custodio N, Carvalho C, Jordan P, Ferreira J and Parreira L (1996) "The topography of chromosomes and genes in the nucleus". *Exp Cell Res* 229:247-52

Carvalho C, Pereira HM, Ferreira J, Pina C, Mendonca D, Rosa AC and Carmo-Fonseca M (2001) "Chromosomal G-dark bands determine the spatial organization of centromeric heterochromatin in the nucleus". *Mol Biol Cell* 12:3563-72

Chambeyron S and Bickmore WA (2004) "Chromatin decondensation and nuclear reorganization of the HoxB locus upon induction of transcription". *Genes Dev* 18:1119-30

Chambeyron S, Da Silva NR, Lawson KA and Bickmore WA (2005) "Nuclear re-organisation of the Hoxb complex during mouse embryonic development". *Development* 132:2215-23

Chen K and Rajewsky N (2007) "The evolution of gene regulation by transcription factors and microRNAs". *Nat Rev Genet* 8:93-103

Cheutin T, McNairn AJ, Jenuwein T, Gilbert DM, Singh PB and Misteli T (2003) "Maintenance of stable heterochromatin domains by dynamic HP1 binding". *Science* 299:721-5

Choo KH (2001) "Domain organization at the centromere and neocentromere". *Dev Cell* 1:165-77

Chuang CH, Carpenter AE, Fuchsova B, Johnson T, de Lanerolle P and Belmont AS (2006) "Long-range directional movement of an interphase chromosome site". *Curr Biol* 16:825-31

Chubb JR, Boyle S, Perry P and Bickmore WA (2002) "Chromatin motion is constrained by association with nuclear compartments in human cells". *Curr Biol* 12:439-45

Cioce M and Lamond AI (2005) "Cajal bodies: a long history of discovery". *Annu Rev Cell Dev Biol* 21:105-31

Clapier CR and Cairns BR (2009) "The biology of chromatin remodeling complexes". *Annu Rev Biochem* 78:273-304

Costantini M, Cammarano R and Bernardi G (2009) "The evolution of isochore patterns in vertebrate genomes". *BMC Genomics* 10:146

Craig JM (2005) "Heterochromatin--many flavours, common themes". *Bioessays* 27:17-28

Cremer T and Cremer C (2001) "Chromosome territories, nuclear architecture and gene regulation in mammalian cells". *Nat Rev Genet* 2:292-301

Cremer T and Cremer M (2010) "Chromosome territories". *Cold Spring Harb Perspect Biol* 2:a003889

Crum CP and McKeon FD (2010) "p63 in epithelial survival, germ cell surveillance, and neoplasia". *Annu* 5:349-71.

de la Serna IL, Ohkawa Y and Imbalzano AN (2006) "Chromatin remodelling in mammalian differentiation: lessons from ATP-dependent remodellers". *Nat Rev Genet* 7:461-73

Dean FB, Nelson JR, Giesler TL and Lasken RS (2001) "Rapid amplification of plasmid and phage DNA using Phi 29 DNA polymerase and multiply-primed rolling circle amplification". *Genome Res* 11:1095-9

Dellaire G and Bazett-Jones DP (2004) "PML nuclear bodies: dynamic sensors of DNA damage and cellular stress". *Bioessays* 26:963-77

Dellambra E, Golisano O, Bondanza S, Siviero E, Lacal P, Molinari M, D'Atri S and De Luca M (2000) "Downregulation of 14-3-3sigma prevents clonal evolution and leads to immortalization of primary human keratinocytes". *J Cell Biol* 149:1117-30

Denslow SA and Wade PA (2007) "The human Mi-2/NuRD complex and gene regulation". *Oncogene* 26:5433-8

Derenzini M, Montanaro L and Trere D (2009) "What the nucleolus says to a tumour pathologist". *Histopathology* 54:753-62

Derenzini M, Trere D, Pession A, Montanaro L, Sirri V and Ochs RL (1998) "Nucleolar function and size in cancer cells". *Am J Pathol* 152:1291-7

Dev VG, Tantravahi R, Miller DA and Miller OJ (1977) "Nucleolus organizers in Mus musculus subspecies and in the RAG mouse cell line". *Genetics* 86:389-98

Dillon N (2004) "Heterochromatin structure and function". *Biol Cell* 96:631-7

Djian P, Easley K and Green H (2000) "Targeted ablation of the murine involucrin gene". *J Cell Biol* 151:381-8

Dundr M and Misteli T "Biogenesis of nuclear bodies". *Cold Spring Harb Perspect Biol* 2:a000711

Dundr M and Misteli T (2010) "Biogenesis of nuclear bodies". *Cold Spring Harb Perspect Biol* 2:a000711

Eckert RL, Broome AM, Ruse M, Robinson N, Ryan D and Lee K (2004) "S100 proteins in the epidermis". *J Invest Dermatol* 123:23-33

Elder JT and Zhao X (2002a) "Evidence for local control of gene expression in the epidermal differentiation complex". *Exp Dermatol.* 11:406-12.

Elder JT and Zhao X (2002b) "Evidence for local control of gene expression in the epidermal differentiation complex". *Exp Dermatol* 11:406-12

Embley TM and Martin W (2006) "Eukaryotic evolution, changes and challenges". *Nature* 440:623-30

Ezhkova E, Pasolli HA, Parker JS, Stokes N, Su IH, Hannon G, Tarakhovsky A and Fuchs E (2009) "Ezh2 orchestrates gene expression for the stepwise differentiation of tissue-specific stem cells". *Cell* 136:1122-35.

Fallon PG, Sasaki T, Sandilands A, Campbell LE, Saunders SP, Mangan NE, Callanan JJ, Kawasaki H, Shiohama A, Kubo A *et al.* (2009) "A homozygous frameshift mutation in the mouse Flg gene facilitates enhanced percutaneous allergen priming". *Nat Genet* 41:602-8

Fedorova E and Zink D (2008) "Nuclear architecture and gene regulation". *Biochim Biophys Acta* 1783:2174-84

Feng W, Gubitz AK, Wan L, Battle DJ, Dostie J, Golembe TJ and Dreyfuss G (2005) "Gemins modulate the expression and activity of the SMN complex". *Hum Mol Genet* 14:1605-11

Ferraris C, Chevalier G, Favier B, Jahoda CA and Dhouailly D (2000) "Adult corneal epithelium basal cells possess the capacity to activate epidermal, pilosebaceous and sweat gland genetic programs in response to embryonic dermal stimuli". *Development* 127:5487-95

Fouse SD, Shen Y, Pellegrini M, Cole S, Meissner A, Van Neste L, Jaenisch R and Fan G (2008) "Promoter CpG methylation contributes to ES cell gene regulation in parallel with Oct4/Nanog, PcG complex, and histone H3 K4/K27 trimethylation". *Cell Stem Cell* 2:160-9

Fox AH, Lam YW, Leung AK, Lyon CE, Andersen J, Mann M and Lamond AI (2002) "Paraspeckles: a novel nuclear domain". *Curr Biol* 12:13-25

Fraser P and Bickmore W (2007) "Nuclear organization of the genome and the potential for gene regulation". *Nature* 447:413-7

Frye M, Fisher AG and Watt FM (2007) "Epidermal stem cells are defined by global histone modifications that are altered by Myc-induced differentiation". *PLoS ONE.* 2:e763.

Gangaraju VK and Bartholomew B (2007) "Mechanisms of ATP dependent chromatin remodeling". *Mutat Res* 618:3-17

Gaszner M and Felsenfeld G (2006) "Insulators: exploiting transcriptional and epigenetic mechanisms". *Nat Rev Genet* 7:703-13

Gaubatz J, Prashad N and Cutler RG (1976) "Ribosomal RNA gene dosage as a function of tissue and age for mouse and human". *Biochim Biophys Acta* 418:358-75

Gaubatz JW and Cutler RG (1978) "Age-related differences in the number of ribosomal RNA genes of mouse tissues". *Gerontology* 24:179-207

Geng S, Mezentsev A, Kalachikov S, Raith K, Roop DR and Panteleyev AA (2006) "Targeted ablation of Arnt in mouse epidermis results in profound defects in desquamation and epidermal barrier function". *J Cell Sci* 119:4901-12

Gibbs S, Fijneman R, Wiegant J, van Kessel AG, van De Putte P and Backendorf C (1993) "Molecular characterization and evolution of the SPRR family of keratinocyte differentiation markers encoding small proline-rich proteins". *Genomics* 16:630-7

Goldman RD, Shumaker DK, Erdos MR, Eriksson M, Goldman AE, Gordon LB, Gruenbaum Y, Khuon S, Mendez M, Varga R *et al.* (2004) "Accumulation of mutant lamin A causes progressive changes in nuclear architecture in Hutchinson-Gilford progeria syndrome". *Proc Natl Acad Sci U S A* 101:8963-8

Goll MG and Bestor TH (2005) "Eukaryotic cytosine methyltransferases". *Annu Rev Biochem* 74:481-514

Grewal SI and Elgin SC (2007) "Transcription and RNA interference in the formation of heterochromatin". *Nature* 447:399-406

Grewal SI and Jia S (2007) "Heterochromatin revisited". *Nat Rev Genet* 8:35-46

Grigoryev SA, Arya G, Correll S, Woodcock CL and Schlick T (2009) "Evidence for heteromorphic chromatin fibers from analysis of nucleosome interactions". *Proc Natl Acad Sci U S A* 106:13317-22

Gruenbaum Y, Margalit A, Goldman RD, Shumaker DK and Wilson KL (2005) "The nuclear lamina comes of age". *Nat Rev Mol Cell Biol* 6:21-31

Gubitz AK, Feng W and Dreyfuss G (2004) "The SMN complex". *Exp Cell Res* 296:51-6

Haaf T and Schmid M (1991) "Chromosome topology in mammalian interphase nuclei". *Exp Cell Res* 192:325-32

Hall LL, Smith KP, Byron M and Lawrence JB (2006) "Molecular anatomy of a speckle". *Anat Rec A Discov Mol Cell Evol Biol* 288:664-75

Han HJ, Russo J, Kohwi Y and Kohwi-Shigematsu T (2008) "SATB1 reprogrammes gene expression to promote breast tumour growth and metastasis". *Nature.* 452:187-93.

Handwerger KE and Gall JG (2006) "Subnuclear organelles: new insights into form and function". *Trends Cell Biol* 16:19-26

Heitz E (1928) "Das heterochromatin der Moose". *I.Jahrb.Wiss.Botanik* 69:762-818

Hernandez-Munoz I, Taghavi P, Kuijl C, Neefjes J and van Lohuizen M (2005) "Association of BMI1 with polycomb bodies is dynamic and requires PRC2/EZH2 and the maintenance DNA methyltransferase DNMT1". *Mol Cell Biol* 25:11047-58

Hernandez-Verdun D (2006) "The nucleolus: a model for the organization of nuclear functions". *Histochem Cell Biol* 126:135-48

Hernandez-Verdun D, Roussel P, Thiry M, Sirri V and Lafontaine DLJ "The nucleolus: structure/function relationship in RNA metabolism". *Wiley Interdisciplinary Reviews: RNA* 1:415-31

Hetzer MW "The nuclear envelope". *Cold Spring Harb Perspect Biol* 2:a000539

Hoffjan S and Stemmler S (2007) "On the role of the epidermal differentiation complex in ichthyosis vulgaris, atopic dermatitis and psoriasis". *Br J Dermatol* 157:441-9

Hoffmann K, Dreger CK, Olins AL, Olins DE, Shultz LD, Lucke B, Karl H, Kaps R, Muller D, Vaya A *et al.* (2002) "Mutations in the gene encoding the lamin B receptor produce an altered nuclear morphology in granulocytes (Pelger-Huet anomaly)". *Nat Genet* 31:410-4

Hogan C and Varga-Weisz P (2007) "The regulation of ATP-dependent nucleosome remodelling factors". *Mutat Res* 618:41-51

Hohl D, Mehrel T, Lichti U, Turner ML, Roop DR and Steinert PM (1991) "Characterization of human loricrin. Structure and function of a new class of epidermal cell envelope proteins". *J Biol Chem* 266:6626-36

Hohl D, Ruf Olano B, de Viragh PA, Huber M, Detrisac CJ, Schnyder UW and Roop DR (1993) "Expression patterns of loricrin in various species and tissues". *Differentiation* 54:25-34

Holmer L and Worman HJ (2001) "Inner nuclear membrane proteins: functions and targeting". *Cell Mol Life Sci* 58:1741-7

Horn PJ and Peterson CL (2006) "Heterochromatin assembly: a new twist on an old model". *Chromosome Res* 14:83-94

Horz W and Altenburger W (1981) "Nucleotide sequence of mouse satellite DNA". *Nucleic Acids Res* 9:683-96

Huber MD and Gerace L (2007) "The size-wise nucleus: nuclear volume control in eukaryotes". *J Cell Biol* 179:583-4

Hurst LD, Pal C and Lercher MJ (2004) "The evolutionary dynamics of eukaryotic gene order". *Nat Rev Genet* 5:299-310

Iborra FJ, Pombo A, Jackson DA and Cook PR (1996) "Active RNA polymerases are localized within discrete transcription "factories' in human nuclei". *J Cell Sci* 109 (Pt 6):1427-36

Indra AK, Dupe V, Bornert JM, Messaddeq N, Yaniv M, Mark M, Chambon P and Metzger D (2005) "Temporally controlled targeted somatic mutagenesis in embryonic surface ectoderm and fetal epidermal keratinocytes unveils two distinct developmental functions of BRG1 in limb morphogenesis and skin barrier formation". *Development* 132:4533-44

Irizarry RA, Ladd-Acosta C, Wen B, Wu Z, Montano C, Onyango P, Cui H, Gabo K, Rongione M, Webster M *et al.* (2009) "The human colon cancer methylome shows similar hypo- and hypermethylation at conserved tissue-specific CpG island shores". *Nat Genet* 41:178-86

Ito S, D'Alessio AC, Taranova OV, Hong K, Sowers LC and Zhang Y (2010) "Role of Tet proteins in 5mC to 5hmC conversion, ES-cell self-renewal and inner cell mass specification". *Nature* 466:1129-33

Ito T, Tsuchiya K, Osawa S, Shibata H and Kanda N (2008) "Mapping of rRNA gene loci in the mice, Mus musculus molossinus (Japan) and Mus musculus musculus (Russia) by double color FISH". *J Vet Med Sci* 70:997-1000

Jackson B, Tilli CM, Hardman MJ, Avilion AA, MacLeod MC, Ashcroft GS and Byrne C (2005) "Late cornified envelope family in differentiating epithelia--response to calcium and ultraviolet irradiation". *J Invest Dermatol* 124:1062-70

Jaenisch R and Bird A (2003) "Epigenetic regulation of gene expression: how the genome integrates intrinsic and environmental signals". *Nat Genet* 33 Suppl:245-54

Jarnik M, de Viragh PA, Scharer E, Bundman D, Simon MN, Roop DR and Steven AC (2002) "Quasi-normal cornified cell envelopes in loricrin knockout mice imply the existence of a loricrin backup system". *J Invest Dermatol* 118:102-9

Jarnik M, Kartasova T, Steinert PM, Lichti U and Steven AC (1996) "Differential expression and cell envelope incorporation of small proline-rich protein 1 in different cornified epithelia". *J Cell Sci* 109 (Pt 6):1381-91

Jenuwein T (2001) "Re-SET-ting heterochromatin by histone methyltransferases". *Trends Cell Biol* 11:266-73

Kalmarova M, Smirnov E, Kovacik L, Popov A and Raska I (2008) "Positioning of the NOR-bearing chromosomes in relation to nucleoli in daughter cells after mitosis". *Physiol Res* 57:421-5

Kalmarova M, Smirnov E, Masata M, Koberna K, Ligasova A, Popov A and Raska I (2007) "Positioning of NORs and NOR-bearing chromosomes in relation to nucleoli". *J Struct Biol* 160:49-56

Kashiwagi M, Morgan BA and Georgopoulos K (2007) "The chromatin remodeler Mi-2beta is required for establishment of the basal epidermis and normal differentiation of its progeny". *Development* 134:1571-82

Kass SU, Landsberger N and Wolffe AP (1997) "DNA methylation directs a time-dependent repression of transcription initiation". *Curr Biol* 7:157-65

Kelly RB, Cozzarelli NR, Deutscher MP, Lehman IR and Kornberg A (1970) "Enzymatic synthesis of deoxyribonucleic acid. XXXII. Replication of duplex deoxyribonucleic acid by polymerase at a single strand break". *J Biol Chem* 245:39-45

Klose RJ and Bird AP (2006) "Genomic DNA methylation: the mark and its mediators". *Trends Biochem Sci* 31:89-97

Koch PJ, de Viragh PA, Scharer E, Bundman D, Longley MA, Bickenbach J, Kawachi Y, Suga Y, Zhou Z, Huber M *et al.* (2000) "Lessons from loricrin-deficient mice: compensatory mechanisms maintaining skin barrier function in the absence of a major cornified envelope protein". *J Cell Biol* 151:389-400

Kosak ST, Skok JA, Medina KL, Riblet R, Le Beau MM, Fisher AG and Singh H (2002) "Subnuclear compartmentalization of immunoglobulin loci during lymphocyte development". *Science* 296:158-62

Koster MI, Kim S, Huang J, Williams T and Roop DR (2006) "TAp63alpha induces AP-2gamma as an early event in epidermal morphogenesis". *Dev Biol* 289:253-61

Koster MI and Roop DR (2007a) "Mechanisms regulating epithelial stratification". *Annu Rev Cell Dev Biol* 9:93-113

Koster MI and Roop DR (2007b) "Mechanisms regulating epithelial stratification". *Annu Rev Cell Dev Biol* 23:93-113

Kriaucionis S and Heintz N (2009) "The nuclear DNA base 5-hydroxymethylcytosine is present in Purkinje neurons and the brain". *Science* 324:929-30

Kurihara Y, Suh DS, Suzuki H and Moriwaki K (1994) "Chromosomal locations of Ag-NORs and clusters of ribosomal DNA in laboratory strains of mice". *Mamm Genome* 5:225-8

Lam YW, Trinkle-Mulcahy L and Lamond AI (2005) "The nucleolus". *J Cell Sci* 118:1335-37

Lamond AI and Sleeman JE (2003) "Nuclear substructure and dynamics". *Curr Biol* 13:R825-8

Lamond AI and Spector DL (2003) "Nuclear speckles: a model for nuclear organelles". *Nat Rev Mol Cell Biol* 4:605-12

Lechler T and Fuchs E (2005) "Asymmetric cell divisions promote stratification and differentiation of mammalian skin". *Nature* 437:275-80

Lercher MJ, Urrutia AO and Hurst LD (2002) "Clustering of housekeeping genes provides a unified model of gene order in the human genome". *Nat Genet* 31:180-3

Lilliefors H (1967) "On the Kolomogorov-Smirnov test for normality with mean and variance unknown". *Journal of the American Statistical Association* 62:399-402

Lim RY and Fahrenkrog B (2006) "The nuclear pore complex up close". *Curr Opin Cell Biol* 18:342-7

Lomvardas S, Barnea G, Pisapia DJ, Mendelsohn M, Kirkland J and Axel R (2006) "Interchromosomal interactions and olfactory receptor choice". *Cell* 126:403-13

Lopez-Garcia P and Moreira D (2006) "Selective forces for the origin of the eukaryotic nucleus". *Bioessays* 28:525-33

Luco RF, Maestro MA, Sadoni N, Zink D and Ferrer J (2008) "Targeted deficiency of the transcriptional activator Hnf1alpha alters subnuclear positioning of its genomic targets". *PLoS Genet* 4:e1000079

Luger K, Mader AW, Richmond RK, Sargent DF and Richmond TJ (1997) "Crystal structure of the nucleosome core particle at 2.8 A resolution". *Nature* 389:251-60

M'Boneko V and Merker HJ (1988) "Development and morphology of the periderm of mouse embryos (days 9-12 of gestation)". *Acta Anat (Basel)* 133:325-36

Maatta A, DiColandrea T, Groot K and Watt FM (2001) "Gene targeting of envoplakin, a cytoskeletal linker protein and precursor of the epidermal cornified envelope". *Mol Cell Biol* 21:7047-53

Maison C and Almouzni G (2004) "HP1 and the dynamics of heterochromatin maintenance". *Nat Rev Mol Cell Biol* 5:296-304

Marfella CG and Imbalzano AN (2007) "The Chd family of chromatin remodelers". *Mutat Res* 618:30-40

Marshall D, Hardman MJ, Nield KM and Byrne C (2001) "Differentially expressed late constituents of the epidermal cornified envelope". *Proc Natl Acad Sci U S A* 98:13031-6

Martin N, Patel S and Segre JA (2004a) "Long-range comparison of human and mouse Sprr loci to identify conserved noncoding sequences involved in coordinate regulation". *Genome Res* 14:2430-8

Martin N, Patel S and Segre JA (2004b) "Long-range comparison of human and mouse Sprr loci to identify conserved noncoding sequences involved in coordinate regulation". *Genome Res.* 14:2430-8.

Matera AG and Frey MR (1998) "Coiled bodies and gems: Janus or gemini?". *Am J Hum Genet* 63:317-21

McKeown PC and Shaw PJ (2009) "Chromatin: linking structure and function in the nucleolus". *Chromosoma* 118:11-23

Mehrel T, Hohl D, Rothnagel JA, Longley MA, Bundman D, Cheng C, Lichti U, Bisher ME, Steven AC, Steinert PM *et al.* (1990) "Identification of a major keratinocyte cell envelope protein, loricrin". *Cell* 61:1103-12

Meissner A, Mikkelsen TS, Gu H, Wernig M, Hanna J, Sivachenko A, Zhang X, Bernstein BE, Nusbaum C, Jaffe DB *et al.* (2008) "Genome-scale DNA methylation maps of pluripotent and differentiated cells". *Nature* 454:766-70

Melcer S and Gruenbaum Y (2006) "Nuclear morphology: when round kernels do the Charleston". *Curr Biol* 16:R195-7

Menon GK, Elias PM, Lee SH and Feingold KR (1992) "Localization of calcium in murine epidermis following disruption and repair of the permeability barrier". *Cell Tissue Res* 270:503-12

Mika S and Rost B (2005) "NMPdb: Database of Nuclear Matrix Proteins". *Nucleic Acids Res* 33:D160-3

Mills AA, Zheng B, Wang XJ, Vogel H, Roop DR and Bradley A (1999) "p63 is a p53 homologue required for limb and epidermal morphogenesis". *Nature* 398:708-13

Mischke D, Korge BP, Marenholz I, Volz A and Ziegler A (1996) "Genes encoding structural proteins of epidermal cornification and S100 calcium-binding proteins form a gene complex ("epidermal differentiation complex") on human chromosome 1q21". *J Invest Dermatol* 106:989-92

Misteli T (2007) "Beyond the sequence: cellular organization of genome function". *Cell* 128:787-800

Mitchell AR, Gosden JR and Miller DA (1985) "A cloned sequence, p82H, of the alphoid repeated DNA family found at the centromeres of all human chromosomes". *Chromosoma* 92:369-77

Mohn F, Weber M, Rebhan M, Roloff TC, Richter J, Stadler MB, Bibel M and Schubeler D (2008) "Lineage-specific polycomb targets and de novo DNA methylation define restriction and potential of neuronal progenitors". *Mol Cell* 30:755-66

Nikolova V, Leimena C, McMahon AC, Tan JC, Chandar S, Jogia D, Kesteven SH, Michalicek J, Otway R, Verheyen F *et al.* (2004) "Defects in nuclear structure and function promote dilated cardiomyopathy in lamin A/C-deficient mice". *J Clin Invest* 113:357-69

North AJ (2006) "Seeing is believing? A beginners' guide to practical pitfalls in image acquisition". *J Cell Biol* 172:9-18

Osborne CS, Chakalova L, Mitchell JA, Horton A, Wood AL, Bolland DJ, Corcoran AE and Fraser P (2007) "Myc dynamically and preferentially relocates to a transcription factory occupied by Igh". *PLoS Biol* 5:e192

Osoegawa K, Tateno M, Woon PY, Frengen E, Mammoser AG, Catanese JJ, Hayashizaki Y and de Jong PJ (2000) "Bacterial artificial chromosome libraries for mouse sequencing and functional analysis". *Genome Res* 10:116-28

Ottaviani D, Lever E, Takousis P and Sheer D (2008) "Anchoring the genome". *Genome Biol* 9:201

Parsa R, Yang A, McKeon F and Green H (1999) "Association of p63 with proliferative potential in normal and neoplastic human keratinocytes". *J Invest Dermatol* 113:1099-105

Pederson T (2000) "Half a century of "the nuclear matrix"". *Mol Biol Cell* 11:799-805

Peters AH, Kubicek S, Mechtler K, O'Sullivan RJ, Derijck AA, Perez-Burgos L, Kohlmaier A, Opravil S, Tachibana M, Shinkai Y *et al.* (2003) "Partitioning and plasticity of repressive histone methylation states in mammalian chromatin". *Mol Cell* 12:1577-89

Pradhan S and Esteve PO (2003) "Allosteric activator domain of maintenance human DNA (cytosine-5) methyltransferase and its role in methylation spreading". *Biochemistry* 42:5321-32

Presland RB, Boggess D, Lewis SP, Hull C, Fleckman P and Sundberg JP (2000) "Loss of normal profilaggrin and filaggrin in flaky tail (ft/ft) mice: an animal model for the filaggrin-deficient skin disease ichthyosis vulgaris". *J Invest Dermatol* 115:1072-81

Presland RB and Dale BA (2000) "Epithelial structural proteins of the skin and oral cavity: function in health and disease". *Crit Rev Oral Biol Med* 11:383-408

Prunuske AJ and Ullman KS (2006) "The nuclear envelope: form and reformation". *Curr Opin Cell Biol* 18:108-16

Rando OJ and Chang HY (2009) "Genome-wide views of chromatin structure". *Annu Rev Biochem* 78:245-71

Raska I (2003) "Oldies but goldies: searching for Christmas trees within the nucleolar architecture". *Trends Cell Biol* 13:517-25

Raska I, Shaw PJ and Cmarko D (2006) "Structure and function of the nucleolus in the spotlight". *Curr Opin Cell Biol* 18:325-34

Razin A and Kantor B (2005) "DNA methylation in epigenetic control of gene expression". *Prog Mol Subcell Biol* 38:151-67

Reik W, Dean W and Walter J (2001) "Epigenetic reprogramming in mammalian development". *Science* 293:1089-93

Reyes JC, Barra J, Muchardt C, Camus A, Babinet C and Yaniv M (1998) "Altered control of cellular proliferation in the absence of mammalian brahma (SNF2alpha)". *EMBO J* 17:6979-91

Rigby PW, Dieckmann M, Rhodes C and Berg P (1977) "Labeling deoxyribonucleic acid to high specific activity in vitro by nick translation with DNA polymerase I". *J Mol Biol* 113:237-51

Rishi V, Bhattacharya P, Chatterjee R, Rozenberg J, Zhao J, Glass K, Fitzgerald P and Vinson C (2010) "CpG methylation of half-CRE sequences creates C/EBPalpha binding sites that activate some tissue-specific genes". *Proc Natl Acad Sci U S A* 107:20311-6

Ronneberger O, Baddeley D, Scheipl F, Verveer PJ, Burkhardt H, Cremer C, Fahrmeir L, Cremer T and Joffe B (2008) "Spatial quantitative analysis of fluorescently labeled nuclear structures: problems, methods, pitfalls". *Chromosome Res* 16:523-62

Rothnagel JA, Longley MA, Bundman DS, Naylor SL, Lalley PA, Jenkins NA, Gilbert DJ, Copeland NG and Roop DR (1994) "Characterization of the mouse loricrin gene: linkage with profilaggrin and the flaky tail and soft coat mutant loci on chromosome 3". *Genomics* 23:450-6

Rothnagel JA and Steinert PM (1990) "The structure of the gene for mouse filaggrin and a comparison of the repeating units". *J Biol Chem* 265:1862-5

Rottach A, Leonhardt H and Spada F (2009) "DNA methylation-mediated epigenetic control". *J Cell Biochem* 108:43-51

Sadoni N, Langer S, Fauth C, Bernardi G, Cremer T, Turner BM and Zink D (1999) "Nuclear organization of mammalian genomes. Polar chromosome territories build up functionally distinct higher order compartments". *J Cell Biol* 146:1211-26

Sandilands A, Sutherland C, Irvine AD and McLean WH (2009) "Filaggrin in the frontline: role in skin barrier function and disease". *J Cell Sci* 122:1285-94

Sandilands A, Terron-Kwiatkowski A, Hull PR, O'Regan GM, Clayton TH, Watson RM, Carrick T, Evans AT, Liao H, Zhao Y *et al.* (2007) "Comprehensive analysis of the gene encoding filaggrin uncovers prevalent and rare mutations in ichthyosis vulgaris and atopic eczema". *Nat Genet* 39:650-4

Saurin AJ, Shiels C, Williamson J, Satijn DP, Otte AP, Sheer D and Freemont PS (1998) "The human polycomb group complex associates with pericentromeric heterochromatin to form a novel nuclear domain". *J Cell Biol* 142:887-98

Savarese F, Davila A, Nechanitzky R, De La Rosa-Velazquez I, Pereira CF, Engelke R, Takahashi K, Jenuwein T, Kohwi-Shigematsu T, Fisher AG *et al.* (2009) "Satb1 and Satb2 regulate embryonic stem cell differentiation and Nanog expression". *Genes Dev* 23:2625-38.

Schalch T, Duda S, Sargent DF and Richmond TJ (2005) "X-ray structure of a tetranucleosome and its implications for the chromatin fibre". *Nature* 436:138-41

Scherthan H, Weich S, Schwegler H, Heyting C, Harle M and Cremer T (1996) "Centromere and telomere movements during early meiotic prophase of mouse and man are associated with the onset of chromosome pairing". *J Cell Biol* 134:1109-25

Schirmer EC and Gerace L (2005) "The nuclear membrane proteome: extending the envelope". *Trends Biochem Sci* 30:551-8

Segre JA (2006a) "Epidermal barrier formation and recovery in skin disorders". *J Clin Invest* 116:1150-8

Segre JA (2006b) "Epidermal differentiation complex yields a secret: mutations in the cornification protein filaggrin underlie ichthyosis vulgaris". *J Invest Dermatol* 126:1202-4

Segre JA, Bauer C and Fuchs E (1999) "Klf4 is a transcription factor required for establishing the barrier function of the skin". *Nat Genet* 22:356-60

Sen GL, Reuter JA, Webster DE, Zhu L and Khavari PA (2010a) "DNMT1 maintains progenitor function in self-renewing somatic tissue". *Nature* 463:563-7. Epub 2010 Jan 17.

Sen GL, Reuter JA, Webster DE, Zhu L and Khavari PA (2010b) "DNMT1 maintains progenitor function in self-renewing somatic tissue". *Nature* 463:563-7

Sevilla LM, Nachat R, Groot KR, Klement JF, Uitto J, Djian P, Maatta A and Watt FM (2007) "Mice deficient in involucrin, envoplakin, and periplakin have a defective epidermal barrier". *J Cell Biol* 179:1599-612

Shilatifard A (2006) "Chromatin modifications by methylation and ubiquitination: implications in the regulation of gene expression". *Annu Rev Biochem* 75:243-69

Shopland LS, Lynch CR, Peterson KA, Thornton K, Kepper N, Hase J, Stein S, Vincent S, Molloy KR, Kreth G *et al.* (2006) "Folding and organization of a contiguous chromosome region according to the gene distribution pattern in primary genomic sequence". *J Cell Biol* 174:27-38

Sirri V, Urcuqui-Inchima S, Roussel P and Hernandez-Verdun D (2008) "Nucleolus: the fascinating nuclear body". *Histochem Cell Biol* 129:13-31

Smart IH (1970) "Variation in the plane of cell cleavage during the process of stratification in the mouse epidermis". *Br J Dermatol* 82:276-82

Smirnov E, Kalmarova M, Koberna K, Zemanova Z, Malinsky J, Masata M, Cvackova Z, Michalova K and Raska I (2006) "NORs and their transcription competence during the cell cycle". *Folia Biol (Praha)* 52:59-70

Smith FJ, Irvine AD, Terron-Kwiatkowski A, Sandilands A, Campbell LE, Zhao Y, Liao H, Evans AT, Goudie DR, Lewis-Jones S *et al.* (2006) "Loss-of-function mutations in the gene encoding filaggrin cause ichthyosis vulgaris". *Nat Genet* 38:337-42

Solovei I, Grandi N, Knoth R, Volk B and Cremer T (2004a) "Positional changes of pericentromeric heterochromatin and nucleoli in postmitotic Purkinje cells during murine cerebellum development". *Cytogenetic and Genome Research* 105:302-10

Solovei I, Kreysing M, Lanctot C, Kosem S, Peichl L, Cremer T, Guck J and Joffe B (2009) "Nuclear architecture of rod photoreceptor cells adapts to vision in mammalian evolution". *Cell* 137:356-68

Solovei I, Schermelleh L, During K, Engelhardt A, Stein S, Cremer C and Cremer T (2004b) "Differences in centromere positioning of cycling and postmitotic human cell types". *Chromosoma* 112:410-23

Song HJ, Poy G, Darwiche N, Lichti U, Kuroki T, Steinert PM and Kartasova T (1999) "Mouse Sprr2 genes: a clustered family of genes showing differential expression in epithelial tissues". *Genomics* 55:28-42

Spector DL (2003) "The dynamics of chromosome organization and gene regulation". *Annu Rev Biochem* 72:573-608

Spector DL (2006) "SnapShot: Cellular bodies". *Cell* 127:1071

Spilianakis CG, Lalioti MD, Town T, Lee GR and Flavell RA (2005) "Interchromosomal associations between alternatively expressed loci". *Nature* 435:637-45

Starr DA (2007) "Communication between the cytoskeleton and the nuclear envelope to position the nucleus". *Mol Biosyst* 3:583-9

Steinert PM, Kartasova T and Marekov LN (1998) "Biochemical evidence that small proline-rich proteins and trichohyalin function in epithelia by modulation of the biomechanical properties of their cornified cell envelopes". *J Biol Chem* 273:11758-69

Steinert PM and Marekov LN (1995) "The proteins elafin, filaggrin, keratin intermediate filaments, loricrin, and small proline-rich proteins 1 and 2 are isodipeptide cross-linked components of the human epidermal cornified cell envelope". *J Biol Chem* 270:17702-11

Steinert PM and Marekov LN (1997) "Direct evidence that involucrin is a major early isopeptide cross-linked component of the keratinocyte cornified cell envelope". *J Biol Chem* 272:2021-30

Steven AC, Bisher ME, Roop DR and Steinert PM (1990) "Biosynthetic pathways of filaggrin and loricrin--two major proteins expressed by terminally differentiated epidermal keratinocytes". *J Struct Biol* 104:150-62

Sullivan GJ, Bridger JM, Cuthbert AP, Newbold RF, Bickmore WA and McStay B (2001) "Human acrocentric chromosomes with transcriptionally silent nucleolar organizer regions associate with nucleoli". *EMBO J* 20:2867-77

Sun HB, Shen J and Yokota H (2000) "Size-dependent positioning of human chromosomes in interphase nuclei". *Biophys J* 79:184-90

Szwagierczak A, Bultmann S, Schmidt CS, Spada F and Leonhardt H (2010) "Sensitive enzymatic quantification of 5-hydroxymethylcytosine in genomic DNA". *Nucleic Acids Res* 38:e181

Taddei A, Hediger F, Neumann FR and Gasser SM (2004) "The function of nuclear architecture: a genetic approach". *Annu Rev Genet* 38:305-45

Tahiliani M, Koh KP, Shen Y, Pastor WA, Bandukwala H, Brudno Y, Agarwal S, Iyer LM, Liu DR, Aravind L *et al.* (2009) "Conversion of 5-methylcytosine to 5-hydroxymethylcytosine in mammalian DNA by MLL partner TET1". *Science* 324:930-5

Tang L, Nogales E and Ciferri C (2010) "Structure and function of SWI/SNF chromatin remodeling complexes and mechanistic implications for transcription". *Prog Biophys Mol Biol* 102:122-8

Telenius H, Carter NP, Bebb CE, Nordenskjold M, Ponder BA and Tunnacliffe A (1992) "Degenerate oligonucleotide-primed PCR: general amplification of target DNA by a single degenerate primer". *Genomics* 13:718-25

Teller K, Solovei I, Buiting K, Horsthemke B and Cremer T (2007) "Maintenance of imprinting and nuclear architecture in cycling cells". *Proc Natl Acad Sci U S A* 104:14970-5

Testillano PS, Sanchez-Pina MA, Olmedilla A, Ollacarizqueta MA, Tandler CJ and Risueno MC (1991) "A specific ultrastructural method to reveal DNA: the NAMA-Ur". *J Histochem Cytochem* 39:1427-38

Truong AB and Khavari PA (2007) "Control of keratinocyte proliferation and differentiation by p63". *Cell Cycle.* 6:295-9. Epub 2007 Feb 28.

Tsutsui KM, Sano K and Tsutsui K (2005) "Dynamic view of the nuclear matrix". *Acta Med Okayama* 59:113-20

Umen JG (2005) "The elusive sizer". *Curr Opin Cell Biol* 17:435-41

Vaezi A, Bauer C, Vasioukhin V and Fuchs E (2002) "Actin cable dynamics and Rho/Rock orchestrate a polarized cytoskeletal architecture in the early steps of assembling a stratified epithelium". *Dev Cell* 3:367-81

Veiko NN, Shubaeva NO, Malashenko AM, Beskova TB, Agapova RK and Liapunova NA (2007) "[Ribosomal genes in inbred mouse strains: interstrain and intrastrain variations of copy number and extent of methylation]". *Genetika* 43:1226-38

Visser T D, Oud J L and J BG (1992) "Refractive index and axial distance measurements in 3-D microscopy.". *Optik* 1:17-19

Volpi EV, Chevret E, Jones T, Vatcheva R, Williamson J, Beck S, Campbell RD, Goldsworthy M, Powis SH, Ragoussis J *et al.* (2000) "Large-scale chromatin organization of the major histocompatibility complex and other regions of human chromosome 6 and its response to interferon in interphase nuclei". *J Cell Sci* 113 (Pt 9):1565-76

Volz A, Korge BP, Compton JG, Ziegler A, Steinert PM and Mischke D (1993) "Physical mapping of a functional cluster of epidermal differentiation genes on chromosome 1q21". *Genomics* 18:92-9

Walter J, Joffe B, Bolzer A, Albiez H, Benedetti PA, Muller S, Speicher MR, Cremer T, Cremer M and Solovei I (2006) "Towards many colors in FISH on 3D-preserved interphase nuclei". *Cytogenet Genome Res* 114:367-78

Wang L, Di LJ, Lv X, Zheng W, Xue Z, Guo ZC, Liu DP and Liang CC (2009) "Inter-MAR association contributes to transcriptionally active looping events in human beta-globin gene cluster". *PLoS ONE.* 4:e4629. Epub 2009 Feb 27.

Waterston RH, Lindblad-Toh K, Birney E, Rogers J, Abril JF, Agarwal P, Agarwala R, Ainscough R, Alexandersson M, An P *et al.* (2002) "Initial sequencing and comparative analysis of the mouse genome". *Nature* 420:520-62

Watt FM and Green H (1982) "Stratification and terminal differentiation of cultured epidermal cells". *Nature* 295:434-6

Wei X, Somanathan S, Samarabandu J and Berezney R (1999) "Three-dimensional visualization of transcription sites and their association with splicing factor-rich nuclear speckles". *J Cell Biol* 146:543-58

Weierich C, Brero A, Stein S, von Hase J, Cremer C, Cremer T and Solovei I (2003) "Three-dimensional arrangements of centromeres and telomeres in nuclei of human and murine lymphocytes". *Chromosome Res* 11:485-502

Weipoltshammer K, Schofer C, Almeder M, Sylvester J and Wachtler F (1996) "Spatial distribution of sex chromosomes and ribosomal genes: a study on human lymphocytes and testicular cells". *Cytogenet Cell Genet* 73:108-13

Williams CJ, Naito T, Arco PG, Seavitt JR, Cashman SM, De Souza B, Qi X, Keables P, Von Andrian UH and Georgopoulos K (2004) "The chromatin remodeler Mi-2beta is required for CD4 expression and T cell development". *Immunity* 20:719-33

Williams RR, Azuara V, Perry P, Sauer S, Dvorkina M, Jorgensen H, Roix J, McQueen P, Misteli T, Merkenschlager M *et al.* (2006) "Neural induction promotes large-scale chromatin reorganisation of the Mash1 locus". *J Cell Sci* 119:132-40

Williams RR, Broad S, Sheer D and Ragoussis J (2002a) "Subchromosomal positioning of the epidermal differentiation complex (EDC) in keratinocyte and lymphoblast interphase nuclei". *Exp Cell Res.* 272:163-75.

Williams RR, Broad S, Sheer D and Ragoussis J (2002b) "Subchromosomal positioning of the epidermal differentiation complex (EDC) in keratinocyte and lymphoblast interphase nuclei". *Exp Cell Res* 272:163-75

Wilson KL and Berk JM "The nuclear envelope at a glance". *J Cell Sci* 123:1973-8

Woodcock CL and Ghosh RP "Chromatin higher-order structure and dynamics". *Cold Spring Harb Perspect Biol* 2:a000596

Xie SQ, Martin S, Guillot PV, Bentley DL and Pombo A (2006) "Splicing speckles are not reservoirs of RNA polymerase II, but contain an inactive form, phosphorylated on serine2 residues of the C-terminal domain". *Mol Biol Cell* 17:1723-33

Yang A, Kaghad M, Wang Y, Gillett E, Fleming MD, Dotsch V, Andrews NC, Caput D and McKeon F (1998) "p63, a p53 homolog at 3q27-29, encodes multiple products with transactivating, death-inducing, and dominant-negative activities". *Mol Cell* 2:305-16

Yang A, Schweitzer R, Sun D, Kaghad M, Walker N, Bronson RT, Tabin C, Sharpe A, Caput D, Crum C *et al.* (1999) "p63 is essential for regenerative proliferation in limb, craniofacial and epithelial development". *Nature* 398:714-8

Yasuhara JC and Wakimoto BT (2006) "Oxymoron no more: the expanding world of heterochromatic genes". *Trends Genet* 22:330-8

Young PJ, Le TT, Dunckley M, Nguyen TM, Burghes AH and Morris GE (2001) "Nuclear gems and Cajal (coiled) bodies in fetal tissues: nucleolar distribution of the spinal muscular atrophy protein, SMN". *Exp Cell Res* 265:252-61

Zhang CT and Zhang R (2003) "An isochore map of the human genome based on the Z curve method". *Gene* 317:127-35

Zhang L, Kasif S, Cantor CR and Broude NE (2004) "GC/AT-content spikes as genomic punctuation marks". *Proc Natl Acad Sci U S A* 101:16855-60

Zimmermann N, Doepker MP, Witte DP, Stringer KF, Fulkerson PC, Pope SM, Brandt EB, Mishra A, King NE, Nikolaidis NM *et al.* (2005) "Expression and regulation of small proline-rich protein 2 in allergic inflammation". *Am J Respir Cell Mol Biol* 32:428-35

Zink D, Amaral MD, Englmann A, Lang S, Clarke LA, Rudolph C, Alt F, Luther K, Braz C, Sadoni N *et al.* (2004) "Transcription-dependent spatial arrangements of CFTR and adjacent genes in human cell nuclei". *J Cell Biol* 166:815-25